

**AN EVALUATION OF THE COAL BED METHANE  
POTENTIAL OF THE MID-ZAMBEZI AND  
NORTHEASTERN KALAHARI KAROO BASINS**

**By**

**Johannes Hermanus Jacobus Potgieter**

**Dissertation submitted in fulfilment of the requirements for the  
degree of**

**MASTER OF SCIENCE**

**In the Faculty of Natural and Agricultural Sciences**

**Department of Geology**

**University of the Free State**

**Bloemfontein**

**South Africa**

UNIVERSITY OF THE  
FREE STATE  
UNIVERSITEIT VAN DIE  
VRYSTAAT  
YUNIVESITHI YA  
FREISTATA



2017

Internal Supervisor:

Prof. W.A. v.d. Westhuizen

External Supervisor:

Dr. L. Nel

## DECLARATION

I declare that this thesis is my own, unaided work. It is being submitted for the degree of Master of Science in the Department of Geology, University of the Free State, Bloemfontein. This thesis has not been submitted previously for any degree or any examination at any other University.

---

Johannes Hermanus Jacobus Potgieter

This \_\_\_\_\_ day of \_\_\_\_\_, 2017

*“Do or do not, there is no try”*

- Jedi Master Yoda

## ABSTRACT

*With the growing energy demand worldwide it is very important to identify any new fossil fuel resources for future use. Coal remains the most widely used fossil fuel for electricity generation in Southern Africa but over the past two decades gas has been seen as a possible supplement and ultimate replacement for the coal. A lack of world class conventional gas accumulations in Southern Africa, unconventional gas deposits, hosted in the Karoo Supergroup, have been investigated as an alternative gas source. The primary unconventional resource focussed on in north-eastern Botswana and north-western Zimbabwe to date has been coal bed methane (CBM), a natural gas generated during the coalification process and stored within internal coal structures. A major limiting factor for a regional investigation into the CBM resource potential is the lack of exploration information specifically focussed on gas rather than coal. The gas saturation state of coal has a notable impact on the measureable gas content value as well as the production potential within an area. One of the assumptions of previous semi-regional assessments was that the coal is fully saturated, which has not been the case from dedicated gas exploration campaigns in the region. As part of this evaluation the coal ranks, obtained from historic borehole data over the study area, were compared to the laboratory measured maximum sorptive capacities to determine the theoretical gas content of the coal. Investigations of two regional analogous coal fields showed that the coals are unlikely to be fully saturated and for a resource evaluation based on coal rank it is imperative to use a range of saturations for the final data inputs. Schlumberger's GeoX software was used for a probabilistic resource calculation using Monte Carlo simulations with ten thousand iterations. The resource estimation results showed a wide distribution of probable values. Even with a resource value of 22Tcf, the major basins in Canada and the US have significantly higher resource densities than that of the Study Area indicating a lower prospectivity for CBM.*

### **Key words:**

Coal bed methane, Coal, Saturation Kalahari Karoo Basin, Mid-Zambezi Basin, Karoo Supergroup, Wankie, Nata.

## **ACKNOWLEDGEMENTS**

I would like to thank the following people and institutions who were all instrumental in the completion of this investigation:

- Dr. Alexei Milkov for introducing me to the world of volumetric evaluations and the statistical modelling of regional data investigation.
- Juan Botillo for your patience, guidance and motivation during my early days of resource evaluation.
- Neil Andersen for introducing me to the Karoo and CBM.
- Dr Leon Nel for his guidance through the review process.
- Prof. Willem van der Westhuizen for your calls and mails that got me back on track when I let my mind wander onto other matters.
- Sasol Limited for the financial backing and access to GeoX during the completion of the dissertation.
- All the field exploration teams that have for the past 120 years endured many hardships and epic travels to give us the information that we use every day of our geological lives.

# **TABLE OF CONTENTS**

<b>1. INTRODUCTION</b>	<b>1</b>
1.1. Gas as an Alternative Energy Source to Coal	1
1.2. Study Aim	5
1.3. Evaluation Methodology	5
1.4. Study Area	6
<b>2. COAL BED METHANE AS AN UNCONVENTIONAL RESOURCE</b>	<b>7</b>
2.1. Coal bed methane Generation, Storage and Migration	7
2.2. Coal Bed Methane Production	10
2.3. The Importance of the Gas Saturation State of Coal	13
2.4. Coal Bed Methane in Southern Africa	15
<b>3. REGIONAL GEOLOGICAL SETTING</b>	<b>17</b>
3.1. Development and Preservation of the Karoo Supergroup	23
3.1.1. The Karoo in Botswana and Zimbabwe	26
3.2. Karoo Supergroup in the Study Area	32
3.2.1. The Pre-Ecca Formations	37
3.2.2. Ecca Formations	38
3.2.2.1. Lower Ecca Formations	38
3.2.2.1.1. Botswana	38
3.2.2.1.1.1. Tswane Formation	39
3.2.2.1.1.2. Mea Arkose Formation	40
3.2.2.1.2. Zimbabwe	42
3.2.2.2. Upper Ecca Formations	44
3.2.2.2.1. Botswana	44
3.2.2.2.1.1. Northeastern Botswana	44
3.2.2.2.2. Zimbabwe	46

3.2.2.2.1. Wankie, Entuba and Western Areas	
Coalfields	46
3.2.2.2.2. Lubimbi Coalfield	47
3.2.2.2.3. Sengwa Coalfield	47
3.2.2.2.4. Gokwe Coalfield	48
3.2.2.2.5. Tjolutjo, Sawmills, and Insuza Areas	48
3.2.2.2.6. Upper Wankie Sandstone Formation	49
3.2.2.2.7. Tshale Formation	50
3.2.2.2.8. Ridge Sandstone Formation	50
3.2.3. The Post-Ecca Formations	51
3.2.3.1. Botswana	51
3.2.3.1.1. Tlhabala Formation	53
3.2.3.1.2. Lebung Group	54
3.2.3.2. Zimbabwe	57
3.2.3.2.1. Madumabisa Mudstones	57
3.2.3.2.2. Escarpment Grit	57
3.2.3.2.3. Pebbly Arkose Formation	58
3.2.3.2.4. Forest Sandstones	58
3.2.3.3. Volcanic Rocks in the Study Area	58
<b>3.3. The Post-Karoo Sediments</b>	<b>61</b>
<b>4. COAL DEVELOPMENT AND CHARACTERISTICS IN THE STUDY AREA</b>	<b>71</b>
4.1. Coal Quality and Rank	75
4.2. Coal Thickness, Depth and Regional Continuity	80
<b>5. ASSESSMENT OF THE CBM RESOURCE OF THE STUDY AREA</b>	<b>83</b>
5.1. Area	86
5.2. Coal Thickness	86
5.3. Coal Density	87
5.4. Gas Content	90

5.4.1.	Hydrocarbon Generation Potential of Coal	93
5.4.2.	Estimation of the Gas Content of the Coal in the Study Area	97
5.4.3.	The Impact of Gas Saturation Levels within the Coal Seams	109
<b>5.5.</b>	<b>Resource Evaluation</b>	<b>117</b>
<b>6.</b>	<b>CHALLENGES WITH DATA ACQUISITION AND MITIGATION MEASURES FOR FUTURE EXPLORATION</b>	<b>122</b>
6.1.	Data to be Acquired During Exploration Programmes	122
6.2.	Guidelines for CBM Exploration Data Collection, Sampling and Reporting	123
6.2.1.	Programme Planning and Logistics	125
6.2.1.1.	Drilling Techniques	125
6.2.1.2.	Desorption Equipment	126
6.2.1.2.1.	Desorption Canisters	126
6.2.1.2.2.	Canister Spacers	128
6.2.1.2.3.	Water Baths and Hot Boxes	128
6.2.2.	In-Field Sampling	129
6.2.2.1.	Sampling Strategy	130
6.2.2.2.	Sample Identification and Collection	130
6.2.3.	Gas Content Measurements	134
6.2.3.1.	Measureable Gas	134
6.2.3.2.	Lost Gas	138
6.2.3.3.	Residual Gas	141
6.2.3.4.	Total Gas Content	142
6.2.4.	Wireline Logging	144
6.2.5.	Post-Desorption Sample Analyses	147
6.2.5.1.	Basic Analyses	147
6.2.5.2.	Specialised Analyses	147
6.2.6.	Data Reporting	152

<b>7. SUMMARY</b>	<b>154</b>
<b>8. CONCLUSIONS</b>	<b>158</b>
<b>9. RECOMMENDATIONS</b>	<b>159</b>
<b>10. REFERENCES</b>	<b>160</b>
<b>11. APPENDICES</b>	<b>171</b>

## LIST OF FIGURES

Figure 1	The geology of conventional and unconventional hydrocarbons (Armaretti, 2014).	2
Figure 2	Projected contributions of specific hydrocarbon sources to the fossil fuel energy pool (U.S. Energy Information Administration, 2011).	3
Figure 3	Petroleum exploration and production activities in South Africa with the Waterberg CBM (blue) and Karoo shale gas (red) projects highlighted (after Petroleum Agency of South Africa, 2015; Dowling, 2006 and Shell, 2012).	4
Figure 4	Location of the study area superimposed onto a Google Earth image.	6
Figure 5	The coalification process (Alberta Energy, 2012).	7
Figure 6	Flow dynamics in coals (Al-Jubori, et al., 2009).	8
Figure 7	Coal cleat geometries (Laubach, et al., 1998).	9
Figure 8	Methane adsorption in coal cleats and pores (Flores, 2002).	10
Figure 9	CBM extraction methods.	12
Figure 10	The effect of saturation on the production from a CBM well (after Aminian, 2005 & Crain, 2015).	14
Figure 11	Locations of the areas previously assessed for CBM potential.	16
Figure 12	Permian basins of southern Godwana.	18
Figure 13	Geological time scale (Walker, et al., 2012).	19
Figure 14	The study area (red polygon) superimposed onto the Karoo basins of Southern Africa, (after Catuneanu, et al., 2005).	20
Figure 15	Location of the Smith (1984) and Anglo Coal Botswana (2010) boreholes in North East Botswana superimposed onto the SRTM image (after National	

	Aeronautics and Space Administration, 2006; Smith, 1984 and Anglo Coal Botswana, 2010).	22
Figure 16	Major structural provinces and tectonic units of Botswana (Potgieter & Andersen, 2012).	24
Figure 17	Ice flow directions in the Kalahari Karoo Basin (Jansson, 2010).	25
Figure 18	Simplified Pre-Karoo basement of Botswana (after Geological Survey Department, 1984).	27
Figure 19	Distribution of the Karoo basins and formations in Botswana (after Smith, 1984).	28
Figure 20	Distribution of the Karoo Supergroup in North East Botswana (after Smith, 1984).	29
Figure 21	Cross section of the postulated Nata Sub-Basin (after Smith, 1984).	29
Figure 22	The descriptive subdivisions of the Mid-Zambezi Basin as used by Oesterlen & Lepper (2005).	31
Figure 23	Boreholes that intersected the lower Karoo formations in north-eastern Botswana, superimposed onto the outline of the Kalahari-Karoo and Mid-Zambezi Basins after (Anglo Coal Botswana, 2010; Pitfield, 1996; Mothibi, 1999 and Persits, et al., 2011).	33
Figure 24	Southwest–northeast trending cross-section of correlation of the Karoo lithostratigraphic units through the Aranos, Kalahari, Mid-Zambesi and Cabora Bassa basins with the study area stratigraphic correlation highlighted (Catuneanu, et al., 2005).	34
Figure 25	Distribution of the Upper and Lower Karoo across the study area (after Mothibi, 1999; Pitfield, 1996 and Persits, et al., 2011).	36
Figure 26	Location of the Smith (1984) and Anglo Coal Botswana (2010) boreholes in Botswana.	41

Figure 27	Stratigraphy of the lower Karoo Supergroup in the Mid-Zambezi Basin in Zimbabwe (after Thompson, 1981; Moyo, 2012 and Oesterlen & Lepper, 2005).	43
Figure 28	Distribution map of the Late Carboniferous-Early Jurassic Karoo Supergroup in the Kalarhari Karoo Basin of Botswana showing the regional divisions of the basin, the borehole localities and palaeo-current directions in the coal-bearing Eccca Group (Bordy, 2009).	46
Figure 29	Postulated depositional environments of the coal bearing formations in the Mid-Zambezi Basin (Oesterlen & Lepper, 2005).	49
Figure 30	Lower Lebung Group distribution throughout Botswana Bordy, et al. (2010) <sup>b</sup> .	56
Figure 31	Location of the major Karoo igneous unit throughout Southern Africa (Jourdan, et al., 2004).	60
Figure 32	Map of African Karoo flood basalts, sills, and related dyke swarms (Jourdan, et al., 2005).	60
Figure 33	Isopach and distribution of the Kalahari Group (Haddon & McCarthy, 2005).	62
Figure 34	Representative borehole logs from different locations across the Kalahari basin (Haddon & McCarthy, 2005).	63
Figure 35	Map of Botswana showing the location of the Makgadikagi Pans (SA-Venues).	65
Figure 36	Lake Paleo-Makgadikgadi levels (Himmelsbach, et al., 2008).	68
Figure 37	Neotectonism of Lake Paleo-Makgadikgadi (Himmelsbach, et al., 2008).	69
Figure 38	Lake Palaeo-Makgadikgadi extents and bounding ridges (Partridge & Maud, 2000).	70
Figure 39	Coal occurrences in Southern Africa with the basins of interest highlighted (Cairncross, 2001). See Table 8 for a brief description of the coal occurrences.	72

Figure 40	Investigation areas and regions used in this evaluation.	74
Figure 41	Alteration of peat into coal (Kentucky Geological Survey, 2011).	76
Figure 42	Coal types and uses (World Coal Institute, 2005).	76
Figure 43	Graphical differentiation of coal constituent distributions, based on proximate analysis (constructed after Krishan, 1940; Middelkoop, 2009 and Cardott, 2012).	78
Figure 44	The Wankie Main Seam (k2-3) lithofacies changes at the Wankie Concession (Oesterlen & Lepper, 2005).	81
Figure 45	A typical vertical section through the Wankie Main Seam, Zimbabwe (Cairncross, 2001).	81
Figure 46	Shangani Energy exploration and production grants in Zimbabwe showing the test location from which CBM was produced (Maponga, 2014).	83
Figure 47	Location of the study area showing investigation areas in Zimbabwe, exploration boreholes in north-eastern Botswana and the Kubu Energy boreholes.	85
Figure 48	Extent of the mapped Karoo Supergroup in the study area (after Pitfield, 1996; Mothibi, 1999 and Persits, et al., 2011).	86
Figure 49	Distribution of total coal thickness data.	87
Figure 50	Formation density logging tool and compensated density log indicating coal seams.	88
Figure 51	Distribution of densities from the compensated density logs of all values less than 1.75g/cm <sup>3</sup> collected from 9 coal exploration boreholes in Botswana (after Kubu Energy, 2014).	89
Figure 52	Investigation areas in Zimbabwe and boreholes in Botswana used in this evaluation (after Thompson, 1981; Palloks, 1984; Smith, 1984; Oesterlen & Lepper, 2005; Barker, 2006 and Anglo Coal Botswana, 2010).	92

Figure 53	Correlation of maturity and coal type (Corrado, et al., 2010).	94
Figure 54	The temperature transformation of kerogen with increased depth and temperature (McCarthy, et al., 2011).	94
Figure 55	Coal rank classification based on maturity, moisture content, volatile matter content and heating value (Smith, et al., 1994).	95
Figure 56	Relative gas production amounts from coal in selected Australian basins (Faiz, et al., 2012).	96
Figure 57	Simplified elevation cross-section across the Kubu area showing the encountered coal seams and dolerite intrusions (Faiz, et al., 2013).	98
Figure 58	Langmuir isotherm parameters (IHS Inc., 2014).	101
Figure 59	Relationship between rank, depth, and sorptive capacity (Eddy, et al., 1982).	104
Figure 60	Digitised trend lines of the relationship between rank, depth, and sorptive capacity after Eddy, et al. (1982).	105
Figure 61	Correlation between the Langmuir isotherm and Eddy, et al. (1982) trend line equation gas content values.	106
Figure 62	Desorption testing results from Zimbabwe (Barker, 2006).	110
Figure 63	Digitised gas contents from the Shangani Energy measurement data graph compared to the maximum sorptive capacity (after Barker, 2006 and Eddy, et al., 1982).	111
Figure 64	Evaluations of the Permian coals collected during the Kubu Energy exploration campaign in Botswana (Faiz, et al., 2014).	112
Figure 65	Gas measurement data from the Shangani graph plotted on theoretical sorptive capacities of a high	

	volatile bituminous A coal type (after Barker, 2006 and Eddy, et al., 1982).	113
Figure 66	Distribution of gas content values from the calculated, digitised and measured datasets.	116
Figure 67	Distribution of the results of the GeoX Monte Carlo resource calculation.	120
Figure 68	Well stratigraphy and coal measure zonation as used in the guidelines.	124
Figure 69	Coring sizes (Sandvik Mining and Construction, 2015).	125
Figure 70	Test sample canister (Stoeckinger, 1991).	127
Figure 71	Clamp type aluminium HQ3 canisters (Potgieter, 2015).	127
Figure 72	Water bath (GEO Data, n.d.).	129
Figure 73	Desorption canisters in a water bath (Waechter, et al., 2004).	129
Figure 74	Desorption sample collection strategy.	131
Figure 75	The wireline coring system collection mechanism (Massenga Drilling Rigs, n.d.)	133
Figure 76	Sample identification and collection (CBM Asia Development Corporation, 2012)	133
Figure 77	Coal sample selected for desorption on digital scale (Potgieter, 2015)	133
Figure 78	Desorption canister with purge and thermocouple valve (GEO Data, n.d.)	133
Figure 79	Single sample desorbed gas content measuring apparatus (Weatherford Laboratories, n.d.).	135
Figure 80	Continuous multiple sample desorbed gas content measuring apparatus (CSG Exploration & Production Services, n.d.).	135
Figure 81	Cumulative measureable desorbed gas curve (Faiz, et al., 2013).	136
Figure 82	IsoTube gas sampling receptacle (Fieldwork Group, n.d.).	138

Figure 83	Curve fit lost gas estimations (Waechter, et al., 2004).	139
Figure 84	Comparison of linear and polynomial fits in a coal with high gas content and high diffusion rate over a 4.4 hour period (Waechter, et al., 2004).	140
Figure 85	Core slabbing equipment (GeoGas Pty Ltd, 2016).	141
Figure 86	Residual gas content measurement milling canister (Weatherford Laboratories, n.d.).	142
Figure 87	Residual gas mill pot in a shaker (GeoGas Pty Ltd, 2016).	142
Figure 88	Desorption summary sheet (Kubu Energy, 2014).	143
Figure 89	Examples of wireline logging units.	146
Figure 90	Hypothetical production dynamics of 2 coal types and similar depths.	148
Figure 91	Isotherm sample selection.	150
Figure 92	Example of desorption and coal data over a heterogeneous sampling zone.	151

## LIST OF TABLES

Table 1	Corner coordinates of the study area.	6
Table 2	Lithostratigraphic subdivisions of the Karoo Supergroup in the Mid-Zambezi Basin (Oesterlen & Lepper, 2005).	30
Table 3	Correlation of the Karoo Supergroup formations in the Ellisras (Lephalale), North East Botswana and Northern Belt and Mid-Zambezi basins.	35
Table 4	The Post-Ecca Formations across the study area.	51
Table 5	Karoo stratigraphic units Upper Karoo in Southern Africa (Catuneanu, et al., 2005).	52
Table 6	Stratigraphic nomenclature of the Lebung Group used in this study with relation to Green (1966), Smith (1984), Anglo Coal Botswana (2010) and Bordy, et al., (2010) <sup>b</sup> .	55
Table 7	Attempted correlation of the Kalahari Group stratigraphy across the basin (Haddon & McCarthy, 2005).	64
Table 8	Main characteristics of the coal occurrences shown in Figure 39 after, (Cairncross, 2001; Sparrow, 2012 and Barker, 2012)	73
Table 9	Coal classification properties on ash free basis (constructed after Krishan, 1940 and Cardott, 2012).	77
Table 10	Coal ranks across the study area derived from ash-free proximate analyses.	79
Table 11	Minimum, maximum and average coal thicknesses and top depths from borehole records.	82
Table 12	CBM recovery factors for three North American plays.	84
Table 13	Summarised statistics of all total coal thickness values across the study area.	87

Table 14	Summarised statistics of density values less than 1.75g/cm <sup>3</sup> obtained from the Kubu Energy (2014) wireline logs.	89
Table 15	Data sources and types used throughout this evaluation.	91
Table 16	Kerogen types as determined by visual kerogen analysis, origin, and hydrocarbon potential (SPE UGM SC, 2014).	93
Table 17	Selection parameters and thresholds.	99
Table 18	Subset of samples used in the gas content evaluations.	100
Table 19	Data evaluation of the select Kubu samples (after Kubu Energy, 2014).	103
Table 20	Trend line equation calculations derived from the sorptive capacity graphs by Eddy, et al. (1982).	105
Table 21	Langmuir isotherm and Eddy, et al. (1982) trend line equations gas content calculations for the Kubu sample subset.	107
Table 22	Calculated gas contents for the coal seams using the trend line equations based on the coal qualities and depth.	108
Table 23	Summarised statistics of the gas content data digitised from the Shangani Energy measurement data graph (after Barker, 2006).	110
Table 24	Coal saturation levels of the Kubu data subset (after Kubu Energy, 2014).	114
Table 25	The effect of gas saturation state of the coal on the calculated gas content data using the trend lines derived from Eddy, et al. (1982).	115
Table 26	Summarised statistics measured, digitised and calculated gas content values with incorporating the effect of saturation levels of the coal.	116
Table 27	Summary of original and filtered data inputs used in GeoX.	118

Table 28	Summary of the inputs used in GeoX.	119
Table 29	Result of the GeoX volumetric resource calculation showing the P10, P50, $P_{mean}$ and P90 values.	120
Table 30	Resource densities for the basins used in this (after APF Energy, 2004).	121
Table 31	Aspects addressed as part of the guidelines for CBM exploration data collection and sampling.	123
Table 32	Sampling sequence of events.	132
Table 33	Suggested desorption measurement intervals (Potgieter, 2015).	137
Table 34	Wireline logging tool specifications and logging speeds (Farr, 2012).	145
Table 35	Proposed coding library for CBM exploration borehole, sampling and analysis information.	153

## **LIST OF EQUATIONS**

Equation 1	Ash-free content estimation formulae (Snyman, 1998).	77
Equation 2	Calculation of gas in place volumes (Aminian, 2005).	83
Equation 3	Determination of gas content from a Langmuir isotherm (IHS Inc., 2014).	102
Equation 4	Determination of dry, ash-free gas content from a Langmuir isotherm (IHS Inc., 2014).	102
Equation 5	Determination of dry, ash-free gas content (after Snyman, 1998).	102
Equation 6	Resource density calculation method.	121

## **LIST OF APPENDICES**

Appendix A	Schedule of borehole data, indicating coal depth and thickness used in this study.	172
Appendix B	Schedule of borehole data, indicating coal quality and coal rank estimated from the ash-free fixed carbon, volatile matter and moisture values used in this evaluation.	180
Appendix C	Schedule of borehole data showing the Gas Content Calculated from the Eddy, et al. (1982) trend line Equations used in this evaluation.	196
Appendix D	List of isotherm samples collected and analysed by Kubu Energy (after Faiz, et al., 2013).	205
Appendix E	Gas content values from the Shangani Energy exploration data digitised from the Barker (2006) graph.	207

## **1. INTRODUCTION**

According to the World Coal Association (2010) coal is still the most widely used energy source worldwide and accounts for approximately 41% of electricity generation. With South Africa's coal resources diminishing and political instability in Zimbabwe, Southern African exploration activities are primarily being focused on Southern Botswana and Mozambique. However, the quality of coal in Wankie is of great importance as there is an economic coking grade fraction in the succession (Sable Mining Africa Ltd, 2011). Any extension of this coal province into the politically more stable Botswana is of cardinal economic importance to Southern Africa.

### **1.1. Gas as an Alternative Energy Source to Coal**

This growing energy demand coupled with finite coal supply has resulted in industry leaders identifying and investigating new energy sources for future use. According to Origin Energy (2015) natural gas is an important transitional fuel during the period where reliable, affordable, safe and low-carbon alternatives to coal and nuclear sources are investigated. In North America natural gas is being used extensively as the preferred energy source for domestic use and is one of the cleanest fossil fuels used for electricity generation (Alberta Energy, 2008). One trillion cubic feet (Tcf) of natural gas is capable of supplying a 1000MW power station with fuel for approximately 20 years (Rycroft, 2014).

Currently there are two primary types of gas resources being exploited (Figure 1). Conventional gas resources, hosted in highly permeable sandstone reservoirs that can be reached with traditional well-drilling techniques (Origin Energy, 2015). Unconventional gas resources are exploited from formations with much lower permeability such as shale and siltstone, and is very technology driven (Armaretti, 2014). The most well-known of the unconventional gasses is Shale Gas that gained notoriety as a result of the completion method known as fracking, also referred to as fracking, hydraulic fracturing or hydraulic stimulation. Another unconventional resource, currently being exploited in North America and Australia, is coal bed methane (CBM) where deep coal seams are exploited and gas produced.

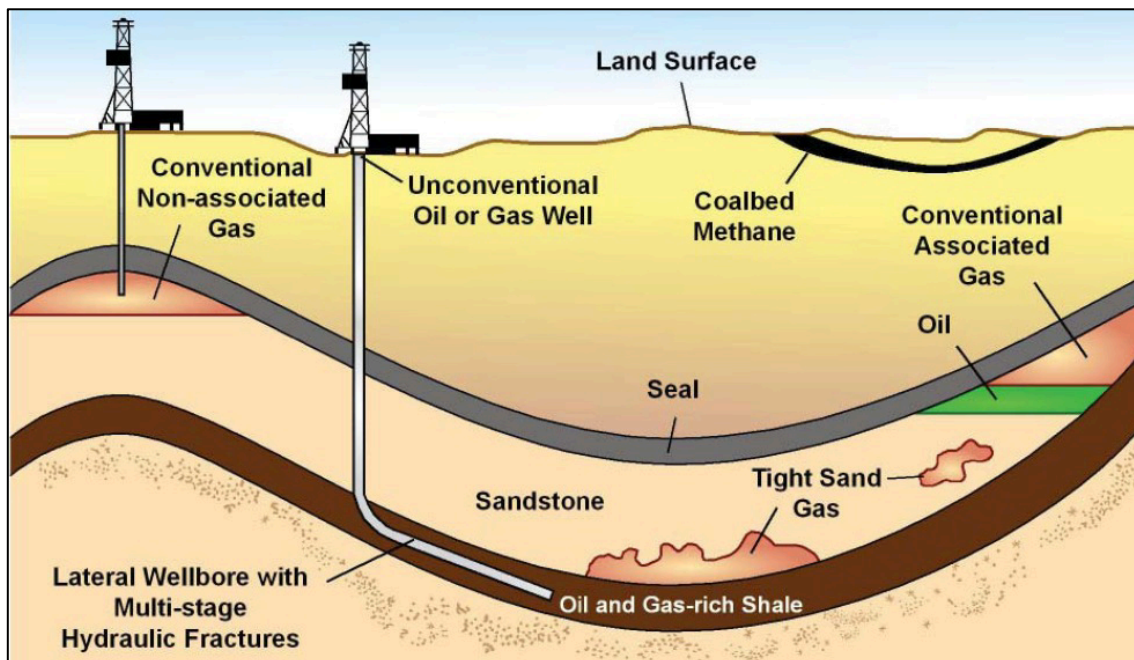


**Figure 1** The geology of conventional and unconventional hydrocarbons (Armaretti, 2014).

Southern Africa has very few producing conventional gas fields, mostly off-shore South Africa and Namibia. Currently the only commercially producing onshore field is in Mozambique, operated by Sasol. Worldwide the number of conventional fields being discovered continues to decline year on year. As a result of this, unconventional gas resources have in the past two decades, become much more important in the global energy market and so too in Southern Africa. Forecasts show that shale gas and CBM could account for up to 56% (Figure 2) of the United States energy pool (U.S. Energy Information Administration, 2011).

The vast marine shales of the Main Karoo Basin, in South Africa, and coal fields in Southern Africa have been the focus of these exploration efforts. The most notable programmes are the Waterberg CBM near Ellisras, operated by Anglo Coal (Dowling, 2006) and planned Karoo shale gas project, operated by Shell (Shell, 2012), in South Africa (Figure 3). The coal fields of north-eastern Botswana and north-western Zimbabwe, for their CBM potential, will be the focus of this evaluation.

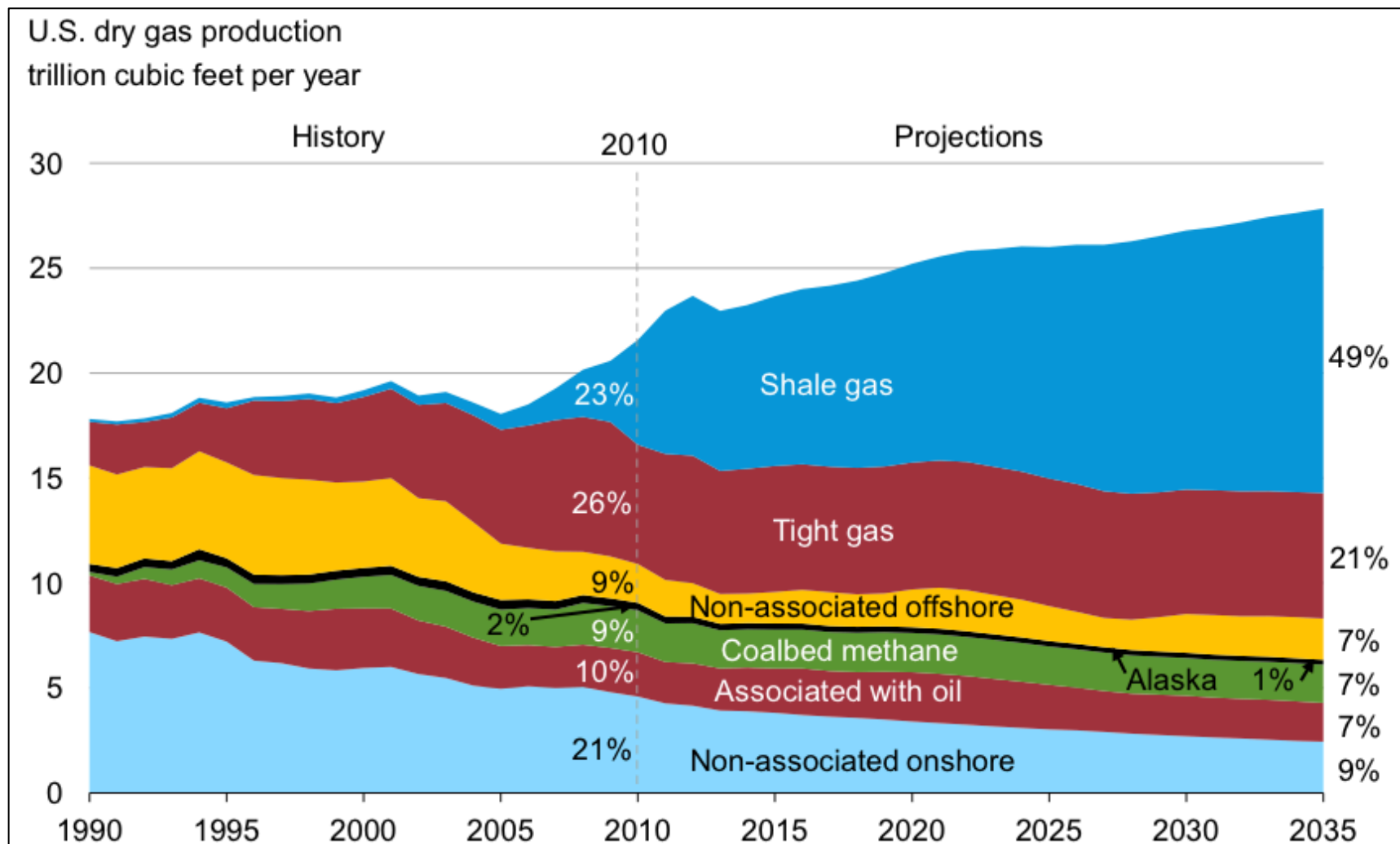


Figure 2 Projected contributions of specific hydrocarbon sources to the fossil fuel energy pool (U.S. Energy Information Administration, 2011).

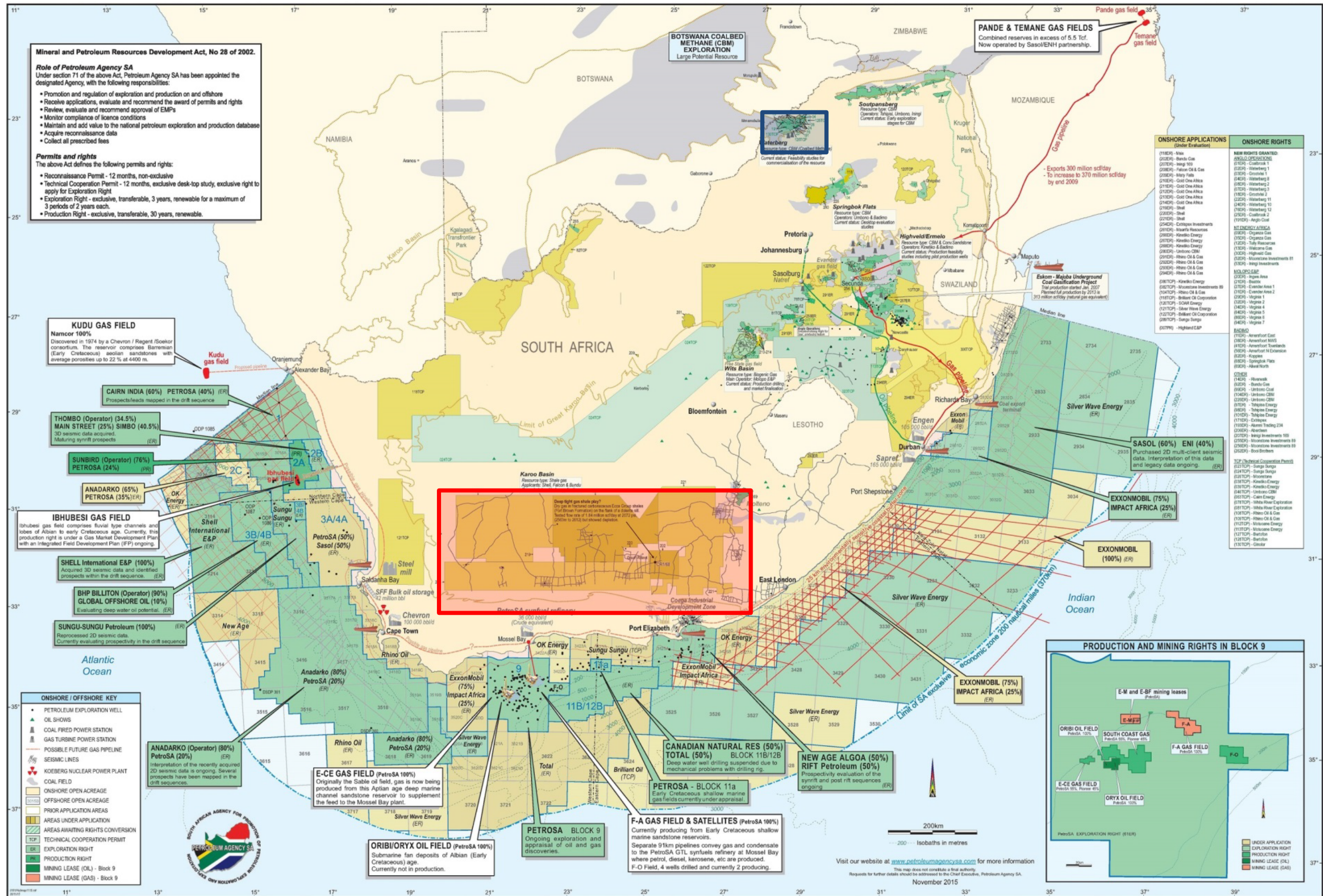


Figure 3 Petroleum exploration and production activities in South Africa with the Waterberg CBM (blue) and Karoo shale gas (red) projects highlighted (after Petroleum Agency of South Africa, 2015; Dowling, 2006 and Shell, 2012).

## **1.2. Study Aim**

This study aimed to evaluate the CBM resource potential within the study area with respect to the gas in place (GIP) CBM volumes. GIP values are one of the criteria to determine exploration success.

## **1.3. Evaluation Methodology**

The evaluation of available borehole information over the area of interest with respect to key aspects of coal and CBM exploration, formed the basis of the study. The most accurate geological information was obtained from historic borehole logs and published reports. For this study, a detailed examination of all available published information was completed as the primary source of data. Parameters that were extracted are coal quality, gas content measurements, stratigraphic depths and nett coal thicknesses, determined from geological borehole logs. It was not possible to view any core as the mudstones of the Karoo Supergroup tend to weather very quickly if not stored properly. This deterioration affects both the geological description and made correct depth correlation impossible.

The regional geological continuity and correlations were determined from existing literature and supplemented by drilling records derived primarily from Anglo Coal Botswana exploration operations from 2008 to 2010 (Anglo Coal Botswana, 2010). The review of the data included an investigation into the nett thickness of the coal in the region. During the evaluation the rank of the coal and gas generation and holding capability was established and combined with gas saturation measurements taken from analogous fields in the region. These datasets were used as inputs to the GIP calculations in GeoX.

For comparative purposes the resource evaluation results were compared to a number of other basins globally.

## 1.4. Study Area

An area with a surface extent of 166 931 km<sup>2</sup> covering the north-eastern part of Botswana and the north-western part of Zimbabwe was selected as the focus for this study (Table 1 and Figure 4). The study area covers portions of the Kalahari Karoo and Mid Zambezi Karoo Basins.

**Table 1** Corner coordinates of the study area.

Corner	Latitude	Longitude
West	19°15'22"S	23°49'18"E
North	16°19'41"S	27°16'29"E
East	18°27'4"S	29°32'53"E
South	21°26'57"S	26°13'48"E



**Figure 4** Location of the study area superimposed onto a Google Earth image.

## 2. COAL BED METHANE AS AN UNCONVENTIONAL RESOURCE

Coal Bed Methane (CBM) is the term used for the natural gas that is generated by thermogenic alterations of coal or by biogenic action of indigenous microbes on the coal (Simpson, 2008). CBM along with shale gas are the two most prominent unconventional gas resources currently being exploited. An unconventional source is defined as a natural gas source where the source rock acts as the reservoir with no or very little gas migration. These unconventional plays are often associated with very low permeability and porosity.

### 2.1. Coal bed methane Generation, Storage and Migration

Thermogenic methane is generated during the coalification process (Figure 5) when organic debris is deposited in swamps, swamp-like lakes and overbank levees where peat is formed. As the peat is buried deeper it changes to brown coal, lignite, bituminous coal and ultimately anthracite depending on the pressure and temperature the coals are exposed to. During this process the decomposition of the organic material produces methane gas which along with other gases, including nitrogen and carbon dioxide, is adsorbed in the coal (Alberta Energy, 2012). Biogenic methane is generated by microbial activity post coalification under anaerobic conditions to produce methane (Faiz, et al., 2012). The generation capability of biogenic methane is very difficult to measure or predict. Biogenic enhancement has, however, been investigated as a possible reservoir enrichment technique (Fallgren, et al., 2013).

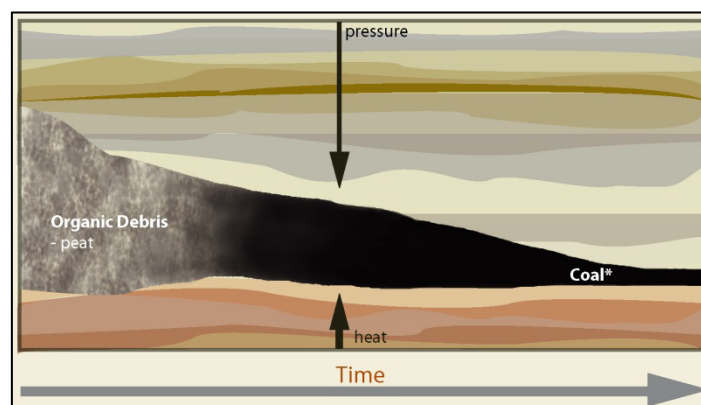
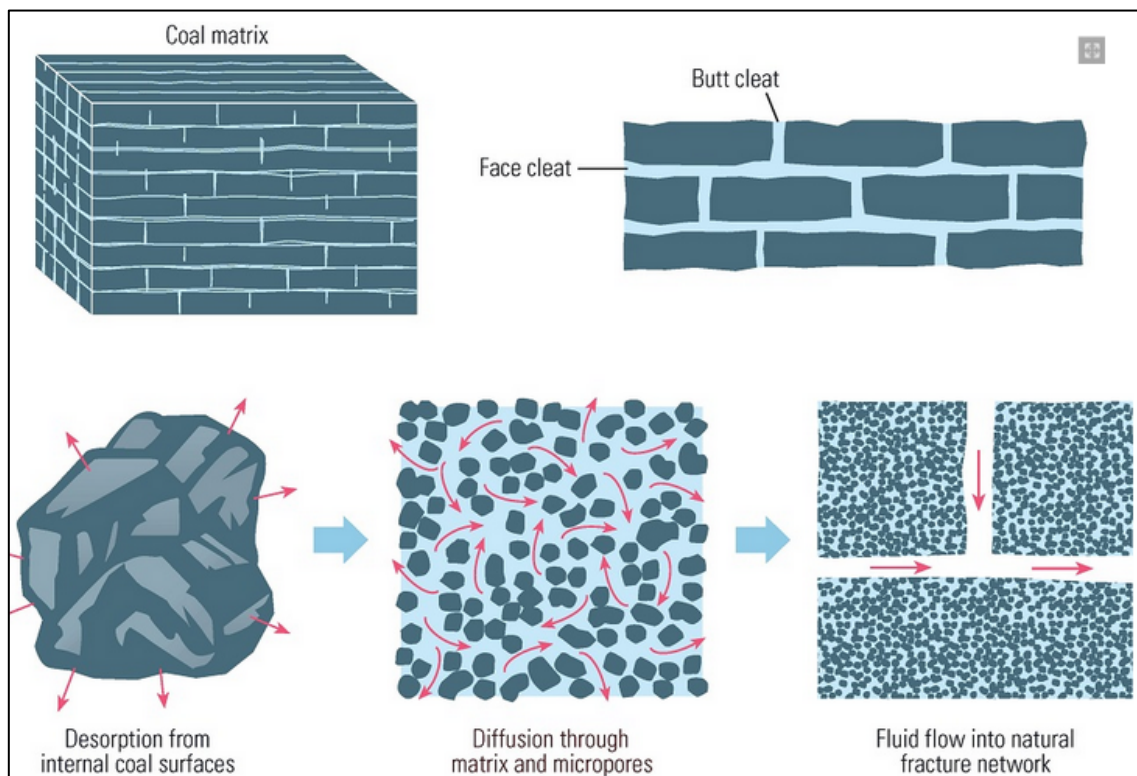


Figure 5 The coalification process (Alberta Energy, 2012).

CBM is often not pure methane but a mixture of gasses of with the most prominent three being methane, nitrogen and carbon dioxide. During economic evaluations of small scale projects the understanding of the gas composition of the CBM is essential. Carbon dioxide is corrosive and requires specialised completion and reticulation equipment whereas nitrogen is thermally inert and can be seen as the equivalent of ash in coal. Gas composition changes are often localised and inconsistencies in sampling procedures could have significant effects on the gas content values (Potgieter, 2015).

The majority of the gas (>95%) in coal is stored in micropores that are estimated to have diameters ranging from 0.5 to 1 nm (Laubach, et al., 1998). These small diameters mean the coal matrix has little to no effective porosity. The cleat-fracture porosity in coal to be between 0.5 and as much as 2.5% and is regarded as the primary conduits for flow and migration (Figure 6). The remainder of the gas in the coal is free gas that exists in fracture systems (Laubach, et al., 1998).



**Figure 6** Flow dynamics in coals (Al-Jubori, et al., 2009).

Cleats are natural opening-mode fractures that usually occur in two sets that are mutually perpendicular and also perpendicular to bedding in coal beds (Laubach, et al., 1998). These cleats account for most of the permeability and much of the porosity of CBM reservoirs and can have a significant effect on the stimulation and production of a reservoir (Laubach, et al., 1998 and Flores, 2002). Figure 7 illustrates coal cleat geometries (a) depicts cleat-trace patterns in plan view and (b) cleat hierarchies in cross-section view. These conventions used for cleat measurement are:

- LENGTH is parallel to cleat surface and parallel to bedding
- HEIGHT is parallel to cleat surface and perpendicular to bedding
- APERTURE is perpendicular to fracture surface
- SPACING between two cleats of the same set is a distance between them at right angles to the cleat surface (Laubach, et al., 1998)

Face and butt cleat systems are the primary and secondary permeability fractures, respectively, used by gas and water flows in the coal. Methane molecules are adsorbed along the surfaces of these cleats and related porosity by weak van der Waals bonds (Flores, 2002), Figure 8.

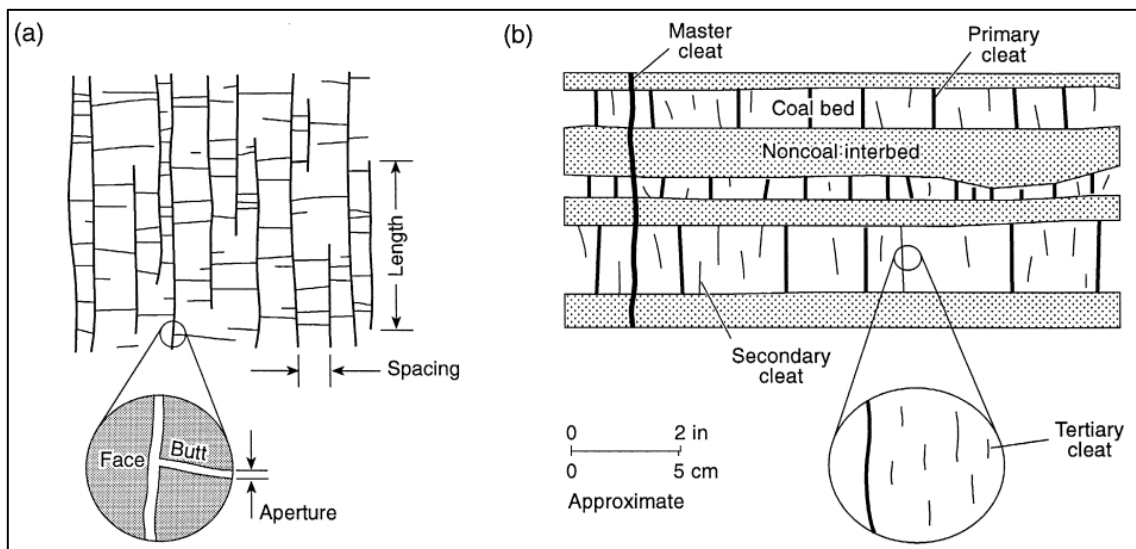


**Figure 7 Coal cleat geometries (Laubach, et al., 1998).**

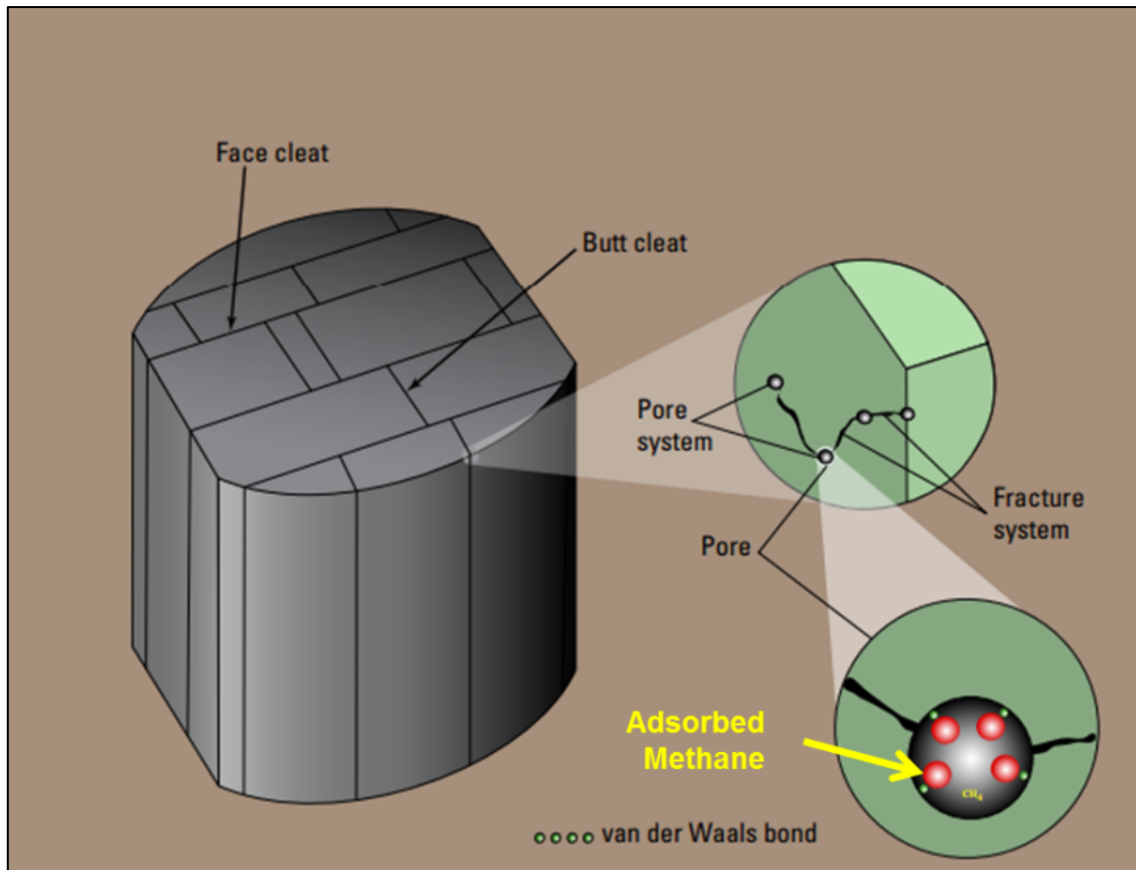


Figure 8 Methane adsorption in coal cleats and pores (Flores, 2002).

## Coal Bed Methane Production

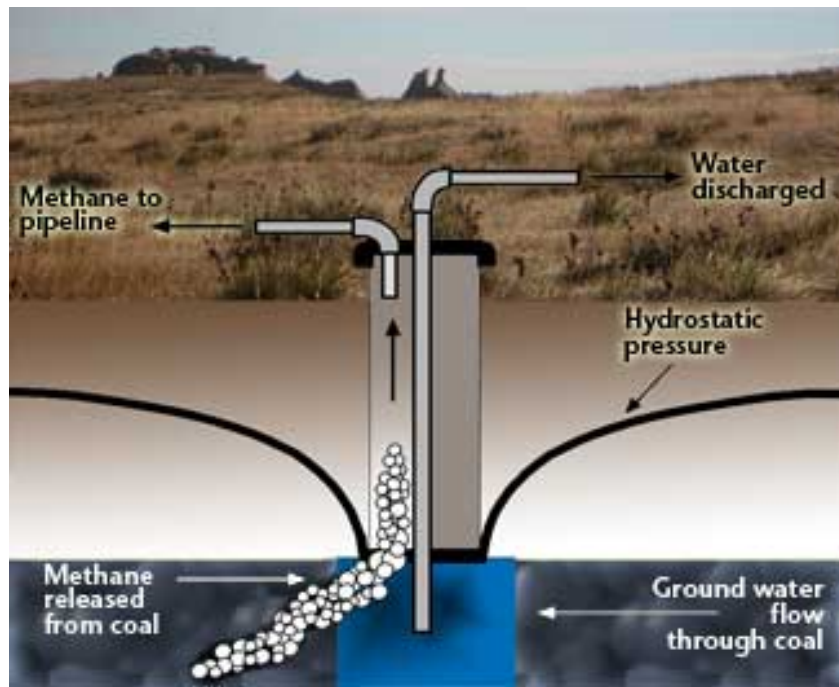
In the United States, CBM has been produced commercially since the mid 1970's when operators started to modify existing petroleum industry technology. This led to a new branch of unconventional reservoir enhancement and production techniques such as long reach, shallow horizontal drilling and multi stage hydraulic fracturing (Hollub & Schafer, 1992). One limitation that did exist was that conventional oil and gas technology did not always work, mainly because the geology of the coals differed from that of conventional oil and gas deposits (Hollub & Schafer, 1992).

Formation water that saturates the coal provides the hydrostatic pressure to hold the CBM in an adsorbed state (Dowling, 2006). Only when this hydrostatic pressure is reduced will the gas molecules be capable of being desorbed (Figure 9). Dewatering reduces the hydrostatic pressure and promotes gas desorption from coal (Al-Jubori, et al., 2009). The production of gas is governed by the rate at which gas desorbs from coal. The permeability of the gas-water system in the cleat network and

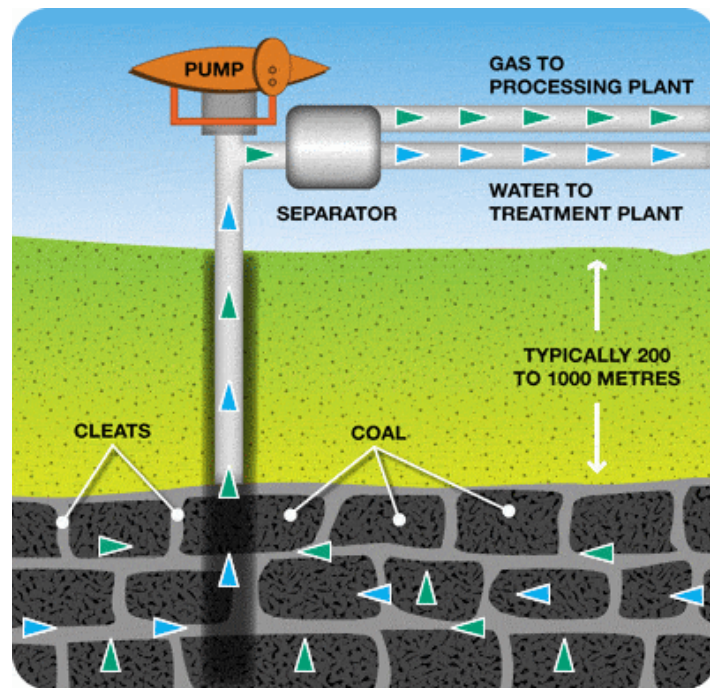
stimulated fractures controls the flow of gas through the beds (Al-Jubori, et al., 2009) and (Laubach, et al., 1998). Once the dewatering is ceased and the hydrostatic pressure returns to normal production will cease too.

Gas producing coal seams with no water have been discovered and commercially exploited. In these reservoirs, the adsorbed gas is held in place by free gas in the cleats. Consequently, gas production consists of both free gas from the cleat system and desorbed gas from the matrix (Al-Jubori, et al., 2009).

The CBM capability of the Bowen Basin in Australia is regarded as world class and will act as the main feeder for the Australia Pacific Liquefied Natural Gas (APLNG) Project in Queensland (Australia Pacific LNG, 2011).



a) CBM extraction showing the hydrostatic pressure cone of depression (Montana Bureau of Mines and Geology, n.d.)



b) CBM production and associated water production using a separator from a vertical well in Australia (Australia Pacific LNG, 2011)

Figure 9 CBM extraction methods.

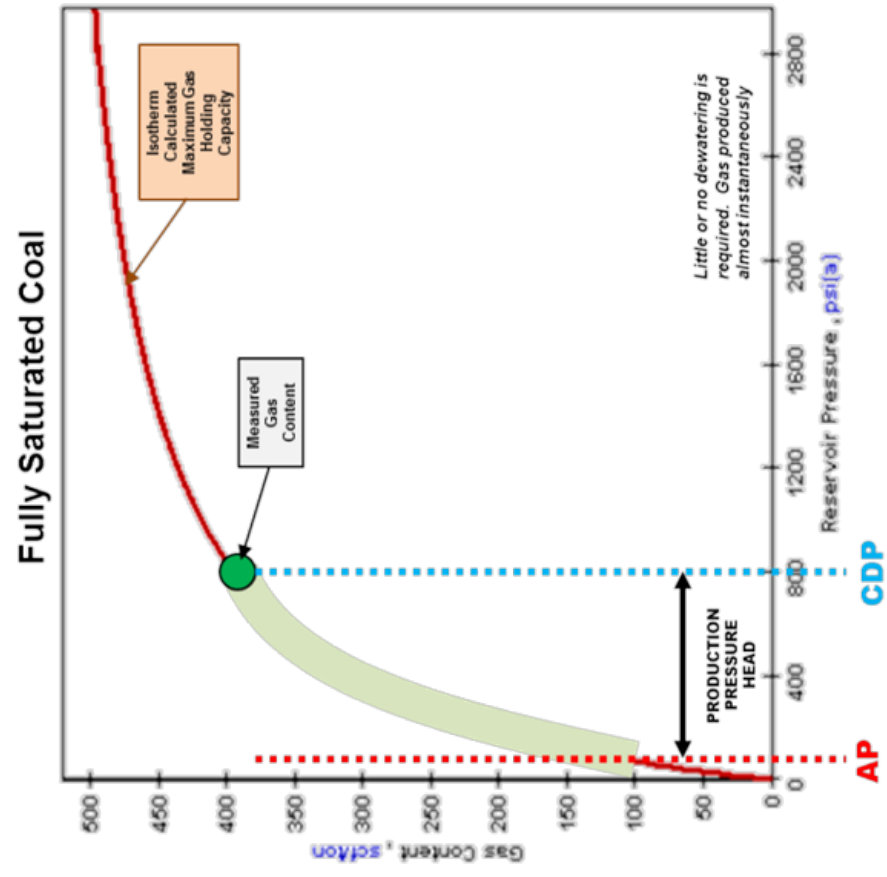
## **2.2. The Importance of the Gas Saturation State of Coal**

The saturation state of a coal seam is determined by comparing the measured gas content to the maximum sorptive capacity of the coal. The maximum sorptive or gas holding capacity of the coal is measured in a laboratory by isotherm analysis (Eddy, et al., 1982; Stoeckinger, 1991 and Faiz, et al., 2013).

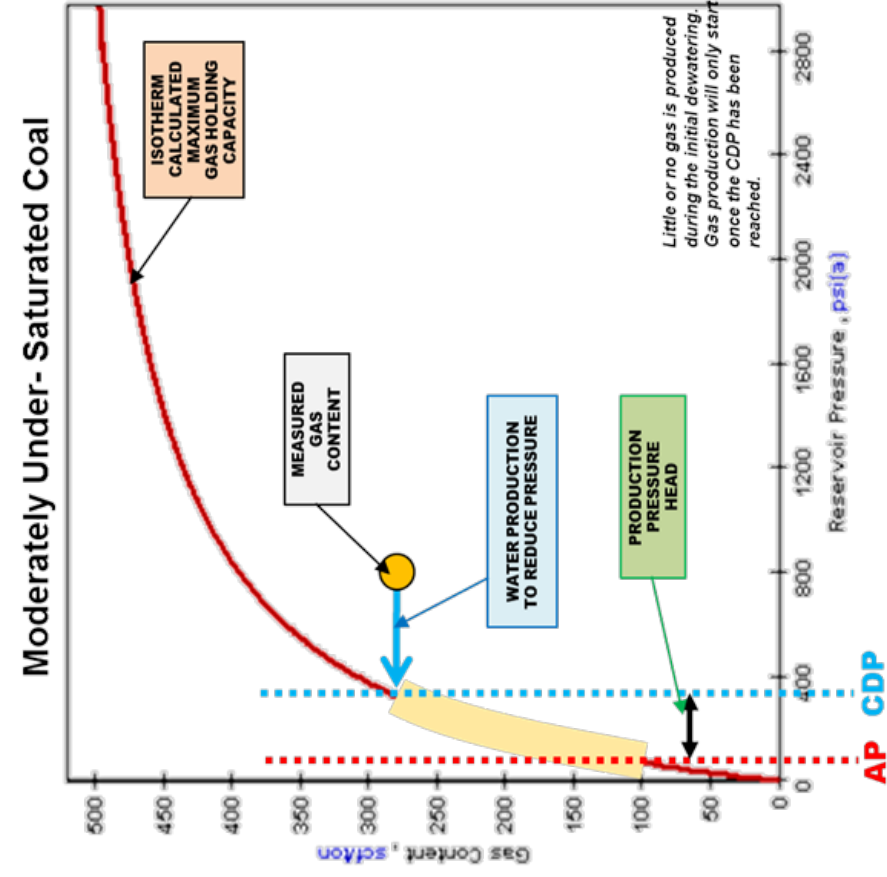
In an area where measured gas content, permeability testing and isotherm data is available the saturation state information is used to determine the production dynamics of an asset (Swindell, 2007). CBM production is associated with the simultaneous abstraction of water from the coal seam. The pumping of water reduces the hydrostatic pressure in the reservoir resulting in unassisted flow of gas from the production well. Aminian (2005) demonstrated that the ratio between the produced water and gas at different times of the life of a well is determined by the saturation.

A saturated coal seam will produce gas nearly simultaneous to the initiation of the water pumping, whereas there is a long period of water abstraction required prior to any gas production in under-saturated seams. The instance where the hydrostatic pressure has been reduced sufficiently to start the production of gas from the coal seam, is referred to as the critical desorption pressure (CDP).

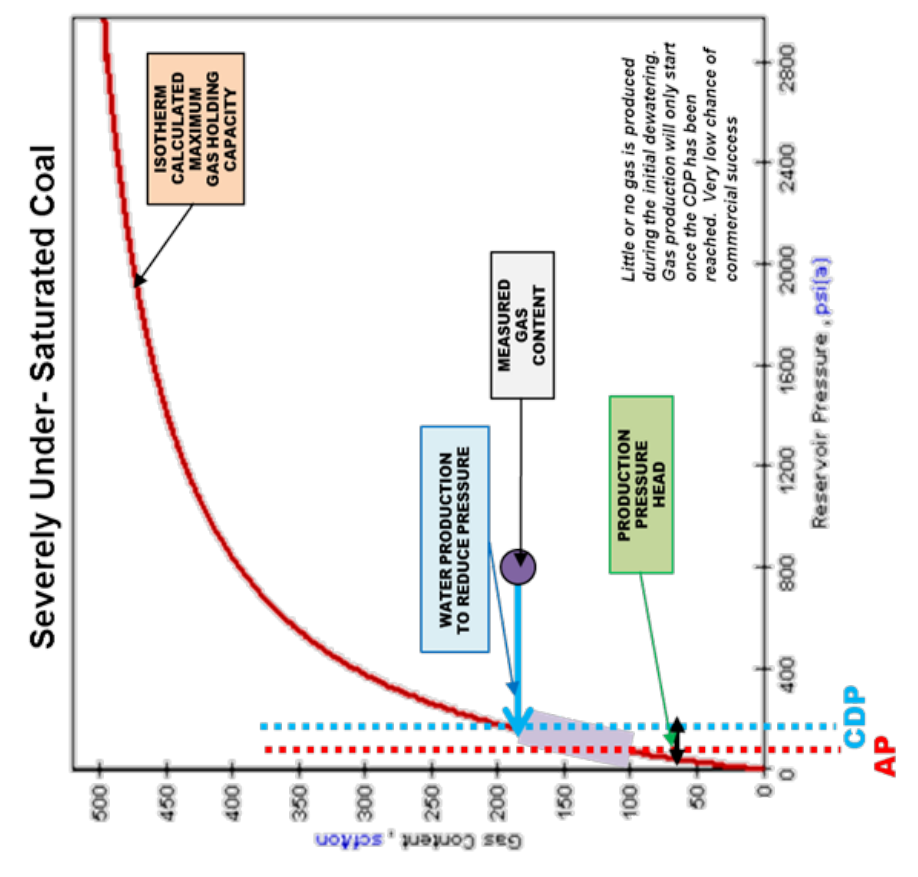
Once the well has been depressurised to a point where no gas and only water is abstracted, it is plugged and abandoned. This point is known as the abandonment pressure (AP) (Crain, 2015). Under-saturated coal seams have a shorter production life than wells with saturated coals (Figure 10).



a)



b)



c)

Figure 10 The effect of saturation on the production from a CBM well (after Aminian, 2005 & Crain, 2015).

### **2.3. Coal Bed Methane in Southern Africa**

The primary target for these unconventional resources in Southern Africa is the Karoo Supergroup, specifically the Ecca Group for its terrestrial coal and marine shale deposits as possible CBM, shale gas and conventional hydrocarbon source rock targets (Hiller & Shoko, 1996; Segwabe, 2008; Potgieter & Andersen, 2012 and Faiz, et al., 2014).

According to Catuneanu, et al. (2005) the Karoo Supergroup in north-eastern Botswana is structurally, depositionally and sedimentologically controlled, and the uniform continuation of the Mid-Zambezi Basin into Botswana. The deposition is limited to a small localized sub-basin, the Nata sub-basin, as described by (Smith, 1984). Taking Oesterlen & Lepper (2005) into account, CBM as well as some minor shale gas plays can be hosted by the Karoo Supergroup. The CBM resources in Botswana and Zimbabwe have been regarded as potentially exploitable gas deposits and over time, a substitute for coal as the primary energy source in the region. Current convention is that terrestrial deposits are likely to host coal resources and marine shale deposits are considered to be prospective for shale gas (Boyer et al., 2011).

To date there has been a great deal of speculation on the size of the potential resource, with values ranging from as high as 27Tcf in just the Hwange/Lupane Fields (Mukwakwami, 2013) to values as low as 0.2Tcf for the Lupane-Binga area (Mthandazo, 2015). Sibanda (2015) reported resource values of 40Tcf in Lupane-Lubimbi (Figure 11). The resource estimation values are often based on either proprietary data or single point datasets that have been extrapolated to fit a regional study area (Potgieter, 2015). Currently there are no commercially producing CBM fields in Southern Africa. However, Anglo Coal has had exploration success in the Waterberg Basin in South Africa with a pilot production study commencing in 2004 (Dowling, 2006) while Tlou Energy plans to commence their full scale pilot study on Central Botswana in 2015/2016 (Tlou Energy, 2014).

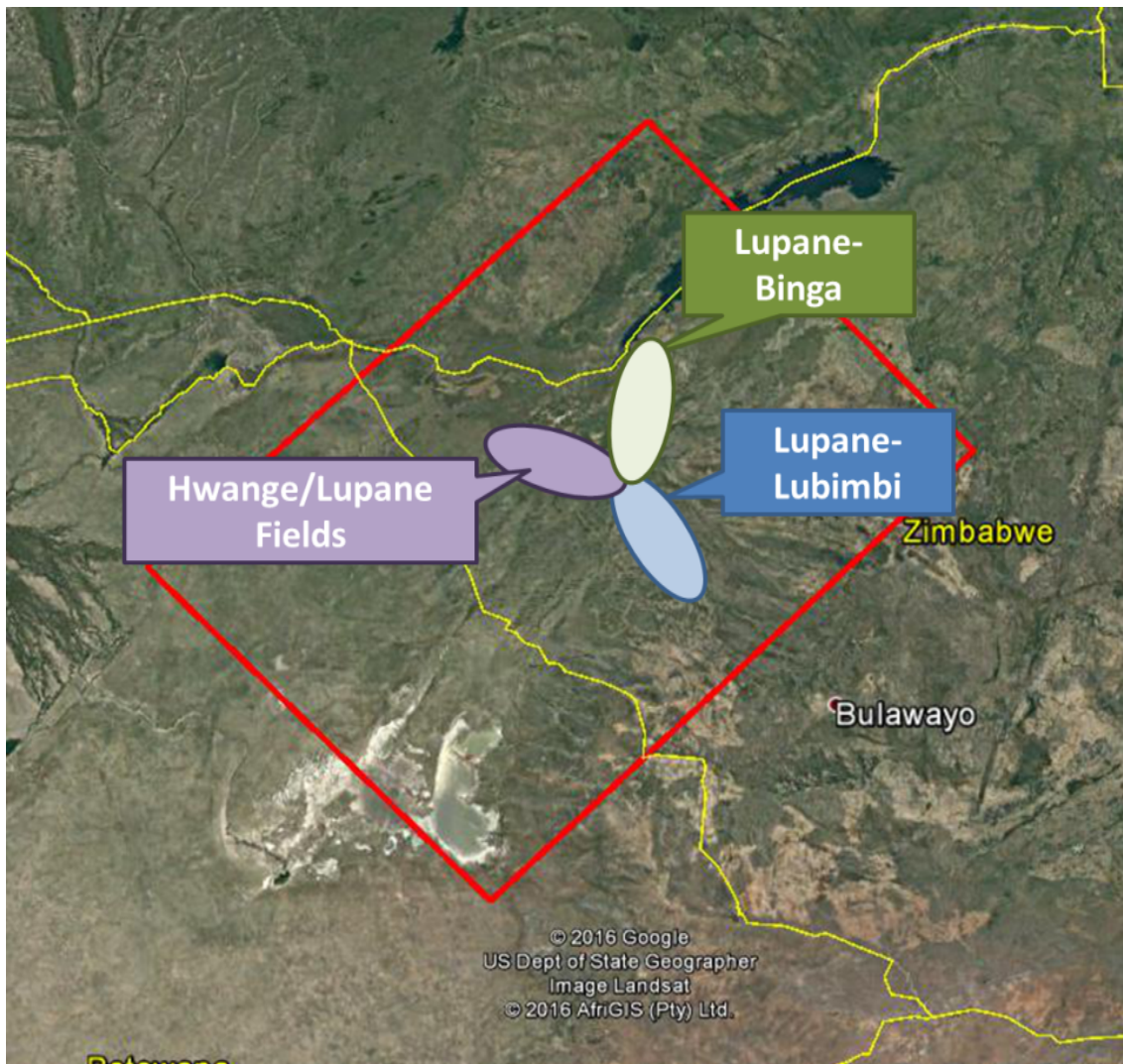


**Figure 11** Locations of the areas previously assessed for CBM potential.

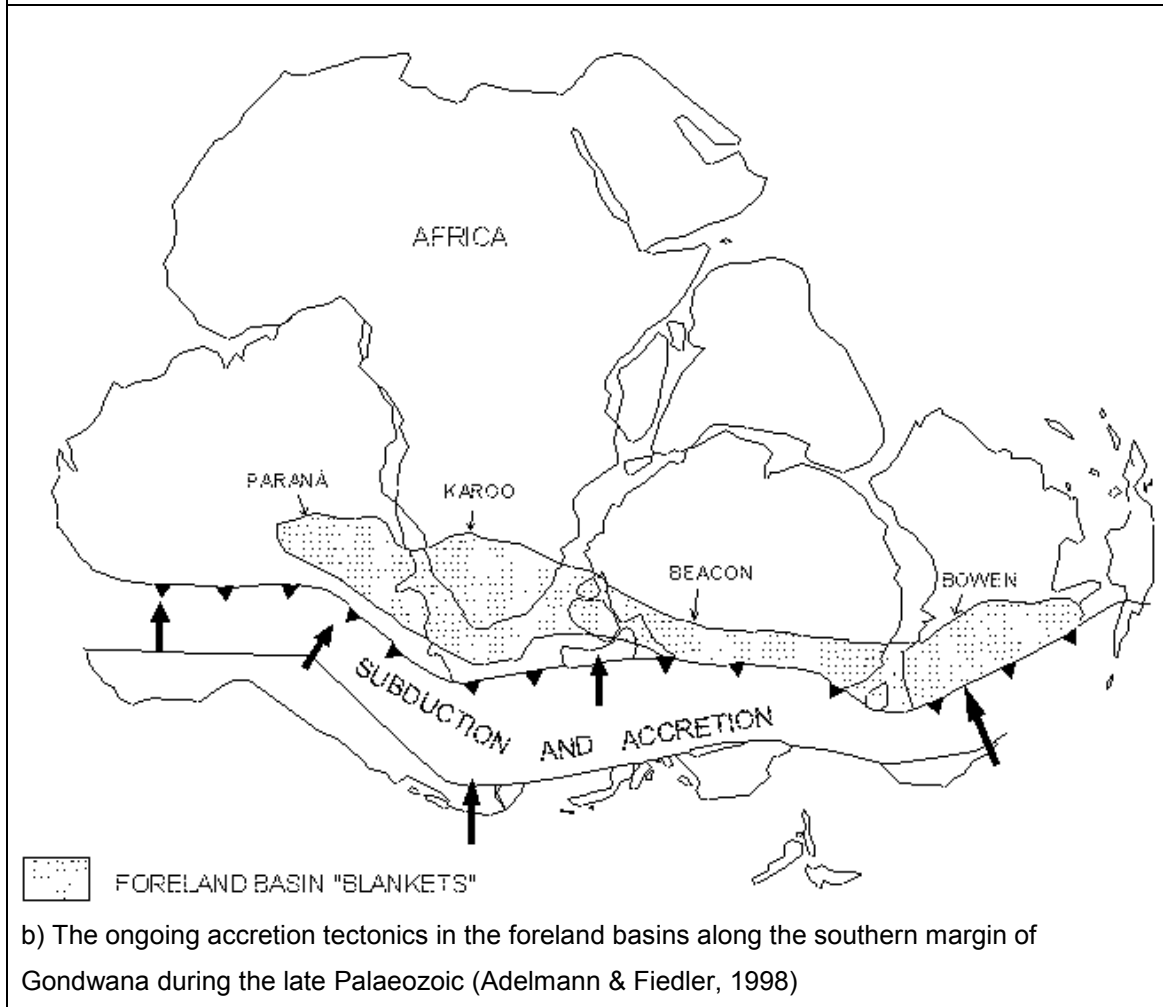
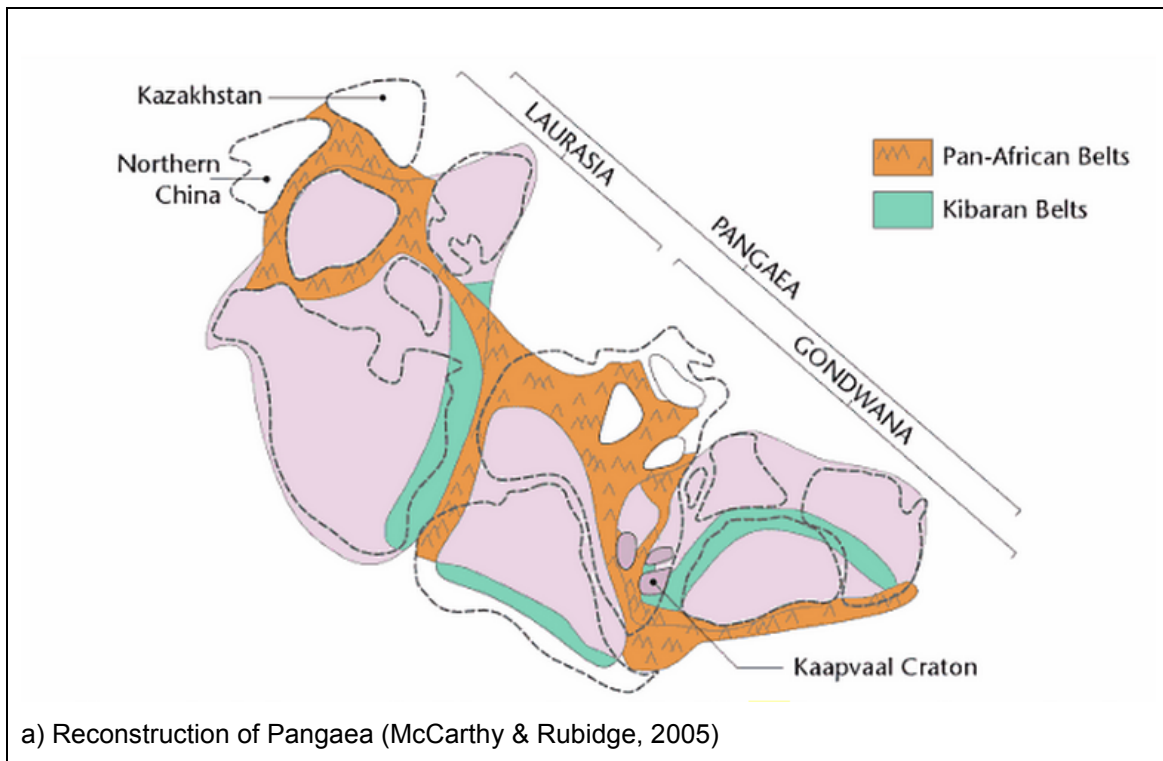
One of the major limitations noted with previous CBM resource evaluations was the lack of compensation for lower saturations. In a number of the existing evaluations full saturation levels were presumed (Potgieter, 2015) as opposed to lower saturation values noted in a number of exploration assessments by Faiz, et al. (2014) and Rainbow Gas and Coal Exploration (Pty) Ltd, (2011) in Central Botswana. The change in assumed saturation has a notable effect on the CBM resource potential across the study area and will be addressed in this evaluation.

### **3. REGIONAL GEOLOGICAL SETTING**

The study area is underlain by formations ranging from the Precambrian to Cenozoic ages. The main focus of the study was the formations of Palaeozoic and Mesozoic rocks of the Karoo Supergroup (Figure 13). The Carboniferous to Jurassic ages of the Karoo Supergroup are highlighted by the red shaded blocks.

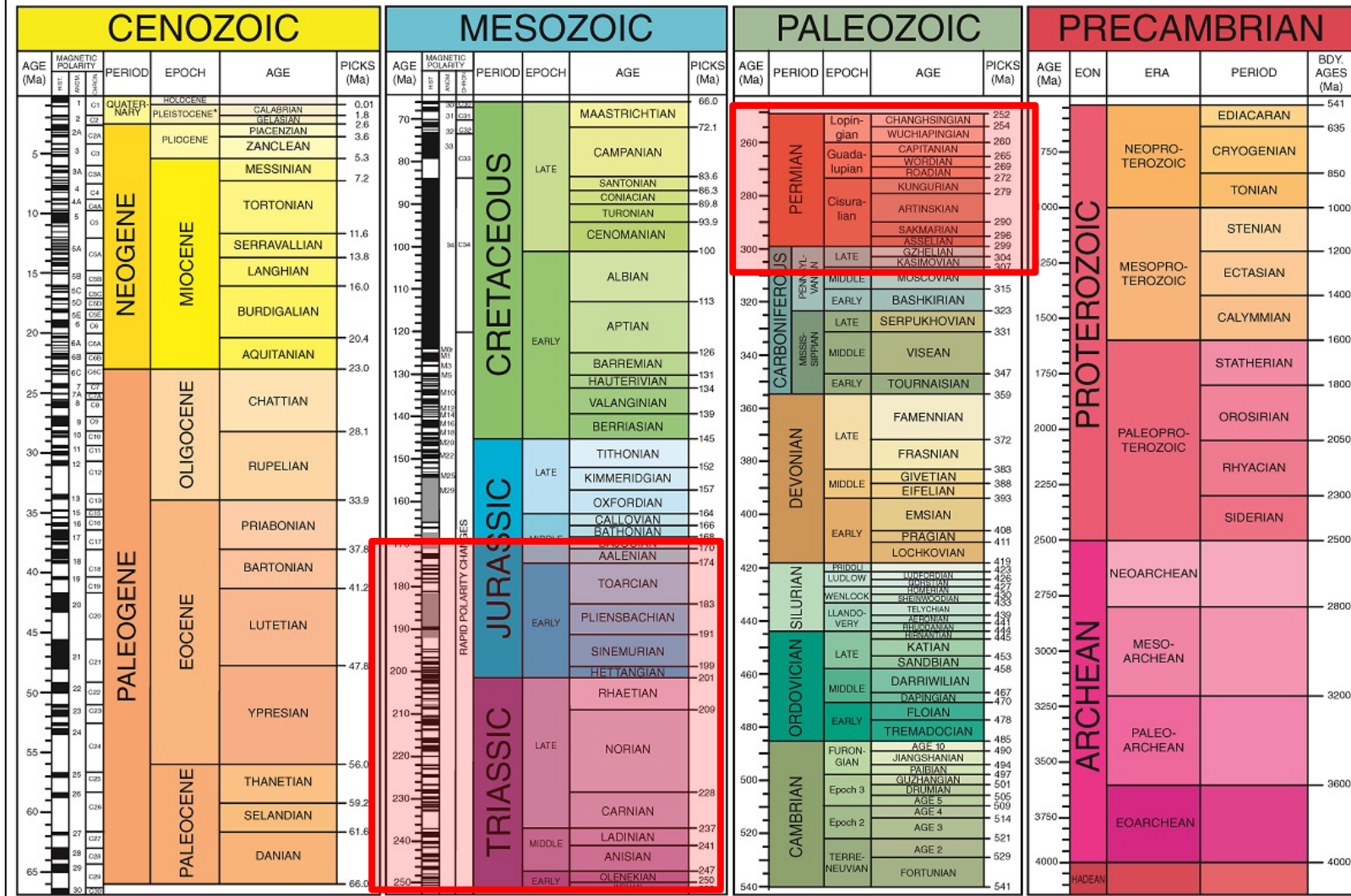
The Karoo Supergroup is appreciated for both its geological value and for its variety of well-preserved animals and plant fossils. The well preserved fossil records of the Karoo provide distinct indications of the climate, ecology, fauna and flora of the Permian and Triassic times (Potgieter & Andersen, 2012). The term Karoo Supergroup refers to sedimentary basins which occurred as the result of a major inversion tectonic event along the southern margin of Gondwana (Figure 12) during Late Carboniferous times (Catuneanu, et al., 2005). Sedimentation in these basins continued until the Middle Jurassic, around 178Ma, when widespread basalt flows and mafic dyke and sill intrusions occurred across the super continent Gondwana (Jourdan, et al., 2004).

For this study, the focus area will be the northeastern part of the Kalahari Karoo Basin in Botswana and Mid-Zambezi Basin in Zimbabwe as indicated on Figure 14. Green (1966); Smith; (1984), Catuneanu, et al. (2005) and Modie (2007) postulated that the north-eastern portion of the Kalahari Karoo Basin extend eastwards into the Mid-Zambezi Karoo basin in Zimbabwe where the Wankie coal field is one of the most important coal deposits in Southern Africa (Figure 14). This extension led explorers and the Botswana Geological Survey to believe that the North East Botswana basin has a high potential of hosting economic coal deposits (Cairncross, 2001).



**Figure 12 Permian basins of southern Godwana.**

# GSA GEOLOGIC TIME SCALE v. 4.0



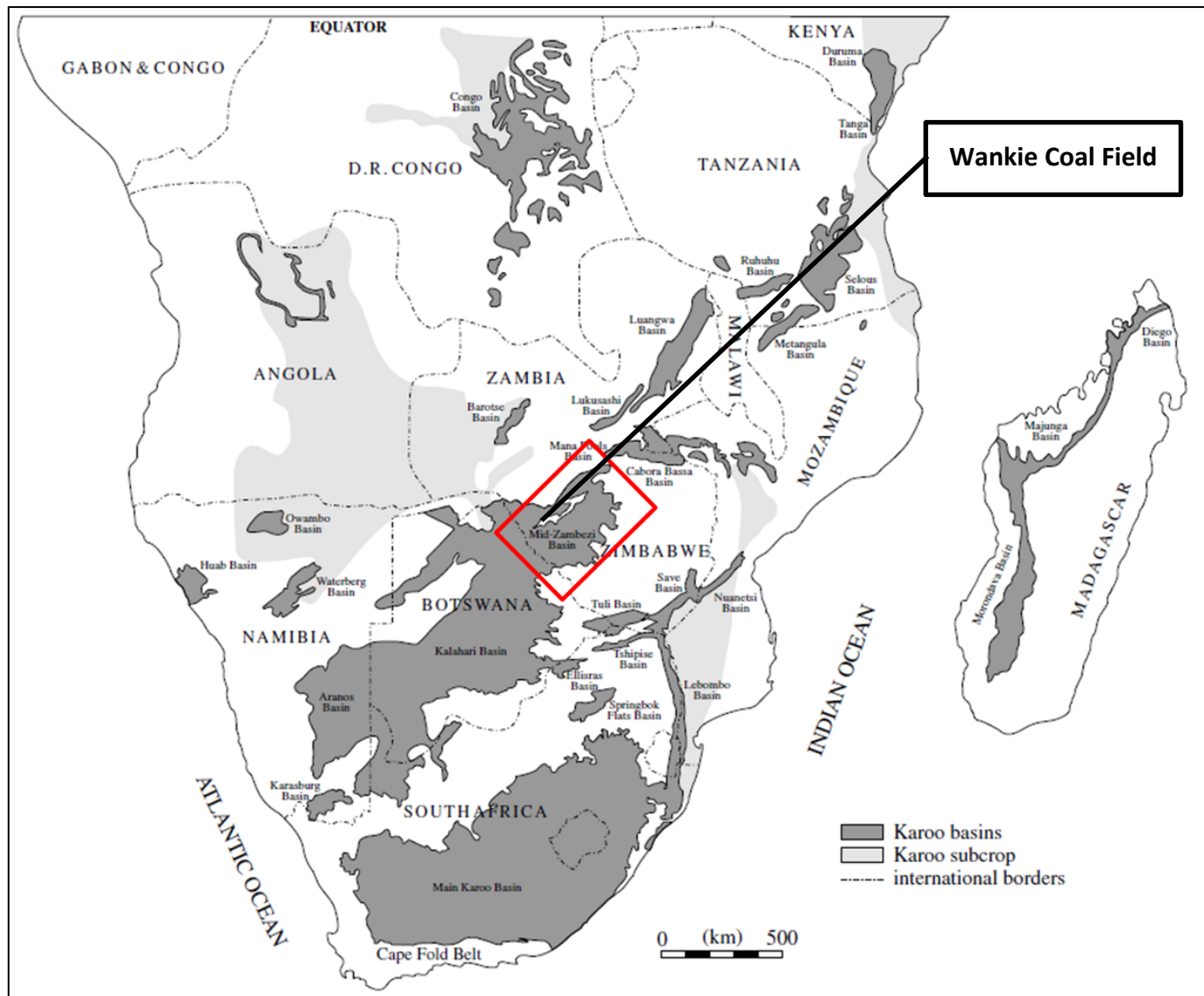


Figure 14 The study area (red polygon) superimposed onto the Karoo basins of Southern Africa, (after Catuneanu, et al., 2005).

In the study area, the Karoo is poorly exposed and only a few outcrop descriptions could be made by Green (1966). The stratigraphic descriptions by Smith (1984) were mainly obtained from limited deep boreholes drilled by Shell Coal and Anglo Botswana Coal in the 1970's aided by a deep resistivity survey by Shell Coal (Smith, 1984). The most complete drilling records through the coal measures in north-eastern Botswana are from the Dukwi area. For correlation and formation identification purposes this area was used as the stratigraphic analogue by Smith (1984). This was however, subjective, as at the time of the correlation very little deep Karoo beds were intersected in the boreholes north of Nata and the correlation with the condensed Karoo beds around Dukwi proved to be extremely tentative (Smith, 1984).

As a result of the increased CBM interest in Botswana since the publication of the Advanced Resources International, Inc. (2003) report on the CBM and shale gas potential of the Central Kalahari Basin, a number of companies applied for prospecting licences (PL). Anglo Coal Botswana (ACB) was the most notable contributor to additional deep level drilling in north-eastern Botswana. A total of twelve exploration boreholes were drilled by ACB over 23 PLs from 2007 to 2009 (Figure 15), to further delineate the lower Karoo strata north of Nata. The coordinates for the ACB exploration boreholes were obtained from the Anglo Coal Botswana (2010) relinquishment report submitted to the Department Geological Surveys and the historic borehole coordinates were obtained by georeferencing and orthorectifying the maps by Smith (1984).

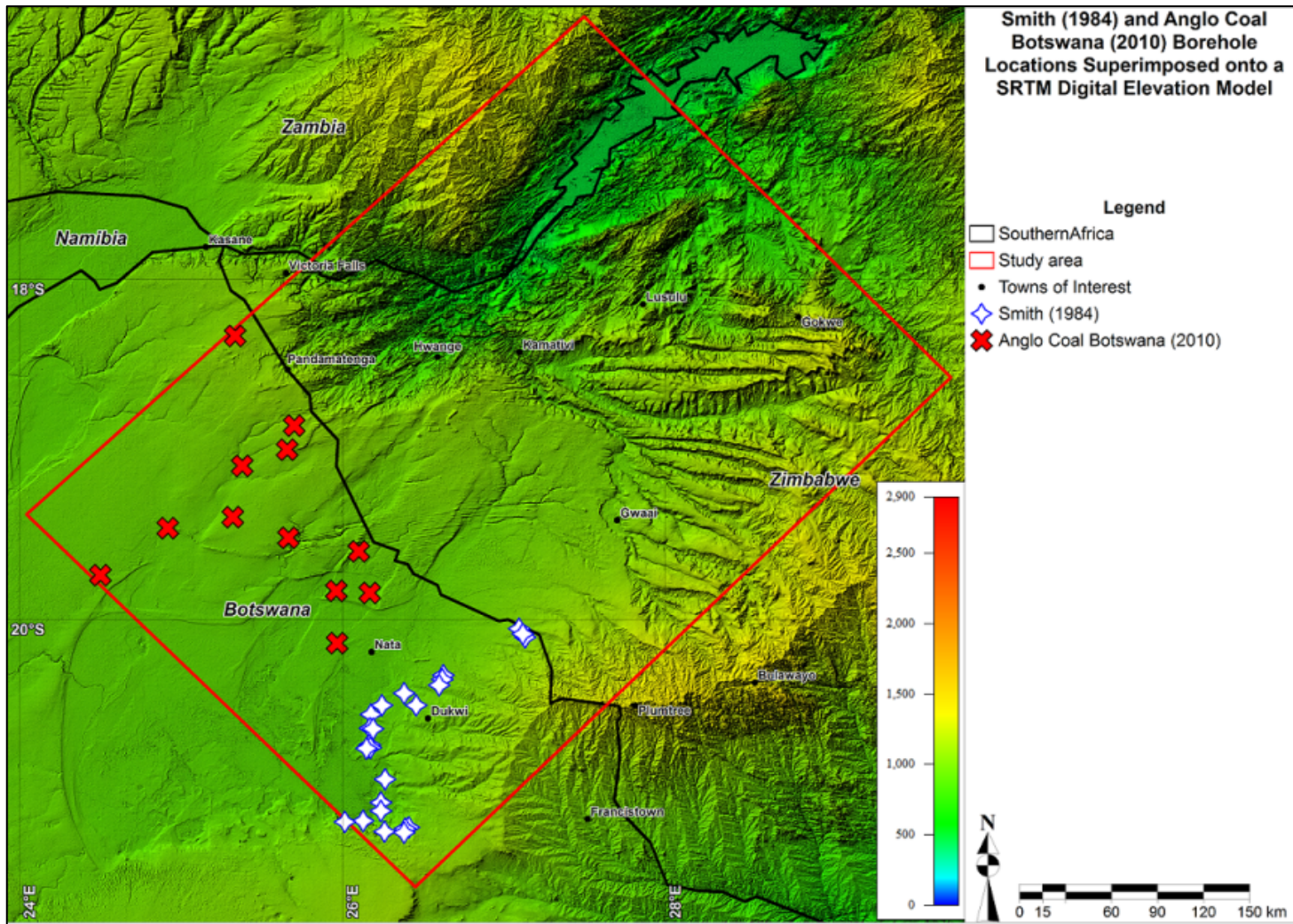


Figure 15 Location of the Smith (1984) and Anglo Coal Botswana (2010) boreholes in North East Botswana superimposed onto the SRTM image (after National Aeronautics and Space Administration, 2006; Smith, 1984 and Anglo Coal Botswana, 2010).

### **3.1. Development and Preservation of the Karoo Supergroup**

The development of the Kalahari Karoo Basin began in the late Carboniferous times to early Permian and was mainly influenced by tectonics and climate. The tectonic development of the Kalahari Karoo Basin is not well documented but there is evidence of rejuvenation of faults related to the Zoetfontein Fault (Figure 16) and a series of uplift and sagging events over the interior of the basin (Potgieter & Andersen, 2012). Le Gall, et al. (2002) found that one of the mafic dykes from the Okavango Dyke Swarm (ODS) yielded a minimum age of  $883 \pm 4$  Ma. This dyke was chemically distinct (low-Ti tholeiite) from the other ODS dykes, showing that the ODS contains both Proterozoic and Jurassic dykes (Potgieter & Andersen, 2012). This indicates that the failed rift (triple junction) as postulated by Jourdan, et al. (2006) probably propagated an ancient zone of weakness. The tectonic regimes in the study area vary from predominantly flexural systems in the south related to the subduction, accretion and mountain building processes along the Panthalassan (Palaeo-Pacific) margin to predominantly extensional regimes, related to the spreading of the Tethyan margin, in the north of Gondwana (Catuneanu, et al., 2005).

Further to the tectonic influences, the regional climate changes had a notable control of the stratigraphic deposition from cold, semi-arid environments in the Late Carboniferous to increasingly warmer climates with fluctuating levels of precipitation (Catuneanu, et al., 2005). The most recent glaciations in Africa lasted from 302Ma to 290Ma and during the maximum glaciations the South Pole was located in Southern Africa. This glacial advance occurred in a number of phases starting north of the Polar Regions and moving towards the tropical latitudes resulting in approximately 150Ma of major climatic change prior to the final ice sheet retreat (Catuneanu, et al., 2005 and Jansson, 2010). This retreat led to deposition of sedimentary rocks that record a change in geological environment from glacial cool, moist conditions during which the Dwyka Group sediments were deposited (Jansson, 2010). Figure 17 shows the minor and major ice-flow directions in and around the Kalahari Basin controlled by changes in topography or differences in deglaciation between ice sheets.

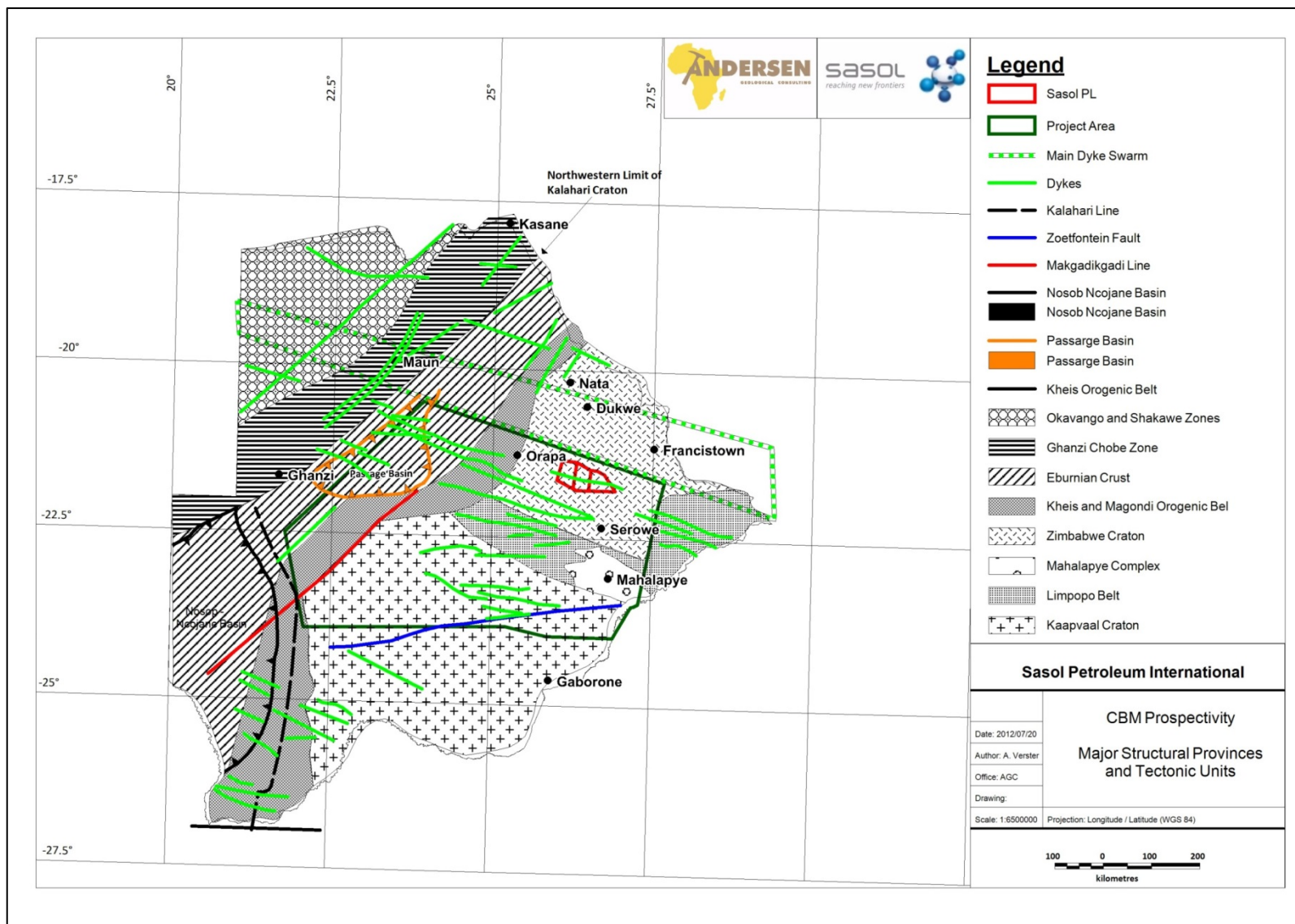


Figure 16 Major structural provinces and tectonic units of Botswana (Potgieter & Andersen, 2012).

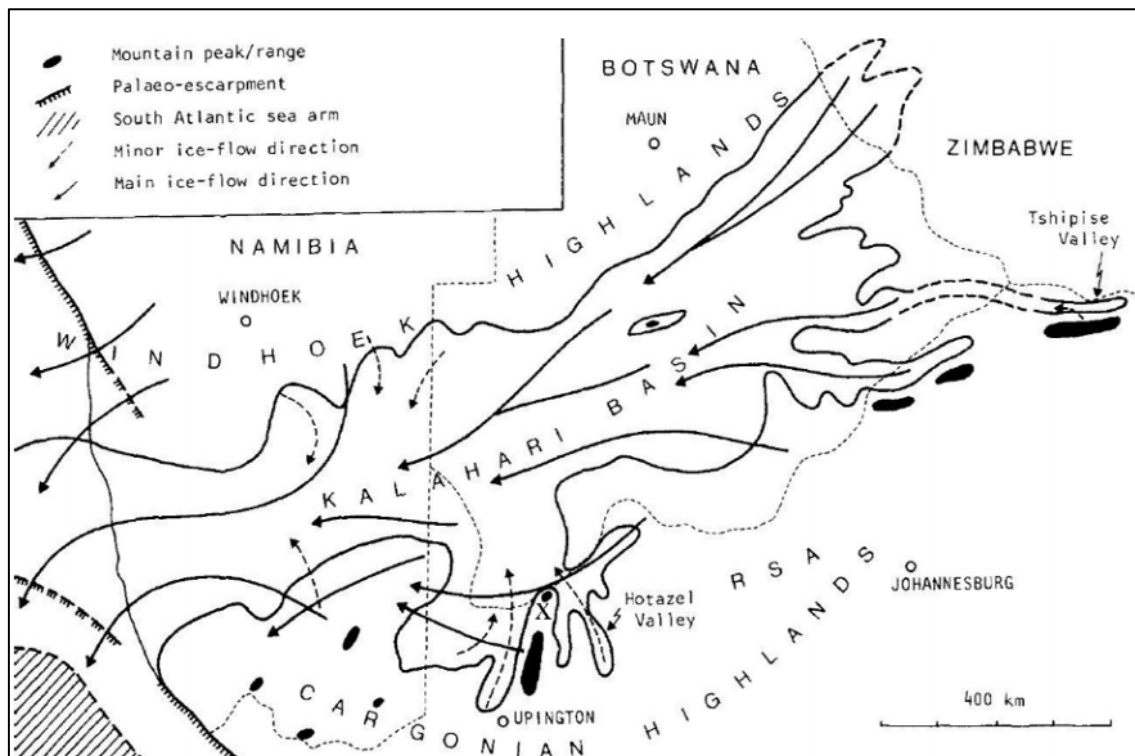


Figure 17 Ice flow directions in the Kalahari Karoo Basin (Jansson, 2010).

During the Permian period organic-rich postglacial sedimentary rocks were deposited in lacustrine, deltaic and fluvial environments (Johnson, et al., 1996). The rocks of the Permian is suggestive of tundra-type peat bog deposition caused by a northward shift of Africa from polar to sub-polar regions (Segwabe, 2008). Prograding deltas caused the formation of extensive plains capable of supporting stable vegetation growth (Segwabe, 2008). The Permian deposits in the Kalahari-Karoo basin comprise fluvio-deltaic sands, muds and peat (Smith, 1984; Segwabe, 2008)

The Beaufort Group strata, deposited from the late Permian to middle Triassic, consist dominantly of mudstones and siltstones with lenticular and tabular sandstones deposited by a variety of fluvial systems (Potgieter & Andersen, 2012). There was a gradual change in the mechanism responsible for the sedimentary deposits from flexural subsidence to extensional tectonics which took place during the Beaufort (Potgieter & Andersen, 2012).

A significant tectonic event ended the Beaufort sedimentation, as depicted by the base-Molteno angular unconformity which is developed in many basins where it can be seen overstepping the older Karoo units onto basement rocks (Potgieter & Andersen, 2012). The rocks of the Molteno Formation were deposited by large braided rivers. A climate change resulted in the formation of the Red Beds of the Elliot Formation in South Africa. Continued global warming led to increasing aridification with the deposition of regional aeolian sandstones widely referred to as cave sandstones (Catuneanu, et al., 2005; Potgieter & Andersen, 2012 and Palloks, 1984).

Sedimentation in the Karoo Basin was terminated abruptly approximately 180 Ma ago when the crust ruptured and large volumes of basaltic lava flowed out covering virtually the whole of southern Africa. These eruptions heralded the breakup of Gondwanaland and occurred mainly from long crack-like fissures through which the magma welled. Lava flows were typically between 10m and 20m thick, and flow after flow erupted building up a pile of lava over 1 600m in South Africa, but usually not more than 400m in Botswana and Zimbabwe (Potgieter & Andersen, 2012; Jones, et al., 2001 and Jourdan, et al., 2004). The magma that did not reach the surface was injected under pressure into the sedimentary layers of the Karoo rocks crystallizing to form dolerite sills. These vary in thickness from a few centimetres to more than 100m (Jourdan, et al., 2004 and Rainbow Gas and Coal Exploration (Pty) Ltd, 2011). Magma also solidified in the fissures producing dolerite dykes. This Karoo Volcanic event was very short lived, lasting only about 2 million years. The Okavango Dyke Swarm, formed a prominent feeder to the magmatic event in Botswana (Jourdan, et al., 2005 and Potgieter & Andersen, 2012).

### *3.1.1. The Karoo in Botswana and Zimbabwe*

The Karoo Supergroup in north-east Botswana overlies the Ghanzi-Chobe foldbelt to the north and west of the basin. This foldbelt is believed to be a palaeotopographic high onto which the Karoo sediments onlapped during sedimentation (Smith, 1984). This onlapping nature of the Karoo Supergroup was noted in a number of the boreholes reported by Anglo Coal Botswana (2010). As shown on Figure 18 north-eastern Botswana is underlain by Archaean Basement that is represented as a ridge,

south of Dukwi. This ridge has been postulated by Smith (1984), Green (1966) and Stansfield, (1973) to have affected the Karoo sedimentation and is generally regarded as the southern limit of the North East Botswana Karoo Basin.

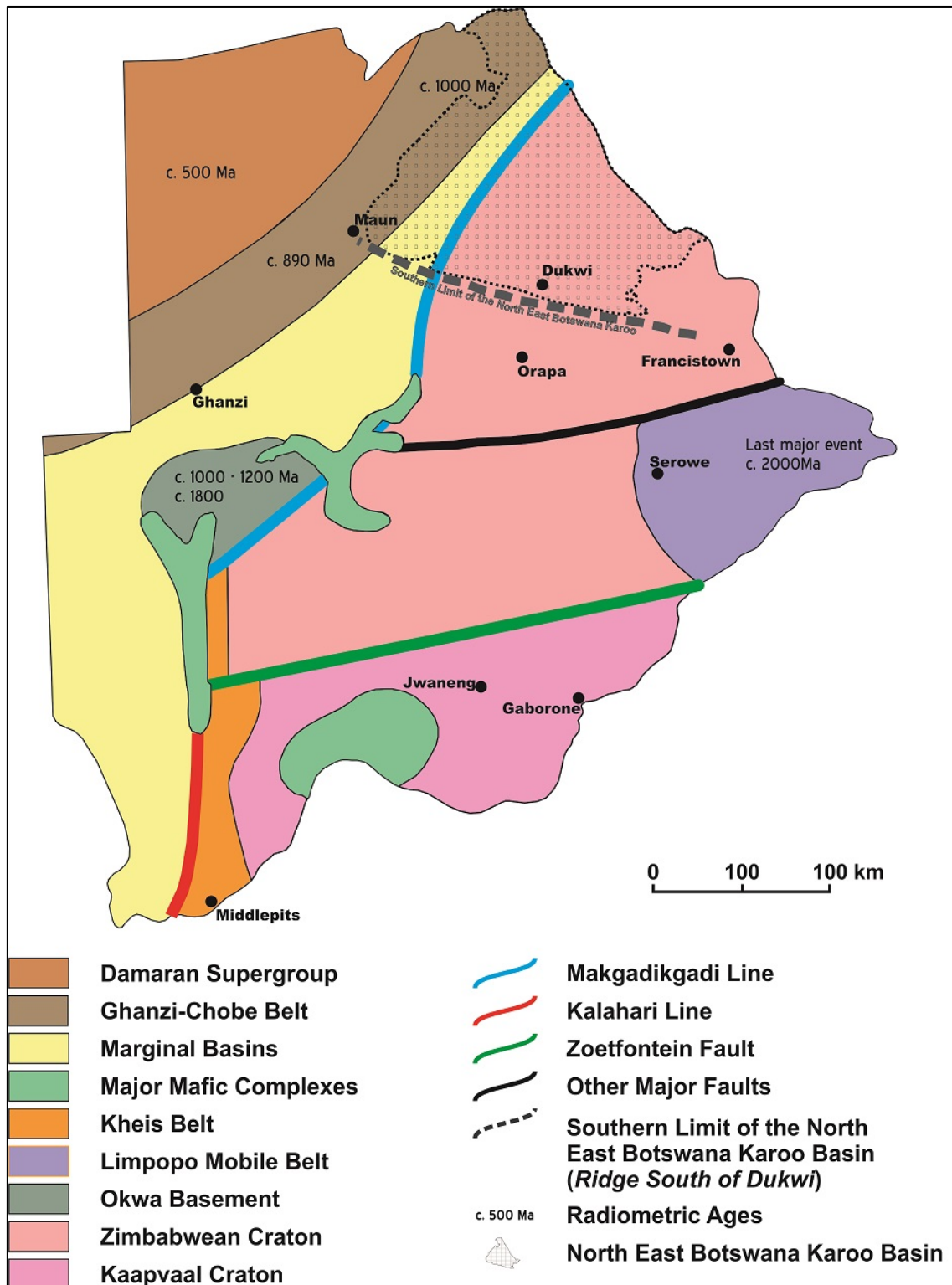
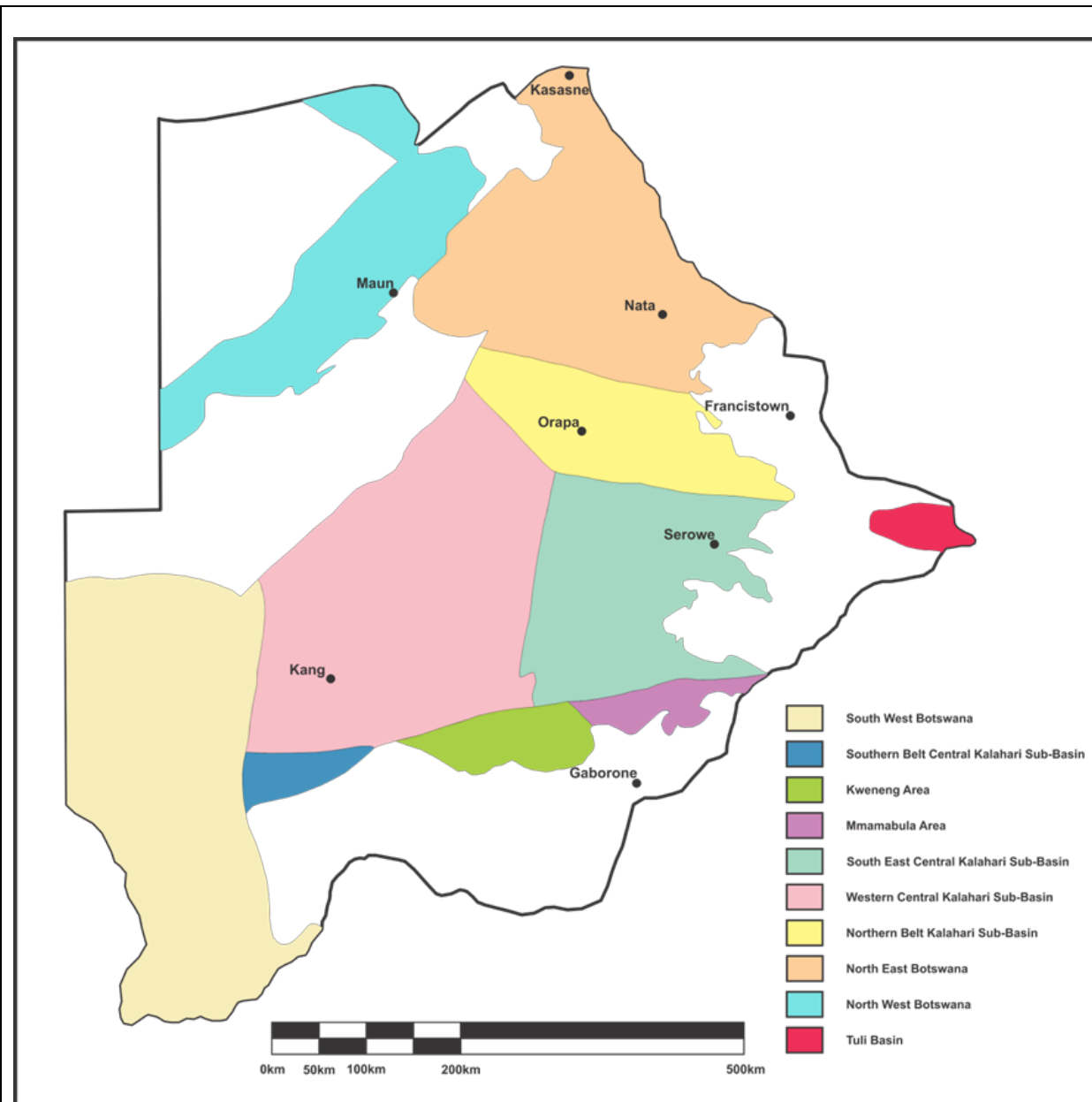


Figure 18 Simplified Pre-Karoo basement of Botswana (after Geological Survey Department, 1984).



a) Spatial distribution of the Karoo basins in Botswana.

GROUPS	1 SOUTH WEST BOTSWANA	2 KWENENG AND WESTERN CENTRAL KALAHARI	3 MMAMABULA	4 MORUPULE AND SOUTH EASTERN CENTRAL KALAHARI	5 NORTH EAST BOTSWANA AND NORTHERN BELT	6 NORTH WEST BOTSWANA	7 TULI BASIN (BOTSWANA)	
STORMBERG LAVA (~U. Stormberg Series)	STORMBERG LAVA GROUP (undivided)						BOBONONG LAVA FM.	
LEBUNG (~L. Stormberg Series)	NAKALATLOU FM.	NTANE SANDSTONE FM.				BODIBENG SILTSTONE FM.	TSHEUNG SILTSTONE FM.	
	DONDONG FM.	MOSOLOTSANE FM.			(N.E ONLY) NGWASHA FM. PANDAMATENGA FM.	SAVUTI FM.	THUNE FM. KOREBO FM.	
(~Beaufort Series)	KULE FM.	KWETLA FM.	TLHABALA FM.			?	SESWE FM	
ECCA (~Ecca Series)	OTSHE FM.	BORITSE FM.	KOROTLO FM.	SEROWE FM.	TLAPANA FM.	MARAKWENA FM.		
			MMAMABULA FM.	MORUPULE FM.		TALE FM.		
	KOBE FM.	BORI FM.	KWENENG FM.	MOSOMANE FM.	KAMOTAKA FM.	MEA ARKOSE FM.		?
			BORI FM.	MAKORO FM.	TSWANE FM.	?		
Dwyka (~Dwyka Series)	MIDDLEPITS FM.	DUKWI FORMATION				?	?	
	KHUIS FM.							
	MALOGONG FM.							

b) Formations of the Karoo Supergroup – This study will focus on the Northern Belt of the Central Kalahari and North East Botswana basins.

Figure 19 Distribution of the Karoo basins and formations in Botswana (after Smith, 1984).

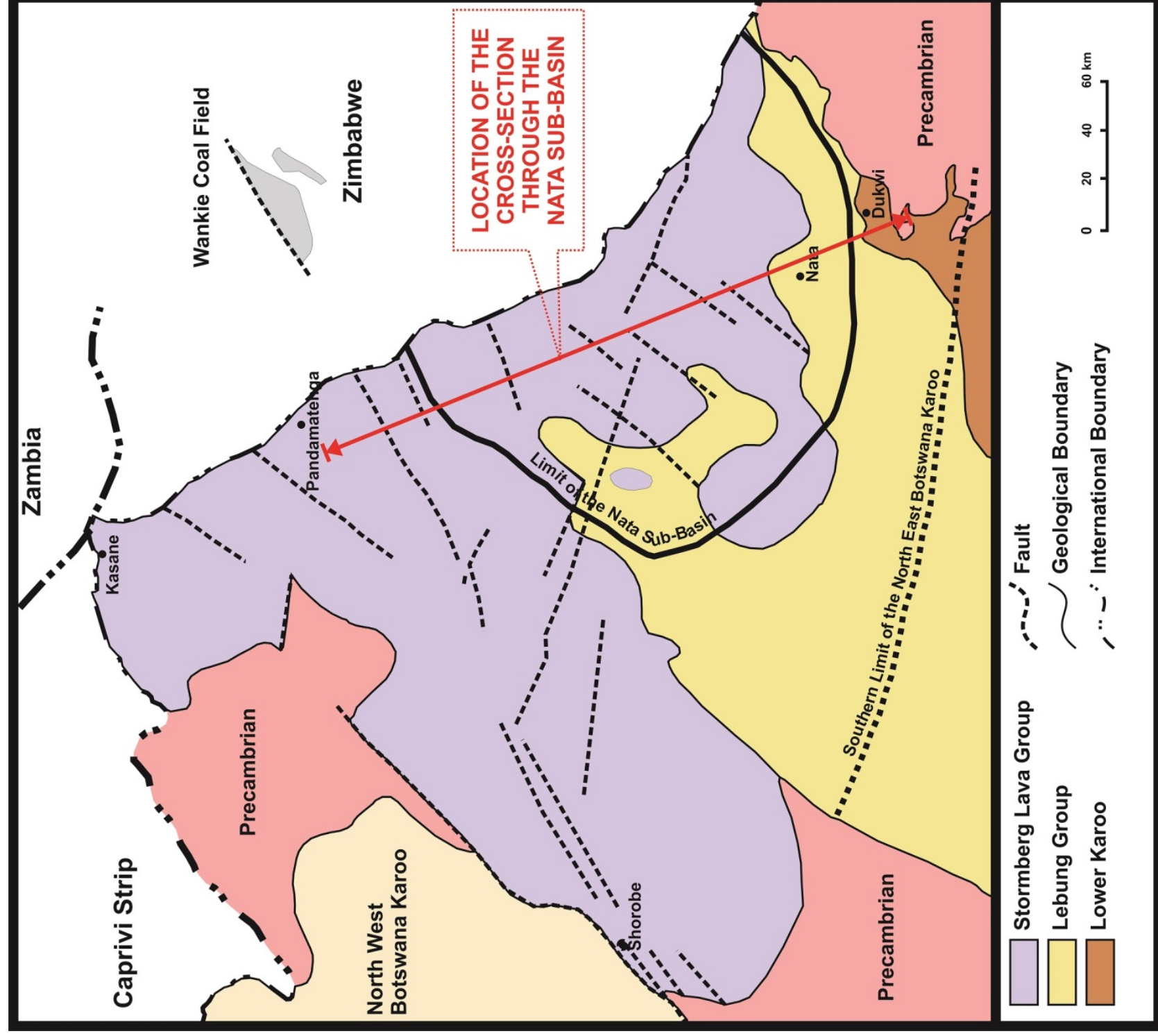


Figure 20 Distribution of the Karoo Supergroup in North East Botswana (after Smith, 1984).

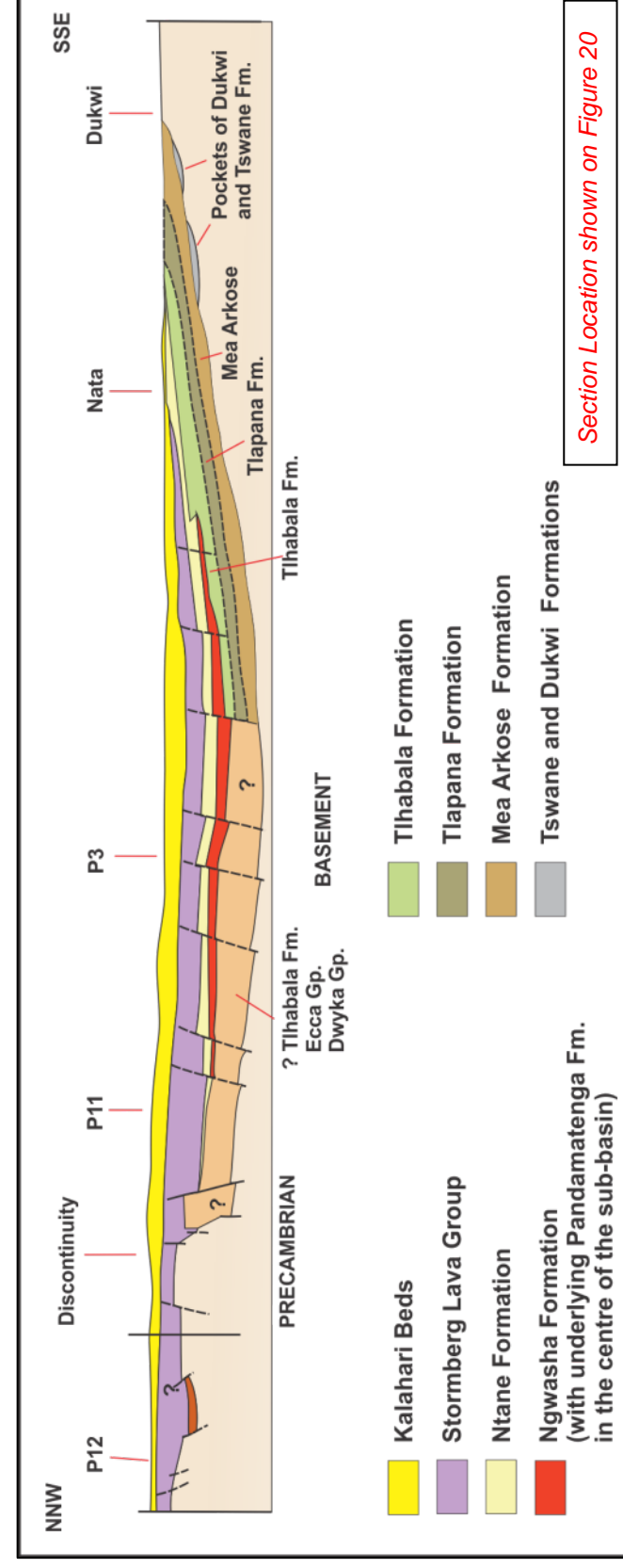


Figure 21 Cross section of the postulated Nata Sub-Basin (after Smith, 1984).

The Karoo Supergroup was deposited in a number of basins in Zimbabwe (Table 2) of which the Mid-Zambezi is economically the most prospective basin as it hosts the world famous Wankie and Entuba coal deposits (Thompson, 1981; Palloks, 1984 and Sable Mining Africa Ltd, 2011). The search for coal in North West Zimbabwe dates back to 1894 with the discovery of the Wankie coal deposits which has delivered an abundance of geological exploration data (Palloks, 1984).

**Table 2 Lithostratigraphic subdivisions of the Karoo Supergroup in the Mid-Zambezi Basin (Oesterlen & Lepper, 2005).**

Period	Group	Gair (1959)	Bond (1967)	Sutton (1979)	Hosking (1981)	Oesterlen (1999)		
Cretaceous	Late	Post	Gokwe	White sandstone M.	Gokwe	Gokwe		
	Middle	Karoo		Gokwe				
	Early			Calcareous M.				
Jurassic	Late	Upper Karoo	Batoka basalt	Batoka basalt	Batoka basalt	Batoka basalt		
	Middle							
Triassic	Early	Karoo	Batoka basalt	Batoka basalt	Batoka basalt	Batoka basalt		
	Late		Red sandstone	Forest sandstone			Forest sandstone	
			Sandstone and Interbedded mudstone	Pebbly arkose			Pebbly arkose	Tashinga
Permian	Middle	Lower Karoo	Escarpment grit	Escarpment grit	Escarpment	Escarpment		
							Early	
	Late	Madumabisa mudstone	Upper Madumabisa mudstone		Madumabisa	Madumabisa (k 5)		
Carbonifer.	Late	Gwembe coal	Black shale and coal	Lower Madumabisa mudstone	Wankie	Upper Wankie sandstone (k 4)		
				Upper Wankie sandstone			Lower Wankie sandstone	Wankie Black shale and coal (k 2-3)
				Black shale and coal			Lower Wankie sandstone	Lower Wankie sandstone (k 1)
		Red mudstone and Basal sandstone	Lower Wankie sandstone	Lower Wankie sandstone	Dwyka	Dwyka (k 0)		
		Basal beds	Tillites and varved shales	Tillites and varved shales				
Region		Gwembe area/ Zambia	MZB, Zimbabwe	Gokwe area, Zimbabwe	MZB, Zimbabwe	MZB, Zimbabwe		

The Wankie Black Shale and Coal unit of the Ecca Group has been studied in great detail as a result of the economic potential of the coal seams in the region as well as the postulated hydrocarbon potential as investigated by Hiller & Shoko (1996) and CBM exploration companies such as Afpenn, Lupane Gas and Shangani Energy. Thompson (1981) described the Wankie Black Shale and Coal, hosting the most economic coal seams, as the formation directly underlying the Madumabisa mudstones and overlying the Lower Wankie sandstone. In their re-evaluation of the

Wankie Black Shale and Coal, Oesterlen & Lepper (2005) confirmed the findings of Duguid (1986) that the drilling records of the Wankie coalfield and other areas in the basin showed great lithological variability within the unit. As a result of this variability Oesterlen & Lepper (2005) defined the basin in a number of subdivisions as shown in Figure 22.

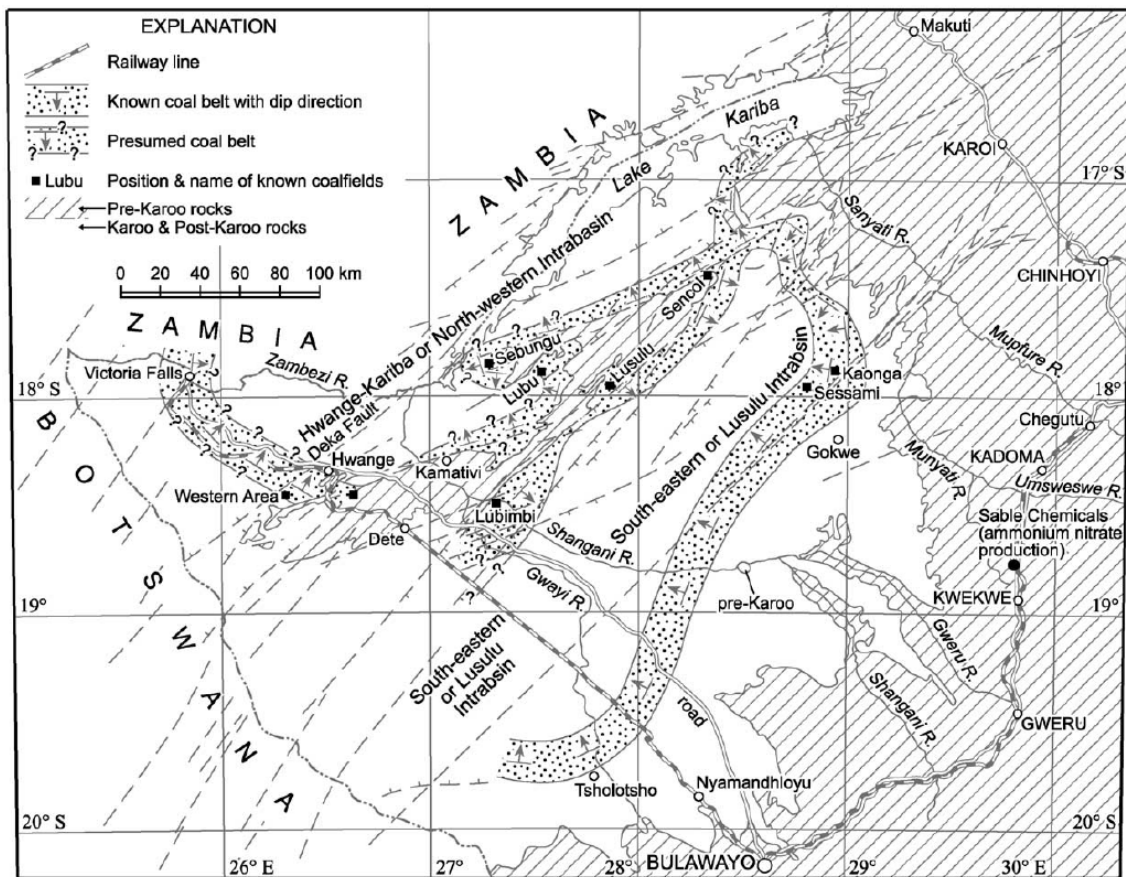


Figure 22 The descriptive subdivisions of the Mid-Zambezi Basin as used by Oesterlen & Lepper (2005).

### 3.2. Karoo Supergroup in the Study Area

All boreholes drilled by Anglo Coal Botswana (2010) were terminated in the basement. An onlap of the upper Karoo onto the Precambrian Basement was noted towards the north-east with the lower Karoo being absent in all but 4 of the wells (Anglo Coal Botswana, 2010) (Figure 23). Catuneanu, et al. (2005) showed a correlation between the Mid-Zambezi and North East Botswana Karoo Basins (Figure 24). In this correlation it was indicated that the formations of the Karoo are correlatable with some minor adjustments to formations noted in Botswana. These adjustment can be attributed to both thinning of the deposits and/or lack of regional drilling data in Botswana.

The study is focused on the Eccca Group coal measures and this stratigraphic unit was isolated as an individual unit and correlated across the study area. For ease of reference the formations described were correlated with the Ellisras (Lephalale) basin in South Africa. This correlation is shown in Table 3 along with the informal nomenclature that was used for the identification of the units of interest during this evaluation.

- The “Pre-Eccca Formations” comprise the Dwyka Group equivalents;
- The “Eccca Formations” hosting the coal measures encompasses all coal bearing formations hosted in the Eccca Group equivalents. Further subdivided into the Upper and Lower units and;
- The “Post-Eccca Formations” comprises all formations from the top of the Eccca to the Jurassic volcanic formations.

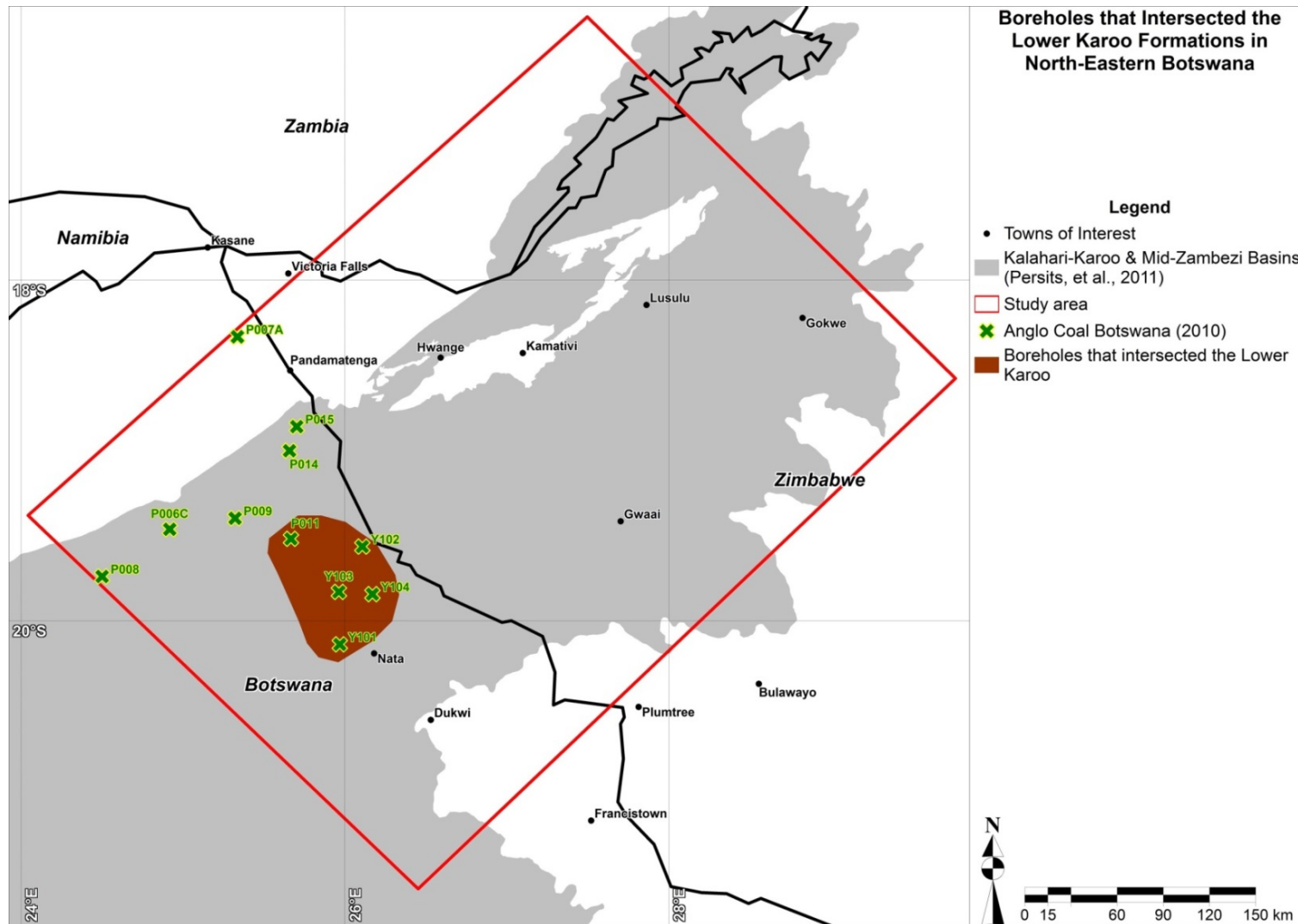


**Figure 23** Boreholes that intersected the lower Karoo formations in north-eastern Botswana, superimposed onto the outline of the Kalahari-Karoo and Mid-Zambezi Basins after (Anglo Coal Botswana, 2010; Pitfield, 1996; Mothibi, 1999 and Persits, et al., 2011).

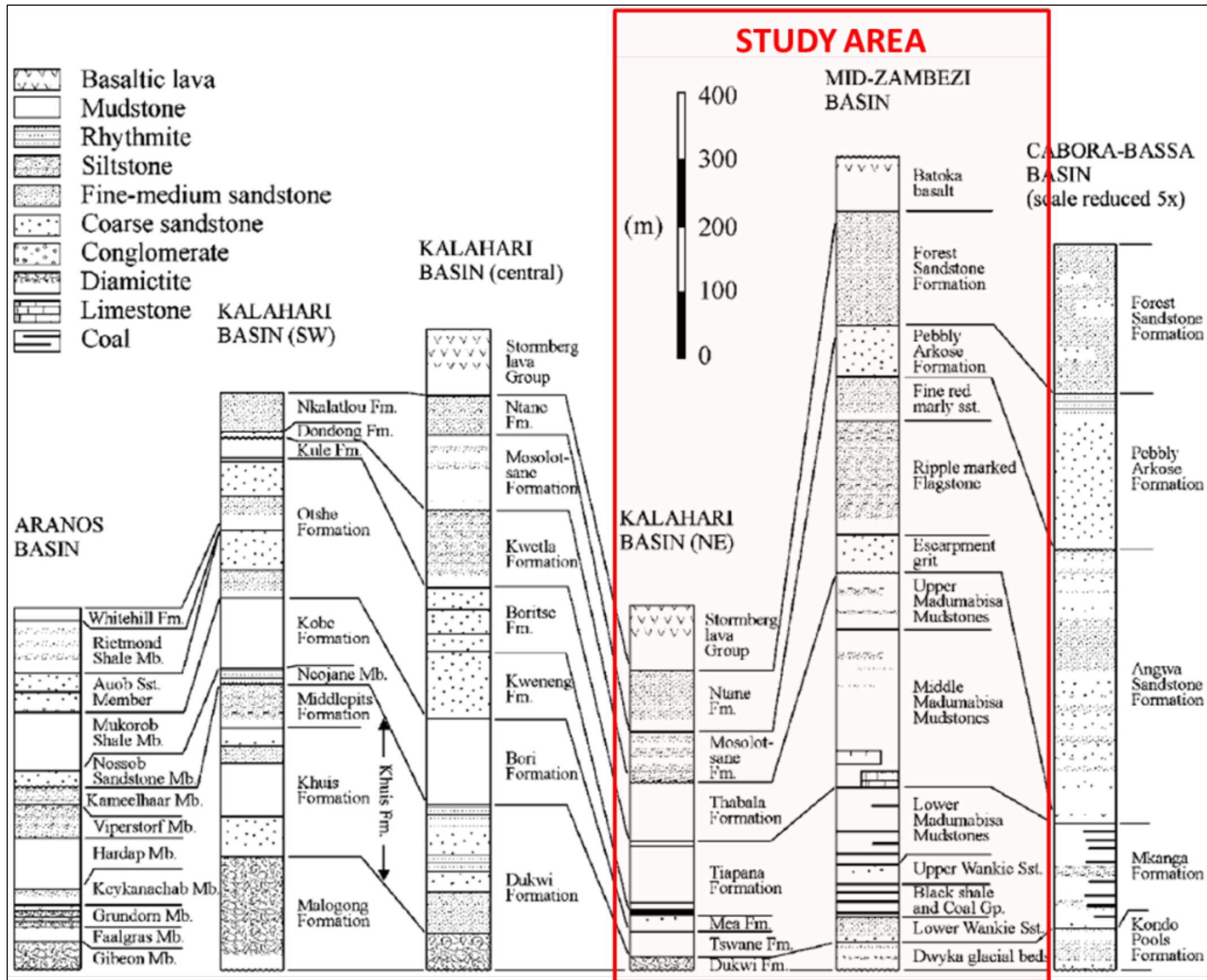


Figure 24 Southwest–northeast trending cross-section of correlation of the Karoo lithostratigraphic units through the Aranos, Kalahari, Mid-Zambesi and Cabora Bassa basins with the study area stratigraphic correlation highlighted (Catuneanu, et al., 2005).

**Table 3 Correlation of the Karoo Supergroup formations in the Ellisras (Lephalale), North East Botswana and Northern Belt and Mid-Zambezi basins.**

PERIOD	EPOCH	GROUP	ELLISRAS BASIN	NORTH EAST BOTSWANA AND NORTHERN BELT OF THE CENTRAL KALAHARI BASINS	MID-ZAMBEZI BASIN	THIS STUDY*		
			FORMATION					
JURASSIC	Early	STORMBERG GROUP	Letaba Formation	Stormberg lava Group	Batoka basalt	UPPER KAROO	POST-ECCA FORMATIONS	
			Clarens Formation	Ntane Formation	Forest Sandstone Formation			
TRIASSIC	Late		Lisbon Formation	Mosolotsane Formation	Pebbly Arkose Formation			
			Middle		Greenwich Formation			Fine red marly sandstone
	Ripple marked Flagstone							
PERMIAN	Early		BEAUFORT GROUP	Eendragtpan Formation	Tlhabala Formation			Upper Madumabisa Mudstones
		Late				Grootegeluk Formation	Tlapana Formation	Lower Madumabisa Mudstones
	Early		SWARTRAND FORMATION	Mea Arkose Formation	Upper Wankie Sandstone			
		ECCA GROUP			Tswane Formation	Lower Wankie Sandstone	Black shale and Coal Group	
	Late		Dwyka Group	Wellington Formation			Dukwi Formation	Dwyka glacial Beds
		Early			Waterkloof Formation	Dukwi Formation		
PRE-ECCA FORMATIONS								
Sources	Bordy, et al., (2010) <sup>a</sup> ; Catuneanu, et al., (2005); Smith, (1984); Anglo Coal Botswana, (2010); Bordy, et al., (2010) <sup>b</sup> ; Palloks, (1984); Thompson, (1981) and Oesterlen & Lepper, (2005)							
*	The nomenclature will be used for this study for the combination of units into chronostratigraphic equivalents across the study area							

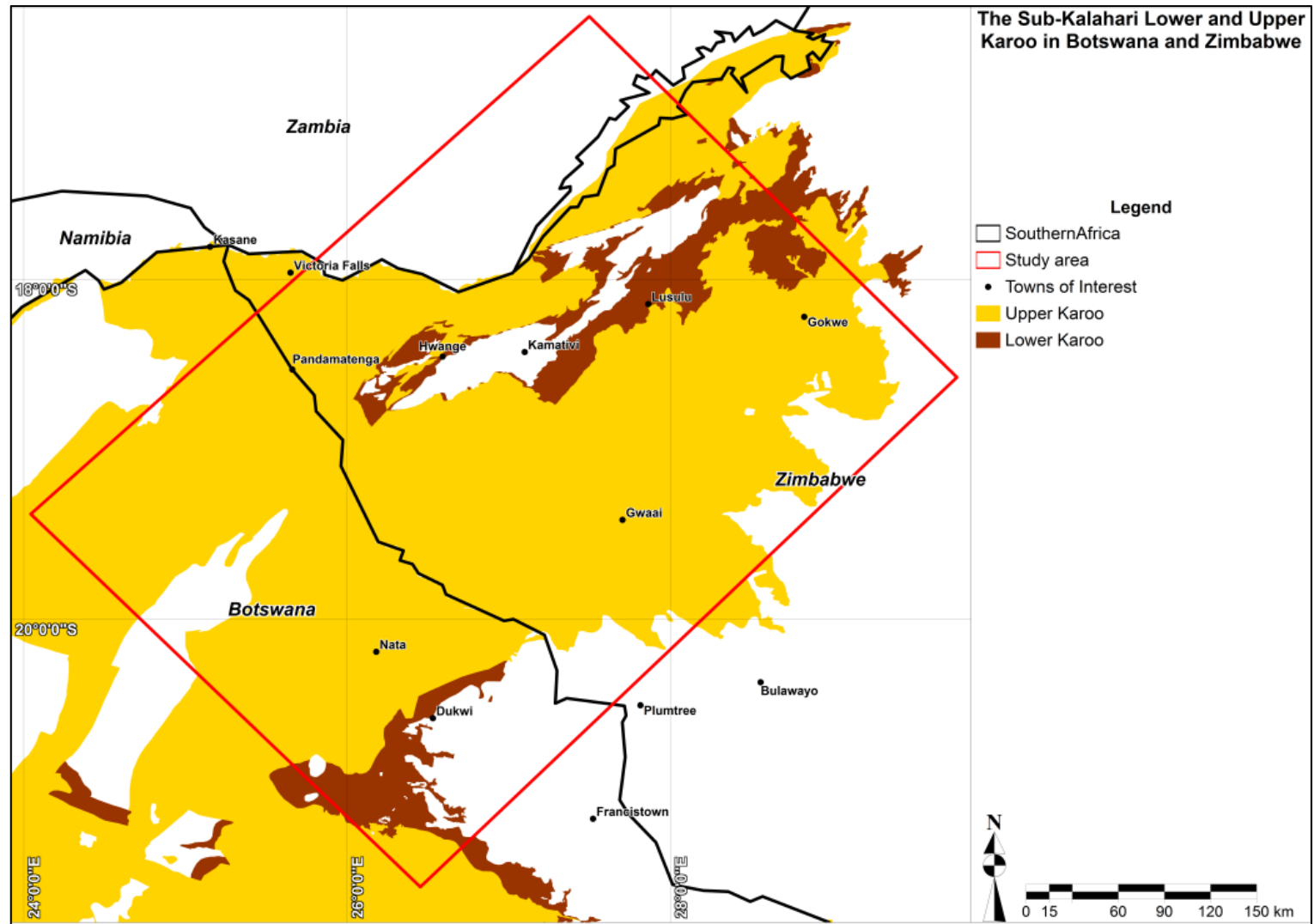


Figure 25 Distribution of the Upper and Lower Karoo across the study area (after Mothibi, 1999; Pitfield, 1996 and Persits, et al., 2011).

### 3.2.1. *The Pre-Ecca Formations*

All glaciogenic sediments of the Dwyka Group in Botswana were grouped into a single formation known as the Dukwi Formation by Stansfield (1973). Smith (1984) noted the presence of this formation in two boreholes drilled near the town of Dukwi, ACB intersected the glacial sediments of the Dukwi Formation in 5 boreholes. The base of this formation is regarded as the sediments unconformably overlying the Precambrian Basement and the top is taken as the youngest beds with glacial characteristics (Smith, 1984). Drilling records show that the formation consists of a lower member approximately 16m thick, comprising a tillite with siltstones and sparse pebbly siltstones (Stansfield, 1973). A re-evaluation of the sediment descriptions by Smith (1984) suggested that they are more likely to be proglacial, water lain deposits rather than true glacial debris deposits. The 3 m upper member encountered comprises varved siltstones and mudstones with a thin conglomerate towards the top of the member.

Smith (1984) found that during the early Dwyka Group times an ice sheet moved in a south-westerly direction from central Botswana which coincides with the minimal striation records available along the Molopo River. A basal tillite was deposited beneath this ice sheet and thickens in basement depressions. Smith (1984) proposed that the pockets of tillite or reworked till were deposited on an uneven pre-Karoo surface and was subsequently overlain by glaciolacustrine sediment deposits. Green (1966) showed that variations in the sedimentation rates were related to palaeoclimatic effects of glacial retreat. This theory is supported by the “patchy” nature of the formation specifically in the eastern regions suggesting that the primary under-sheet process was that of erosion. It was postulated that the Precambrian basement formed a topographical high and that the current Dwyka Group distribution is close to the original depositional extent (Smith, 1984).

Glacial tillite deposits of the Dwyka Group have been noted in many parts of the Mid-Zambezi basin, predominantly from exploration drilling records. Thompson (1981) referred to the glacially deposited formations as the Lubimbi Glacials of the Dwyka Series, whereas Oesterlen & Lepper (2005) classified these formations as the undivided Dwyka Group (Table 2). The thickness distribution of the Dwyka Group is

extremely variable as a result of the uneven nature of pre-Karoo topography and the thickest intersection, 100m, was encountered in the Matabola borehole approximately 60km north-east of Lubimbi (Thompson, 1981).

Thompson (1981) described the rocks of the Dwyka Group as largely consisting of coarse tillite and fine- to medium grained sandy material. The sandy material is indicative of outwash sands from retreating glaciers. From the outcrops noted in the Bari, Lubimbi and Gwaai River areas it was noted that coarse, pebbly deposits occur frequently in major river beds with rounded fragments up to 30cm in diameter. The glacial deposits were found to be fairly heterogeneous and described to be hard, pale grey to greyish yellow colour, unevenly tinged and containing red iron oxides (Thompson, 1981). In the Lubimbi area dull coal and bituminous shales, with intercalated siltstone and shale layers, were frequently intersected, indicating that during the Dwyka times conditions were already favourable for the accumulation of coaly material in localised embayments (Thompson, 1981).

### 3.2.2. *Ecce Formations*

The Ecce Formations in the study area (Table 3) is defined as all sediments that directly overly the Dwyka Group up to the youngest carbonaceous mudstone or coal (Smith, 1984; Catuneanu, et al., 2005 and Palloks, 1984).

#### 3.2.2.1. Lower Ecce Formations

##### 3.2.2.1.1. Botswana

According to Smith (1984) the broad pattern of the lower Ecce in Botswana is analogous with sedimentation in a widespread body of water opening to the sea. The sediments show that the basin was filled with prodeltaic sediments followed by increasingly arenaceous deposits indicating the presence of a fluvial dominated delta system (Smith, 1984).

### 3.2.2.1.1.1. Tswane Formation

Stansfield (1973) described the sediments directly overlying the Dukwi Formation as consisting of red and black shales with grey mudstones and referred to the unit as the Dukwe Mudstone. Although the naming of the unit seems to suggest association with the glacial sediments of the Dukwi Formation, Green (1966) grouped the beds with the Lower Ecca Group. Smith (1984) named the unit Tswane Formation, the currently accepted formation name, after a town by the same name approximately 20km southwest of the discovery borehole. There is no Tswane outcrop in the region and the lithological description by Green, (1966); Stansfield (1973) and Smith (1984) were based on drilling records from boreholes providing the most complete intersection of 7.5m. The base of this formation is characterised by grey mudstones grading into black, carbonaceous mudstones and a shaly coal with minor vitrinite bands. Towards the top of the unit the beds are black carbonaceous shales and red fissile shales. Smith (1984) postulated that the deposition initially occurred in open, aerobic conditions gradually becoming more euxinic and that the red colouration of the upper shales relates to the overlying unconformity with the Mea Arkose Formation as postulated by Stansfield (1973). During the ACB exploration programme the Tswane Formation was intersected in three boreholes (Y1-02, Y1-03 and PDM011, Figure 23) with the formation reaching a maximum thickness of 24.55m in Y1-03. The intersections noted in the three ACB boreholes showed a sequence of grey to black, carbonaceous mudstones and minor coal bands with some bright stringers in the middle of the unit (Anglo Coal Botswana, 2010). The argillaceous sediments of the Tswane formation were probably deposited conformably over the glaciolacustrine Dukwi Formation in broad lake systems which developed as a result of the final glacial retreat. This accumulation of the carbonaceous sediments soon after the glacial event suggests a cool to temperate environment (Smith, 1984).

### 3.2.2.1.1.2. Mea Arkose Formation

The term Mea Arkose was first described by Stansfield (1973) from widely spaced “patchy” outcrops in the Shuane and Lepashe Rivers and at Mea Pan. Drilling records showed an even greater lateral extent of the formation. Green (1966) defined the formation as part of the Middle Ecca and describe samples as unique from any other formation in the area. Smith (1984) extrapolated the formation name Mea Arkose to the North East Botswana Basin and described it as the arenaceous unit directly overlying the Tswane Formation in turn overlain by the first carbonaceous unit.

The base of the formation is described a coarse grained feldspathic sandstone directly overlying either the Tswane Formation or Pre-Karoo rocks. The top of the formation has been described as a cream-white fine to coarse-grained feldspathic sandstone. Grey-green shale partings have been noted towards the base (Smith, 1984). Historic drilling records show that the unit may also contain a number of thin shale beds with the thickest Mea Arkose intersection being 109.73m (Stansfield, 1973).

ACB reported Mea Arkose intersections in six boreholes (Y1-01, Y1-02, Y1-03, Y1-04, PDM009 and PDM011) with the thickest intersection of 52.44m being in Y1-03 (Anglo Coal Botswana, 2010). Stansfield (1973) postulated a fluvial sediment transport direction from east to west based on local provenance and crossbedding. In the thicker sequences to the north a deltaic sandstone sequence with mudstone and coaly horizons may have developed.

The Mea Arkose was recognised as an aquifer by Chilume (2002) in North East Botswana and from personal experience, posed difficulties with massive water intersections and losses during the ACB exploration drilling programme. It was not possible to analyse water samples but the water qualities varied greatly from highly saline to potable (Potgieter, 2015).

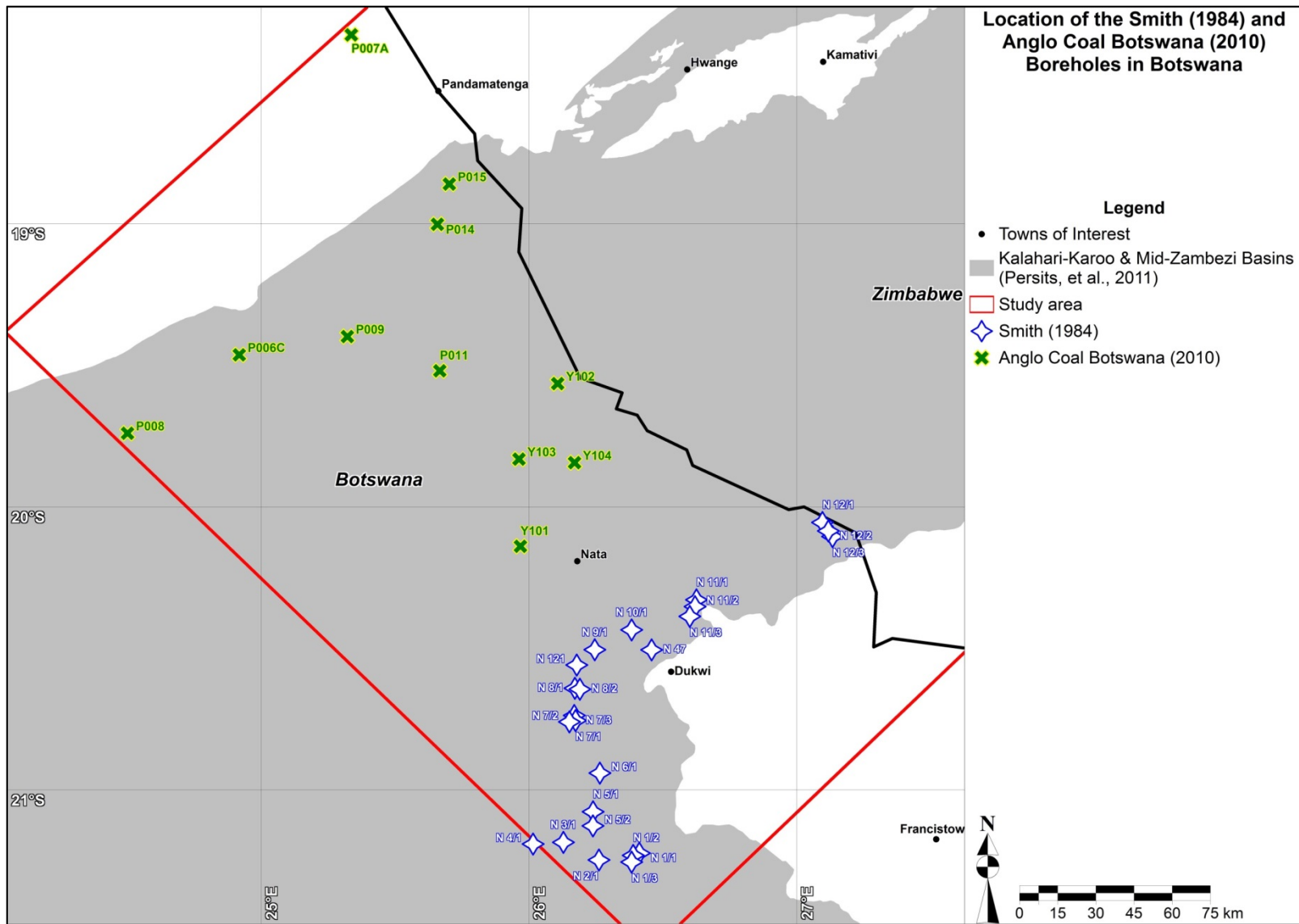


Figure 26 Location of the Smith (1984) and Anglo Coal Botswana (2010) boreholes in Botswana.

#### 3.2.2.1.2. Zimbabwe

In Zimbabwe, the basal succession, i.e. the Lower Wankie Sandstone, is invariably arenaceous with occasional fluvioglacial sediments and is the formation upon which the Wankie Main Seam rests (Figure 27). Thompson (1981) described the Lower Wankie Sandstone as a widely distributed fluvial deposit consisting of subangular to subrounded, coarse-grained, cross-bedded feldspathic sandstones, grits and pebble layers which outcrop along the edge of Kamitivi Inlier and gently dips eastwards with a maximum thickness of 45m.

The rocks of the Lower Wankie Sandstones are commonly light coloured with some iron oxide staining giving rise to brown or reddish patches and the feldspar content is high enough in certain areas to term the lithological unit an arkose (Thompson, 1981). The deposition of this formation was most likely soon after the end of glaciation and poor sorting of the sediments in the region was noted by Thompson (1981) and Palloks (1984) suggests short transport distances of the material in a medium to high energy environment.

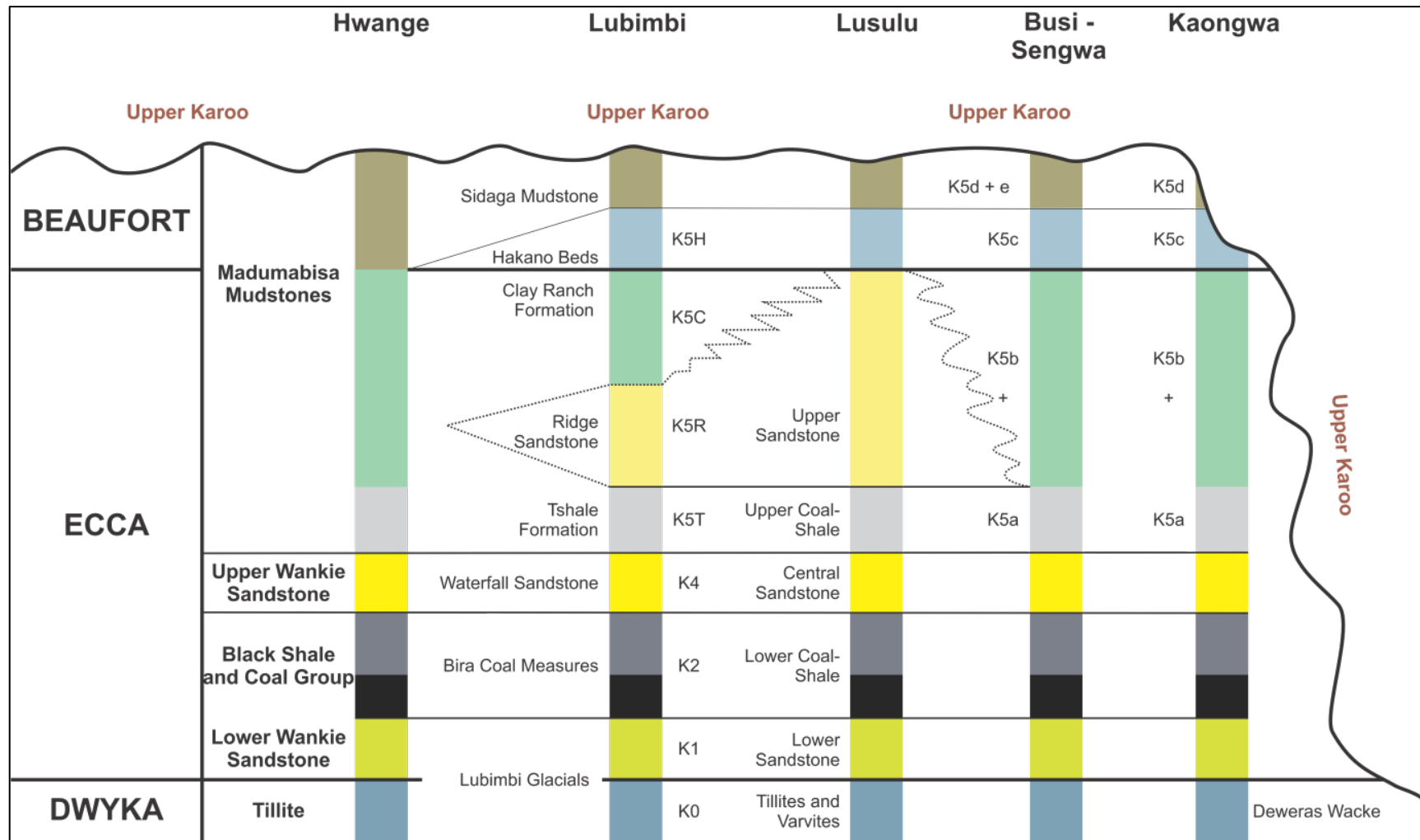


Figure 27 Stratigraphy of the lower Karoo Supergroup in the Mid-Zambezi Basin in Zimbabwe (after Thompson, 1981; Moyo, 2012 and Oesterlen & Lepper, 2005).

### 3.2.2.2. Upper Eccca Formations

The Upper Eccca is defined as the unit that directly overlies the sediments containing the greatest amount of carbonaceous sediments and coal (Smith, 1984). This unit is believed to have been deposited in swampy, shallow water deltas over a widespread area in Botswana being the most favoured environment for the development of peat swamps and bogs (Smith, 1984).

#### 3.2.2.2.1. Botswana

##### 3.2.2.2.1.1. Northeastern Botswana

The Tlapana Formation is arguably the most important Karoo Formation in north-eastern Botswana from an economic perspective because of potentially large scale coal deposits. Extensive coal exploration programmes were undertaken by Shell Coal and Anglo Botswana with drilling focussed around the Dukwe area and minor regional reconnaissance drilling and geophysical surveys between Nata and Pandamatenga. In 2007 ACB acquired 2 prospecting licences from Sekaname for CBM exploration and drilled 4 exploration boreholes with 7 additional holes being drilled on 19 further licences acquired in 2009. This data greatly aided in the further understanding of the Lower Karoo as outcrops of the sediments are very rare. The Tlapana Formation, mainly identified in the N series boreholes, was described as the mudstones, siltstones, carbonaceous mudstones and coals that overly the Mea Arkose Formation and which are overlain by the non-carbonaceous mudstones and siltstones of the Beaufort Group (Stansfield, 1973). Smith (1984) extrapolated the name Tlapana Formation to the North East Botswana Basin from the northern belt of the Central Kalahari basin. This formation was intersected in a number of the historic and ACB boreholes that contained coal seams thicker than 0.3 m with the maximum thickness intersected in N10/1 being 77.71m (Smith, 1984). The thickest intersection in the recent ACB boreholes was 66m in borehole Y1-01 (Anglo Coal Botswana, 2010).

Smith (1984) used the drilling records from borehole N10/1 to describe the Tlapana Formation (Figure 26). The lower section of the formation is characterized as a 24m

thick succession hosting at least 26 bands of mixed bright and dull coal with carbonaceous and thin brown-grey mudstone interbeds. Of the 26 coal bands only 6 are thicker than 30cm. Siderite and pyrite nodules are common. A 1.2m thick hard, brown sideritic siltstone separates the middle and lower sections. The middle section is characterized as a succession of thin coal and coaly shales with siderite, intercalated with carbonaceous mudstones. The upper section consists of pale grey and dark grey shales with plant imprints capped by a 67cm coal seam and a further 38cm of carbonaceous mudstone. This upper unit is also regarded as the top of the Eccra Group (Smith 1984).

Smith (1984) proposed that the coals of the Tlapana Formation were probably deposited in a gently subsiding swamp into which herbaceous material and debris drifted with interspersed mud flows during periods of fluctuating energy and flow rates. A distinct facies change was noted from borehole N10/1 toward the Precambrian basement high to the extent that in borehole N8/2 (Figure 26) the formation is thinner but a 6.42m coal zone, mainly consisting of dull coal with thin pyritic bands and carbonaceous mudstone partings, developed at the base of the formation (Smith, 1984). Above the coal in N8/2 the presence of intercalated sandstone sequence suggesting deposition in an impersistent channel that cannot be correlated in any other borehole supports this postulated facies change (Smith, 1984). This sandstone sequence was not reported in the ACB drilling records either. In a detailed sedimentological study for Anglo Coal Botswana, Bordy (2009) described the unit as intersected in four boreholes (Y1-01, Y1-02, Y1-03 and Y1-04) as being mudstone dominated with rare upward fining cycles suggesting deposition in a fluctuating energy environment (Figure 26). This was consistent with the findings by Smith (1984). During this study Bordy (2009) also re-evaluated the palaeo-flow directions throughout Botswana but was not able to improve on the findings by Smith (1984) in northeast Botswana (Figure 28).

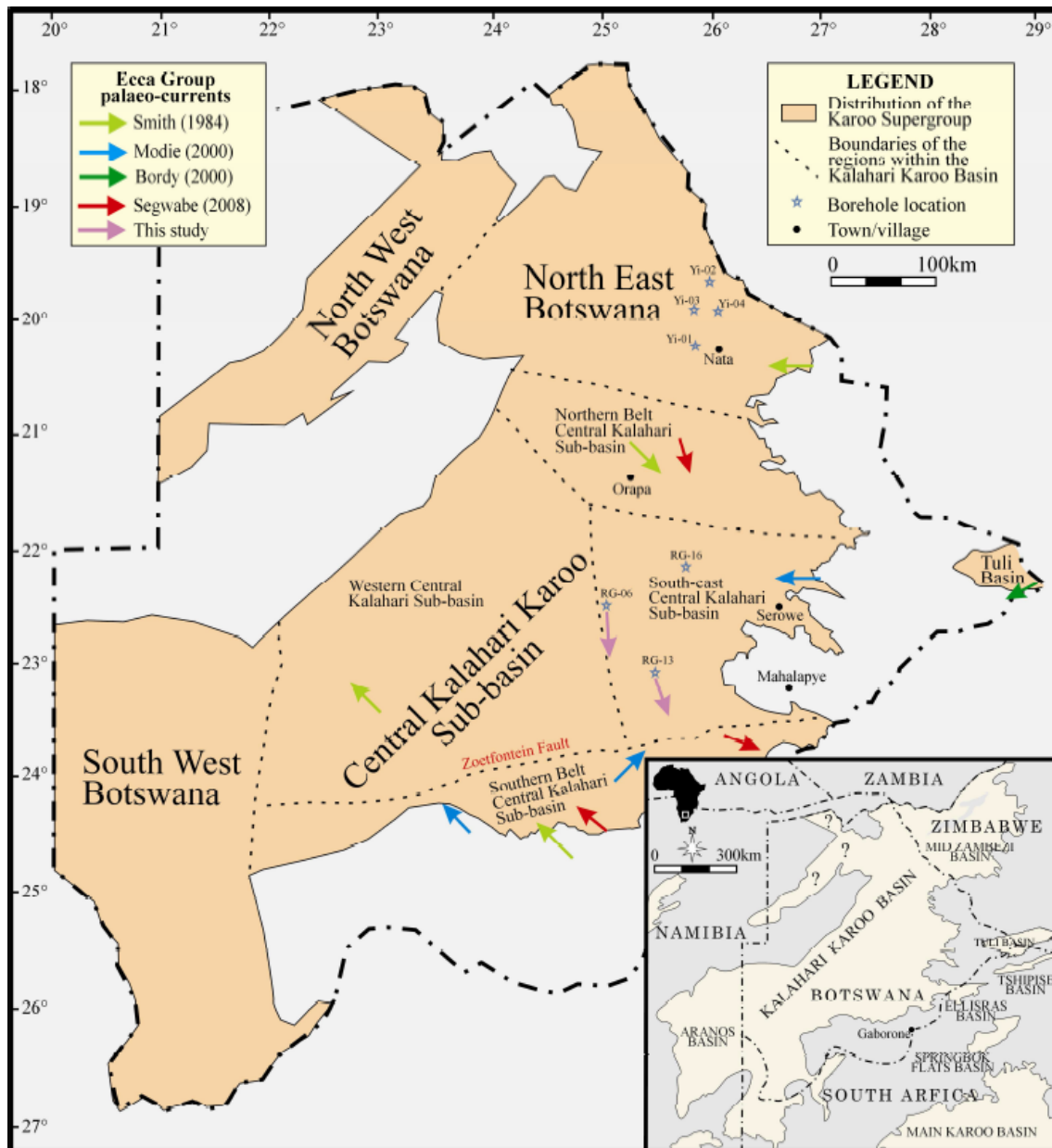


**Figure 28** Distribution map of the Late Carboniferous-Early Jurassic Karoo Supergroup in the Kalarhari Karoo Basin of Botswana showing the regional divisions of the basin, the borehole localities and palaeo-current directions in the coal-bearing Ecca Group (Bordy, 2009).

### 3.2.2.2. Zimbabwe

#### 3.2.2.2.1. Wankie, Entuba and Western Areas Coalfields

In the Wankie, Entuba and Western Areas coalfields the Wankie Black Shale and Coal formation grades from a thick basal coal seam, with coking coal, and mudstone succession to a carbonaceous mudstone unit with coal being replaced by pelitic or

clastic sediment around Entuba (Oesterlen & Lepper, 2005). In the Wankie Concession the formation typically consists of the Main Seam at the base, up to 14m thick, which is overlain by a carbonaceous mudstone succession, approximately 20m thick, and in some places intersected in the upper part by a thin coal seam and a 6m thick fireclay horizon. This pelite–coal lithology changes in the Western Areas Concession gradationally replacing the coal with clastic intercalations in the Main margin on one side representing the shore of the ancient Mid-Zambezi lake, and its down-dip lacustrine facies in the other direction (Oesterlen & Lepper, 2005). The Wankie Main Seam grades from a discrete coal seam to carbonaceous shale both laterally and vertically. The Upper Wankie sandstone overlies the main coal seam and these sandstones thin towards the centre of the palaeodepositional valley and into Zambia (Cairncross, 2001; Oesterlen & Lepper, 2005 and, Thompson, 1981).

#### 3.2.2.2.2. Lubimbi Coalfield

The lithology of the Lubimbi coalfields was found to be markedly different from that of the Wankie coalfields. The 40 to 50m thick succession consisting of bright and dull coal, carbonaceous mudstone, mudstone and a grey shale marker horizon, petrographically similar to the fireclay at Wankie and usually containing six coal horizons (Oesterlen & Lepper, 2005). Palkos (1984) described the Black shale and coal Formation at Lubu as reaching a thickness of 50 to 70m, hosting the Main Coal Seam. This formation is overlain by carbonaceous mudstone containing a number of subordinate coal seams with some intercalated sandstone.

#### 3.2.2.2.3. Sengwa Coalfield

The Sengwa area has been divided into 2 further areas, Sengwa North and Sengwa South, by Palkos (1984) based on the geographic distribution north and south of the Sijarira Inlier. Oesterlen & Lepper (2005) also described the lithologies of the Wankie black shale and coal to be almost identical in the two areas. The base of the sequence is the Main Coal Seam overlain by the lower carbonaceous shale, the Upper Coal Seam and finally the upper carbonaceous shale. Both the lower and upper carbonaceous shales can be categorised as carbonaceous mudstones with thin barcoded coal laminae. Some of the differences between the areas are that the

fireclay is developed in the north but not in the south and that in some cases the Upper Coal Seam is poorly developed or even absent in the South (Palloks, 1984).

#### 3.2.2.2.4. Gokwe Coalfield

The coal bearing formation around Gokwe varies greatly from the aforementioned areas and is composed of various lithologies changing rapidly in a lateral direction (Oesterlen & Lepper 2005). Occasionally the Main Seam occurs at the base, with a maximum of 9 m thickness, overlain by siltstone and from other drilling records it appears that the sequence is represented only by carbonaceous mudstone, siltstone or sandstone and in cases it is completely missing. The package is thinner in comparison with an average thickness of only 15m.

#### 3.2.2.2.5. Tjolutjo, Sawmills, and Insuza Areas

Oesterlen & Lepper (2005) provided further information on the coal-bearing succession resulting from the three deep research boreholes drilled at Tjolutjo, Sawmills, and Insuza; all located in the Nyamandlovu district approximately 200km southeast of Wankie. Similar lithologies were encountered in the 3 holes and described by Oesterlen & Lepper (2005) as one or several thin coal seams are interbedded in an alternation of carbonaceous mudstone, with siltstone or sandstone. In general the sequence is upward coarsening with a decrease in organic material towards the contact with the overlying formations indicative of a deltaic deposition (Oesterlen & Lepper, 2005). It was found that the sequences closely resembled those of Gokwe indicating deposition on an alluvial plain as well. Figure 29 shows the depositional dynamics as postulated by Oesterlen & Lepper (2005) showing the locations of the interpreted alluvial plane, deltas and Mid-Zambezi Lake.

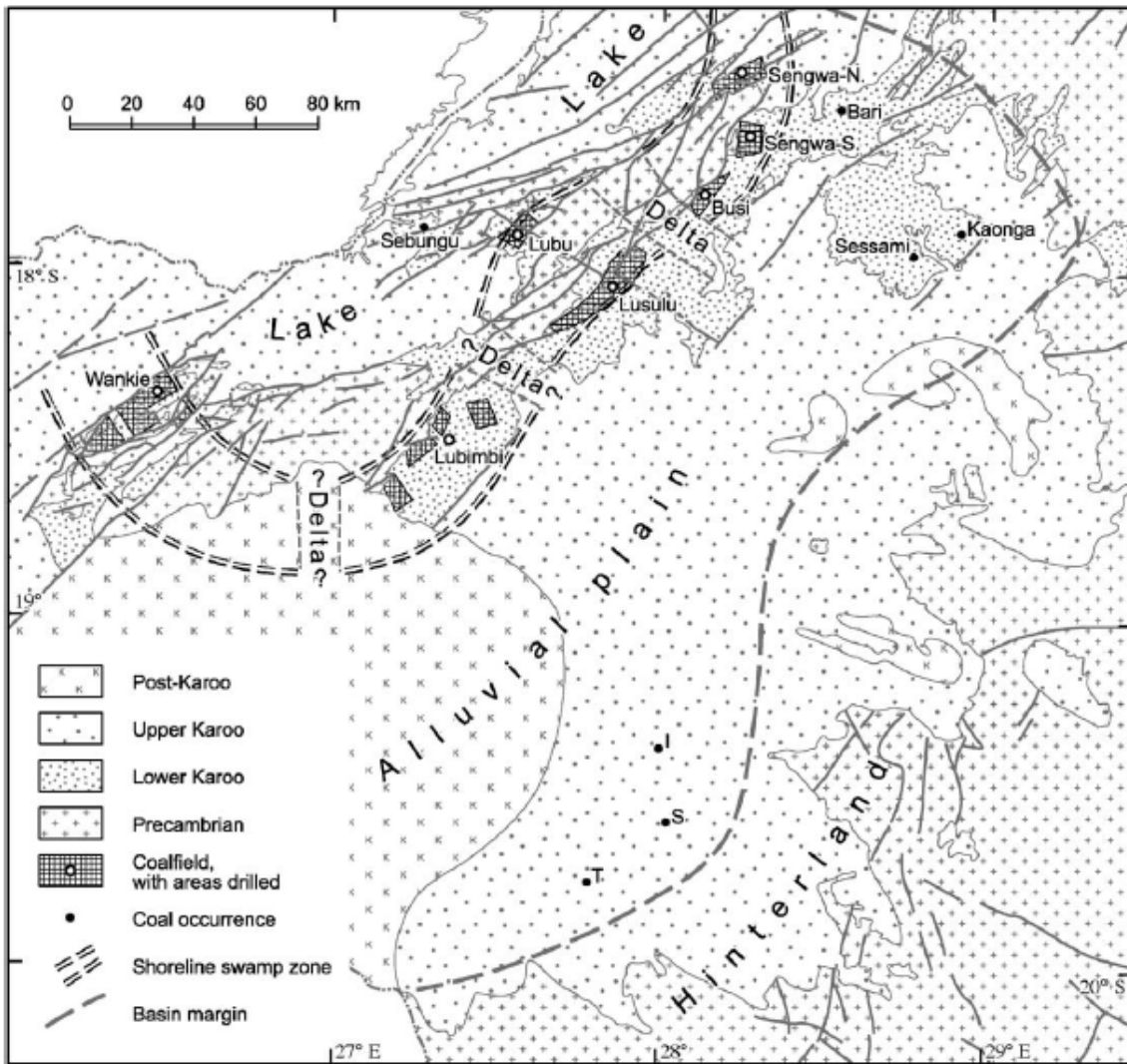


**Figure 29** Postulated depositional environments of the coal bearing formations in the Mid-Zambezi Basin (Oesterlen & Lepper, 2005).

#### 3.2.2.2.6. Upper Wankie Sandstone Formation

Thompson (1981) described the Upper Wankie Sandstone Formation as coarse, cross-bedded deltaic sandstones, grits and pebble layers deposited on a relatively level surface. The Upper Wankie Sandstone and equivalent Waterfall Sandstone (Figure 27) is widely encountered across Zimbabwe and marks the end of a major accumulation of organic matter within the basin. The unit is predominantly arenaceous with only one argillaceous parting noted at Lubimbi. The thickest development described is at Gwaai where it forms a 70m escarpment (Thompson, 1981).

#### 3.2.2.2.7. Tshale Formation

Following the deposition of the Upper Wankie Sandstone, is the Tshale Formation a sequence of alternating sandstones and shales. Thompson (1981) postulated that the Tshale Formation is equivalent to the argillaceous parting noted in the Upper Wankie Sandstone at Hwange but is much thicker, with an average thickness of 37m and could host potentially economic coal deposits. The Tshale formation distribution parallels that of the Waterfall Sandstone on a regional scale and notable outcrops of black carbonaceous shale occur along the banks of the Tshale River. Tshale coals, in general, have higher ash contents than the lower coal measures (Thompson, 1981).

#### 3.2.2.2.8. Ridge Sandstone Formation

The Ridge Sandstone Formation (Figure 27) is regarded to be the continuation of the Waterfall Sandstone and is well exposed on the Dhalia-Lubimbi road (Thompson, 1981). Where the unit directly overlies the Waterfall Sandstone it is difficult to distinguish between the lithologies. The unit varies in thickness from 67m to 192m, averaging 30m, thinning east wards (Thompson, 1981). Overlying the Ridge Sandstone is a thick unit consisting of massive mudstone with minor siltstone and sandstone lenses known as the Madumabisa Mudstone, the uppermost unit of the Lower Karoo in Zimbabwe. There is no lithological break between the Madumabisa Mudstone and the carbonaceous mudstones of the Tshale Formation at Wankie (Mapani, et al., 2013).

### 3.2.3. The Post-Ecca Formations

#### 3.2.3.1. Botswana

The Post-Ecca Karoo deposits comprise formations ranging from late Permian to Cenozoic in age, distributed throughout the study area (Table 4) (Raath, et al., 1992) and (Oesterlen & Lepper, 2005). All groups, with the exception of the Stormberg Volcanic Group, are sediments. The Ntane Formation of the Lebung Group has been investigated widely, for its geohydrological wealth, in Botswana. Table 5 shows the stratigraphic units of the late Triassic and Jurassic formations of the Upper Karoo in Southern Africa compared to the Main Karoo Basin in South Africa (Catuneanu, et al., 2005). Approximate thicknesses are shown as the values in brackets, and ages are the italics.

**Table 4 The Post-Ecca Formations across the study area.**

PERIOD	EPOCH	GROUP	NORTH EAST BOTSWANA AND NORTHERN BELT	MID-ZAMBEZI	THIS STUDY				
<b>JURASSIC</b>	<i>Early</i>	<b>STORMBERG GROUP</b>	Stormberg lava Group	Batoka basalt	<b>POST-ECCA FORMATIONS</b>				
			Ntane Formation	Forest Sandstone Formation					
<b>TRIASSIC</b>	<i>Late</i>		Mosolotsane Formation	Pebbly Arkose Formation			<b>PERMIAN</b>	<i>Late</i>	<b>ECCA GROUP</b>
				Fine red marly sandstone					
	Ripple marked Flagstone								
	<i>Middle</i>			Escarpment Grit					
	<i>Early</i>	<b>BEAUFORT GROUP</b>	Tihabala Formation	Upper Madumabisa Mudstones	<b>PERMIAN</b>	<b>ECCA GROUP</b>			
Middle Madumabisa Mudstones									
	<i>Late</i>	<b>ECCA GROUP</b>	Tlapanana Formation	Lower Madumabisa Mudstones	<b>PERMIAN</b>	<b>ECCA GROUP</b>			
	<i>Early</i>			Upper Wankie Sandstone			<i>Upper</i>		
				Black shale and Coal Group					
				Mea Arkose Formation	Lower Wankie Sandstone	<i>Lower</i>			
		Tswane Formation							
<b>CARBONIFEROUS</b>	<i>Late</i>	<b>DWYKA GROUP</b>	Dukwi Formation	Dwyka glacial Beds	<b>PRE-ECCA FORMATIONS</b>				

**Table 5 Karoo stratigraphic units Upper Karoo in Southern Africa (Catuneanu, et al., 2005).**

BASIN	Molteno equivalent unit	Elliot equivalent unit	Clarens equivalent unit	Drakensberg equivalent unit	References
Main Karoo	Molteno (460m) <i>Carnian-Norian</i>	Elliot (480m) <i>Norian-Liassic</i>	Clarens (c. 300m) <i>Liassic-Dogger</i>	Drakensberg (1370m) <i>Dogger</i>	Visser (1984); Smith et al. (1993); Johnson et al. (1996); Catuneanu and Bowker (2001)
Lebombo	Ntabene ("100m)	Nyoka (250m)	Clarens (45m)	Lebombo (>10km)	SACS (1980)
Springbok Flats	Codrington member (c.10m)	Upper Irrigasie (Worthing member; c.80m)	Clarens (c.80m)	Letaba	Roberts (1992); Johnson et al. (1996)
Tshipise	Klopperfontein (20m)	Bosbokpoort and Red Rocks (<280m)	Clarens (150m)	Letaba	Johnson (1994); Johnson et al. (1996)
Tuli	Middle Unit (c.70m)	Upper Unit (200-280m) <i>Norian-Liassic</i>	Clarens (140m)	Letaba	Bordy and Catuneanu (2001, 2002a and b)
Save	Upper Mkururwe (c.25m)	Bond, Sandota and Oasis (c.300m)	Aeolian Sandstone (c.130m)	lavas	Johnson et al. (1996)
Ellisras	Greenwich (c. 30m)	Lisbon (c.100m)	Clarens (>120m)	X	Johnson (1994); Johnson et al. (1996)
Kalahari-SW	Lowermost Dondong (very thin)	Upper Dondong (thin)	Nkalatlou (c.60m)	X	Johnson et al. (1996)
Kalahari-central	Lowermost Mosolotsane (<10m)	Upper Mosolotsane (c. 110m)	Ntane (c.60m)	Stormberg	Smith (1984); Johnson et al. (1996)
Kalahari-NE	Lowermost Mosolotsane (<10m)	Upper Mosolotsane (c.70m)	Ntane (c.90m)	Stormberg	Smith (1984); Johnson et al. (1996)
Waterberg	Lower Omingonde (c.220m)	Upper Omingonde (100m)	Etjo (c.140m)	X	Holzförster et al. (1999)
Huab	X	X(?)	Twyfelfontein (150-300m) <i>Early Cretaceous</i>	Etendeka	Mountney et al. (1998); Marsh et al. (2003)
Mid-Zambezi	Escarpment Grit (c.55m) <i>Upper Scythian</i>	Ripple Marked Flagstone, Fine Red Marly Sandstone, Pebbly Arkose (c. 340m) <i>Scythian-Anisian</i>	Forest (c. 160m) <i>Norian</i>	Batoka	Nyambe and Utting (1997); Nyambe (1999)

### 3.2.3.1.1. Tlhabala Formation

The Beaufort Group in north east Botswana is represented by a single formation, the Tlhabala Formation (Smith, 1984 and Potgieter & Andersen, 2012). The formation continues from the Central Kalahari Basin over the Makgadikgadi basement high into the North East Botswana Basin (Smith, 1984). The base of the formation is regarded to be the contact with the carbonaceous mudstones and coal of the Tlapana Formation while the top is taken at the junction between the non-carbonaceous unit and the red beds of the Lebung Group. The 100m borehole intersection described by Stansfield (1973) showed deep weathering of the top of the formation and the true contact between the Tlhabala Formation and Lebung Group could not be established by Stansfield (1973) or Smith (1984). The unit mainly consists of brittle, grey, non-carbonaceous mudstones and siltstones and some minor limestone bands. The base of the formation was described as a 29cm thick non-carbonaceous mudstone with some carbonaceous fossil fragments directly overlying the youngest coal followed by a 3m bed of greenish mud-flake breccia. The 60m succession of mudstones that follow gradually becomes khaki yellow in colour and contains a number of limestone beds with interspersed calcite stringers up to 30cm thick Smith (1984). During his regional evaluation of the Karoo Supergroup, Smith (1984) had no data available of the Tlhabala Formation being intersected north of Nata but postulated that the formation could have been intersected in N12/1 had it been drilled deeper (Figure 26). ACB intersected this formation in six boreholes (Y1-01, Y1-02, Y1-03, Y1-04, PDM009 and PDM011) with the thickest intersection, 122m, achieved in Y1-03 (Figure 26). The ACB drilling strategy and basic borehole design was to drill percussion or mud rotary pre-collars to within the Tlhabala Formation and cored sections to below the Dukwi Formation (Anglo Coal Botswana, 2010). As a result of this the sections of the base of the Tlhabala Formation were described from drill chips and not core. The Tlhabala Formation was most likely deposited in a shallow, fairly quiet open water system into which very little arenaceous detrital material flowed and the basal fossil rich mudstones are indicative of a change from a peat swamp to an open widespread lake system (Smith, 1984).

### 3.2.3.1.2. Lebung Group

The fluvial and aeolian deposits of the Lebung Group in Botswana has an affinity for the development for red beds and have previously been compared to the Stormberg Group (Molteno, Elliott and Clarens Formations) of South Africa by Green (1966) and Carney, et al. (1994). The ~150 m thick Group consists of red mudstones, sandstones and medium- and coarse-grained, orange to white sandstones which are either massive or cross-bedded and contain sand grains with frosted surfaces, indicating accumulation under aeolian conditions (Segwabe, 2008). The Lebung Group consists of a succession of red mudstones, siltstones and fine- to coarse-grained, red, orange and white, massive and cross-bedded sandstones. The group is underlain by a well-documented regional unconformity and is mostly conformably overlain by volcanic rocks of the Stormberg Lava Group over most of the Kalahari Karoo Basin (Bordy, et al., 2010<sup>b</sup>). In North East Botswana the group is represented by the Pandamtenga, Ngwasha and Ntane Sandstone Formations. The latter being the primary of potable aquifer in the region (UNESCO, 2004).

Borehole P8 (Figure 26), although it did not intersect the base of the Pandamatenga Formation, was regarded as the most complete intersection and used to describe the lithology. The formation comprises medium-grained calcareous sandstones that become gritty parts or containing mud-flake breccias and conglomerates. Some intercalated purple-brown siltstones, silty mudstones and impure concretionary limestones were also identified (Smith, 1984). It is believed that the argillaceous beds were contorted by possible water-escape or quick-sand structures indicative of a rapid deposition in a relatively high energy aqueous environment (Smith, 1984). The lack of transportation of some of the mudstone fragments was interpreted to be suggestive of a bank-collapse fluvial regime, however, the development of the concretionary limestones are indicative of a semi-arid terrestrial depositional environment (Smith, 1984). The sediments Ngwasha Formation was correlated with the red beds of the Karoo Supergroup by Green (1966), but Smith (1984) named the formation after Ngwasha Pan close to borehole P8 near the border with Zimbabwe. The base of this formation is characterized by a 4.86m thick red muddy siltstone with calcareous mudstone followed by a sequence of greyish cross-bedded and laminated sandstones and red-brown siltstones. The upper 24m consists of grey,

fine-grained sandstone and siltstone succeeded by grey sandstone with purple argillaceous stringers (Smith, 1984). The environment of deposition has been described as a semi-arid fluvial environment and carbonate rich ground water evaporation, oxidising conditions giving rise to the red colouration (Smith, 1984).

The Pandamtenga and Ngwasha Formations were not described separately by Anglo Coal Botswana (2010) and Bordy, et al. (2010)<sup>b</sup> and will be referred to as the Lower Lebung Group for the purposes of this study (Table 6).

**Table 6** Stratigraphic nomenclature of the Lebung Group used in this study with relation to Green (1966), Smith (1984), Anglo Coal Botswana (2010) and Bordy, et al., (2010)<sup>b</sup>.

Group	Formation				
	Green (1966)	Smith (1984)	ACB (2010)	Bordy (2010)	This Study
Lebung Group	Cave Sandstone Stage	Ntane Sandstone Formation			
	Red Beds Stage	Ngwasha Formation	Mosolotsane Formation		Lower Lebung Group
	Molteno Stage	Pandamatenga Formation			

ACB obtained full intersections of the Lower Lebung Group in six boreholes (Y1-01, Y1-02, Y1-03, Y1-04, PDM009 and PDM011) with the thickest intersection, 148m, achieved in Y1-04 (Anglo Coal Botswana, 2010) (Figure 26). A regional distribution map produced by Bordy, et al. (2010)<sup>b</sup> shows the Lower Lebung possibly attains a thickness greater than 100m in the far north-eastern portion of Botswana (Figure 30). The ACB distribution data correlates with this thickness distribution but shows development further west.

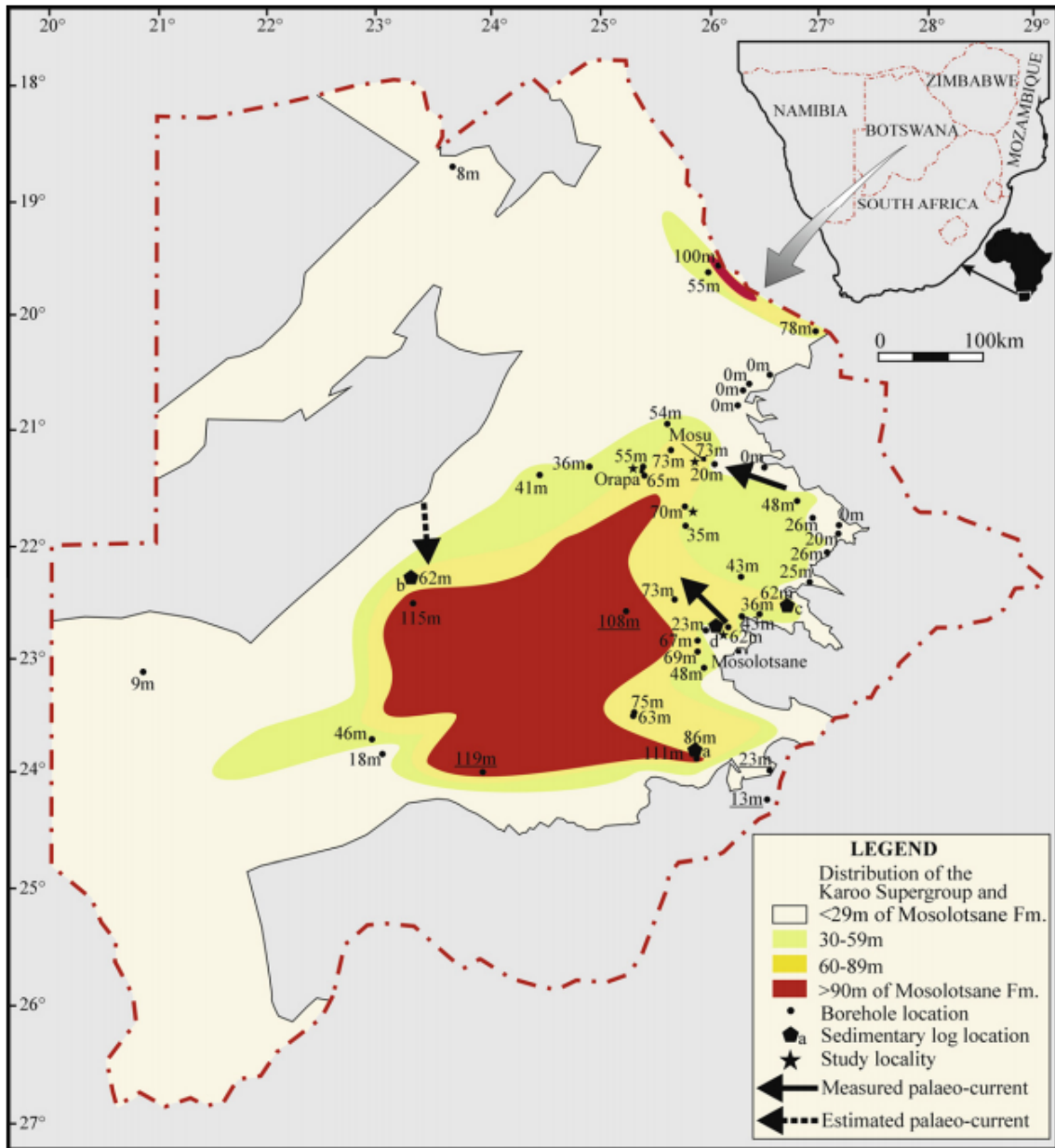


**Figure 30** Lower Lebung Group distribution throughout Botswana Bordy, et al. (2010)<sup>b</sup>.

The Ntane Formation, the uppermost sedimentary unit of the Karoo Suppergroup, described by Stansfield (1973) in the Central Kalahari Basin was extrapolated to the North East Botswana basin because of the uniform aeolian sandstone deposits underlying the Stormberg Lava Group by Smith (1984). This formation is the primary source of potable groundwater throughout the majority of Botswana (Chilume, 2002), resulting in great number of borehole drilling records being available for regional mapping. This formation forms an extensive cover over the majority of the older Karoo formation overstepping basement highs and the base generally unconformably, in some cases condensed, overlies the older rocks (Smith, 1984). At

the base of the formation lies a thin greyish breccia containing polymict clasts suspected by Smith (1984) to lie above an unconformity marking a certain change from a silty to sandy facies as described in borehole P8. Similar breccia zones were noted throughout the sequence in some of the other boreholes described by Smith, (1984). As with the Lower Lebung ACB intersected the Ntane Formation in six boreholes (Y1-01, Y1-02, Y1-03, Y1-04, PDM009 and PDM011), with 88m being intersected in Y1-03 (Anglo Coal Botswana, 2010). The depositional environment is believed to be dry, aeolian with a predominant wind direction from east to west (Smith, 1984).

### 3.2.3.2. Zimbabwe

#### 3.2.3.2.1. Madumabisa Mudstones

In Zimbabwe, the basal formation of the upper Karoo is a thick unit consisting of massive mudstone with minor siltstone and sandstone lenses known as the Madumabisa Mudstone. There is no lithological break between the Madumabisa Mudstone and the carbonaceous mudstones of the Tshale Formation at Wankie (Mapani, et al., 2013). The Clay Ranch Formation described at Lubimbi is considered to be the equivalent of the lower section and the Hakano Beds the middle section of the Madumabisa Mudstones (Thompson 1981). At Lubimbi Thompson, (1981) found the Sidaga Mudstones of the Beaufort Group to be the equivalent to the lower Madumabisa Mudstones and the first true Triassic Formation.

#### 3.2.3.2.2. Escarpment Grit

In Zimbabwe, the Escarpment Grit was described as a fluvially deposited, coarse-grained massive bedded sandstone formation by Raath, et al. (1992). Titley (2013) described the Escarpment Grit to consist of coarse to very coarse-grained sandstone, locally conglomeratic, that fines upwards into more fine grained sandstones and intercalated mudstones. The unit has been subdivided into two informal members based on the facies. The lower member, called the braided facies is characterised by poorly sorted sandstones and pebbly sandstones with mudclasts, whereas the overlying meandering facies comprises of well sorted, upward fining

sandstones with mudclasts and pebble lag layers with laterally extensive mudstones (Titley, 2013). The Escarpment Grit sediments were observed at Sengwa by Palloks (1984). Best described as soft, earthy, red siltstones or very fine sandstones, the Triassic Fine Red Marly Sandstone Formation overly the Escarpment Grits and are poorly exposed and rarely described in borehole records. The clay minerals derived from weathered feldspar partly act as matrix cement and iron oxides introduced laterally give the sediment the distinct reddish colouring (Thompson, 1981).

#### 3.2.3.2.3. Pebbly Arkose Formation

Outcrops of the Pebbly Arkose Formation are more common than that of the Escarpment Grits and are believed to be a more transgressive unit. The arkose is coarse grained with randomly scattered quartz pebbles of varying sizes in irregular disturbed bands (Thompson, 1981). The formation is often a reddish brown due to the presence of iron oxides, however white to light yellow varieties of the arkose has been noted. The unit has been intersected in a number of boreholes with one intersection of 28.5m of Pebbly Arkose (Thompson, 1981).

#### 3.2.3.2.4. Forest Sandstones

The Forest Sandstones were the final sediments deposited in the Mid-Zambezi Basin prior to the eruption of the regional basalts of the Jurassic. Although outcrops are confined to small areas Thompson (1981) described the formation, from borehole logs and small scale mapping, as fine grained white to cream coloured quartzose aeolian sandstones with feldspar contents of up to 50%, iron oxide stained outcrops show a reddish colour. The general thickness of the formation is believed to be less than 30m.

#### 3.2.3.3. Volcanic Rocks in the Study Area

Green (1966) described the igneous unit directly overlying the youngest sediments of the Karoo Supergroup as equivocal to the Drakensberg Lavas found in South Africa. Stansfield (1973) named this unit of rocks the Stormberg Lava Group as encountered in the Central Kalahari sub-basin, a name that was extrapolated to the

remainder on Botswana, except in the Tuli Basin, where it is known as the Bobonong Lava Formation by Smith (1984). The succession generally consists of a number of amygdaloidal basalt flows up to 50m thick with the basal flows being finer grained and richer in amygdales, vesicles and thin tuffaceous bands. The vesicles and amygdales often constitute zeolites, chlorite and calcite with partial quartz infill (Smith, 1984). ACB intersected the Stormberg Lavas in every hole drilled (Anglo Coal Botswana, 2010). The wide-spread non explosive nature of the basalts suggest the flows emanated as relatively quiet pulses from fissures and plugs from the northeast (Smith, 1984). The majority of the Karoo aged dolerite intrusions (Figure 31), visible as both dykes and sills, dated by Jourdan et al. (2004) were found to have been emplaced between 178.4 and 180.9Ma (Figure 32). It was also suggested that the dykes were emplaced at the same time as the basalt flows noted in north-west Zimbabwe as part of the greater Karoo Igneous Province (Jourdan, et al., 2004 and Jourdan, et al., 2005). Jones, et al. (2001) describes the Batoka Basalts, equivalent to the Stormberg Lava, as a succession of up to thirteen near horizontal flows ranging from 10m to 80m in thickness that form a flat plateau. The lack of sedimentary interbeds between the flows is suggestive of a very short eruption time for the entire formation (Jones, et al., 2001). The Botaka Basalts is chronologically and mineralogically identical to the Stormberg Lavas in Botswana and was deposited between 178Ma and 180Ma ago during the Jurassic (Jourdan, et al., 2005).

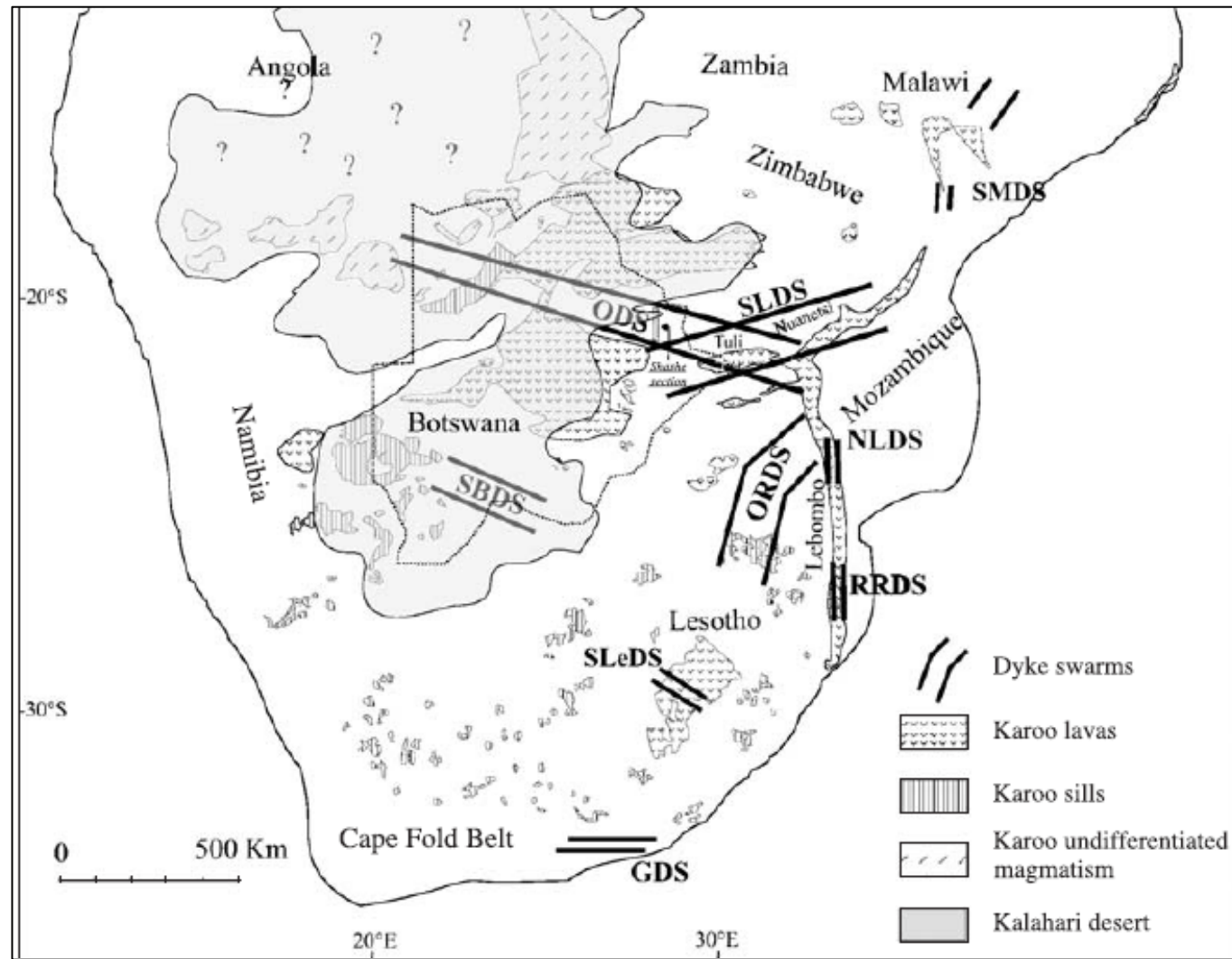


Figure 31 Location of the major Karoo igneous unit throughout Southern Africa (Jourdan, et al., 2004).

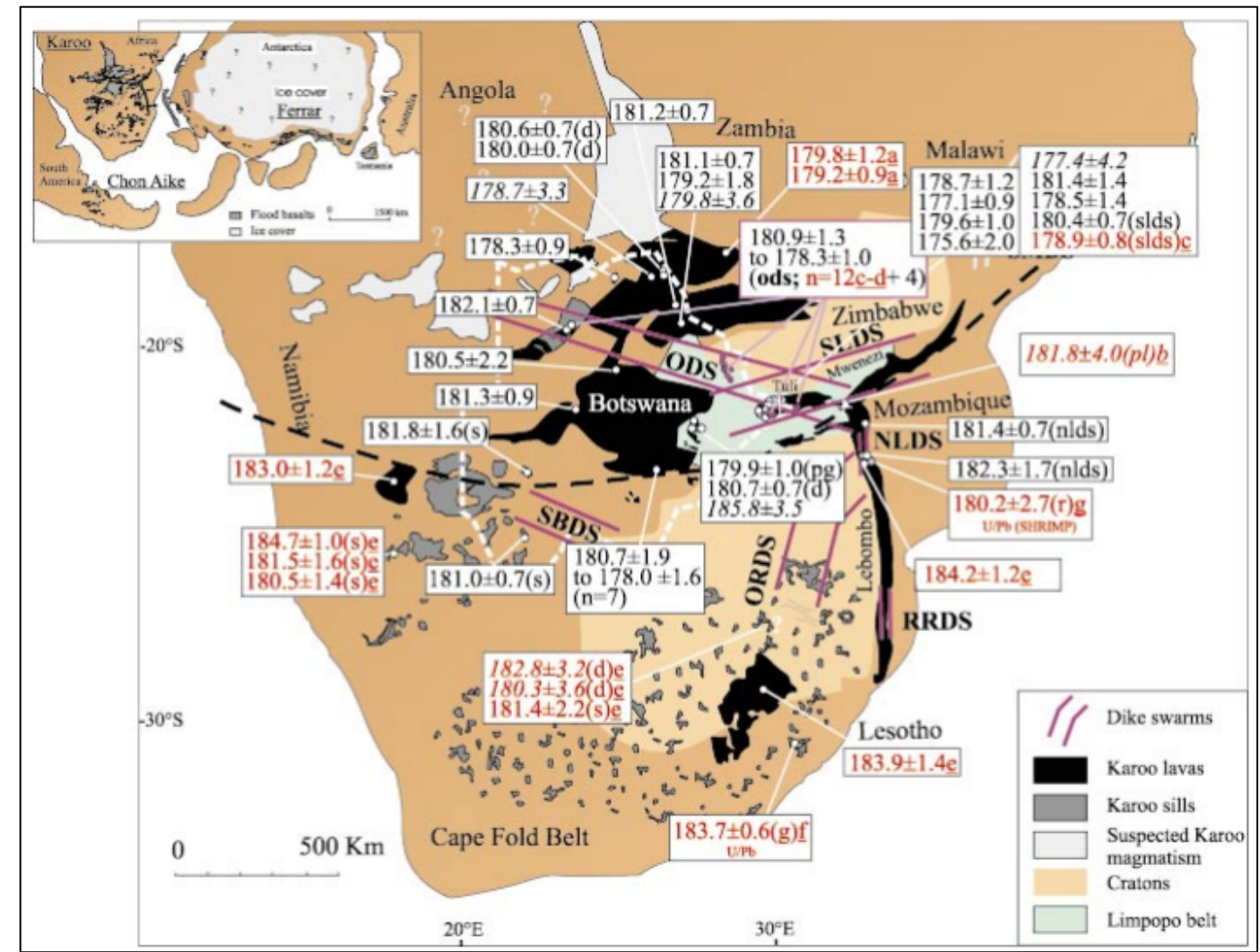


Figure 32 Map of African Karoo flood basalts, sills, and related dyke swarms (Jourdan, et al., 2005).

**Notes:**

**Dyke Swarms Mapped**

(Jourdan, et al., 2004 and Jourdan, et al., 2005)

- ODS: Okavango dyke swarm, ORDS: Olifants River dyke swarm (undated; intruding basement)
- SBDS: south Botswana dyke swarm (undated; intruding Karoo formations)
- SLDS: Sabi–Limpopo dyke swarm (mostly undated; intruding basement and Karoo formations)
- SLeDS: south Lesotho dyke swarm (undated; intruding Karoo lava pile)
- SMDS: south Malawi dyke swarm (undated; intruding basement and Karoo group)
- RRDS: Rooi Rand dyke swarm (undated, intruding Karoo lava pile)
- NLDS: north Lebombo dyke swarm (undated, intruding Karoo lava pile)
- GDS: Gap dyke swarm (undated, intruding Karoo sediments).

**Notes on the Mapping of Data**

(Jourdan, et al., 2004 and Jourdan, et al., 2005)

Botswana and western Zimbabwe are mostly covered by desert sand and that the Karoo volcanic rocks are therefore extrapolated from scarce outcrops, boreholes and aeromagnetic data

### **3.3. The Post-Karoo Sediments**

The Post-Karoo Sediments in the study area consist of the Late Cenozoic to Cretaceous Kalahari Group and some younger pan sediments, most notably those of the Makgadikgadi Pans in Botswana.

The sediments of the Kalahari Group were deposited in a large basin stretching some 2200 km from South Africa in the south northwards through Botswana and Angola into the Democratic Republic of the Congo (Haddon & McCarthy, 2005). The thickness of these sediments can vary from less than 1m to 450m. The average thickness across the study area is approximately 100m thinning from west to east and being absent east of the Hwange Park in Zimbabwe (Figure 33). The accumulation of gravels continued as the down-warp of the basin progressed with interbedding of the gravel layers with sand and finer sediment carried by the rivers. Thick clay beds accumulated in the lakes that formed as a result of the back-tilting of rivers, with sandstone being deposited in braided streams interfingering with the clays (Haddon & McCarthy, 2005).

A period of relative tectonic stability during the mid-Miocene saw the silcretisation and calcretisation of older Kalahari Group lithologies (Figure 34 & Table 7). This was followed in the late Miocene by relatively minor uplift of the eastern side of southern Africa and along certain epeirogenic axes in the interior.

More significant uplift that followed in the Pliocene along epeirogenic axes may have elevated the Karoo Supergroup and basal Kalahari Group sedimentary rocks above the Kalahari basin floor where they were exposed to erosion (Haddon & McCarthy, 2005). The eroded sand was washed into the basin where it was reworked and redeposited by aeolian processes during drier periods, resulting in the extensive dune fields that are preserved today (Haddon & McCarthy, 2005).

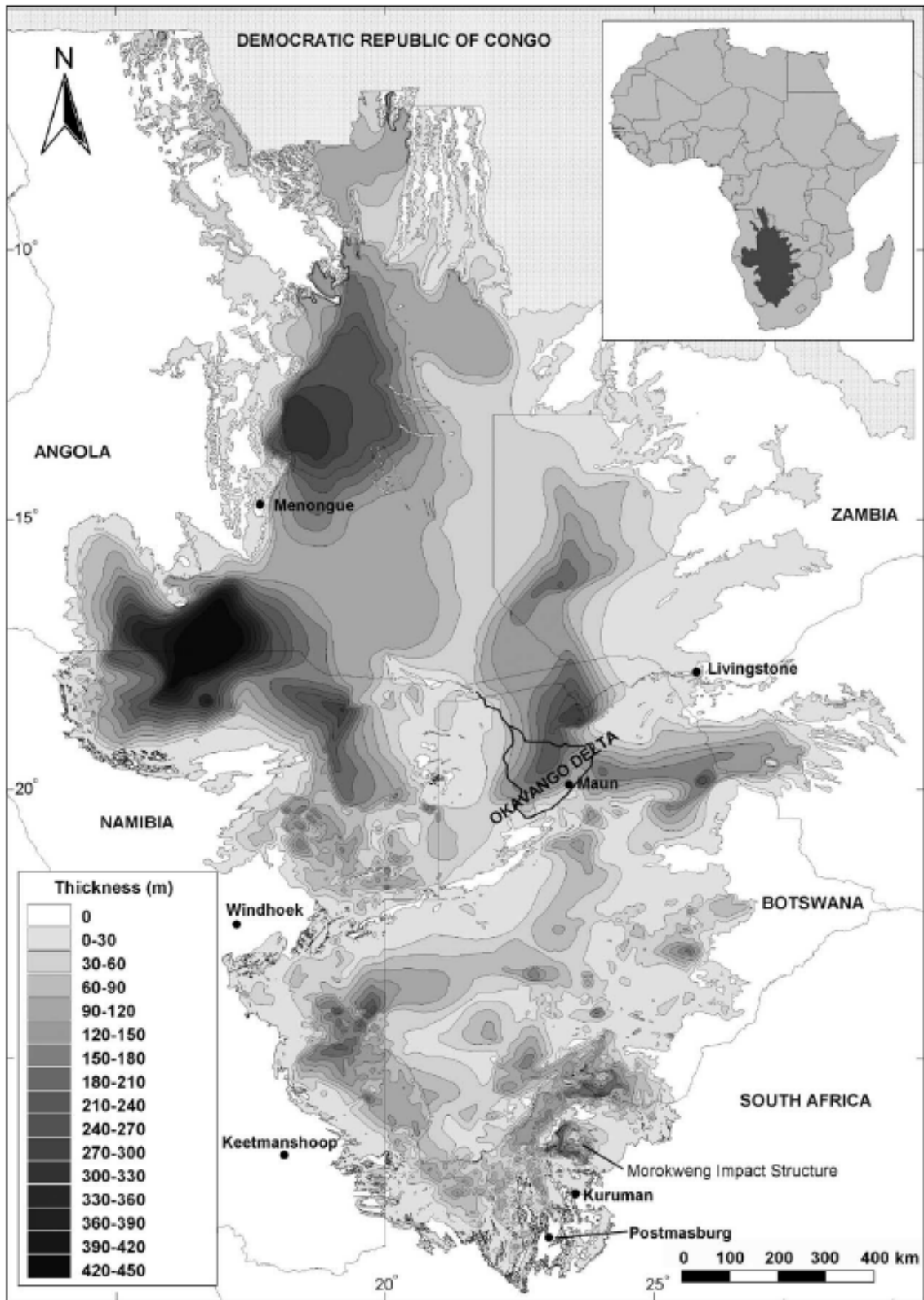
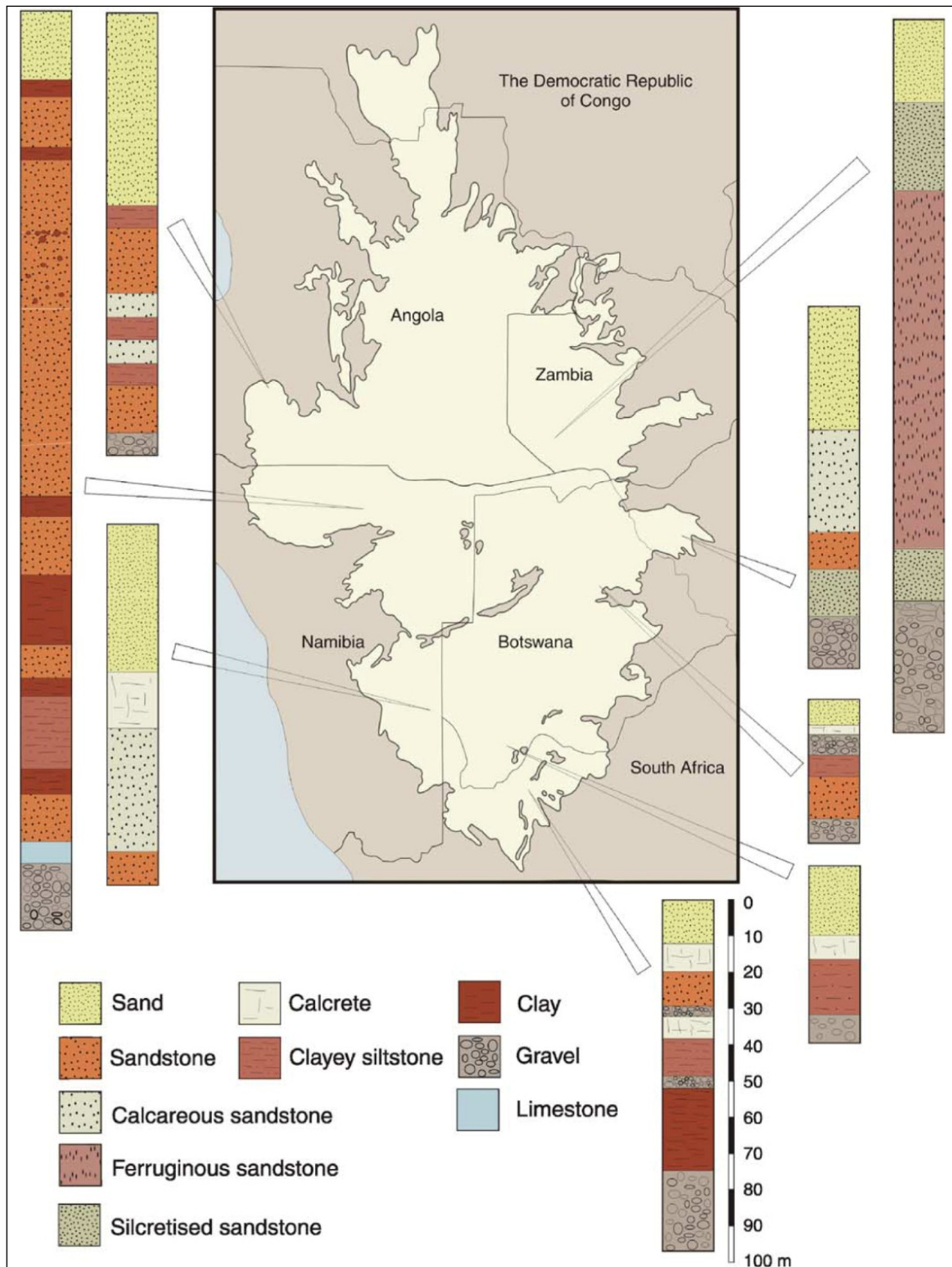


Figure 33 Isopach and distribution of the Kalahari Group (Haddon & McCarthy, 2005).



**Figure 34** Representative borehole logs from different locations across the Kalahari basin (Haddon & McCarthy, 2005).

**Table 7** Attempted correlation of the Kalahari Group stratigraphy across the basin (Haddon & McCarthy, 2005).

South Africa (Smit, 1977) (Thomas, 1981)*	Southern Namibia (SACS, 1980)	Northern Namibia (SACS, 1980) (Miller, 1992)*	Northeastern Namibia (SACS, 1980)	Zimbabwe (Maufe, 1939)	DRC (Cahen & Lepersonne, 1952, 1954) (Claeys, 1947)*	Angola (Pachero, 1976)	Zambia (Money, 1972)	Botswana (Passarge, 1904)	Botswana (Du Plessis, 1993)
<b>Lonely Fm*</b> (diatomaceous limestone) <b>Goeboe Goeboe Fm*</b> (pan sediments) <b>Obobogorop Fm*</b> (gravels)						<b>Série Superior</b> (unconsolidated sand, duricrusts, pan sediments)	<b>Zambezi Fm</b> (limestone and clays on pan floors, duricrusts)	<b>Alluviale Bildungen</b> (alluvium)	
<b>Gordonia Fm</b> (unconsolidated sand)		<b>Andoni Fm</b> (clayey sand or sandy clay)		<b>Kalahari Sand</b> (unconsolidated sand)	<b>Sable Ochres (Etage Superieur)*</b> (unconsolidated sand)		<b>Zambezi Fm Mongu sand member</b> (unconsolidated sand)	<b>Kalahari Sand</b> (4 subgroups) (unconsolidated sand)	<b>Gordonia Fm</b> (unconsolidated sand)
<b>Mokalanen Fm*</b> (calcrete)	<b>Weissrand Fm</b> (basal conglomerate and sandy limestone)			<b>Omatoko Fm</b> (ferricrete and ferruginous sandstone)	<b>Pipe Sandstone</b> (sandstone)	<b>Grès Polymorphes (Etage Moyen)*</b>  (silicified sandstones, chalcedonic limestones)	<b>Série Inferior</b> (sandstones and conglomerates, some clay)	<b>Upper Barotse Fm</b> (massive sandstones and conglomerates)	<b>Kalahari Kalk</b> (limestone, pan deposits)
<b>Eden Fm</b> (sandstones)		<b>Olukonda Fm</b> (calcareous sandstone)	<b>Eiseb Fm</b> (silicified and calcretised sand, sandstone and limestone )	<b>Kalahari Chalcedony</b> (silicified limestone)	<b>Middle Barotse Fm</b> (bedded, ferruginous sandstones)			<b>Bottleschichten</b> (sandstone, sandy limestone) (chalcedonic limestone) (cemented regolith)	<b>LSL Fm</b> (gravel bed)
<b>Budin Fm</b> (clay)		<b>Beiseb Fm</b> (gritty to conglomeratic sandstone)					<b>Mmashoro Fm</b> (sandstone and siltstone) (basal conglomerate)		
<b>Wessels Fm</b> (basal gravels)			<b>Tsumkwe Fm</b> (lime-cemented conglomerate and sand)					<b>Lower Barotse Fm</b> (conglomerate)	
			<b>Ombalantu Fm*</b> (siltstone, mudstone)						

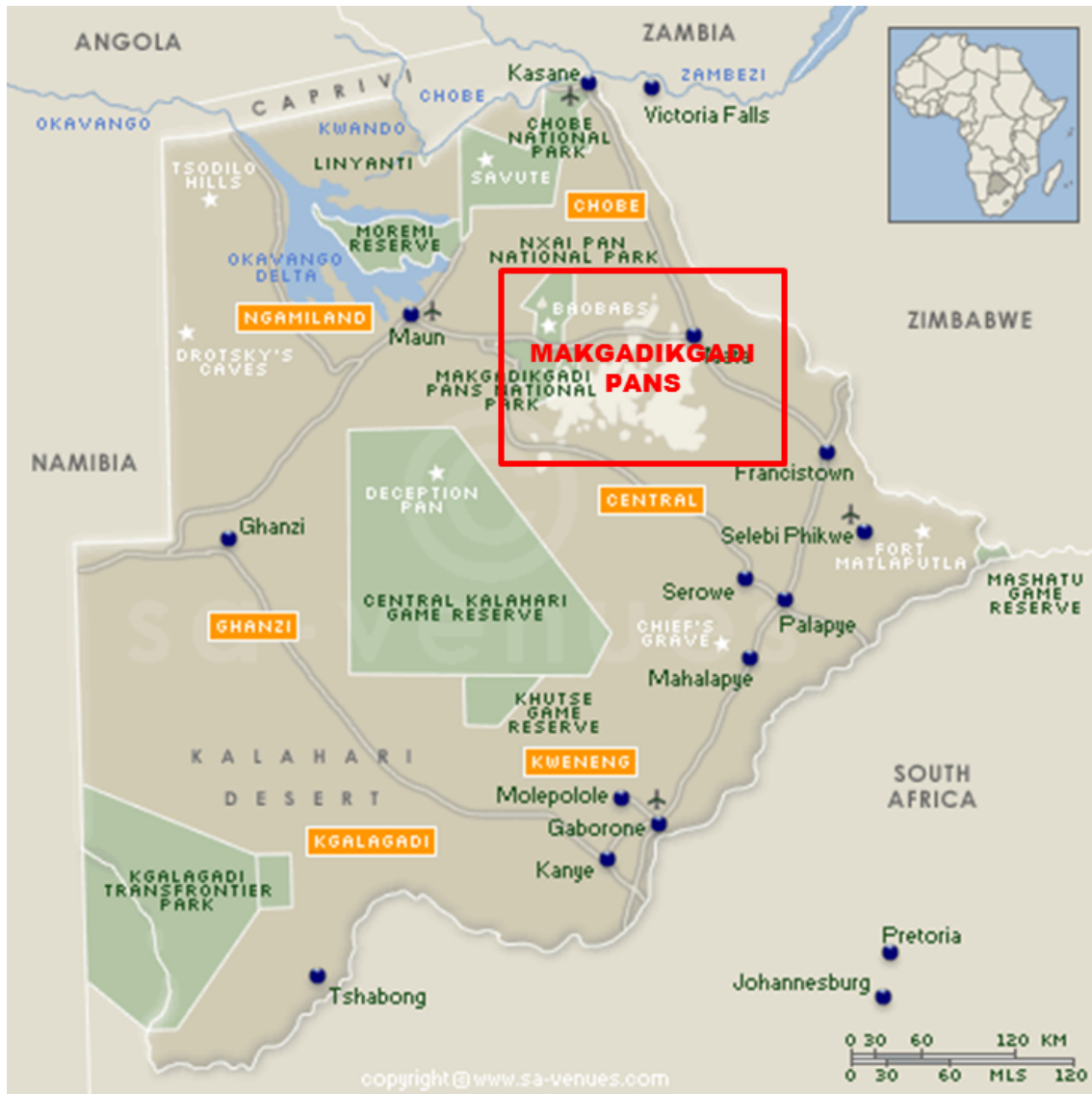


Figure 35 Map of Botswana showing the location of the Makgadikgadi Pans (SA-Venues).

The best studied pans in the region are those of the Makgadikgadi Pan System (Figure 35) and the focus will remain on these for discussion. The pans can be regarded as an analogue for the smaller pans found towards the eastern boundary of Botswana (Potgieter, 2015).

The Makgadikgadi Pans is a large hyper saline lake system in Central Botswana. The system is composed of a number of ephemeral pans with the largest ones being the Sua and Nwetwe Pans (Hogan, 2011). The paleo-lake that occupied the greater Makgadikgadi Basin was much larger than the present day extents. As shown on Figure 36 to Figure 38, the palaeo-lake covered a total area of 37 000km<sup>2</sup>, stretching

from about 100km east of the present day Okavango Delta, to which it is joined by the Boteti River (Figure 38). The long axis of the basin is controlled by recent faults and it is bounded to the north and west by the Gidikwe Ridge (Himmelsbach, et al., 2008). The crest elevation of this feature is 940-945m above sea level, indicating unity of Ngami-Mababe-Makgadikgadi System at the time of its maximum extent. The entire system has been named Lake Paleo-Makgadikgadi and had a maximum areal extent in excess of 80 000km<sup>2</sup> which was larger than the present day Lake Victoria (Partridge & Maud, 2000). This Lake Paleo-Makgadikgadi probably formed during the Late Pleistocene times (~500ka ago) with the Zambezi, Okavango and Chobe Rivers entering the system. The lake reached a maximum level of 945m above sea level ~35ka ago after which the tectonically induced inclination of the system cut off the Zambezi River and this maximum water level would never be reached again (Himmelsbach, et al., 2008). Subsequent tectonism reduced the volume of water fed into the system by the Okavango and Chobe Rivers and drying out of the lake increased the salinity (Himmelsbach, et al., 2008).

The development of the Makgadikgadi-Okavango-Zambezi (MOZ) basin was controlled by a series of mainly NE–SW trending faults that formed grabens in the underlying basement complex and the Karoo sequence. Tectonic activity along this trend resulted in uplift along the Zimbabwe-Kalahari axis and displacement along northeast–southwest trending faults (Himmelsbach, et al., 2008 and Kinabo, et al., 2007). This neotectonic activity resulted in the impoundment of the proto Okavango, Kwando, and upper Zambezi rivers and the development of the proto Makgadikgadi, Ngami and Mababe sub-basins (Kinabo, et al., 2007).

Neotectonic activity related to the rifting in the Okavango Rift Zone (ORZ) has greatly influenced the geomorphology and drainage patterns of the MOZ basin resulting in the formation of the intra-continental Okavango alluvial fan (one of the world's largest inland fan/deltas). Although the timing of initial rifting within the ORZ is not known, palaeoenvironmental reconstruction suggests that feeder rivers promoted extensive flow beyond the Thamalakane and Kunyere faults circa and beyond 120ka ago into the Makgadikgadi pans. However, between 120ka ago and ~40ka ago vertical movements along these rift-related faults caused the impoundment of the Okavango River and cutting off water supply to the pans. Thus it is possible that the 40ka ago

age represents a lower estimate of when active rifting was initiated within the ORZ (Kinabo, et al., 2007).

The large pans Sua and Nwetwe are primarily composed of saline clays and efflorescence approximately 50 to 100 metres deep. Equilibrium between stabilised dunes and pans is driven by aeolian forces. Fluctuations in groundwater levels during interpluvials has led to hardpan formation of calcretes and silcretes resulting in low permeability. Annual rainfall accrues here averaging 500mm (Hogan, 2011). The highly saline water table is quite near the surface for such a semi-arid region, resulting from the fact that these pans are actually the termini of a large closed drainage basin (Hogan, 2011).

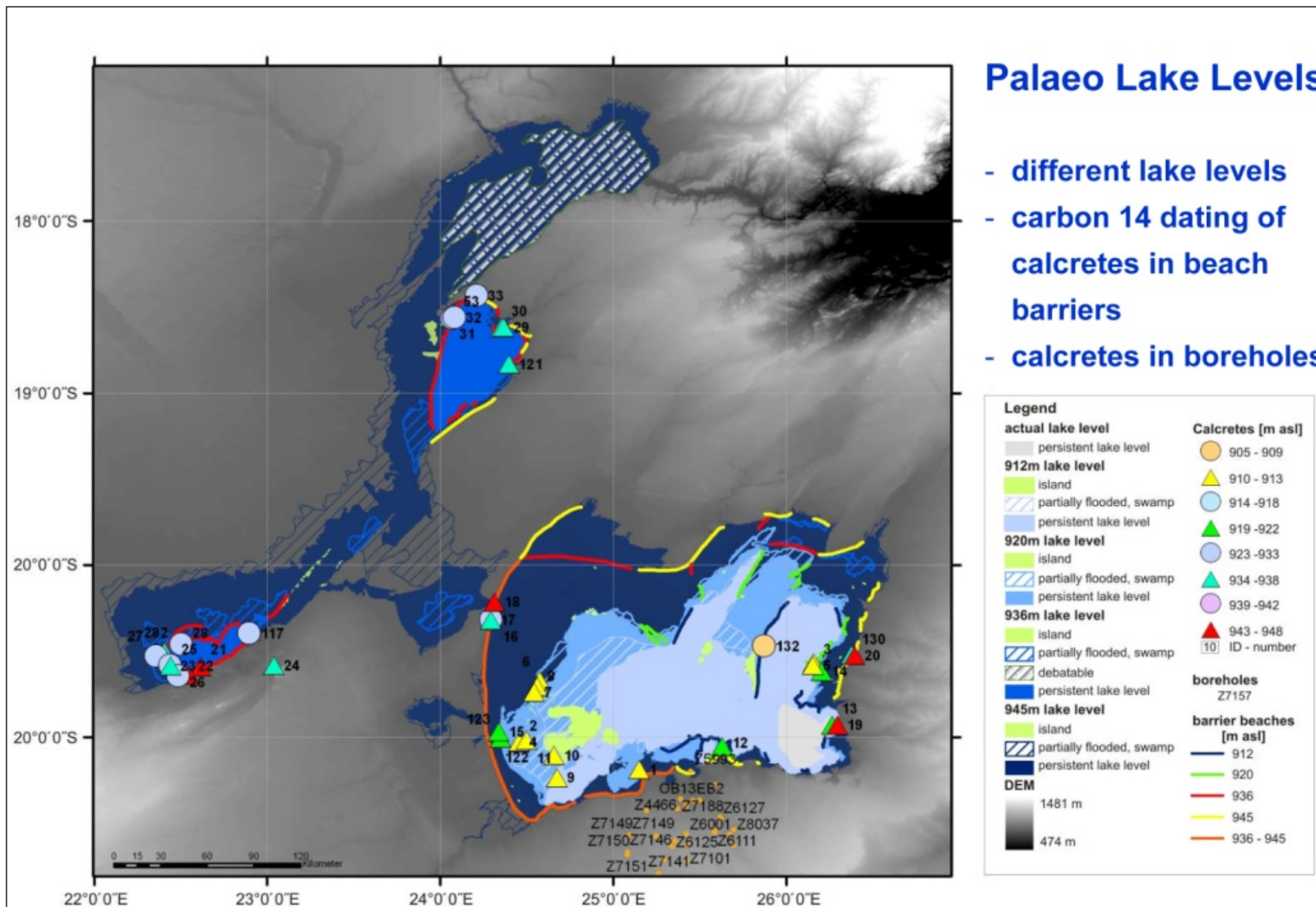
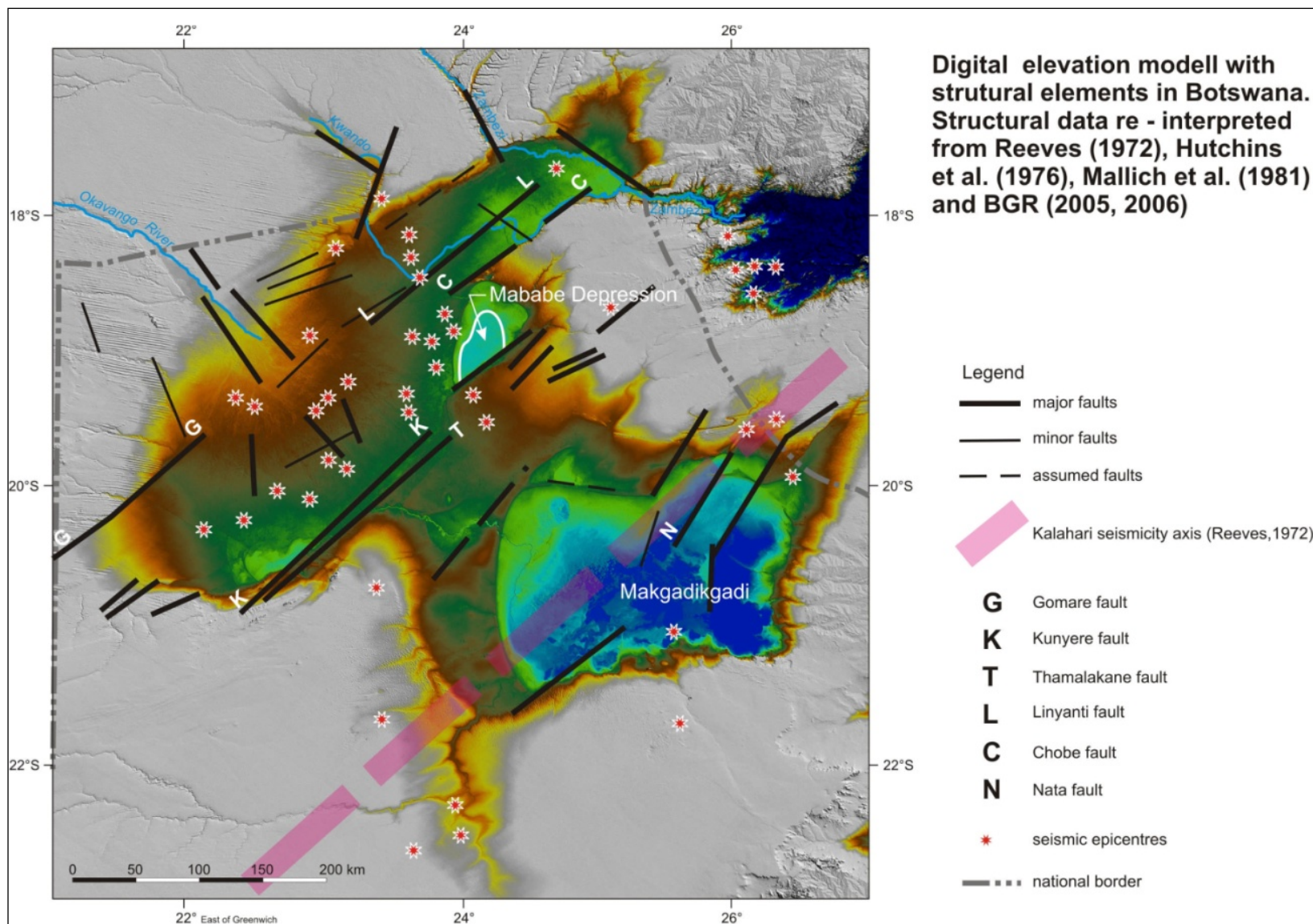


Figure 36 Lake Paleo-Makgadikgadi levels (Himmelsbach, et al., 2008).



**Figure 37** Neotectonism of Lake Paleo-Makgadikgadi (Himmelsbach, et al., 2008).

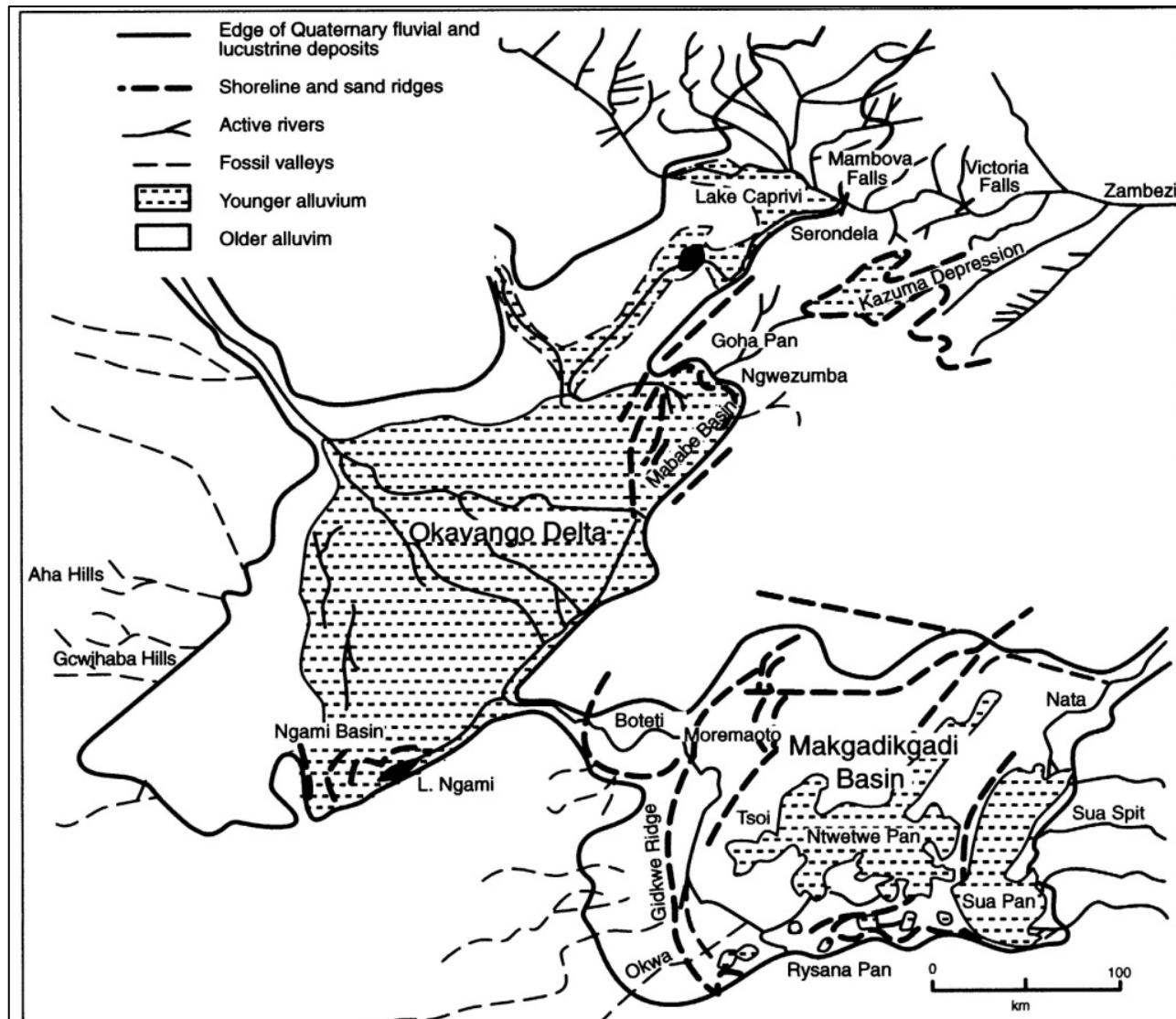


Figure 38 Lake Palaeo-Makgadikgadi extents and bounding ridges (Partridge & Maud, 2000).

#### **4. COAL DEVELOPMENT AND CHARACTERISTICS IN THE STUDY AREA**

Historically South Africa has enjoyed the greatest level of coal mining activity in Southern Africa, mainly due to better infrastructure and access to local and export markets. It has been estimated that Zimbabwe has in situ reserves of 11 billion tonnes of which 2.5 billion tonnes are believed to be shallow enough for opencast exploitation (Cairncross, 2001). In Zimbabwe the coal deposits are found in 2 main regions Save-Limpopo in the South and Mid-Zambezi in the north (Figure 39 and Table 8) (Cairncross, 2001).

Abundant coal seams and interbedded carbonaceous mudstones are found in the upper Ecca Formations in Botswana, which could be a source rock for hydrocarbons (Hiller & Shoko, 1996; Cairncross, 2001 and Faiz, et al., 2013). Carney, et al. (1994) postulated that the thicker and better quality coal seams are found along the eastern margin of the Karoo basin. As a generalisation, the coal has high ash content and is of medium calorific value (Cairncross, 2001). The best coals located to-date are found in the Kgaswe coal field, near Palapye (Morupule Colliery) and, at the Mmamabula coal field in southern Botswana. In Botswana the furthest northern coal field is found at Dukwe (Cairncross, 2001 and Smith, 1984). In northeast Botswana the coal typically occurs in thin seams with mudstone and carbonaceous mudstone partings in the Tlapana Formation with minor stringers in the Tshwane Formation (Anglo Coal Botswana, 2010). Economic coal deposits are found throughout the Mid-Zambezi Basin in Zimbabwe with the best known deposits found at Wankie and Western Areas. The general quality of the coal in the Mid-Zambezi Basin is a high ash low rank bituminous coal with pockets of semi-anthracite. These pockets of higher rank coals have been attributed to localised thermal maturation by dolerite intrusions by Cairncross (2001).

Key exploration reports, covering a range of coal fields and prospective regions, were used in this evaluation (Figure 40). The coordinates provided for the majority of the boreholes in Zimbabwe are on a local survey reference as used by the mine surveyors it was not possible to plot these in the map. For the evaluation the data was grouped per study area and evaluated as such.

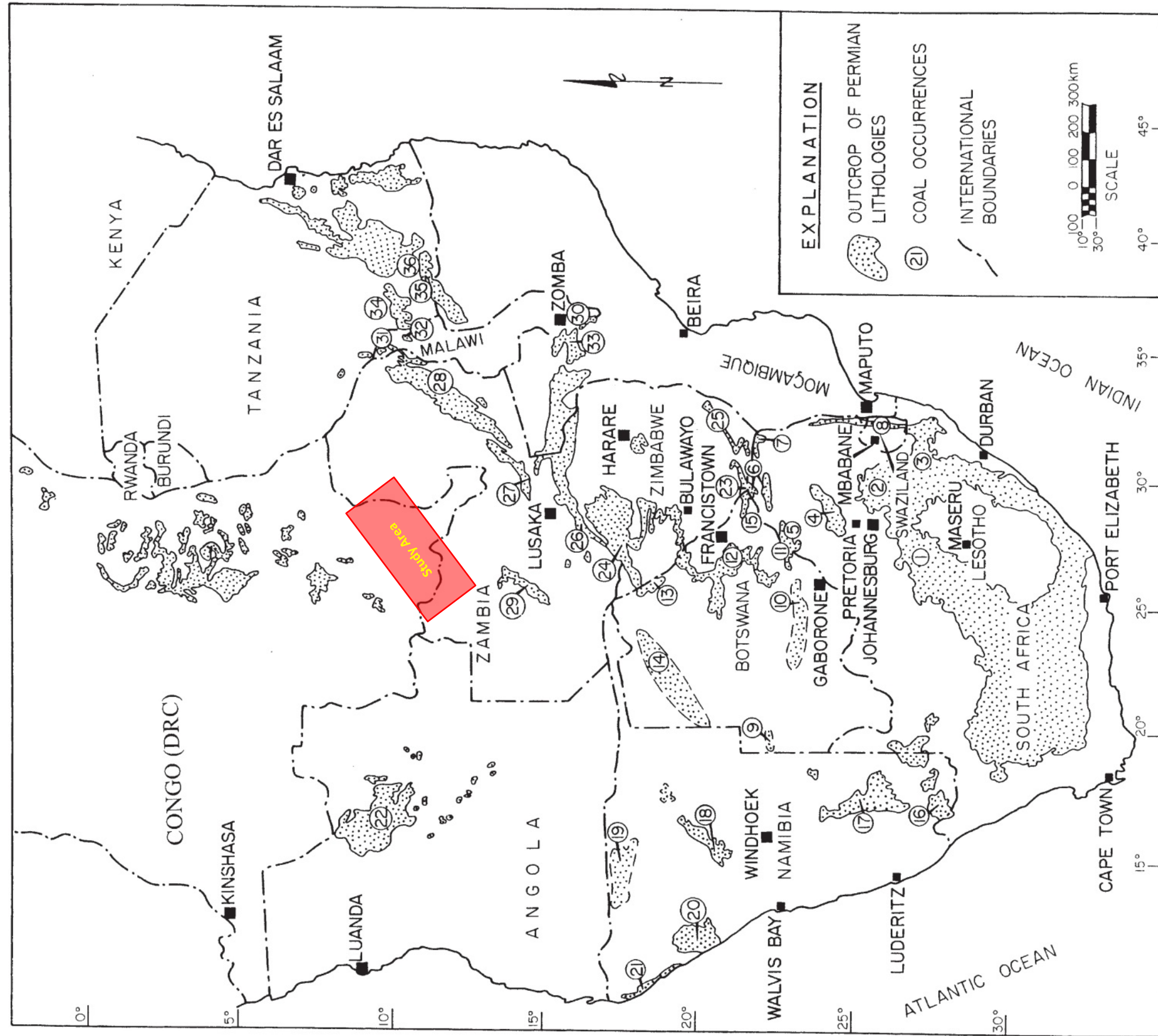


Figure 39 Coal occurrences in Southern Africa with the basins of interest highlighted (Cairncross, 2001). See Table 8 for a brief description of the coal occurrences.

**Table 8 Main characteristics of the coal occurrences shown in Figure 39 after, (Cairncross, 2001; Sparrow, 2012 and Barker, 2012)**

Occurrence Number	Country	Basin	Occurrence Name	Formation	Age			
1.	South Africa	Main Karoo	Free State	Vryheid	Early Permian	Artinskian		
2.			North Eastern Coalfield	Vryheid	Early Permian	Artinskian		
3.			Kwazulu-Natal Coalfield	Vryheid	Early Permian	Artinskian		
4.		Springbok Flats	Springbok Flats Coalfield	Warmbad	Late Permian	Kazanian		
5.				Turfpan	Early Permian	Artinskian		
6.		Lephalale	Ellisras	Grootegeluk	Late Permian	Kazanian		
7.		Limpopo	Limpopo Coalfield	Vryheid	Early Permian	Artinskian		
8.				Mikabeni	Late Permian	Kazanian		
9.	Tshipise	Pafuri Coalfield	Madzaringwe	Early Permian	Artinskian			
10.			Mikabeni	Late Permian	Kazanian			
11.	Swaziland	Swaziland	Volksrust	Late Permian	Kazanian			
12.			Vryheid	Early Permian	Artinskian			
13.	Botswana	Kalahari Karoo	Southwest	No coal intersections				
14.			Kweneng	Boritse	Late Permian	Kazanian		
15.			Mmamabula	Mmamabula	Early Permian	Artinskian		
16.		Morupule		Serowe	Late Permian	Kazanian		
17.				Morupule	Early Permian	Artinskian		
18.		Northeast		Tlapana	Late Permian	Kazanian		
19.				Northwest		No coal intersections		
20.						Tuli	Seswe	Early Permian
21.	Namibia	Karasburg	Karasburg	No coal intersections				
22.				Aranos	Prince Albert	Early Permian	Artinskian	
23.		Waterberg	Waterberg	Teverede	Early Permian	Artinskian		
24.		Ovambo	Ovambo	Prince Albert	Early Permian	Artinskian		
25.		Huab	Huab	Verbrande Berg	Early Permian	Artinskian		
26.		Kaokoland / Damaraland	Kaokoland / Damaraland	No coal intersections				
27.	Angola	Luanda	Luanda	No coal intersections				
28.		Mazunga	No coal intersections					
29.	Zimbabwe	Mid-Zambezi	Mid-Zambezi	Black Shale and Coal Wankie Main	Early Permian	Artinskian		
30.		Sabi-Lundi	Sabi-Lundi	Marare	Late Permian	Kazanian		
31.				Malilongwe	Early Permian	Kungurian		
32.	Zambia	Gwembe (Mid-Zambezi)	Gwembe (Mid-Zambezi)	Lower Mkushuwe	Early Permian	Artinskian		
33.				Main Coal Seam	Early Permian	Artinskian		
34.				Luano	Gwembe Coal	Early Permian	Kungurian	
35.		Luangwa	Luangwa	Luwumbu	Early Permian	Artinskian		
36.		Barotse	Barotse	Luampa	Early Permian	Artinskian		
37.	Malawi	Malawi	Southern Coalfield	Unnammed Coal & Sandstone	Late Permian	Tatarian		
38.			Ngana Area	Coal Measures	Early Permian	Artinskian		
39.			Livingstonia Area	Unnammed Coal & Sandstone	Early Permian	Artinskian		
40.	Mozambique	Moatize/Tete	Moatize/Tete	Productive Series	Early Permian	Artinskian		
41.				Tanzania	Ruhuru	Upper Coal Measures	Late Permian	Ufimian
42.	Lower Coal Measures	Early Permian	Artinskian					
43.	Mhukuru	Mhukuru	Upper Coal Measures			Late Permian	Ufimian	
44.	Luwegu	Luwegu	No coal intersections					

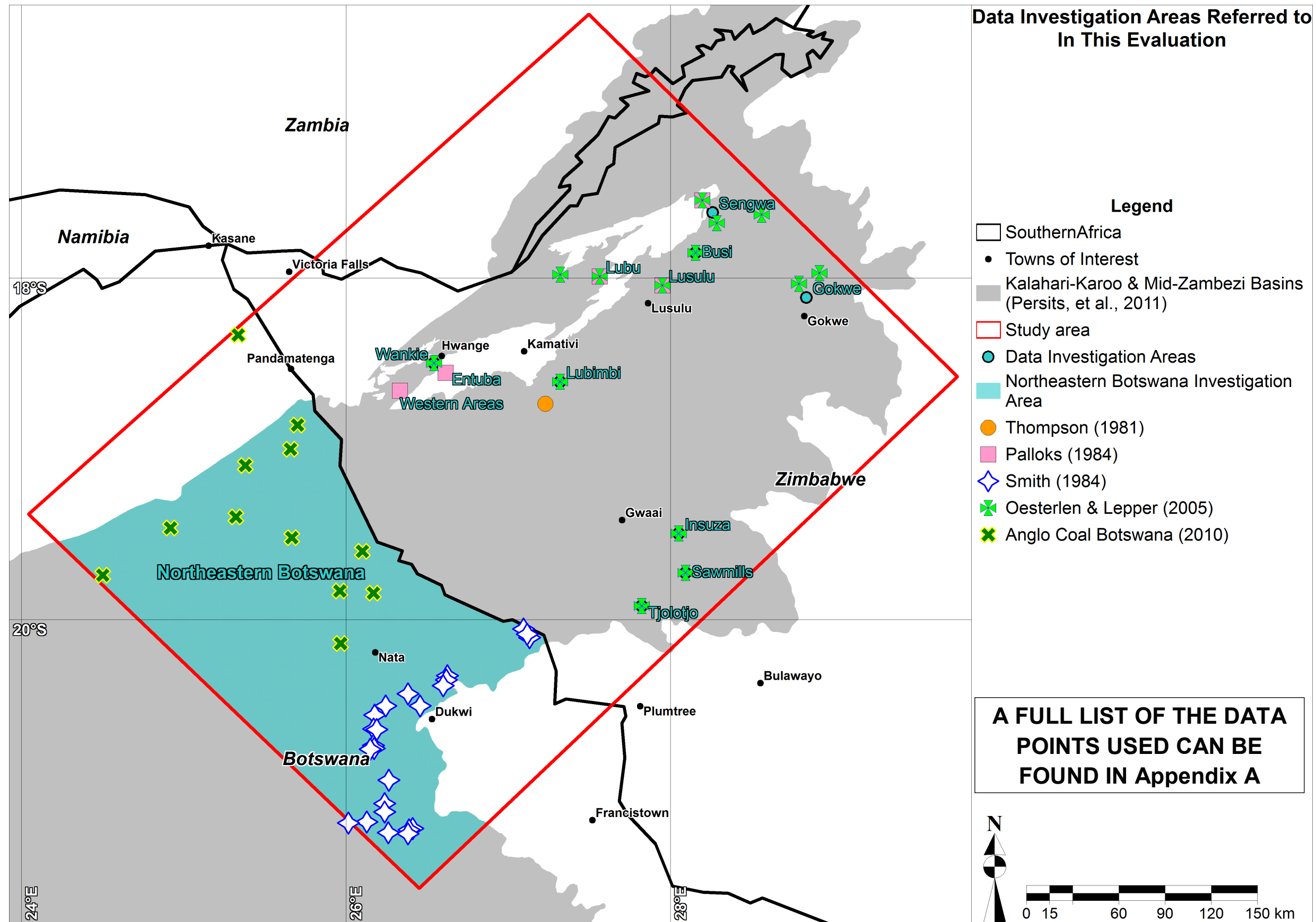


Figure 40 Investigation areas and regions used in this evaluation.

#### **4.1. Coal Quality and Rank**

Coal is ranked based on the constituents, physical properties and thermal maturity changes as the raw peat is transformed to anthracite (World Coal Institute, 2005). The primary characteristics of the coal used for ranking are 1) the amount of carbon present in the sample, termed the Fixed Carbon Content, 2) the amount of moisture 3) the amount of non-combustible material referred to as the Ash Content, 4) the volatile matter content and 5) the heat value expressed as energy per weight.

In the Mid-Zambezi Basin an apparent decrease in the coal rank over relatively short distance north-eastwards from Wankie to Sengwa and between Lusulu and Sengwa, has been noted (Cairncross, 2001). In Botswana, the Panadamatenga field has not been investigated extensively due to the inhibitive coal depths (Smith, 1984). One government borehole showed that the coal seams could be up to 700m deep as a result of thick Kalahari Group and Upper Karoo Supergroup development. Evaluations of the Dukwi field indicated that the coal is also of low rank (Cairncross, 2001). Two ACB boreholes, Y1-02 and Y1-03 intersected coal at a 705m, reinforcing these depth postulations (Anglo Coal Botswana, 2010).

Proximate analyses are used to determine the fixed carbon, ash, moisture and volatile matter contents as percentages on air dried coal samples, the sum of the constituents must add up to 100%. The physical changes within the coal are caused by temperature and pressure resulting from the burial of the sediments containing the coal measures (Figure 41). As the coal is matured in high pressure, high temperature environments the ash, moisture and volatile matter components decrease (Figure 42) causing a relative increase in fixed carbon per weight and this increase causes an increase in the heating value (World Coal Institute, 2005).

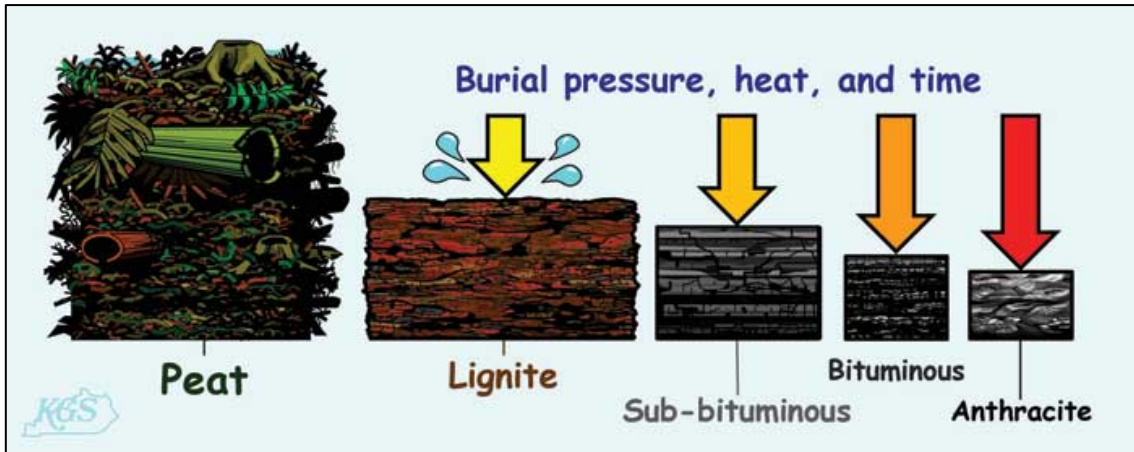


Figure 41 Alteration of peat into coal (Kentucky Geological Survey, 2011).

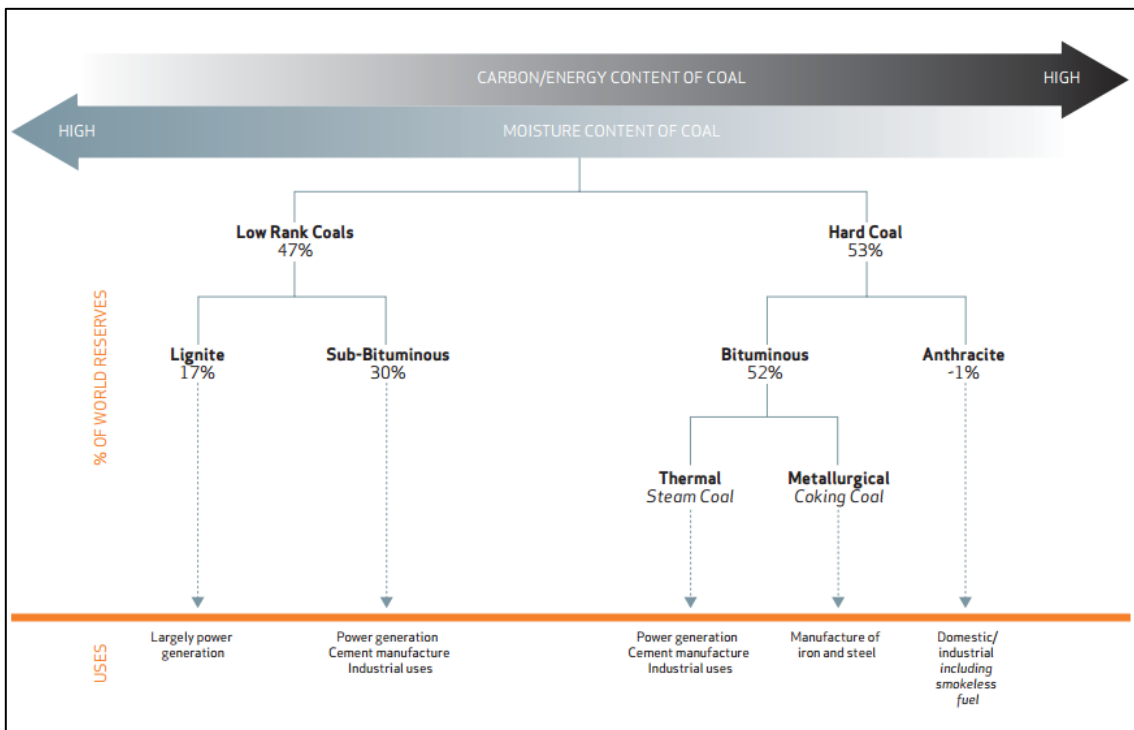


Figure 42 Coal types and uses (World Coal Institute, 2005).

Thompson (1981) and Palloks, (1984) reported detailed proximate analytical data for a number of coal occurrences in the Mid-Zambezi Basin and; generalised quality information was obtained from a number of other sources. Anglo Coal Botswana, (2010) evaluated the coals intersected in four CBM exploration boreholes drilled in the Nata area, Cairncross (2001) reported key quality parameters for the Dukwe Field in Botswana. The variation in depth and rank across the study area is reflected in the level of exploration drilling activity in each of exploration areas. For the evaluation the ASTM standard on coal rank classification was used as it is relatable

to the maximum amount of gas that the coal can generate and store as determined by Eddy, et al., (1982).

Krishan (1940) and Cardott (2012) demonstrated that the general ranking of coal can be determined based on the ash-free fixed carbon, and moisture contents (Figure 43 and Table 9). For these evaluations all analyses were corrected to ash-free values using the equations (Equation 1), as shown by Snyman (1998), were used. The coal qualities over the study area were derived from the available data and related to the Cardott (2012) & Krishan (1940) classification system (Table 10).

$C_{(ash-free)} = \frac{C \times 100}{100 - A}$
$V_{(ash-free)} = \frac{V \times 100}{100 - A}$
$M_{(ash-free)} = \frac{M \times 100}{100 - A}$
Where:
A = Ash content (%)
C = Fixed carbon content (%)
V = Volatile matter content (%)
M = Moisture content (%)

Equation 1 Ash-free content estimation formulae (Snyman, 1998).

Table 9 Coal classification properties on ash free basis (constructed after Krishan, 1940 and Cardott, 2012).

Coal Rank		Coal Constituents (Ash-Free Basis)		
		Fixed Carbon	Volatile Matter	Bed Moisture
	Lignite	32	38	30
	Subbituminous - C	37	36	27
	Subbituminous - B	43	35	22
	Subbituminous - A	45	38	17
	High Volatile Bituminous - C	45	40	15
	High Volatile Bituminous - B	53	40	7
	High Volatile Bituminous - A	62	32	6
	Medium Volatile Bituminous	69	25	6
	Low Volatile Bituminous	77	17	6
	Semi Anthracite	85	12	3
	Anthracite	92	5	3

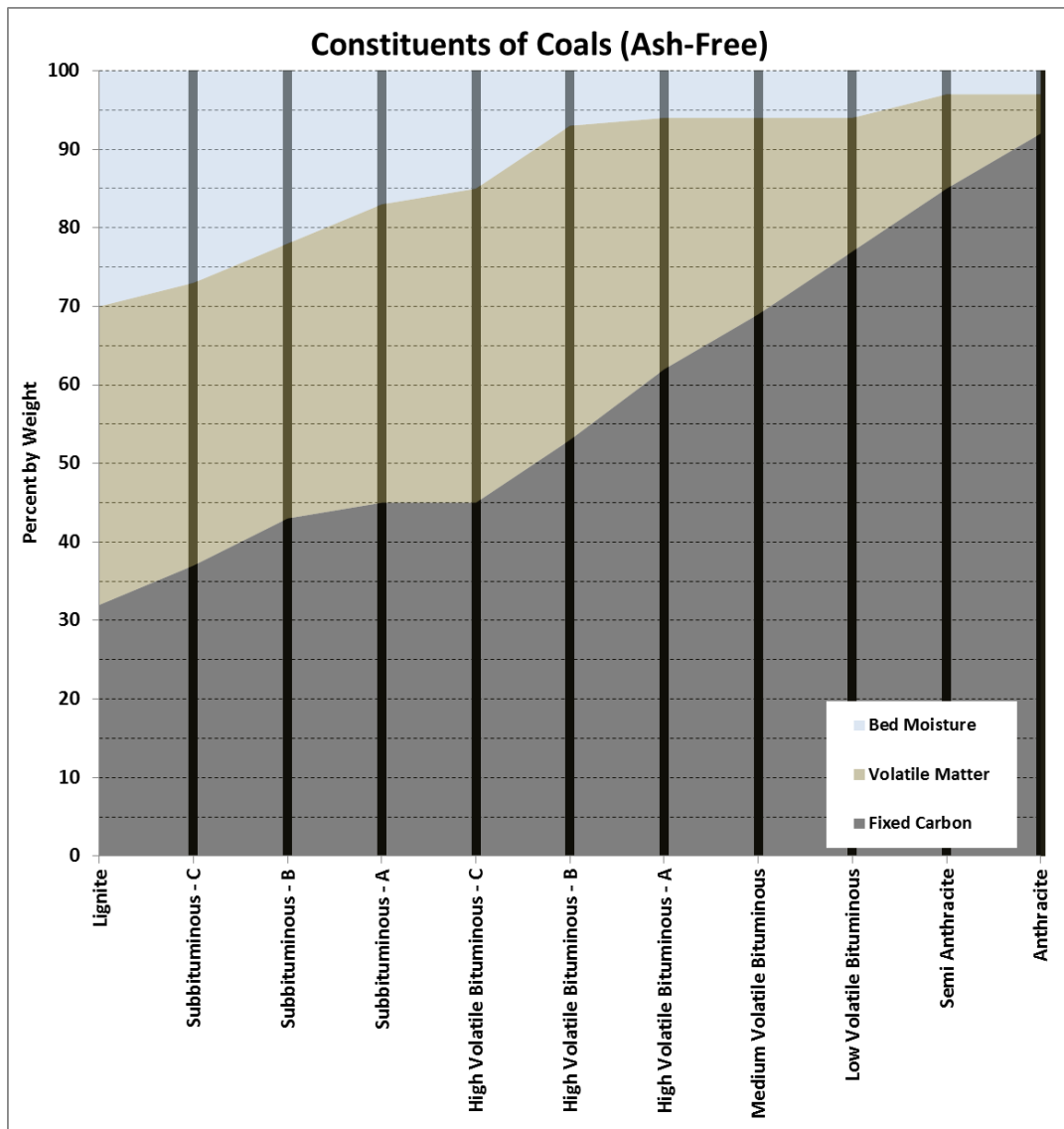


**Figure 43** Graphical differentiation of coal constituent distributions, based on proximate analysis (constructed after Krishan, 1940; Middelkoop, 2009 and Cardott, 2012).

Table 10 Coal ranks across the study area derived from ash-free proximate analyses.

Country	Area	Source(s)	Number of Data Points Evaluated	Minimum			Maximum			Average			General Coal Rank	Comments
				Moisture Content (%)	Volatile Matter (%)	Fixed Carbon (%)	Moisture Content (%)	Volatile Matter (%)	Fixed Carbon (%)	Moisture Content (%)	Volatile Matter (%)	Fixed Carbon (%)		
Zimbabwe	Western Areas	Palloks (1984)	63	1	23	61	3	37	75	2	30	69	High Volatile Bituminous A to Medium Volatile Bituminous	Summarised borehole logs and analyses.
	Entuba		125	0	15	71	8	28	84	1	23	75	Medium Volatile Bituminous	Summarised borehole logs and analyses.
	Lubu		28	1	27	55	4	42	71	2	35	63	High Volatile Bituminous B to High Volatile Bituminous A	Summarised borehole logs and analyses.
	Sengwa South		10	3	25	62	6	33	70	5	28	67	High Volatile Bituminous A	Summarised borehole logs and analyses.
	Sengwa North		11	3	26	64	6	33	69	5	29	66	High Volatile Bituminous A	Summarised borehole logs and analyses.
	Lusulu	Palloks (1984); Mapani, et al. (2013); Padcoal (Pvt) Ltd (2011)	3	14	30	51	16	34	56	15	32	53	High Volatile Bituminous C to High Volatile Bituminous B	Summarised borehole logs and analyses.
	Wankie	Palloks (1984)	2	1	26	73	1	26	73	1	26	73	High Volatile Bituminous C to Medium Volatile Bituminous	Only averages for the Wankie seams given by Mapani et al. (2013). High ash bright thin bands with interbedded mudstone reported, some Fischer oil reported by Padcoal (Pvt) Ltd (2011).
	Gokwe	Oesterlen & Lepper (2005); Padcoal (Pvt) Ltd (2011)	1	5	29	65	5	29	65	5	29	65	High Volatile Bituminous C to Medium Volatile Bituminous	Reported by Padcoal (Pvt) Ltd (2011) as part of an investment brochure. Ash values reported as between 20 & 30 % by Oesterlen & Lepper (2005).
	Lubimbi	Oesterlen & Lepper (2005)	1	*	High ash bright thin bands with interbedded mudstone reported						High Volatile Bituminous C			Described in the text only.
	Busi		1	*	High ash lower quality coal reported						Subbituminous			No quality data is available.
Tjolutjo, Sawmills, and Insuza	1		*	High ash lower quality coal reported						Subbituminous			Described in the text only.	
Botswana	Northeast Botswana	Smith (1984), Anglo Coal Botswana, (2010) Potgieter (2015)	39	**	Smith (1984) and Cairncross (2001) reported high ash low quality coal around Dukwe, Anglo Coal Botswana (2010) only intersected the coal in 4 boreholes and reported generally poor quality.						Subbituminous			Proximate data not published. Personal experience on the project.
*	Quality estimated from literature described as very high ash and lower quality. Low quality subbituminous coal assumed.													
**	Personal experience. Very high ash and very low carbon contents. Subbituminous coal encountered.													

## **4.2. Coal Thickness, Depth and Regional Continuity**

The total coal thickness was evaluated across the study area as this is a pivotal component to the resource assessment. For the purposes of this study the full coal measures were assessed. Once an evaluation of the production capacity is attempted, in a localised field, it is of utmost importance to isolate the discreet primary production seams and establish the continuity or possible compartmentalisation of these seams. However, with the sparse data this is not possible nor is it required at the regional scale of the assessment and the composited coal thickness in a borehole can be used. Composite coal thicknesses for each of the boreholes were calculated and used for this study. The composite was limited to the Eccra Group coals.

In Botswana only four of the Anglo Coal Botswana exploration boreholes intersected coal. These were all placed in the Nata Sub-Basin as identified by Smith (1984). The thickest intersections were towards the west where 12m coal was intersected in boreholes Y1-01 and Y1-03 (Figure 26) at a depth of approximately 500m below surface (Anglo Coal Botswana, 2010).

In the Mid-Zambezi basin the main focus area for coal extraction is in the Wankie Coalfield, a collective name for the coal deposits at the Wankie Concession, Entuba, Western Area, Lubu, Sengwa, Lusulu, Sinamatella and Lukosi, and the Lusulu Coalfield (Oesterlen & Lepper, 2005). In the Wankie Concession the Main Seam (k2-3) varies in depth from 60 to 70m (Figure 44) below ground level (Oesterlen & Lepper, 2005) and in thickness from 2m – 12m with the lower portion having excellent coking properties (Figure 45) with low ash (<10%) values. Some measurements of high sulphur were noted by Cairncross (2001).

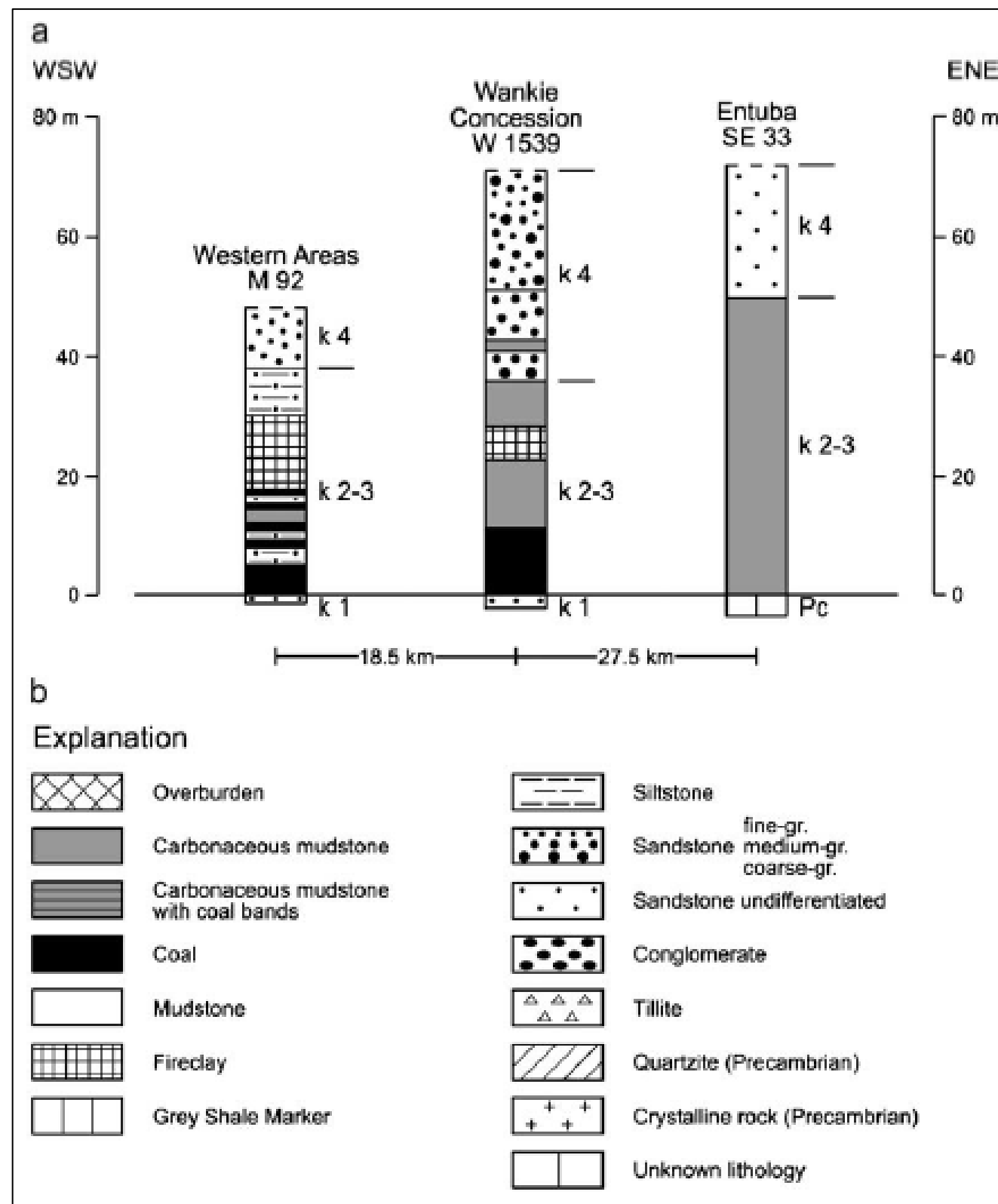


Figure 44 The Wankie Main Seam (k2-3) lithofacies changes at the Wankie Concession (Oesterlen & Lepper, 2005).

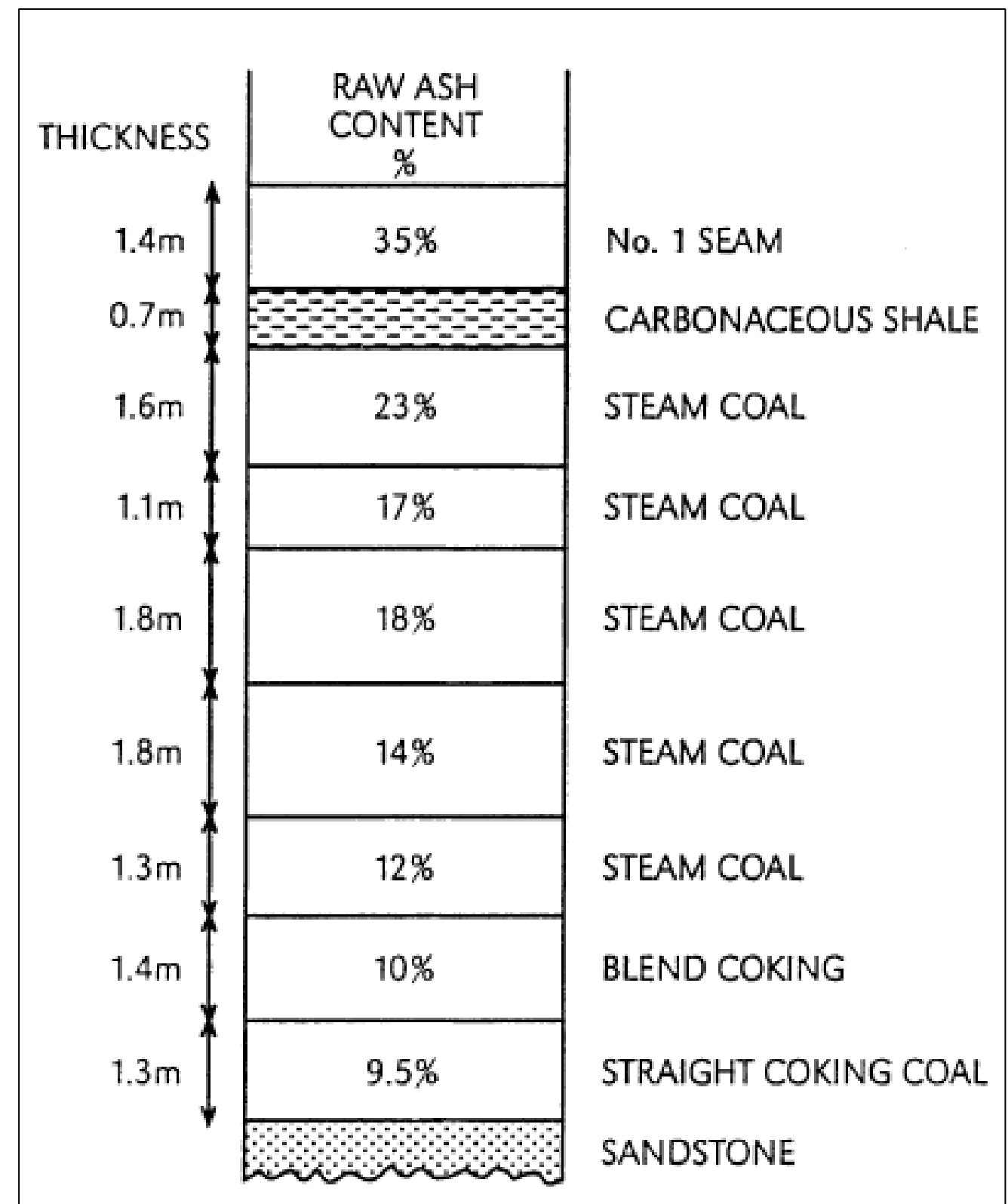


Figure 45 A typical vertical section through the Wankie Main Seam, Zimbabwe (Cairncross, 2001).

Table 11 shows the maximum, minimum and average measured coal thicknesses and top depths from borehole records and published literature for each of the investigated areas. The Botswana measurements were compiled from wireline and geological logs (Anglo Coal Botswana, 2010) and in Zimbabwe the data was taken from historic reports by Palloks (1984) and Thompson (1981). For the resource evaluation all thickness measurement data was combined and statistically analysed.

**Table 11** Minimum, maximum and average coal thicknesses and top depths from borehole records.

Country	Area	Source(s)	Number of Data Points Evaluated	Depth (metres below ground level)			Composite Thickness (metres)		
				Minimum	Maximum	Average	Minimum	Maximum	Average
Zimbabwe	Western Areas	Palloks (1984)	63	4	336	162	2	14	7
	Entuba		125	6	560	118	3	20	11
	Lubu		28	11	112	48	2	18	8
	Sengwa South		10	6	161	82	9	17	12
	Sengwa North		11	0	145	75	8	15	12
	Lusulu	Palloks (1984); Mapani, et al. (2013); Padcoal (Pvt) Ltd (2011)	3	98	197	92	4	9	6
	Wankie	Palloks (1984)	2	100	700	265	8	12	10
	Gokwe	Oesterlen & Lepper (2005); Padcoal (Pvt) Ltd (2011)	1	200	300	250	0	9	5
	Lubimbi	Oesterlen & Lepper (2005)	1	12	190	101	2	47	25
	Busi		1	60	80	70	10	20	15
	Tjolutjo, Sawmills, and Insuza		1	270	330	300	0	9	5
Botswana	Northeast Botswana	Smith (1984), Anglo Coal Botswana, (2010) Potgieter (2015)	39	5	793	96	1	24	10

## 5. ASSESSMENT OF THE CBM RESOURCE OF THE STUDY AREA

Production of CBM in Zimbabwe, has been proven in a number of key wells by Shangani Energy, falling within the study area, indicated in Figure 46 (Maponga, 2014). No production has been proven in north-eastern Botswana to date. For the study Schlumberger GeoX software was used to determine the gas in place (GIP) volumes. The determination of the GIP was achieved by a Monte Carlo simulation of the Aminian (2005) CBM resource equation.

$$GIP = A \times h \times RHOB_{(c)} \times G_{(c)}$$

Where:

A =	Area (km <sup>2</sup> )
h =	Coal thickness (m)
RHOB <sub>(c)</sub> =	Coal density (g/cm <sup>3</sup> )
G <sub>(c)</sub> =	Gas content (scf/tonne)

Equation 2 Calculation of gas in place volumes (Aminian, 2005).

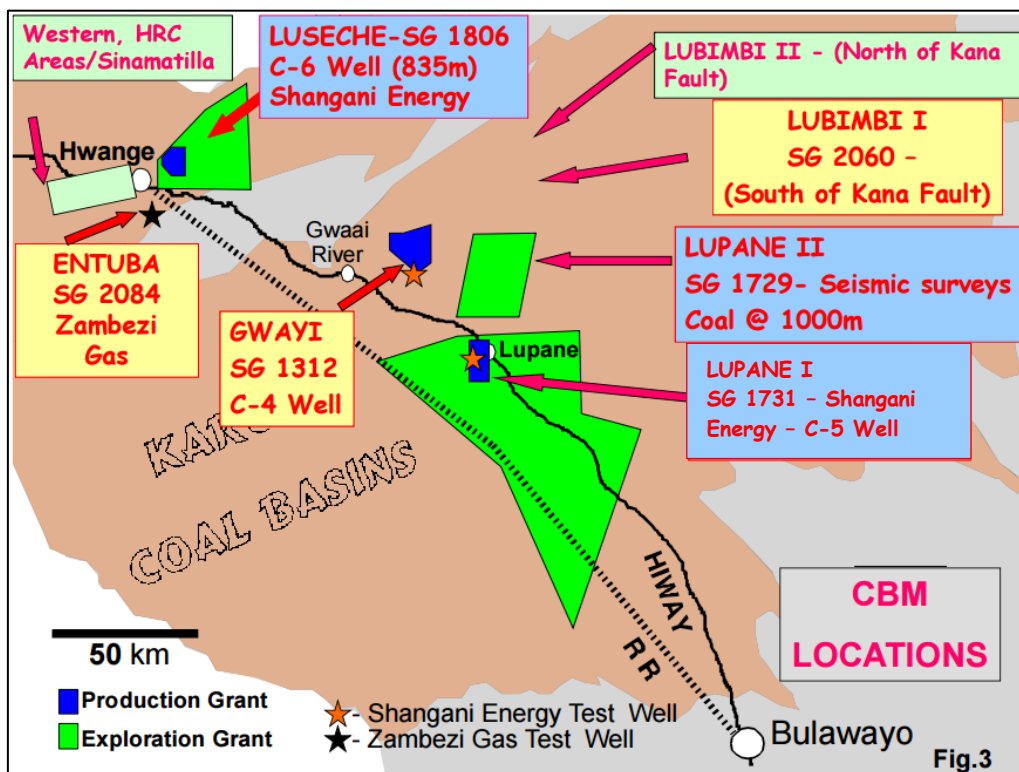


Figure 46 Shangani Energy exploration and production grants in Zimbabwe showing the test location from which CBM was produced (Maponga, 2014).

Not all the inputs required for the resource evaluation were directly measured and reported in the drilling record as some data was not applicable to coal exploration.

The coal thickness measurements (h) were taken from regional drilling records and reports. The extent of the Karoo Supergroup from GIS data was used to determine aerial component (A) of the resource evaluation.

Due to a lack of widely measured Coal Density ( $RHOB_{(c)}$ ) and Gas Content ( $G_{(c)}$ ) data these values had to be inferred using the existing data compared to some sparse measurements taken by mainly Anglo Coal Botswana (2010) in north-eastern Botswana and Kubu Energy (2014) from a coal field in central Botswana. The Kubu Energy (2014) data, comprising nine CBM exploration wells (Figure 47), is one of the most comprehensive collected in the region (Potgieter, 2015). This dataset includes comprehensive geological, gas desorption, proximate, adsorption isotherm and petrological information from all nine boreholes drilled (Kubu Energy, 2014). The Kubu Energy exploration boreholes marginally fall outside the study area within the Northern Belt Central Kalahari sub-basin. Smith (1984) determined that the lithostratigraphic divisions of the Northern Belt Central Kalahari and North East Botswana sub-basins are the same (Figure 19). The Kubu Energy boreholes were not included in the assessment but were used as an analogue for the determination of the poorly measured data that is required for the CBM resource assessment.

Without key production capacity parameters such as permeability tests, detailed isotherm measurements and gas contents it is impossible to estimate a recovery factor for a basin of this size. Reviewing other regional studies where this information was available, in some form, a great deal of variation was noted (Table 12). Recovery factors can also be influenced by adjusting the production well spacing, drilling method, type of reservoir stimulation and biogenic or carbon dioxide enhancement methods (Boyer, et al., 2007; Swindell, 2007; Litynski, et al., 2014 and Fallgren, et al., 2013).

**Table 12 CBM recovery factors for three North American plays.**

Area	Recovery Factor (%)	Source
Horseshoe Canyon	26 - 39	Jenkins (2008)
Mannville	21 - 38	Jenkins (2008)
United States (Lower 48 States) - Generalised	14	Nuccio (2000)

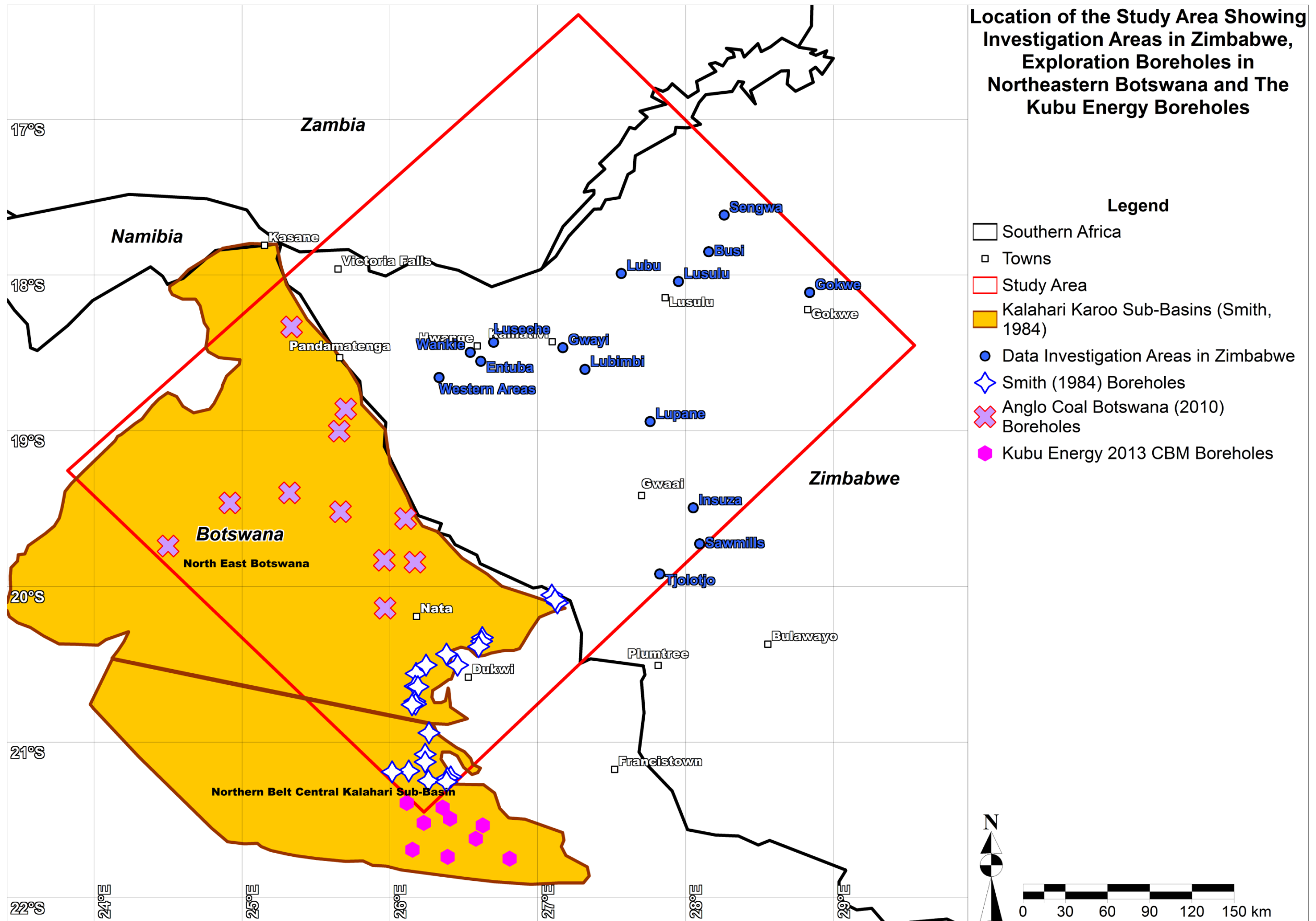
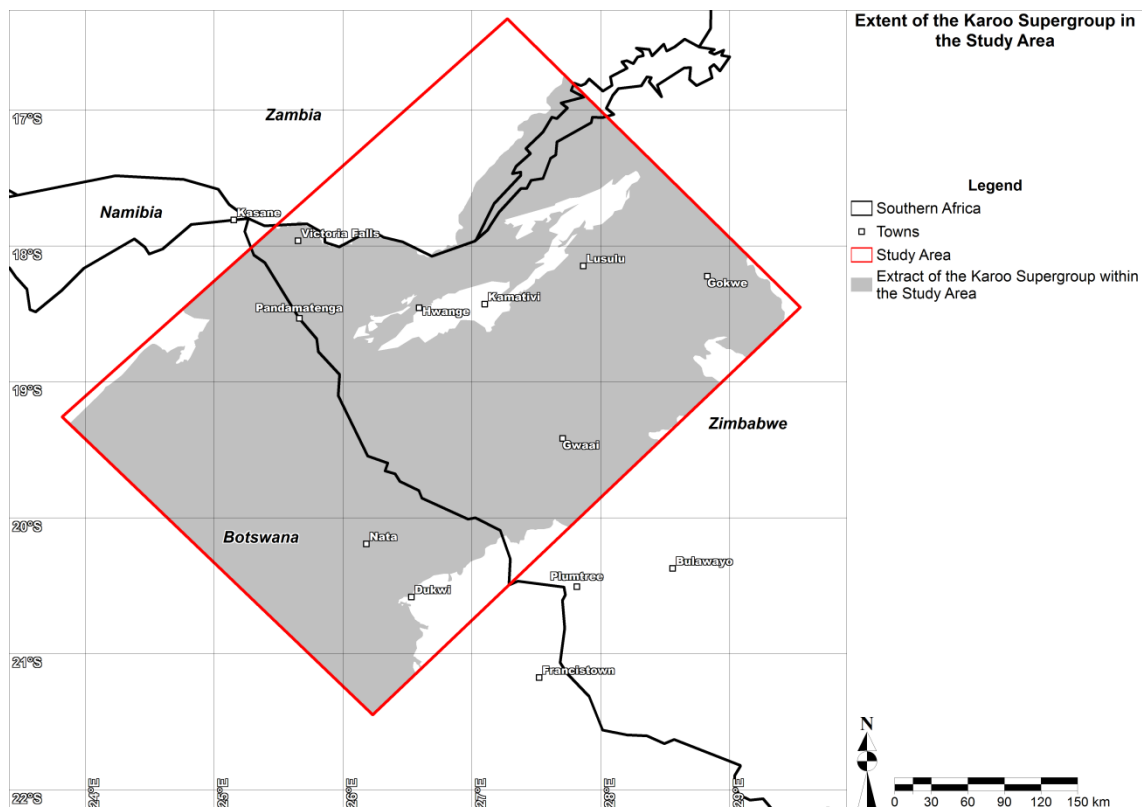


Figure 47 Location of the study area showing investigation areas in Zimbabwe, exploration boreholes in north-eastern Botswana and the Kubu Energy boreholes.

## 5.1. Area

For the Area (A) component of the investigation the mapped Karoo Supergroup from GIS datasets by (Pitfield, 1996), (Mothibi, 1999) and (Persits, et al., 2011) was extracted for only the study area (Figure 48). Even though the study area has a surface extent of 167 057km<sup>2</sup> the area occupied by Karoo Supergroup rocks is only 134 666km<sup>2</sup>.



**Figure 48** Extent of the mapped Karoo Supergroup in the study area (after Pitfield, 1996; Mothibi, 1999 and Persits, et al., 2011).

## 5.2. Coal Thickness

A total of 250 coal thickness (h) measurements available in the reports by Anglo Coal Botswana (2010), Oesterlen & Lepper (2005) Palkos (1984) and Thompson (1981) and Smith, (1984) were statistically analysed (Table 13) to compile a histogram (Figure 49) of the total coal thicknesses. The distribution of the data is lognormal with thicknesses ranging from 1m to 23.65m.

Table 13  
Summarised statistics of all total coal thickness values across the study area.

Summary Statistics of Total Coal Thickness Data (m)	
Mean	9.58
Median	9.66
Mode	11.66
Standard Deviation	3.67
Range	22.65
Minimum	1.00
Maximum	23.65
Count	250

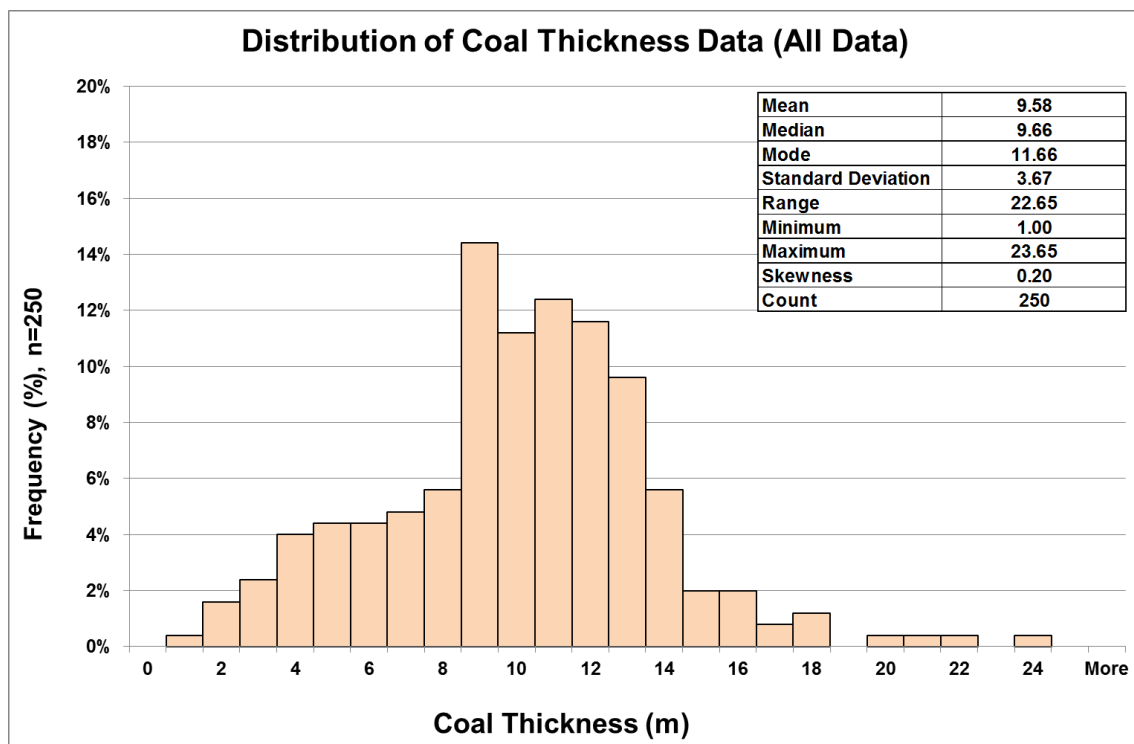
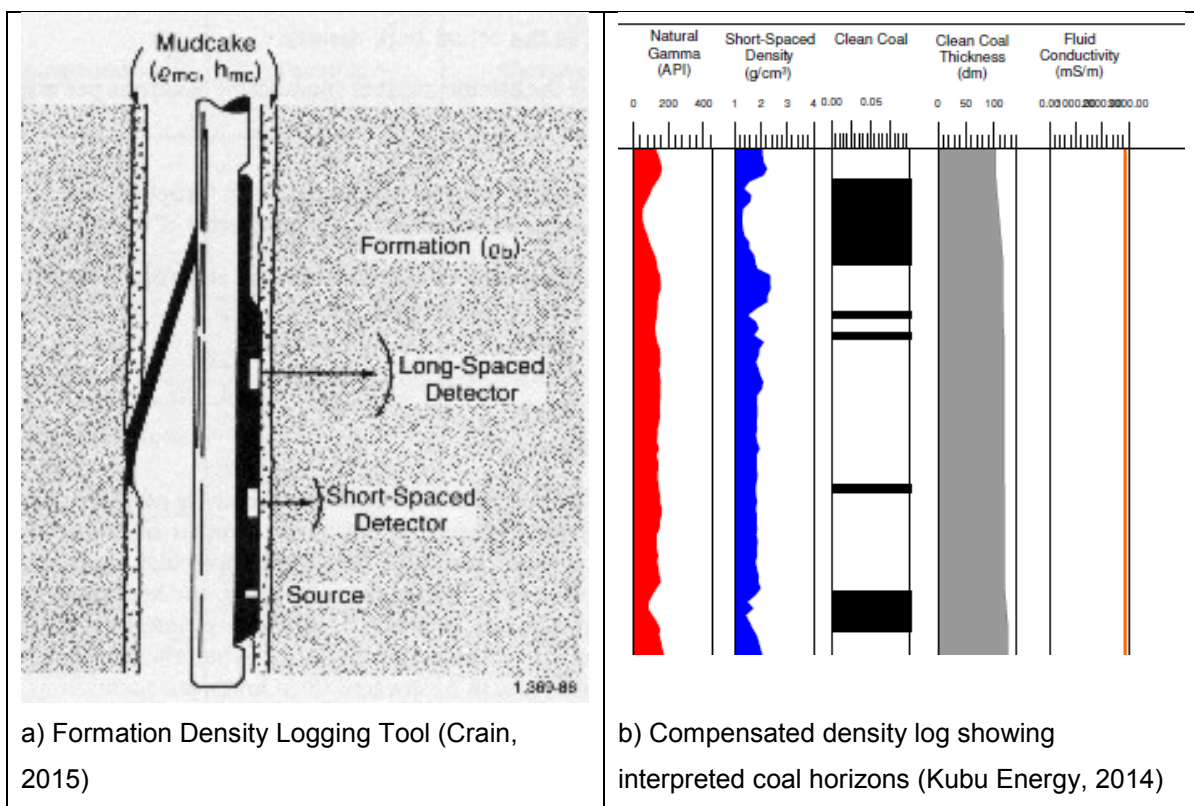


Figure 49 Distribution of total coal thickness data.

### 5.3. Coal Density

The coal density ( $RHOB_{(c)}$ ) values of the coal are used to calculate the bulk weight of the coal along with the thickness (h) and area (A) data. The density can be determined from laboratory analyses and using wireline geophysics. The wireline tools can also be used to identify clean coal in the borehole.

The primary tool used by Anglo Coal Botswana (2010); and Kubu Energy, (2014) for coal identification from exploration boreholes is the formation density logging tool. The tool is sidewall tracking (Figure 50a) with a single arm calliper, measuring the geometry of the borehole. The calliper and density ( $RHOB_{(c)}$ ) data is processed together to remove any false density readings based on sidewall rigosity. The resultant log is referred to as the compensated density log. Anglo Coal Botswana, (2010) used a bulk density cut-off of  $1.8g/cm^3$  and Kubu Energy (2014) a cut-off of  $1.75g/cm^3$ , where all densities lower than the cut-off density are regarded as coal intervals (Figure 50b).



**Figure 50** Formation density logging tool and compensated density log indicating coal seams.

Computer Support Group (2011) reported the laboratory determined density of solid bituminous coal to be  $1346kg/m^3$  ( $1.346g/cm^3$ ) and solid anthracite as  $1506kg/m^3$  ( $1.506g/cm^3$ ). An analysis of the wireline logs from the Kubu Energy drilling campaign in Botswana showed that all measurements less than  $1.75g/cm^3$  measurements were distributed between  $1.1g/cm^3$  and  $1.75g/cm^3$  (Kubu Energy, 2014), the statistically determined mode was  $1.70g/cm^3$  (Table 14 and Figure 51).

Table 14 Summarised statistics of density values less than 1.75g/cm<sup>3</sup> obtained from the Kubu Energy (2014) wireline logs.

Summary Statistics of Wireline Density Data less than 1.75g/cm <sup>3</sup> (g/cm <sup>3</sup> )	
Mean	1.53
Median	1.55
Mode	1.70
Standard Deviation	0.14
Range	0.64
Minimum	1.11
Maximum	1.75
Count	13427

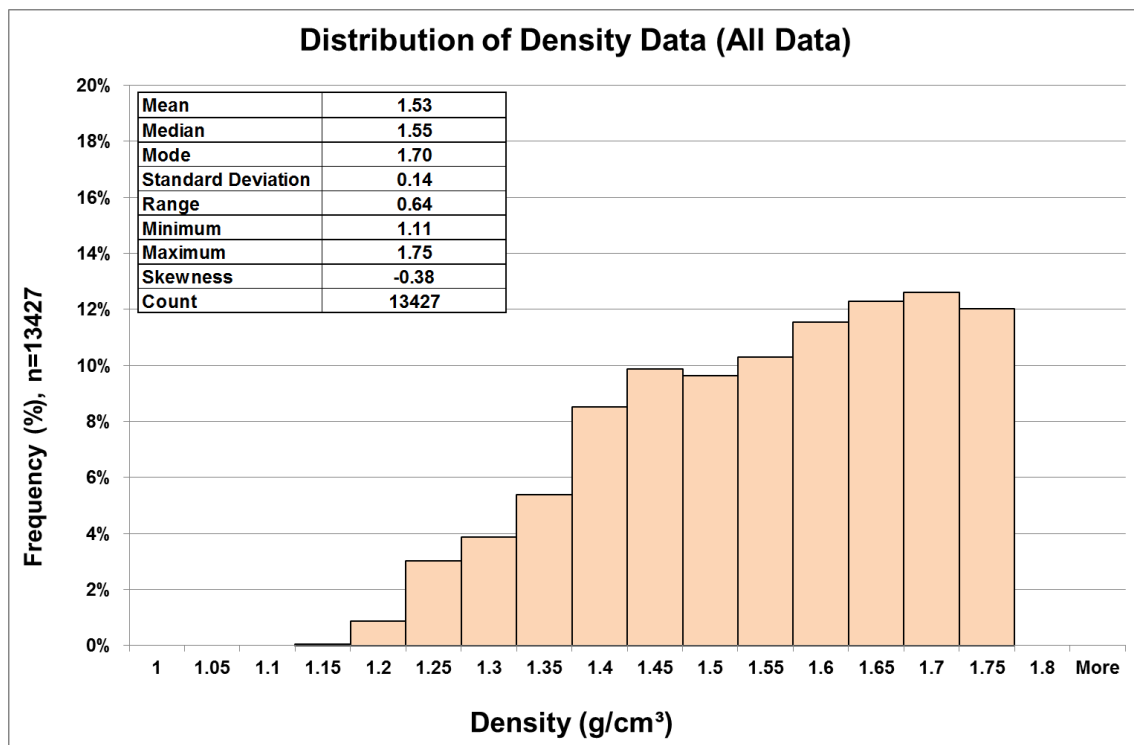


Figure 51 Distribution of densities from the compensated density logs of all values less than 1.75g/cm<sup>3</sup> collected from 9 coal exploration boreholes in Botswana (after Kubu Energy, 2014).

#### 5.4. Gas Content

The measurement and determination of the gas content ( $G_{(c)}$ ) forms an integral part of the resource evaluation. As very little CBM exploration has taken place in the study area it is necessary to infer the potential gas content values of the coal from the coal quality data. This was achieved by evaluating the coal quality measurements and calculating a possible gas content for the coal seams using the graphs published by Eddy, et al. (1982) using the measured depths of the coal seams.

Saturation evaluations require accurate gas content measurements combined with the adsorption isotherm measurements, however, previous investigations in the region have not been consistent in the quality control of measurements and there is a lack of reliable adsorption isotherm data in the public domain (Potgieter, 2015). For the evaluation a range of saturations will be used based on the evaluations by Kubu Energy (Faiz, et al., 2013) and Shangani Energy (Barker, 2006).

A number of sources were used to obtain the depth and thickness of the coal measures. ACB drilled 12 CBM exploration boreholes in north-eastern Botswana (Anglo Coal Botswana, 2010); Thompson (1981), Palloks (1984) and Oesterlen & Lepper (2005) evaluated a series of datasets from the main coal fields in Zimbabwe. Shangani Energy drilled a number of CBM exploration boreholes in Zimbabwe, these borehole results were illustrated by (Barker, 2006) at the Botswana resources sector conference. Figure 52 and Table 15 show the locations and types of data available for this evaluation.

There is a lack of regionally available gas composition data in the public domain with the only freely available dataset being from central Botswana (Kubu Energy, 2014). The incorporation of gas content values in this evaluation was impossible and with the aim of evaluating the total resource in place did not add any material value. In more localised evaluations where gas composition data is available it is essential to fully understand the impact of composition on commerciality.

Table 15

Data sources and types used throughout this evaluation.

Source	Area	Data Types
<b>Anglo Coal Botswana (2010)</b>	Northeastern Botswana	<i>Borehole data, gas content measurements and report on exploration findings</i>
<b>Smith (1984)</b>	Northeastern Botswana	<i>Borehole data, report on regional coal information</i>
<b>Thompson (1981)</b>	Lubimbi	<i>Report on coal occurrences and quality</i>
	Dahlia & Hankano	
<b>Palloks (1984)</b>	Entuba	<i>Report on coal occurrences and quality</i>
	Lubu	
	Lusulu	
	Sengwa	
	Western Areas	
	Wankie	
<b>Oesterlen &amp; Lepper (2005)</b>	Bari	<i>Reporting of coal intersections and general coal quality data</i>
	Busi	
	Insuza	
	Kaonga	
	Lubimbi	
	Lubu	
	Lusulu	
	Sawmills	
	Sebungu	
	Sengwa North	
	Senwa South	
	Sessami	
	Tsholotsho	
	Wankie	
<b>Barker (2006) – Shangani Energy</b>	Entuba	<i>Conference Presentation: Maps and graphs of depths and gas content information</i>
	Gwaai	
	Lupane	
	Sengwa	
	Wankie	

Zimbabwe

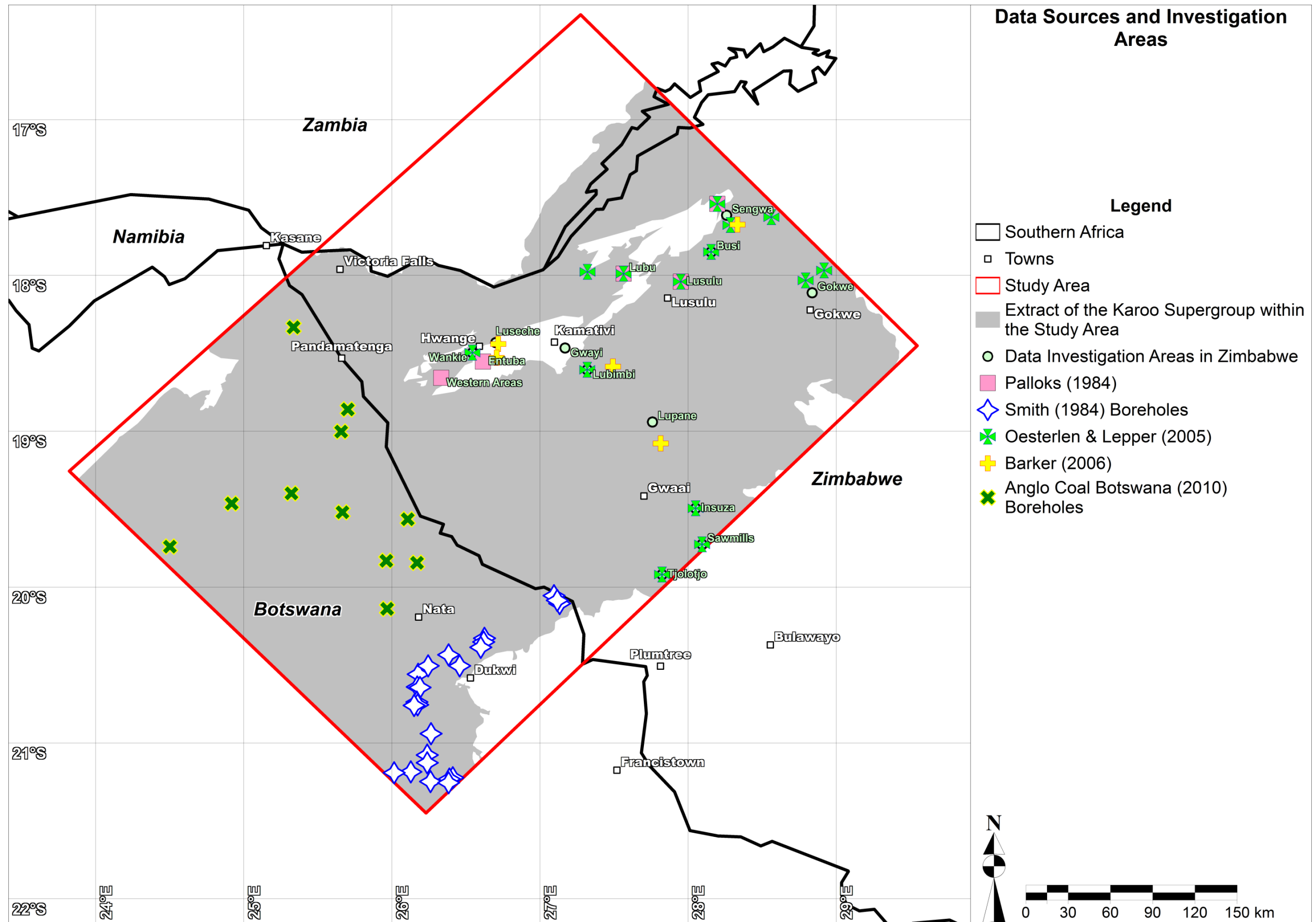


Figure 52 Investigation areas in Zimbabwe and boreholes in Botswana used in this evaluation (after Thompson, 1981; Palkos, 1984; Smith, 1984; Oesterlen & Lepper, 2005; Barker, 2006 and Anglo Coal Botswana, 2010).

### 5.4.1. Hydrocarbon Generation Potential of Coal

Hydrocarbon generation within carbonaceous material is controlled by three components, 1) carbon content, 2) kerogen type and 3) thermal maturity. The carbon content and kerogen type are mainly controlled by the depositional system and provenance of sediments in a basin and the thermal maturity is controlled by the maximum pressures and temperatures to which the kerogen and organic carbon has been subjected to. Coal contains predominantly Type III and IV kerogens (Table 16) and the resulting hydrocarbons are predominantly gas, however, it is possible that some oils may be generated (SPE UGM SC, 2014). Evidence of oil in the coal seams has been noted at Wankie by Palloks (1984) and Thompson (1981) with up to 2.5% oil content in some samples. Thompson (1981) regarded the oil as a Fischer-Tropsch oil and the regional distribution is not understood fully, thus it will not be evaluated as part of this study.

**Table 16 Kerogen types as determined by visual kerogen analysis, origin, and hydrocarbon potential (SPE UGM SC, 2014).**

Depositional Environment	Other	Palynology System	Kerogen Form	Kerogen Type	Hydrocarbon Potential
Lacustrine	Lacustrine Sapropel	Algal (Plankton)	Alginite	I	Oil
Aquatic (typically marine)	Marine Sapropel	Fluorescing Amorphous	Fluorescing Amorphous	I or II	Oil
		Herbaceous	Exinite	II	Oil/Condensate
		"	Resinite	II	"
		"	Liptinite	II	"
		"	Suberinite	II	"
		"	Sporinite	II	"
Terrestrial	Humic	Non-fluorescing Amorphous	Non-fluorescing Amorphous	III or IV	Gas or None
		Woody Cellulose	Vitrinite	III	Gas mainly. May have some oil potential, especially in SE Asia if "HI" is > 150.
		Coaly	Inertinite	IV	Dead Carbon No Potential

Thermal maturity is mainly measured by 1) the reflectance of vitrinite (RoV or RV) during petrological examination and 2) maximum kerogen temperature (Tmax) calculated during Rock-Eval measurements (Figure 53). The maturity is controlled by pressure and temperature which in turn is controlled by the depth of burial.

Different types of hydrocarbons are generated within specific maturity ranges (Figure 54) (McCarthy, et al., 2011).

Maturation rank		Paleo Temp. (1) (°C)	Microscopic parameters				Chemical parameters					
Kerogen	Coal		Vitrinite Reflectance (Ro %)	TAI (2)	SCI (2)	CAI	Fluorescence of alginite	T <sub>max</sub>	Biomarker Isomerization Sterane Hopane		Hydrocarbon main products	
Immature	Peat	50	0.2	1 Yellow	1	1	Bue-green	420	0,10	0,10	Bacterial gas	
	Lignite		0.3				2					Golden yellow
	Sub-bituminous Coal		0.4				3					Yellow
Mature	Bituminous Coal	100	0.5 – 0.55	2 Orange	4	2	Dull yellow	430	0,50	0,50	Immature heavy oil (3)	
Very Mature			0.7				5					Light brown
High Maturity			0.8				6					Orange
			1.0				7					
1.35			8				3 Brown					Red
1.5	9											
Overmature	Semi Anthracite	150	2.0	10	5	Black	500	None	None	Wet gas		
Organic Methamorphisme	Anthracite	200	2.5	4 Brown/Black	9	4 Dark brown	Nonfluorescent	None	None	None	Dry gas	
			3.0									5
	Meta Anthracite	250	4.0	5	Black							
			5.0									

(1) Depending by duration (2) International standard is not available - a lot of correlation scales are present in literature (3) Depending also by kerogen type

Figure 53 Correlation of maturity and coal type (Corrado, et al., 2010).

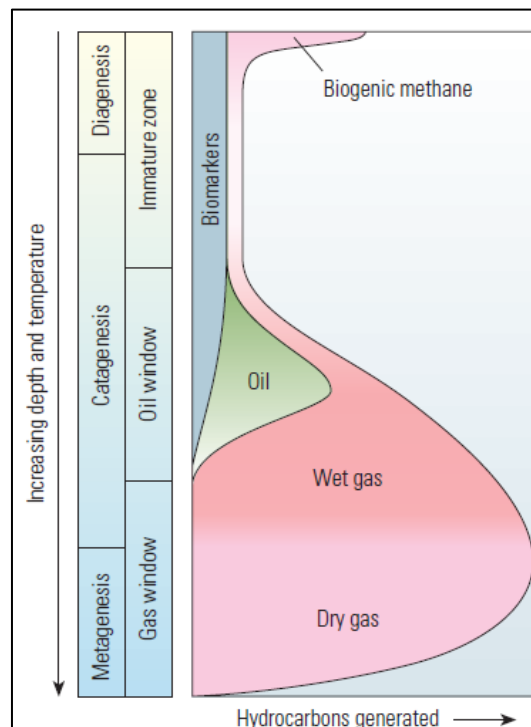


Figure 54 The temperature transformation of kerogen with increased depth and temperature (McCarthy, et al., 2011).

As the coal is subjected to greater pressures and temperatures the vitrinite, derived from cell wall wood material, undergoes different stages of maturation resulting in an increase of the reflectance of vitrinite. Vitrinite Reflectance (RoV) is a measurement of the percentage of light reflected off the vitrinite maceral at 500X magnification in oil immersion (Cardott, 2012). As part of the Western Canada Sedimentary Basin (WCSB) Atlas Smith, et al. (1994) produced a table outlining the expected (RoV) ranges for the volatile matter, moisture and heating value for specific coal ranks (Figure 55).

Coal rank		Vitrinite reflectance (random)	Volatile matter <sup>1</sup> (wt.% dmmf)	Bed moisture (wt %)	Calorific value MJ/kg (moist, rmmf)	Hydro-carbon generation	Principal uses					
Class	Group											
Anthracitic <sup>2</sup>	Meta-anthracite	2.50	2	8-10	32.6	Dry Gas	Space heating Chemical production					
	Anthracite		8									
	Semianthracite		14									
Bituminous	Low volatile bituminous	1.51	22	26.8	30.2	Wet Gas	Metallurgical coke production Cement production Thermal electric power generation					
	Medium volatile bituminous		31									
	High volatile A bituminous	0.50-0.75	31									
	High volatile B bituminous											
	High volatile C bituminous											
	Subbituminous	Subbituminous A <sup>3</sup>	0.50 ?					31	24.4	22.1	Oil and Gas	Thermal electric power generation Conversion to liquid and gaseous petroleum substitutes
		Subbituminous B										
Subbituminous C												
Lignitic	Lignite A	0.42	35	19.3	14.7	Early Gas	Thermal electric power generation Char production Space heating					
	Lignite B											
	Peat		75									

1) dmmf - Dry, mineral matter free  
2) Non-agglomerating; if agglomerating, classified as low volatile bituminous  
3) If agglomerating, classified as high volatile C bituminous

**Figure 55 Coal rank classification based on maturity, moisture content, volatile matter content and heating value (Smith, et al., 1994).**

The generation of hydrocarbons in source rocks are primarily controlled by the process where kerogens are transformed into “dead carbon”, this process is known as cracking and is controlled by depth and pressure increases. The three primary stages of the maturation process are 1) diagenesis, 2) catagenesis and 3) metagenesis which are controlled by thermal and pressure increases, mainly due to an increase in the burial depth as a result of increased sediment load and basin subsidence. During the early stages of diagenesis biologically controlled gas is

mainly formed (McCarthy, et al., 2011). The generation of biogenic methane has been noted as the dominant gas source in the Central Kalahari Basin in Botswana by Faiz (2014). As part of the Kubu Energy drilling campaign a comprehensive sampling and analysis programme was followed (Faiz, et al., 2013). During this programme a far more expanded isotope sampling project of the desorbed methane was conducted compared to the previous ACB campaigns in Botswana (Anglo Coal Botswana, 2010; Faiz, et al., 2014 and Potgieter, 2015). The dominance of biogenic gas has a noted adverse effect on the saturation levels of the coals and subsequently the gas production capacity (Zheng, et al., 2011). A lack of widespread sample data across the region remains one of the shortcomings in the available database for CBM evaluation (Potgieter, 2015).

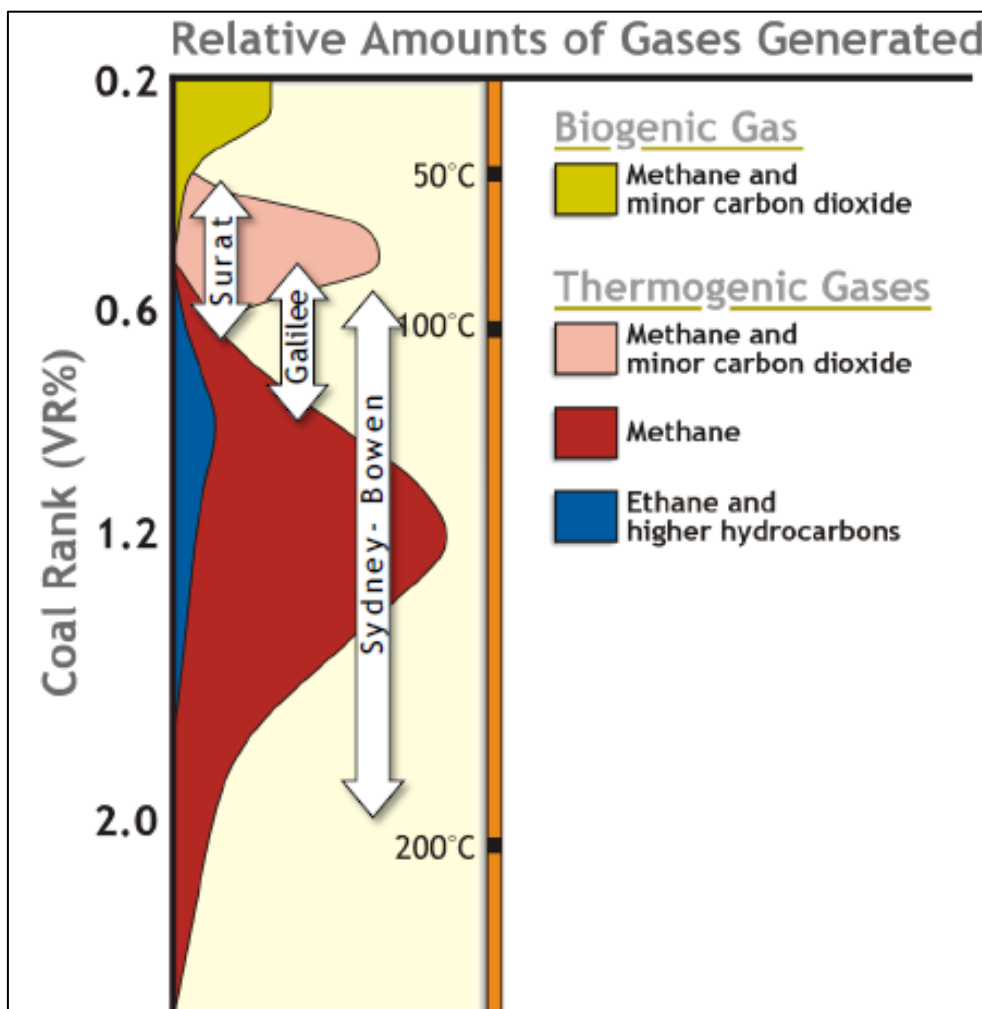


Figure 56 Relative gas production amounts from coal in selected Australian basins (Faiz, et al., 2012).

During catagenesis, resulting from further burial, oil and gas is generated with rich and dry simple gasses being formed at even greater burial depths during metagenesis (McCarthy, et al., 2011). Faiz (2012) showed that the Permian coals of Australia have the ability to generate thermogenic gas across a wide range of thermal maturities. The Bowen Basin in eastern Australia has the potential to produce methane and higher hydrocarbons in a range from 0.6% Vitrinite Reflectance (VR) to greater than 2% VR with peak production around 1.2%VR (Figure 56).

#### 5.4.2. *Estimation of the Gas Content of the Coal in the Study Area*

As part of the Central Kalahari Exploration Campaign in Botswana Kubu Energy sampled the coal intersections extensively and collected a total of 41 isotherm samples (Kubu Energy, 2014). The coals were extensively intruded by dolerite sills that had a noted effect on the coal quality and gas content measurements (Kubu Energy, 2014; Faiz, et al., 2013; Faiz, et al., 2014 and Potgieter, 2015). However, it remains difficult to determine the true effect of intrusives on the apparent rank and maturity of the coal. Faiz (2014) found that in Central Botswana the dolerite intrusion had the potential to increase specific samples from the 0.5%VR average to >4%VR and in a study of coals from the Gunnedah Basin, Australia Gurba & Weber (2001) determined that the intrusions were capable of increasing the rank from the average 0.67%VR to 6%VR. Faiz (2014) demonstrated the effects of the intrusions are localised a generalised rank of the coal across the region was used to determine the potential gas holding capacity.

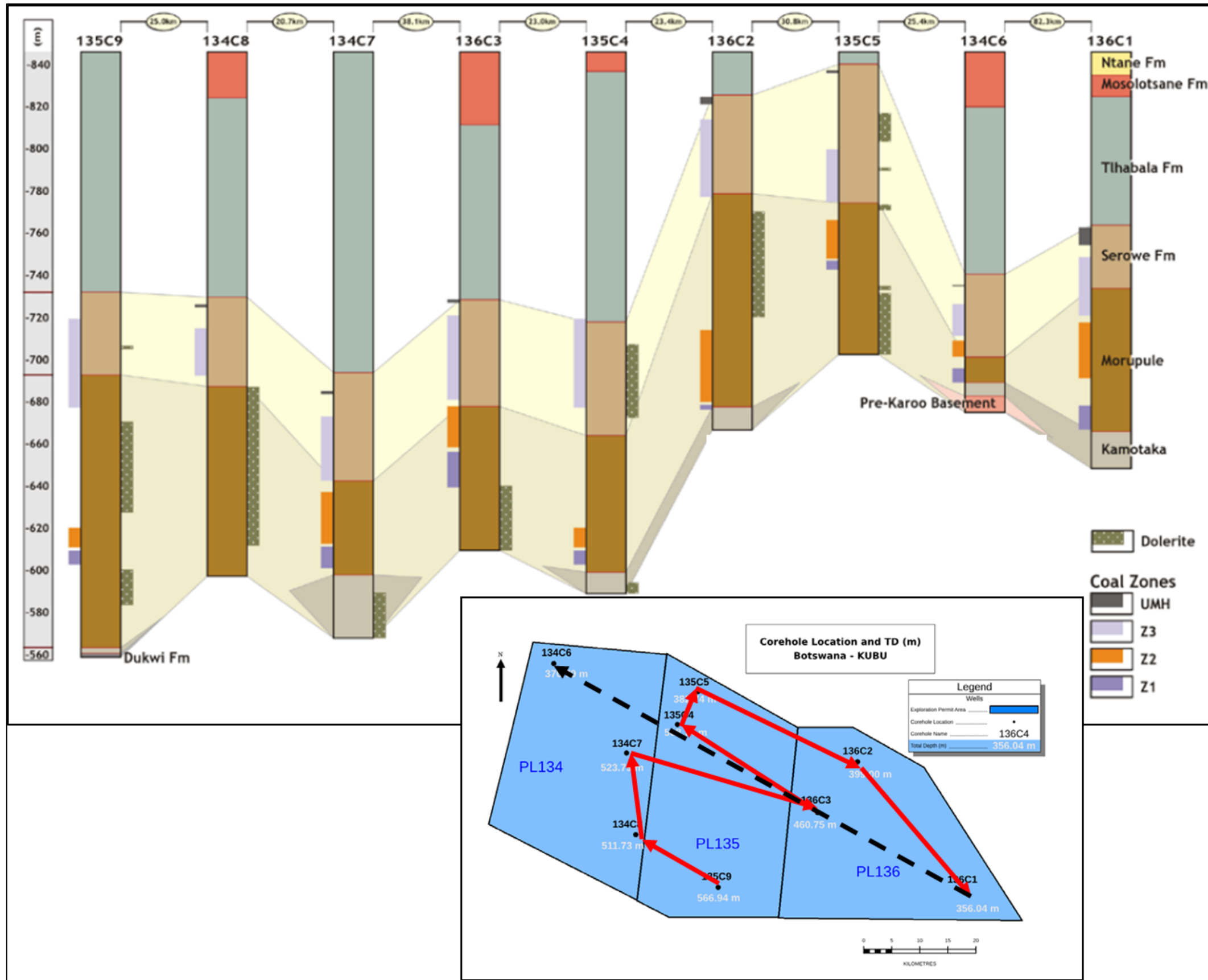


Figure 57 Simplified elevation cross-section across the Kubu area showing the encountered coal seams and dolerite intrusions (Faiz, et al., 2013).

The isotherm samples collected and analysed by Kubu made it possible to calculate the maximum gas holding capacity for each of the coal zones intersected. The dataset was reviewed and boreholes were selected to be evaluated with respect to the gas generation and storage capacity, see Appendix D for the full dataset. For this selection of the data to be analysed additional criteria were used and only samples that comply with the thresholds were evaluated further (Table 17). Of the original 41 samples ten were extracted for further isotherm data evaluation (Table 18).

**Table 17 Selection parameters and thresholds.**

<b>Parameter</b>	<b>Threshold</b>	<b>Threshold Description</b>
<b>1 Dolerite Intrusives</b>	<i>Proximity of sample may not be less than 30m from a dolerite intrusive</i>	The effect of the intrusives is difficult to fully quantify however, Faiz (2014) demonstrated that the effects in borehole 134C7 the coal rank was significantly increased with respect to the surrounding samples.
		The average thickness of the intrusives encountered is 29.9m. A minimum proximity of 30m was selected to compensate for 1:1 thermal effect range around intrusives.
<b>2 Measured Gas Content</b>	<i>Measured gas content values must be greater than 20scf/T</i>	Gas content lower than 20scf/T are regarded as low and was regarded as contributing factors to the sub economic status of the project (Kubu Energy, 2014 and Potgieter, 2015).

**Table 18** Subset of samples used in the gas content evaluations.

Sample Sequence	Borehole	Depth From	Depth To	Sample Mid-Point	Sample Number	Zone	Sampling						Intrusives	
							Gas Description	Isotherm Analyses			Proximate Analysis	Vitrinite Reflectance	Proximity to Intrusive <30m	Vertical Thickest Intrusive Thickness (m)
		Methane	Nitrogen	Carbon Dioxide										
		(m)	(m)	(m)										
12	134C7	462.86	463.14	463.00	CH-7-021	Z2	✓	✓			✓	✓		
14	134C6	319.59	320.19	319.89	CH-6-002	Z3	✓	✓			✓	✓		
15	134C6	328.84	329.40	329.12	CH-6-008	Z3	✓	✓			✓	✓		
16	134C6	340.05	340.64	340.35	CH-6-013	Z2	✓	✓			✓	✓		
25	135C4	450.82	451.40	451.11	CH-04-D7	Z2	✓	✓	✓		✓	✓		
28	136C3	364.70	365.00	364.85	CH-03-005	Z3	✓	✓			✓	✓		
38	136C1	268.38	268.98	268.68	CH-01 D004	Z3	✓	✓			✓	✓		
39	136C1	275.24	275.44	275.34	CH-01 D005	Z3	✓	✓			✓	✓		
40	136C1	277.30	277.90	277.60	CH-01 D006	Z3	✓	✓		✓	✓	✓		
41	136C1	279.96	280.17	280.07	CH-01 D008	Z3	✓	✓	✓	✓	✓	✓		

The isotherm analyses provide information that can be used to determine the maximum sorptive capability of a sample at a specific reservoir pressure. This pressure is related to the depth of a coal seam if the pressure gradient is known. The coal seams evaluated for the Kubu Energydrilling campaign generally were not over-pressured and a hydrostatic pressure gradient of 0.433psi/ft was used in the evaluations (Kubu Energy, 2014 and Potgieter, 2015).

The key parameters (Figure 58) that were derived during the isotherm analysis were the Langmuir Volume ( $V_L$ ), the maximum volume of gas that can be adsorbed by coal at infinite pressure, and Langmuir Pressure ( $P_L$ ) also known as the critical desorption pressure (CDP), the pressure at which one half of the Langmuir volume can be adsorbed by the coal (IHS Inc., 2014).

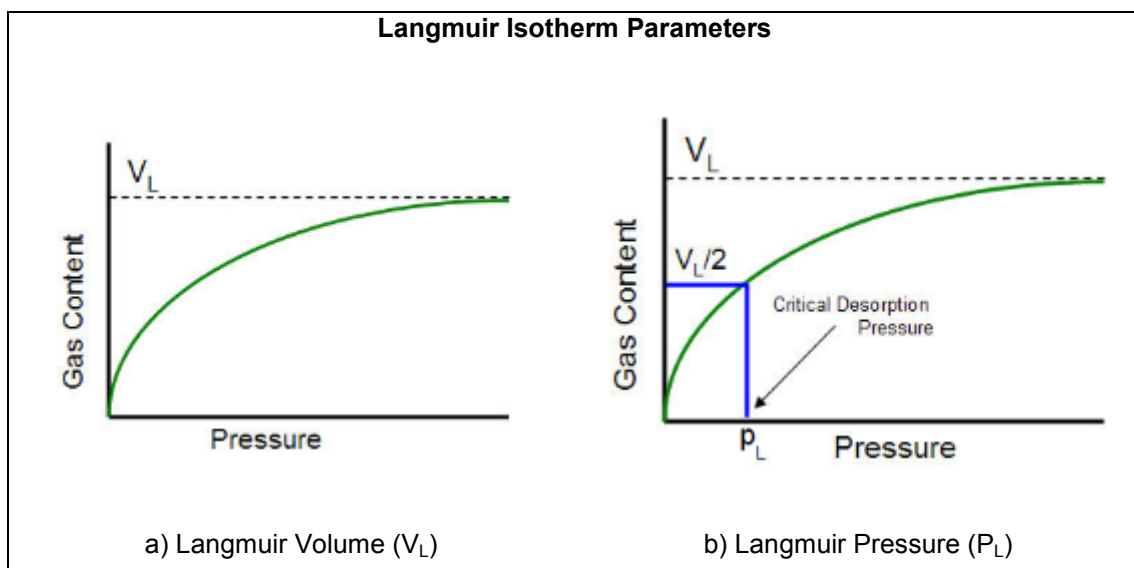


**Figure 58** Langmuir isotherm parameters (IHS Inc., 2014).

IHS Inc. (2014) provided an equation to determine the maximum gas holding capacity for specific pressures (Equation 3). This equation assumes that the entire sample analysed contributes to the gas generation and storage capacity. The ash, volatile matter and moisture contents in the coal are inert in the generation and storage capacity. As a result of this IHS Inc. (2014) showed an equation for calculating the dry, ash-free (DAF) gas contents (Equation 4). The DAF gas content calculation can be simplified, in a similar way as calculating DAF volatiles or fixed carbon equation by Snyman (1998), as used in this evaluation (Equation 5).

$$G_{(c)} = \frac{V_L \rho}{P_L + \rho}$$

Where:

$G_{(c)}$  = Gas content (scf/T)  
 $V_L$  = Langmuir Volume (scf/T)  
 $P_L$  = Langmuir Pressure (psi)  
 $\rho$  = Sample Pressure

**Equation 3** Determination of gas content from a Langmuir isotherm (IHS Inc., 2014).

$$^{DAF}G_{(c)} = (1 - C_a - C_w) \frac{V_L \rho}{P_L + \rho}$$

Where:

$^{DAF}G_{(c)}$  = Dry, Ash-Free Gas Content (scf/T)  
 $C_a$  = Ash Content (decimal fraction)  
 $C_w$  = Moisture Content (decimal fraction)  
 $V_L$  = Langmuir Volume (scf/T)  
 $P_L$  = Langmuir Pressure (psi)  
 $\rho$  = Sample Pressure

**Equation 4** Determination of dry, ash-free gas content from a Langmuir isotherm (IHS Inc., 2014).

$$^{DAF}G_{(c)} = \frac{G_{(c)}}{(100\% - C_a - C_w)}$$

Where:

$^{DAF}G_{(c)}$  = Dry, Ash-Free Gas Content (scf/T)  
 $G_{(c)}$  = Raw Gas content (scf/T)  
 $C_a$  = Ash Content (%)  
 $C_w$  = Moisture Content (%)

**Equation 5** Determination of dry, ash-free gas content (after Snyman, 1998).

The subset of ten samples was evaluated and the maximum gas holding capacities, both raw and DAF were calculated (Table 19). The maximum DAF gas holding capacities ranged from 67scf/T to 239scf/T whereas, the DAF measured gas contents 118scf/T to 319scf/T.

**Table 19** Data evaluation of the select Kubu samples (after Kubu Energy, 2014).

Sample Sequence	Borehole	Sample Mid-Point Depth	Sample Number	Sample Analyses										Data Interpretation							
				Measured Gas Content		Proximate Analysis						Vitrinite Reflectance	Isotherm Analysis			Isotherm Data Interpretation					
		Raw		Dry, Ash-Free	Air Dried			Ash-Free			Langmuir Pressure		Langmuir Volume	Langmuir Volume (Dry, Ash-Free)	Hydrostatic Pressure Gradient	Depth	Formation Pressure	Gas Content (Raw)	Gas Content (Dry, Ash-Free)		
					Moisture	Ash	Volatile Matter	Fixed Carbon	Moisture	Volatile Matter										Fixed Carbon	% VR (mean)
scf/T	scf/T	%	%	%	%	%	%	%	%	%	%	%	psia	scf/T	scf/T	psi/ft	ft	psi	scf/T	scf/T	
12	134C7	463.00	CH-7-021	26.78	32.12	3.72	12.91	32.05	51.33	4.27	36.80	58.94	0.55	749	224	364	0.43	1519.01	672.43	105.97	172.20
14	134C6	319.89	CH-6-002	21.78	42.05	5.99	42.21	23.38	28.41	10.37	40.46	49.17	0.47	1073	223	454	0.43	1049.50	469.13	67.84	138.11
15	134C6	329.12	CH-6-008	37.11	47.18	5.27	16.07	34.62	44.04	6.28	41.25	52.47	0.51	707	307	404	0.43	1079.78	482.24	124.49	163.82
16	134C6	340.35	CH-6-013	39.94	49.05	4.98	13.60	32.00	49.41	5.77	37.04	57.19	0.60	700	308	408	0.43	1116.60	498.19	128.06	169.64
25	135C4	451.11	CH-04-D7	56.73	67.23	2.31	13.30	28.53	55.86	2.66	32.91	64.43	0.84	580	450	601	0.43	1480.00	655.54	238.76	318.87
28	136C3	364.85	CH-03-005	37.55	50.12	2.10	22.98	29.07	45.84	2.73	37.75	59.52	0.83	709	371	534	0.43	1197.00	533.00	159.21	229.16
38	136C1	268.68	CH-01 D004	33.23	44.71	5.45	20.23	31.50	42.82	6.84	39.49	53.68	0.47	867	262	378	0.43	881.49	396.38	82.20	118.60
39	136C1	275.34	CH-01 D005	33.13	45.05	5.43	21.04	30.70	42.84	6.87	38.87	54.25	0.49	757	254	359	0.43	903.34	405.84	88.65	125.29
40	136C1	277.60	CH-01 D006	33.32	51.03	4.71	29.99	25.84	39.46	6.73	36.91	56.36	0.47	771	225	384	0.43	910.75	409.05	77.99	133.11
41	136C1	280.07	CH-01 D008	32.33	39.16	5.08	12.37	32.94	49.62	5.79	37.59	56.62	0.50	894	323	429	0.43	918.84	412.56	101.99	135.46

Based on laboratory measurements Eddy (1982), reported by Stoeckinger (1991), evaluated the sorptive capacity for different coal types and presented it as a gas content versus depth graph (Figure 59). This graph was digitised and trend lines of the sorptive capacity of the coals created (Figure 60).

It was possible to determine equations for these trend lines (Table 20) that could be used to calculate the sorptive capacities based on depth and quality. In all cases a  $R^2$  value greater than 0.9 was found. This is indicative of a strong correlation between the digitised data points and trend line.

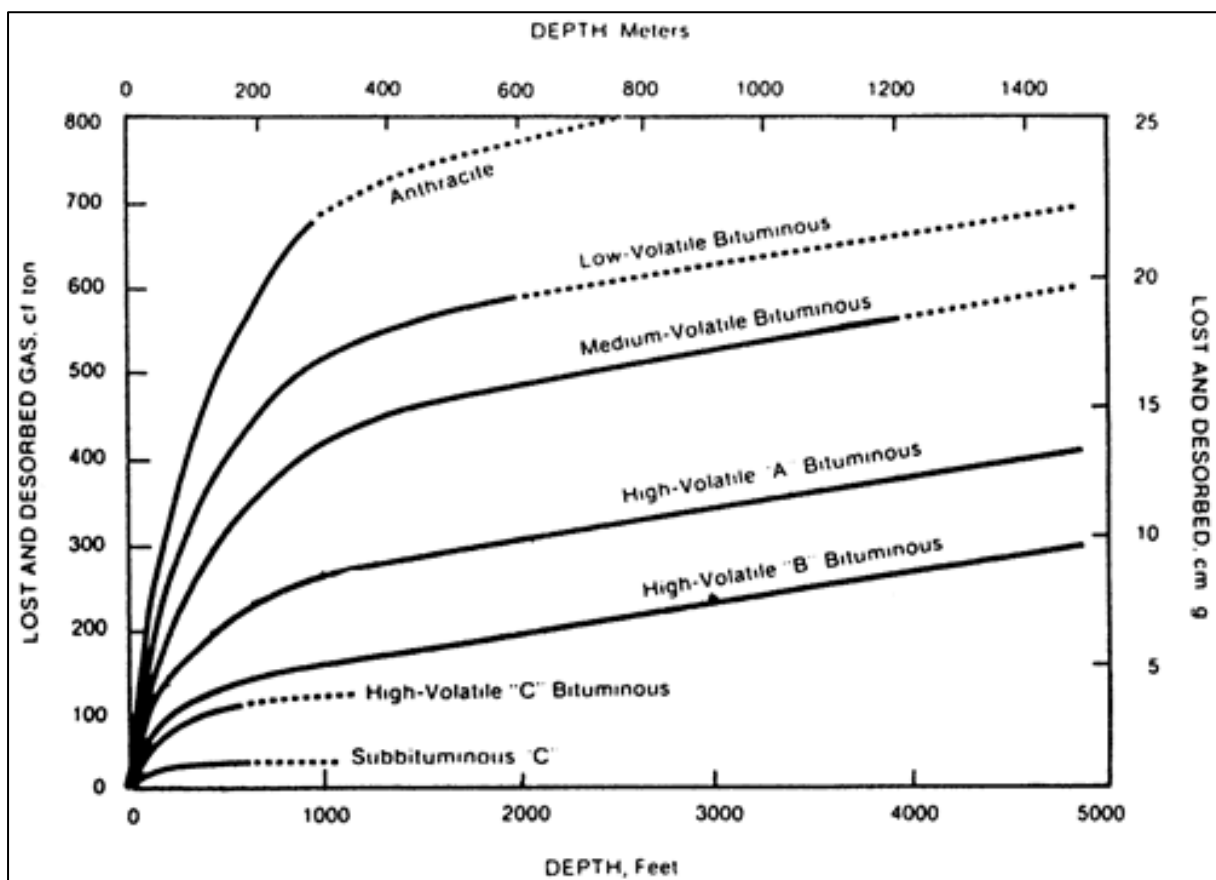


Figure 59 Relationship between rank, depth, and sorptive capacity (Eddy, et al., 1982).

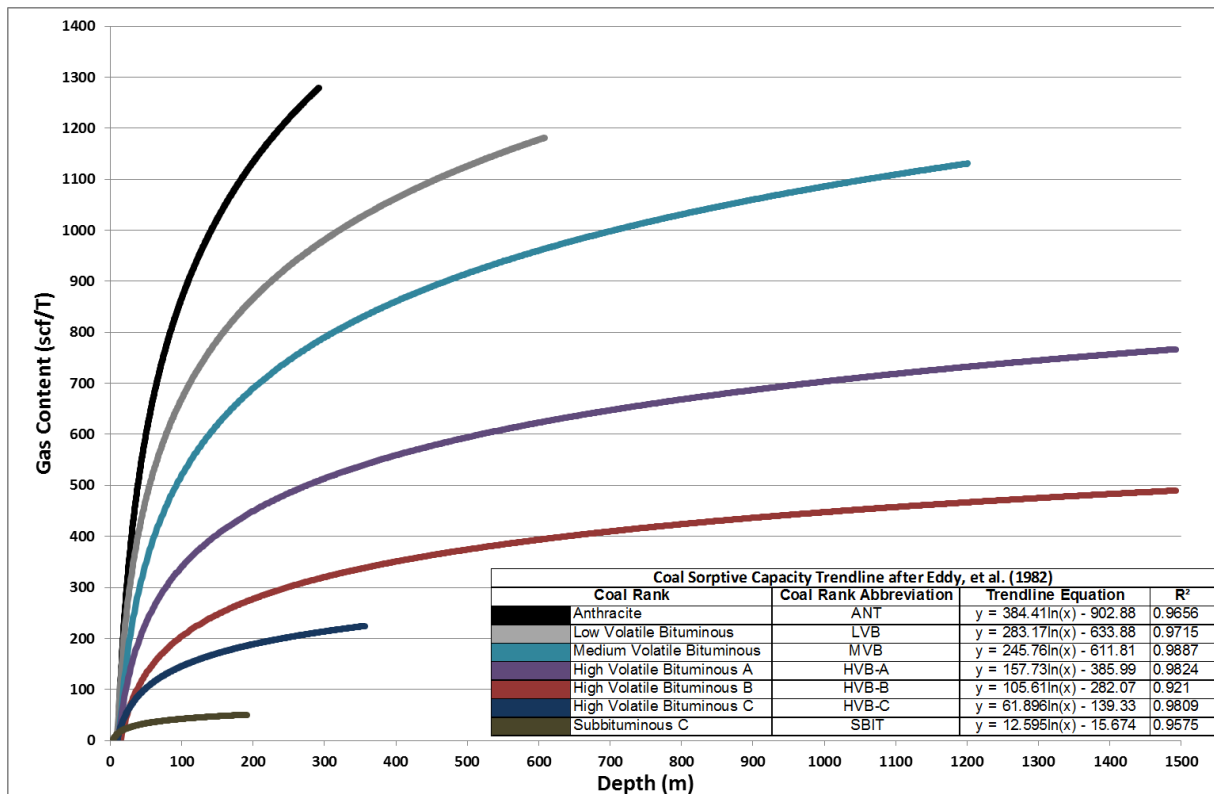


Figure 60 Digitised trend lines of the relationship between rank, depth, and sorptive capacity after Eddy, et al. (1982).

Table 20 Trend line equation calculations derived from the sorptive capacity graphs by Eddy, et al. (1982).

Coal Rank	Coal Rank Abbreviation	Trend line Equation	R <sup>2</sup>
Anthracite	ANT	$y = 192.21\ln(x) - 451.44$	0.9656
Low Volatile Bituminous	LVB	$y = 141.59\ln(x) - 316.94$	0.9715
Medium Volatile Bituminous	MVB	$y = 122.88\ln(x) - 305.91$	0.9887
High Volatile Bituminous A	HVB-A	$y = 78.864\ln(x) - 193.00$	0.9824
High Volatile Bituminous B	HVB-B	$y = 52.803\ln(x) - 141.04$	0.921
High Volatile Bituminous C	HVB-C	$y = 30.948\ln(x) - 69.666$	0.9809
Subbituminous	SBIT	$Y = 6.2975\ln(x) - 7.8369$	0.9575

By classifying the coal types in the Kubu samples subset, using the vitrinite reflectance and ash-free fixed carbon, volatile matter and moisture measurements it was possible to evaluate the correlation between the Langmuir isotherm and the Eddy (1982) trend line equations (Table 21).

The sorptive capacity values calculated using the Eddy (1982) equations differed from the isotherm determined values. For correlative purposes a ratio between the trend line and DAF isotherm results was calculated. The trend line values were generally less with one sample only proving 0.67 of the isotherm calculated value. Of the 2 trend line values higher than the isotherm results the highest ratio was 1.19 (Table 21). The distribution of the ratios was studied and it was found that 8 out of the 10 samples were within the range between 0.75 and 1.1 (Figure 61). This finding indicates that there is a high probability for either under or over estimation of the gas content values using the Eddy (1982) trend line equations. However, by utilising probabilistic simulation methods it is capable to compensate for this, specifically when looking at large datasets for the distribution determination.

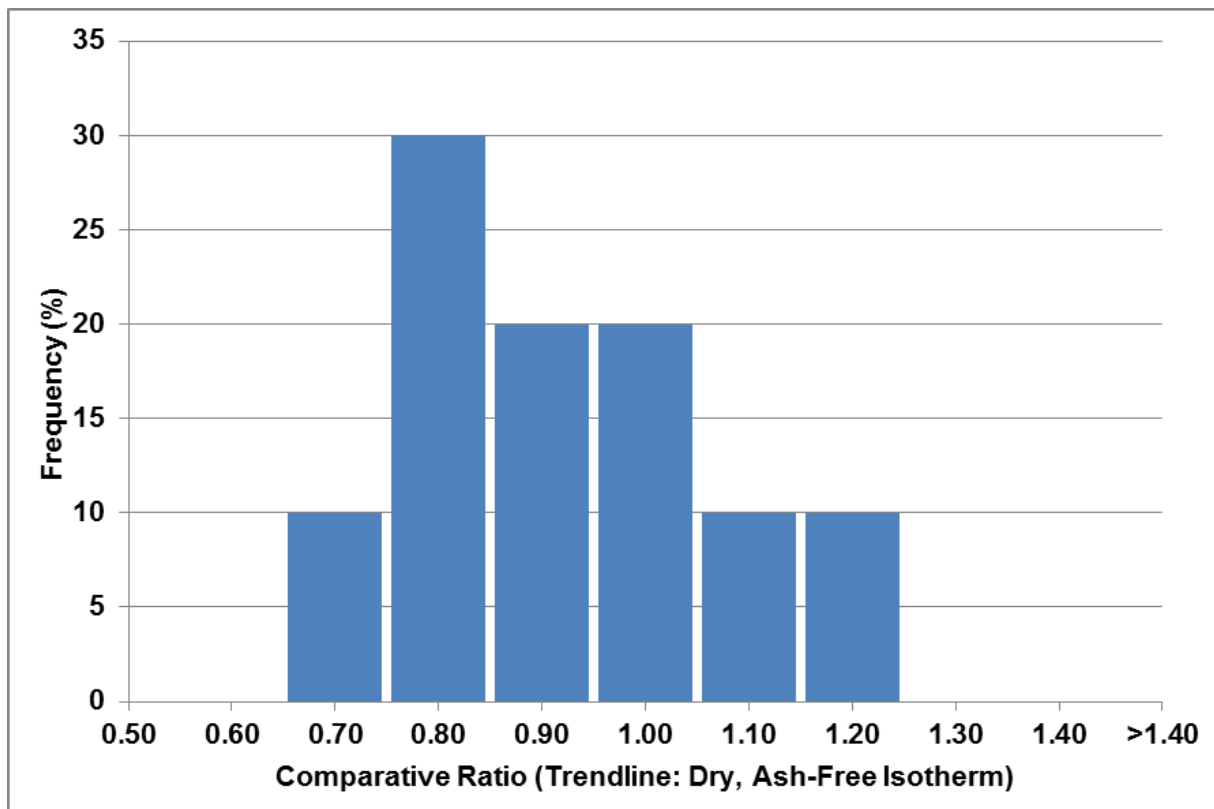


Figure 61 Correlation between the Langmuir isotherm and Eddy, et al. (1982) trend line equation gas content values.

Table 21 Langmuir isotherm and Eddy, et al. (1982) trend line equations gas content calculations for the Kubu sample subset.

Sample Sequence	Borehole	Sample Mid-Point Depth	Sample Number	Measured Gas Content		Depth	Formation Pressure	Gas Content Determined from Langmuir Isotherms		Coal Rank determined from vitrinite reflectance and ash-free fixed carbon, volatile matter and moisture measurements	Stoeckinger (1991) Derived Trend Line Equation	Gas Content Calculated using the Stoeckinger (1991) Derived Trend Line Equation (Dry, Ash-Free)	Comparative Ratio (Trend line: Dry, Ash-Free Isotherm)
		(m)		Raw	Dry, Ash-Free			Gas Content (Raw)	Gas Content (Dry, Ash-Free)			scf/T	
				scf/T	scf/T			ft	psi			scf/T	
12	134C7	463.00	CH-7-021	26.78	32.12	1519.01	672.43	105.97	172.20	High Volatile Bituminous - C	$y = 30.948\ln(x) - 69.666$	183.05	1.06
14	134C6	319.89	CH-6-002	21.78	42.05	1049.50	469.13	67.84	138.11	High Volatile Bituminous - C	$y = 30.948\ln(x) - 69.666$	108.84	0.79
15	134C6	329.12	CH-6-008	37.11	47.18	1079.78	482.24	124.49	163.82	High Volatile Bituminous - C	$y = 30.948\ln(x) - 69.666$	109.72	0.67
16	134C6	340.35	CH-6-013	39.94	49.05	1116.60	498.19	128.06	169.64	High Volatile Bituminous - B	$y = 52.803\ln(x) - 141.04$	166.80	0.98
25	135C4	451.11	CH-04-D7	56.73	67.23	1480.00	655.54	238.76	318.87	High Volatile Bituminous - A	$y = 78.864\ln(x) - 193.00$	288.99	0.91
28	136C3	364.85	CH-03-005	37.55	50.12	1197.00	533.00	159.21	229.16	High Volatile Bituminous - A	$y = 78.864\ln(x) - 193.00$	272.26	1.19
38	136C1	268.68	CH-01 D004	33.23	44.71	881.49	396.38	82.20	118.60	High Volatile Bituminous - C	$y = 30.948\ln(x) - 69.666$	103.44	0.87
39	136C1	275.34	CH-01 D005	33.13	45.05	903.34	405.84	88.65	125.29	High Volatile Bituminous - C	$y = 30.948\ln(x) - 69.666$	104.20	0.83
40	136C1	277.60	CH-01 D006	33.32	51.03	910.75	409.05	77.99	133.11	High Volatile Bituminous - C	$y = 30.948\ln(x) - 69.666$	104.45	0.78
41	136C1	280.07	CH-01 D008	32.33	39.16	918.84	412.56	101.99	135.46	High Volatile Bituminous - C	$y = 30.948\ln(x) - 69.666$	104.73	0.77

The borehole information was evaluated and gas content values calculated using the Eddy (1982) trend line method. A complete database of information is shown in Appendix C. Table 22 shows the summarized calculated gas contents for each of the areas. In the absence of detailed regional evaluation data this proves to be a valuable tool for the resources assessment. Coal occurring at a depth of 30m or less was assigned a gas content of 1 scf/T.

**Table 22** Calculated gas contents for the coal seams using the trend line equations based on the coal qualities and depth.

Country	Area	Source(s)	Number of Data Points Evaluated	Calculated Gas Content (scf/T)		
				Minimum	Maximum	Average
Zimbabwe	Western Areas	Palloks (1984)	63	(1)	363	235
Zimbabwe	Entuba	Palloks (1984)	125	(1)	486	221
Zimbabwe	Lubu	Palloks (1984)	28	(1)	180	73
Zimbabwe	Sengwa South	Palloks (1984)	10	(1)	486	198
Zimbabwe	Sengwa North	Palloks (1984)	11	(1)	145	112
Zimbabwe	Lusulu	Palloks (1984); Mapani, et al. (2013); Padcoal (Pvt) Ltd (2011)	3	54	94	72
Zimbabwe	Wankie	Palloks (1984)	2	176	447	291
Zimbabwe	Gokwe	Oesterlen & Lepper (2005); Padcoal (Pvt) Ltd (2011)	1	160	182	172
Zimbabwe	Lubimbi	Oesterlen & Lepper (2005)	1	(1)	93	73
Zimbabwe	Busi	Oesterlen & Lepper (2005)	1	18	20	19
Zimbabwe	Tjolutjo, Sawmills, and Insuza	Oesterlen & Lepper (2005)	1	27	29	28
Botswana	Northeast Botswana	Smith (1984), Anglo Coal Botswana, (2010) Potgieter (2015)	39	(1)	34	23
<i>Values in brackets indicate values that were below the measurement limit. A default value of 1 was assigned to these estimates</i>						
<i>The full dataset evaluated can be viewed in Appendix B</i>						

#### 5.4.3. *The Impact of Gas Saturation Levels within the Coal Seams*

Analysis of the digitised Shangani data (Appendix E) shows that there is a wide distribution of measurements throughout the sample set. When comparing the data from the trend line data interpreted from Eddy (1982) the maximum measurement in the area, in well C6-Wankie, generally coincides with the High Volatile Bituminous A trend line (Figure 63) inferring that the coal is either of slightly lower quality than in the main mining areas or that the coal is possibly under-saturated.

Barker (2006) described the coal as being deposited in a zone with a thickness greater than 100m and of good quality. However, no mention of coking coal was made alluding that the coal is of a slightly lower quality than at the Wankie Mine. Table 23 shows the summarised descriptive statistics of the data that was digitised from the graph.

These wide distributions of gas content values have been observed in the most Kubu Energy and Shangani Energy drilling campaigns are related to the gas saturation states within the coals. Faiz, et al. (2014) showed that the saturation of the coal seams in Botswana was related to the thermal maturity of the coal and that the gas was predominantly of biogenic origin. Figure 64 shows stratigraphic zonation, maceral composition, burial history and gas origin determined by isotopic analyses. Although the coals are vitrinite dominant they are generally immature and so incapable of generating thermogenic gas.

The measurements with a higher maturity correlate to the proximity of dolerite intrusions and are localised phenomenon. Although these thermally enhanced samples did have higher gas content measurements as well as a mixed (thermogenic and biogenic) isotopic signature the saturation levels were still very low (Faiz, et al. 2014).

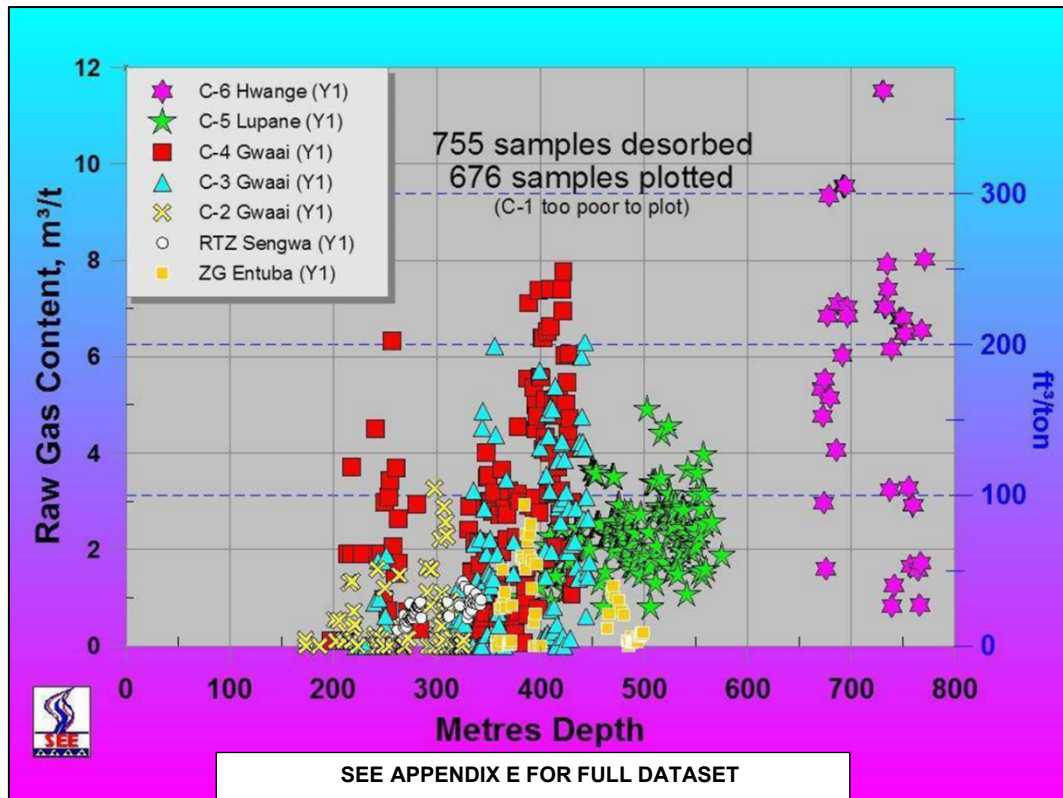


Figure 62 Desorption testing results from Zimbabwe (Barker, 2006).

Table 23 Summarised statistics of the gas content data digitised from the Shangani Energy measurement data graph (after Barker, 2006).

Summary Statistics of Gas Content Data in scf/T	
Mean	90.12
Standard Error	4.16
Median	70.69
Mode	29.09
Standard Deviation	73.55
Range	408.34
Minimum	0.63
Maximum	408.97
Count	313

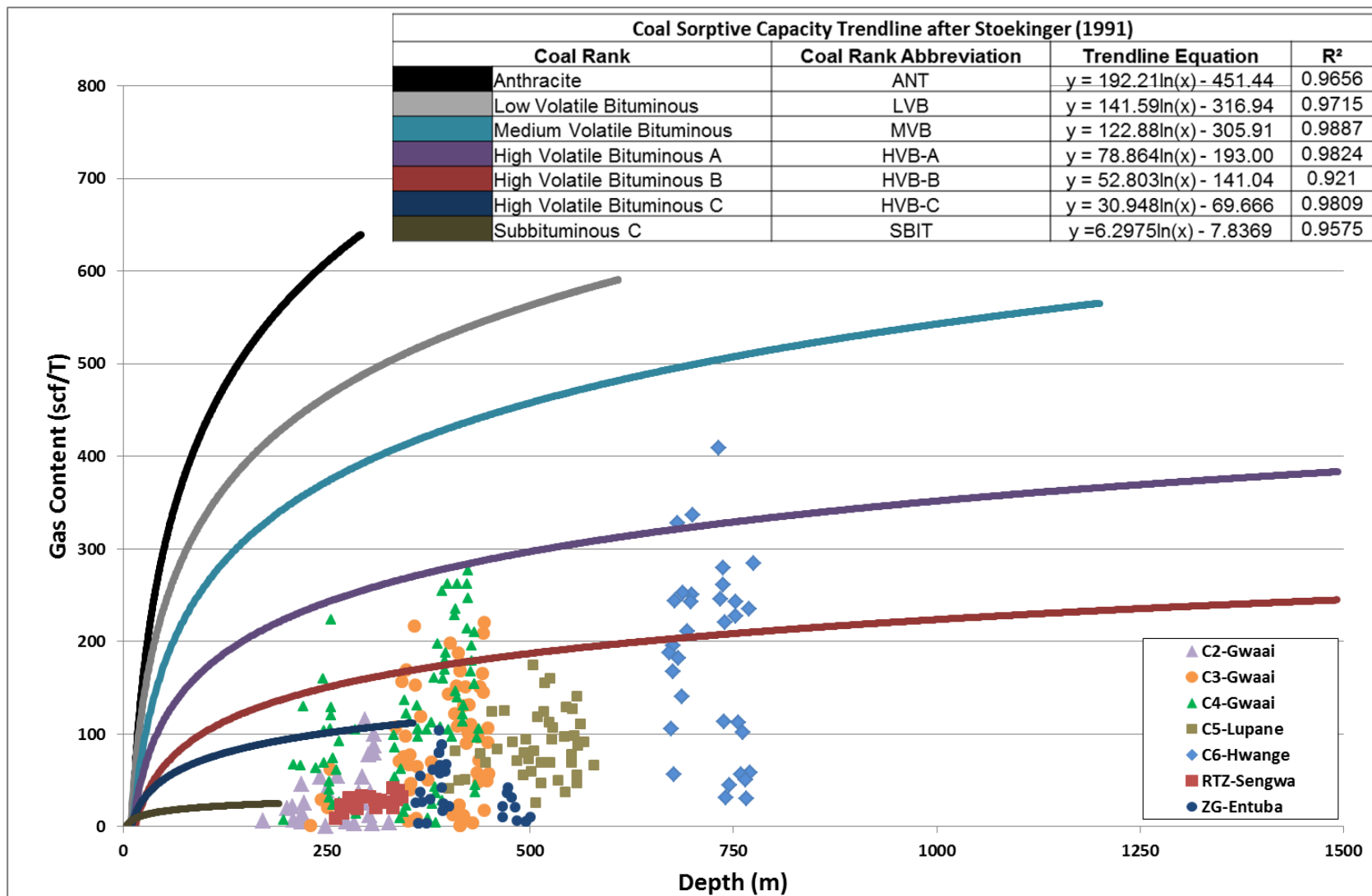


Figure 63 Digitised gas contents from the Shangani Energy measurement data graph compared to the maximum sorptive capacity (after Barker, 2006 and Eddy, et al., 1982).

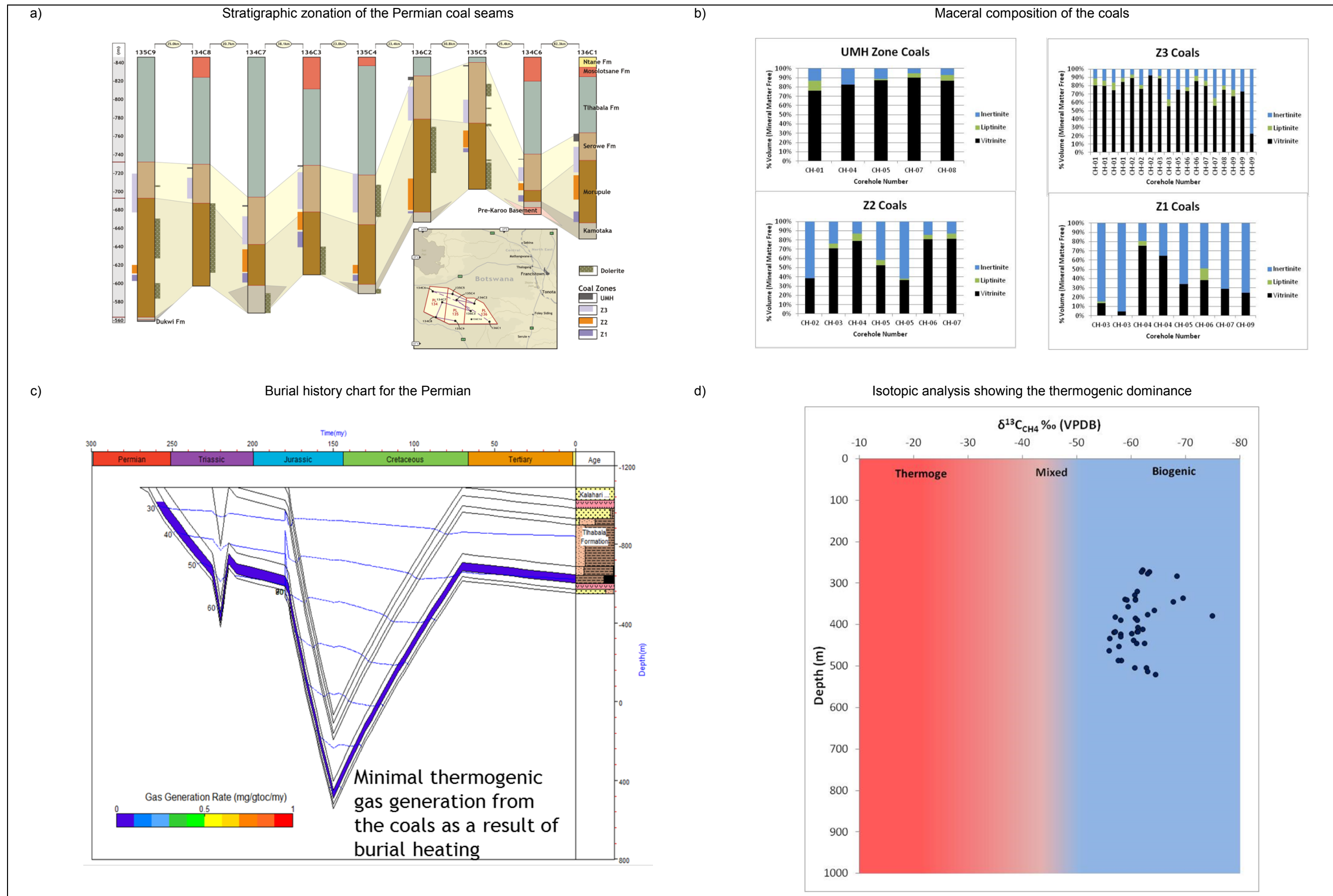
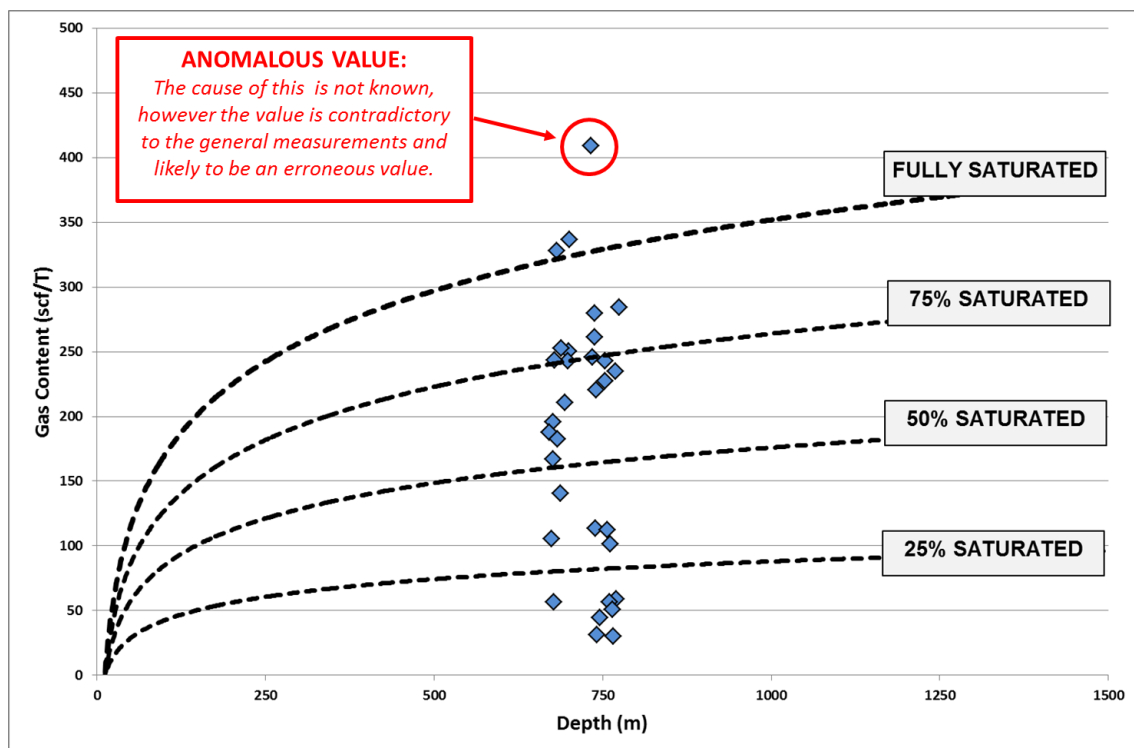


Figure 64 Evaluations of the Permian coals collected during the Kubu Energy exploration campaign in Botswana (Faiz, et al., 2014).

The estimation of saturation levels in this study forms an important basis of the gas content component as the trend line calculated gas contents assume 100% saturation levels. The information digitised from the Shangani presentation show that there is a wide range of saturation levels in Zimbabwe with the majority of the measurements in well C6-Hwange indicating a saturation level less than 75% (Figure 65). Saturation levels in the the Kubu data subset (Table 24) is evidence of generally under-saturated coal (Faiz, et al., 2014; Kubu Energy, 2014; and Potgieter, 2015).

Table 25 demonstrates the effect of saturation levels varying from 100% to 25% on the calculated gas contents. These drastic changes in the gas content will have a notable effect on the final resource determinations as well as the postulated production profiles and economic evaluations that would be completed for a project as part of the New Ventures Screening Process.



**Figure 65** Gas measurement data from the Shangani graph plotted on theoretical sorptive capacities of a high volatile bituminous A coal type (after Barker, 2006 and Eddy, et al., 1982).

Table 24

Coal saturation levels of the Kubu data subset (after Kubu Energy, 2014).

Sample Sequence	Borehole	Sample Mid-Point Depth	Sample Number	Sample Analyses				Gas Content Calculated using the Eddy, et al., (1982) Derived Trend Line Equation (Dry, Ash-Free)	Saturation levels calculated from Isotherm Data (DAF)	Saturation levels calculated from Trendline Equations (DAF)
				Measured Gas Content		Isotherm Data				
		Raw		Dry, Ash-Free	Gas Content (Raw)	Gas Content (Dry, Ash-Free)				
		scf/T		scf/T	scf/T	scf/T				
12	134C7	463.00	CH-7-021	26.78	32.12	105.97	172.20	183.05	30.31	17.54
14	134C6	319.89	CH-6-002	21.78	42.05	67.84	138.11	108.84	61.99	38.64
15	134C6	329.12	CH-6-008	37.11	47.18	124.49	163.82	109.72	37.90	43.00
16	134C6	340.35	CH-6-013	39.94	49.05	128.06	169.64	166.80	38.31	29.41
25	135C4	451.11	CH-04-D7	56.73	67.23	238.76	318.87	288.99	28.16	23.26
28	136C3	364.85	CH-03-005	37.55	50.12	159.21	229.16	272.26	31.48	18.41
38	136C1	268.68	CH-01 D004	33.23	44.71	82.20	118.60	103.44	54.39	43.23
39	136C1	275.34	CH-01 D005	33.13	45.05	88.65	125.29	104.20	50.82	43.23
40	136C1	277.60	CH-01 D006	33.32	51.03	77.99	133.11	104.45	65.43	48.86
41	136C1	280.07	CH-01 D008	32.33	39.16	101.99	135.46	104.73	38.39	37.39

**Table 25** The effect of gas saturation state of the coal on the calculated gas content data using the trend lines derived from Eddy, et al. (1982).

Country	Area	Source(s)	Number of Data Points Evaluated	Estimated Gas Content (scf/T)												
				Fully Saturated			75% Saturated			50% Saturated			25% Saturated			
				Minimum	Maximum	Average	Minimum	Maximum	Average	Minimum	Maximum	Average	Minimum	Maximum	Average	
Zimbabwe	Western Areas	Palloks (1984)	63	(1)	363	235	(1)	272	176	(1)	182	117	(1)	91	59	
Zimbabwe	Entuba	Palloks (1984)	125	(1)	486	221	(1)	365	166	(1)	243	110	(1)	122	55	
Zimbabwe	Lubu	Palloks (1984)	28	(1)	180	73	(1)	135	55	(1)	90	37	(1)	45	18	
Zimbabwe	Sengwa South	Palloks (1984)	10	(1)	486	198	(1)	365	149	(1)	243	99	(1)	122	50	
Zimbabwe	Sengwa North	Palloks (1984)	11	(1)	145	112	(1)	108	84	(1)	72	56	(1)	36	28	
Zimbabwe	Lusulu	Palloks (1984); Mapani, et al. (2013); Padcoal (Pvt) Ltd (2011)	3		54	94	72	41	71	54	27	47	36	14	24	18
Zimbabwe	Wankie	Palloks (1984)	2		176	447	291	132	335	218	88	223	146	44	112	73
Zimbabwe	Gokwe	Oesterlen & Lepper (2005); Padcoal (Pvt) Ltd (2011)	1		160	182	172	120	137	129	80	91	86	40	46	43
Zimbabwe	Lubimbi	Oesterlen & Lepper (2005)	1	(1)	93	73	(1)	70	55	(1)	46	37	(1)	23	18	
Zimbabwe	Busi	Oesterlen & Lepper (2005)	1		18	20	19	13	15	14	9	10	9	4	5	5
Zimbabwe	Tjolojjo, Sawmills, and Insuza	Oesterlen & Lepper (2005)	1		27	29	28	21	22	21	14	14	14	7	7	7
Botswana	Northeast Botswana	Smith (1984), Anglo Coal Botswana, (2010) Potgieter (2015)	39	(1)	34	23	(1)	26	17	(1)	17	12	(1)	9	6	

*Values in brackets indicate values that were below the measurement limit. A default value of 1 was assigned to these estimates*

*The full dataset evaluated can be viewed in Appendix B*

Figure 66 is a distribution curve constructed from the measured, digitised and calculated gas content values. All calculated values were subjected to saturation corrections of 100%, 75%, 50% and 25% prior to the construction of the histogram. A statistical analysis of the data showed is summarised in Table 26.

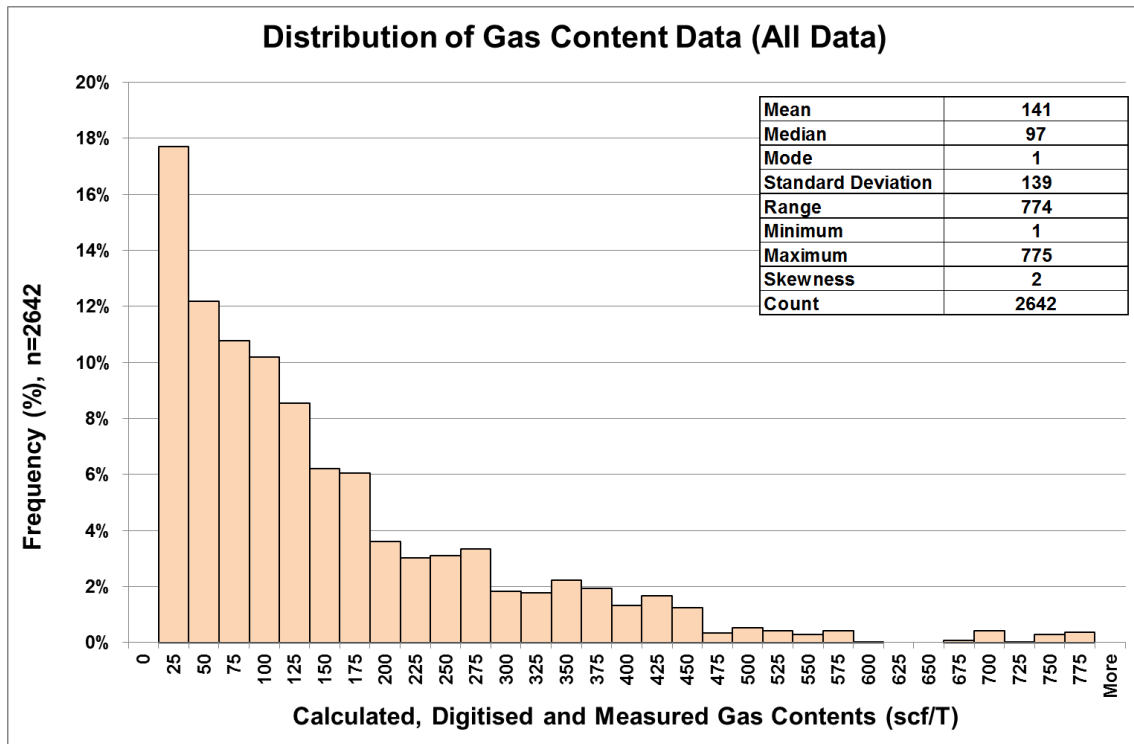


**Figure 66** Distribution of gas content values from the calculated, digitised and measured datasets.

**Table 26** Summarised statistics measured, digitised and calculated gas content values with incorporating the effect of saturation levels of the coal.

Summary Statistics of Gas Content Data in scf/T	
Mean	141
Median	97
Mode	1
Standard Deviation	139
Range	774
Minimum	1
Maximum	775
Count	2642

## 5.5. Resource Evaluation

GeoX is purely a probabilistic volumetric calculator. The software has a CBM component used in this evaluation. Users have the ability to set the parameters used for the resource estimations based on two methods, the first is called the direct method where the gas content information is directly entered into the system as opposed to the indirect method where the gas content is calculated using Langmuir isotherm volumes and pressures. The latter is a very good method, however, it is heavily dependent on the acquisition of reliable desorption and isotherm data that is not readily available across the study area.

Although the distribution function compensates for anomalously high and low values to an extent, it is advised that the input data be evaluated further and a narrower band of values be select and used for the calculations. The coal thickness ( $h$ ), coal density ( $RHOB_{(c)}$ ) and gas content ( $G_{(c)}$ ) data was evaluated further to determine the final GeoX inputs.

The distribution of the coal thickness data was lognormal with 98% of the data falling in the range between 1m and 17.92m (Table 27). The Kubu Energy (2014) wireline density distribution was used as an analogue for the study area. The data evaluation (Table 27) indicated that 93% of 13 427 measurements were distributed between density values of  $1.3\text{g/cm}^3$  and  $1.75\text{g/cm}^3$  with the mode being  $1.70\text{ g/cm}^3$ . The analysis of the measure, digitised and calculated gas content database established that 98% of the measurements are between 1scf/T and 496scf/T (Table 27).

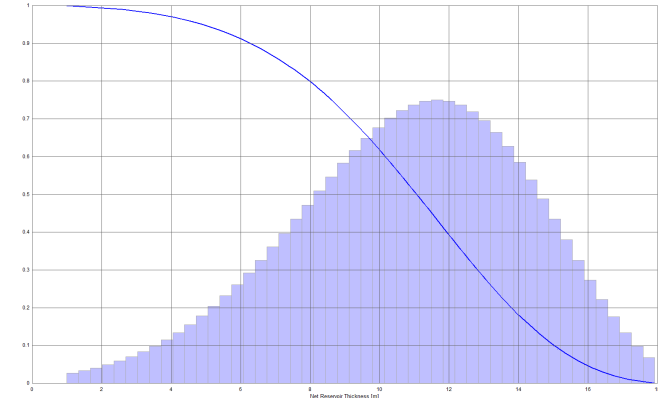
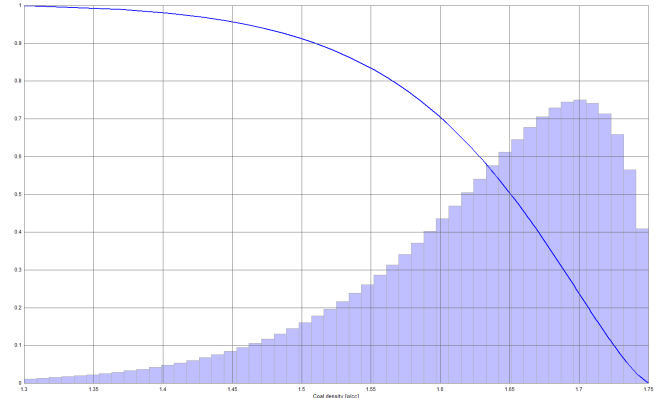
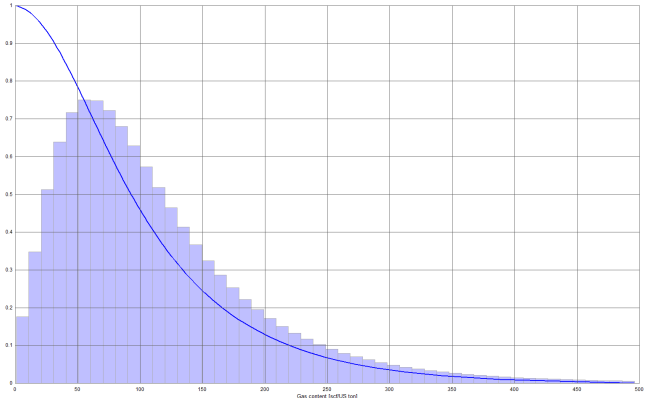
For this evaluation the surface extent of  $134\,666\text{km}^2$  occupied by Karoo Supergroup rocks over the study area was used as a constant for the Area ( $A$ ) component of the resource calculation.

Table 28 summarises the inputs and modelled distributions used during the GeoX estimation.

**Table 27 Summary of original and filtered data inputs used in GeoX.**

Parameter	Data Retained During Filtering	Descriptive Statistics (All Data)		Distribution Curve (All Data)	Descriptive Statistics (Filtered Data)		Distribution Curve (Filtered Data)
<b>Coal Thickness (h).</b>	<b>98%</b>	Mean	9.58		Mean	9.39	
		Median	9.66		Median	9.51	
		Mode	11.66		Mode	11.66	
		Standard Deviation	3.67		Standard Deviation	3.36	
		Range	22.65		Range	16.92	
		Minimum	1.00		Minimum	1.00	
		Maximum	23.65		Maximum	17.92	
		Count	250		Count	246	
<b>Coal Density (RHOB<sub>(c)</sub>)</b>	<b>96%</b>	Mean	1.53		Mean	1.55	
		Median	1.55		Median	1.56	
		Mode	1.65		Mode	1.70	
		Standard Deviation	0.14		Standard Deviation	0.12	
		Range	0.64		Range	0.45	
		Minimum	1.11		Minimum	1.30	
		Maximum	1.75		Maximum	1.75	
		Count	13427		Count	12466	
<b>Gas Content (G<sub>(c)</sub>)</b>	<b>94%</b>	Mean	141		Mean	129	
		Median	97		Median	93	
		Mode	1		Mode	1	
		Standard Deviation	139		Standard Deviation	116	
		Range	774		Range	495	
		Minimum	1		Minimum	1	
		Maximum	775		Maximum	496	
		Count	2642		Count	2578	

**Table 28** Summary of the inputs used in GeoX.

<u>Parameter</u>							
Area		Coal Thickness		Coal Density		Gas Content	
(A)		(h)		$(RHOB_{(c)})$		$(G_{(c)})$	
<u>Unit</u>							
km <sup>2</sup>		m		g/cm <sup>3</sup>		scf/T	
<u>Distribution</u>							
Constant		Stretched Beta		Stretched Beta		Lognormal Based on Median	
Area	134666	Minimum	1.00	Minimum	1.3	Minimum	1
		Maximum	17.92	Maximum	1.75	Maximum	496
		Mode	11.66	Mode	1.70	Median	93
							

A Monte Carlo simulation with 10000 iterations was used to calculate the regional resource estimates. This simulation provides the ability to report values for the P10 (10% probability, least likelihood), P50 (mid-case), P90 (90% probability, highest likelihood). The resource evaluation results show a wide distribution of probable values (Table 29 and Figure 67). This is indicative of a poorly understood region with a great deal of assumption as opposed to good exploration data.

**Table 29** Result of the GeoX volumetric resource calculation showing the P10, P50, P<sub>mean</sub> and P90 values.

Estimated Resource Size			
			
P10	P <sub>mean</sub>	P50	P90
<b><i>Billion Cubic Feet (Bcf)</i></b>			
60196	29582	23105	6917
<b><i>Trillion Cubic Feet (Tcf)</i></b>			
60.1	29.5	23.1	6.9
<b><i>Billion Cubic Metres (Bm<sup>3</sup>)</i></b>			
1595	784	612	183

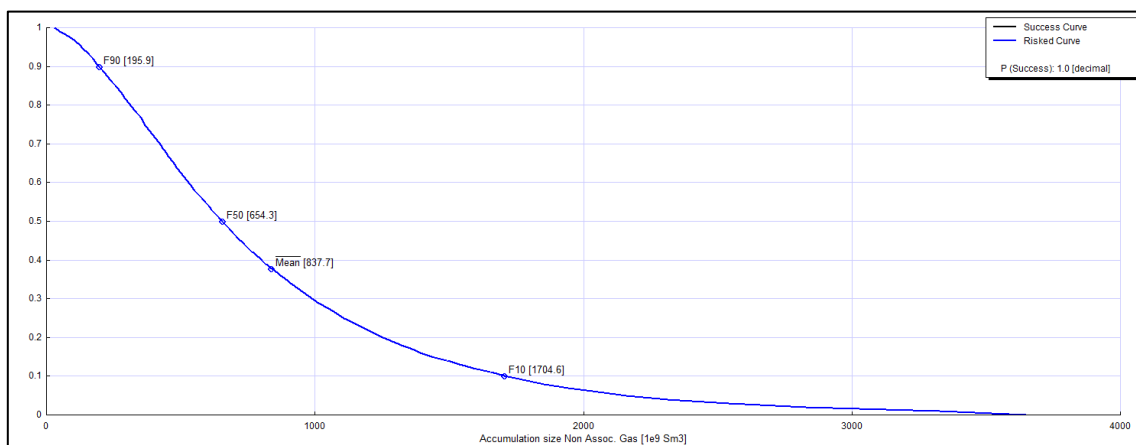


**Figure 67** Distribution of the results of the GeoX Monte Carlo resource calculation.

To fully evaluate the significance of the resource estimates over the study area it is important to compare it to other CBM basins globally. As the basins all differ in surface extent the best comparison tool is to express the values as a concentration

expressed as billion cubic feet per square kilometre expressed as Bcf/km<sup>2</sup>, calculated using the formula shown in Equation 6.

$$RD = \frac{G_{P50}}{A}$$

Where:

*RD* = Resource Density Estimation in Bcf/km<sup>2</sup>  
*G<sub>P50</sub>* = P50 Resource Estimate in Bcf  
*A* = Surface area in km<sup>2</sup>

**Equation 6 Resource density calculation method.**

The Study Area has a P50 Surface Area (*A*) 134 666 km<sup>2</sup> and P50 Resource Estimate (*G<sub>P50</sub>*) of 23 105 Bcf, equating to a resource density of 0.17 Bcf/km<sup>2</sup>. This density was compared to a number of basins in Canada and the USA (Table 30) for comparative purposes. The major basins in Canada and the US have a significantly higher resource density than that of the Study Area indicating a lower prospectivity for CBM. Once more reliable regional data becomes available it will be possible to update this evaluation, however, from previous investigations within the region the general exploration and development potential is low and to date not a single project comparable to the North American basins have been found (Potgieter, 2015).

**Table 30 Resource densities for the basins used in this (after APF Energy, 2004).**

Basin	Country	Resource Density (Bcf/km <sup>2</sup> )
<b>Study Area (Kalahari Karoo and Mid-Zambezi Basins)</b> Range: P90 to P10	Botswana and Zimbabwe	0.06 - 0.3 P50 – 0.18
<b>San Juan</b>	USA	5.8 - 6.8
<b>Black Warrior</b>	USA	3.9 - 4.8
<b>Uinta</b>	USA	5.0 - 6.0
<b>Powder River</b>	USA	0.8 - 1.4
<b>Raton</b>	USA	3.9 - 4.6
<b>Alberta plains shallow</b>	Canada	0.6 - 0.9
<b>Alberta plains deep</b>	Canada	1.2 - 2.5

## **6. CHALLENGES WITH DATA ACQUISITION AND MITIGATION MEASURES FOR FUTURE EXPLORATION**

The primary challenge with the assessment of the study area was the availability of reliable gas content data. If regional data collection and reporting was standardised it would be possible to assess the area with a greater amount of certainty. This section will outline some of these challenges and suggest an achievable guideline for field data collection during CBM exploration programmes in Southern Africa.

As there are no Southern African standards available, companies have been following international standards (Potgieter, 2015). The most widely applied standards for the determination of gas in coal are the Australian (AS 3980-1999) and American (D7569-10) standards (Standards Australia, 1999 and ASTM International, 2010). From personal experience the data gathering procedures in the two standards are not always practical in remote exploration areas such as the study area regarding to cost and equipment availability (Potgieter, 2015). This led to companies inconsistently following sections of the standards compromising the data quality and reliability (Potgieter, 2015).

### **6.1. Data to be Acquired During Exploration Programmes**

When evaluating CBM resources during a dedicated exploration programme it is necessary to collect the following data:

- Coal thickness measured from wireline logs.
- Stratigraphic depths measured during the drilling and refined using the wireline logs.
- Formation temperature from wireline logs.
- Proximate coal analysis.
- Gas content measured from core desorption.
- Gas saturations calculated from the comparison of the measured gas content analyses with the maximum gas holding capacity derived from adsorption isotherm measurements.
- Gas composition measurements using gas chromatography.

Additional data used to further determine the reservoir production capability and gas origin that will impact on the deliverability and ultimate estimated recoverability of the CBM Field include:

- Gas isotope samples for the determination of gas sourcing (biogenic vs thermogenic).
- Coal formation permeability and pressure gradient measured in situ using Drill Stem Tests (DSTs) or Injection Fall-off Tests (IFTs).

## 6.2. Guidelines for CBM Exploration Data Collection, Sampling and Reporting

The following guidelines will cover the aspects listed in Table 31. For illustrative purposes a hypothetical borehole will be used (Figure 68) that is applicable to a range of different deposits and formations.

**Table 31 Aspects addressed as part of the guidelines for CBM exploration data collection and sampling.**

1.	Programme Planning and Logistics
2.	In-Field Sampling
3.	Gas Content Measurements
4.	Wireline Logging
5.	Post Desorption Sample Analyses
6.	Data Reporting

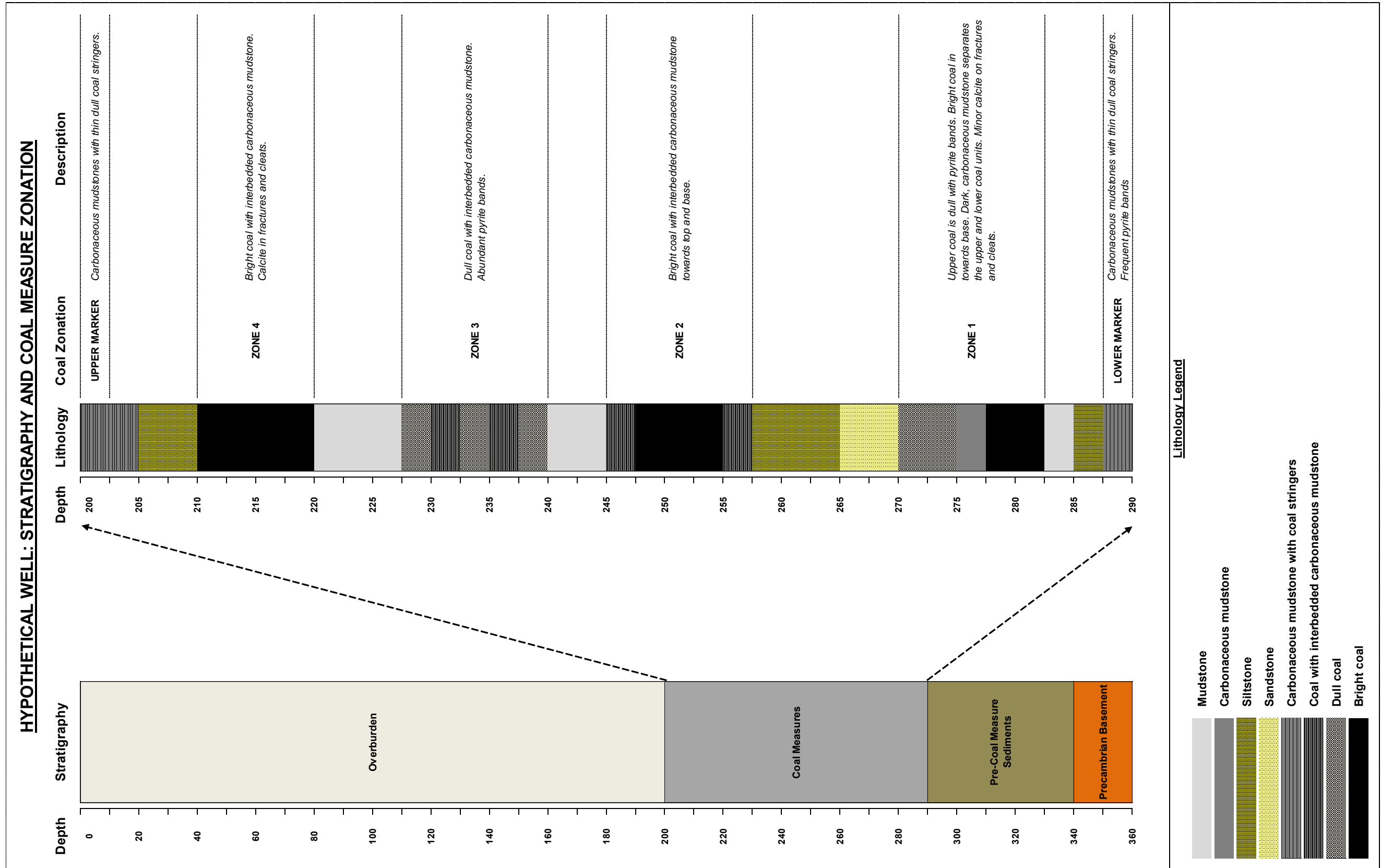


Figure 68 Well stratigraphy and coal measure zonation as used in the guidelines.

### 6.2.1. Programme Planning and Logistics

When planning an exploration programme it is imperative to plan for a CBM programme and not a modified coal exploration campaign. The approach with respect to data gathering is greatly different and will come at higher costs.

#### 6.2.1.1. Drilling Techniques

The preferred drilling technique for CBM exploration should be wireline core drilling as this is the fastest method for getting core to surface from depth. HQ3 and PQ3 triple tube coring systems (Figure 69) are best suited for desorption sampling. The triple tube system causes the least damage to the core during extraction from the barrel and inner tube.

Standard sizes				
Size	Hole diameter		Core diameter	
	mm	in	mm	in
<b>A</b>	48,01	1.890	26,97	1.062
<b>B</b>	59,94	2.360	36,40	1.433
<b>N</b>	75,69	2.980	47,63	1.875
<b>N2</b>	75,69	2.980	50,67	1.995
<b>N3</b>	75,69	2.980	45,09	1.775
<b>H</b>	96,06	3.782	63,50	2.500
<b>H3</b>	96,06	3.782	61,11	2.406
<b>P</b>	122,61	4.827	84,96	3.345
<b>P3</b>	122,61	4.827	83,06	3.270

Figure 69 Coring sizes (Sandvik Mining and Construction, 2015).

#### 6.2.1.2. Desorption Equipment

The contractor appointed to manage the desorption testing of the samples needs to be informed of the core size well in advance of mobilisation. The desorption equipment selected should be sized correctly for the project. It is important to minimize the amount of free space around the core. Depending on the remoteness of the project area it may be necessary to ensure the contractors maintain full redundancy on all essential equipment and specifically on items that may have a long lead replacement schedule such as chromatography equipment.

##### 6.2.1.2.1. Desorption Canisters

Desorption canister (Figure 70) lengths differ and may range from 30cm to 1m. When dealing with barcoded coal sequences as found in north-eastern Botswana filling a 1m canister from a three metre core run may be tricky, whereas 30cm canisters often fail to capture all available data in more discreet seams as found in Zimbabwe. A canister length of approximately 60cm has proven to work very well in Southern Africa (Potgieter, 2015).

These canisters can be made of various materials such as steel, aluminium or PVC and the closing mechanism can be bolted, threaded, clamp (Figure 71) or glued in the case of PVC (Spears, et al., 2014 and Eddy, et al., 1982). The PVC canisters are cheaper to manufacture, however, they remain single use equipment. The preference will be either steel or aluminium with an o-ring in the cap or on the canister for increased seal. Some prototypes of aluminium canisters with double lead threading have been developed but not yet tested (Potgieter, 2015).

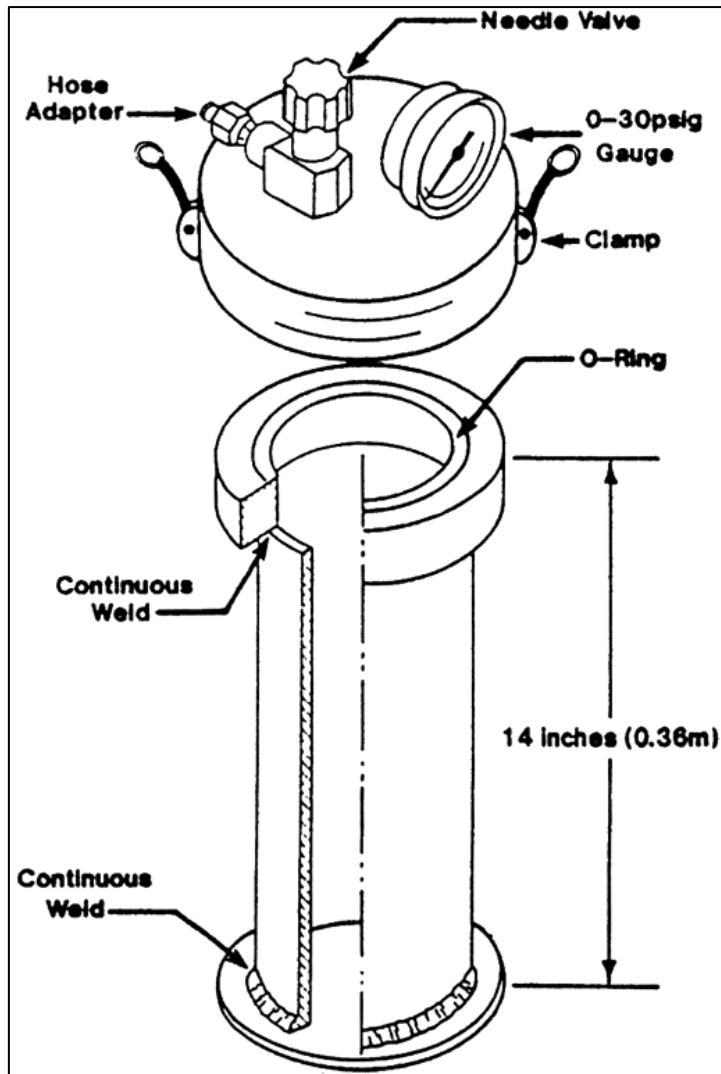


Figure 70 Test sample canister (Stoekinger, 1991).



Figure 71 Clamp type aluminium HQ3 canisters (Potgieter, 2015).

#### 6.2.1.2.2. Canister Spacers

If it is expected that some thin or barcoded coal zones may be intersected it may not be possible to fill an entire canister with a coal sample. In such cases it is necessary to place spacers in the canisters. Spacers need to be made of a substance impermeable and of which the density is consistent. High density polyethylene (HDPE) works very well as spacers due to its nature and ability to mould or mill billets to match the required specifications. The spacer billets can be prepared in two ways:

1. Supply the HDPE billets in 1m lengths and cut the appropriate lengths required on site using a hack saw. This process could be time consuming and actually impact the quality of the desorption data;
2. Have the HDPE billets pre-prepared in specific sizes to be used as spacers. It is possible to use a combination of 1cm, 5cm and 10cm billets for various spacer sizes.

When ordering the spacers it is very important that the density and weight is known and that the billets are manufactured to have the same diameter as the core.

#### 6.2.1.2.3. Water Baths and Hot Boxes

The samples need to be desorbed at the temperature of the formation at the depth where the sample was taken. To ensure this temperature is maintained the desorption canisters need to be placed in either a heated water bath or a hot box with thermal lamps. If possible a water bath (Figures Figure 72 and Figure 73) should be used as water conducts and maintains temperature better than the air in the hot boxes. If the plan is to construct water baths in-house bear in mind that the heating element must be of sufficient size to heat the water evenly and rapidly. An adjustable thermostat must be added to control the water bath temperature.



Figure 72 Water bath (GEO Data, n.d.).



Figure 73 Desorption canisters in a water bath (Waechter, et al., 2004).

### 6.2.2. *In-Field Sampling*

The number of samples taken as part of a Greenfield exploration programme can be a limiting factor. More often than not costs override the value of sampling all the coal

encountered in the initial exploration boreholes. The ideal would be to sample all coal in at least the first couple boreholes to establish a baseline, especially if there is little or no information available regarding the coal deposits in the area. It is very rare that an exploration team is afforded this opportunity or that there is no regional information available for an area.

#### 6.2.2.1. Sampling Strategy

The hypothetical borehole and coal sequence (Figure 68) will be used to illustrate a typical sample collection approach when a limited number of desorption canisters may be used. In this scenario the maximum number of samples that may be taken is thirty (30). The sample collection strategy outlined in Figure 74 was developed to analyse the thickest and brightest coal zones more rigorously than the dull, thin and barcoded zones.

When limited in the number of samples that can be taken it is advised to have a number of samples, around 10%, as contingent samples. These can either be reserved for specific zones, as in the hypothetical case, or in the event that an unexpected horizon, such as a 30cm bright stringer in a barcoded sequence or thicker than expected coal zone, is encountered.

#### 6.2.2.2. Sample Identification and Collection

Time is of the essence when collecting desorption samples. As the core is brought to surface it loses gas and it is of utmost importance to minimise the time it takes to bring the core to surface, extract it from the core barrel, identify the samples and place in the desorption canisters (Waechter, et al., 2004; Potgieter, 2015 and Halliburton, 2008). A field exploration geologist with CBM exploration experience is essential for this phase as long delays may have a detrimental effect on the data quality. Table 32 demonstrates the sequence of events and points at which time recordings have to be taken during the sample collection process.

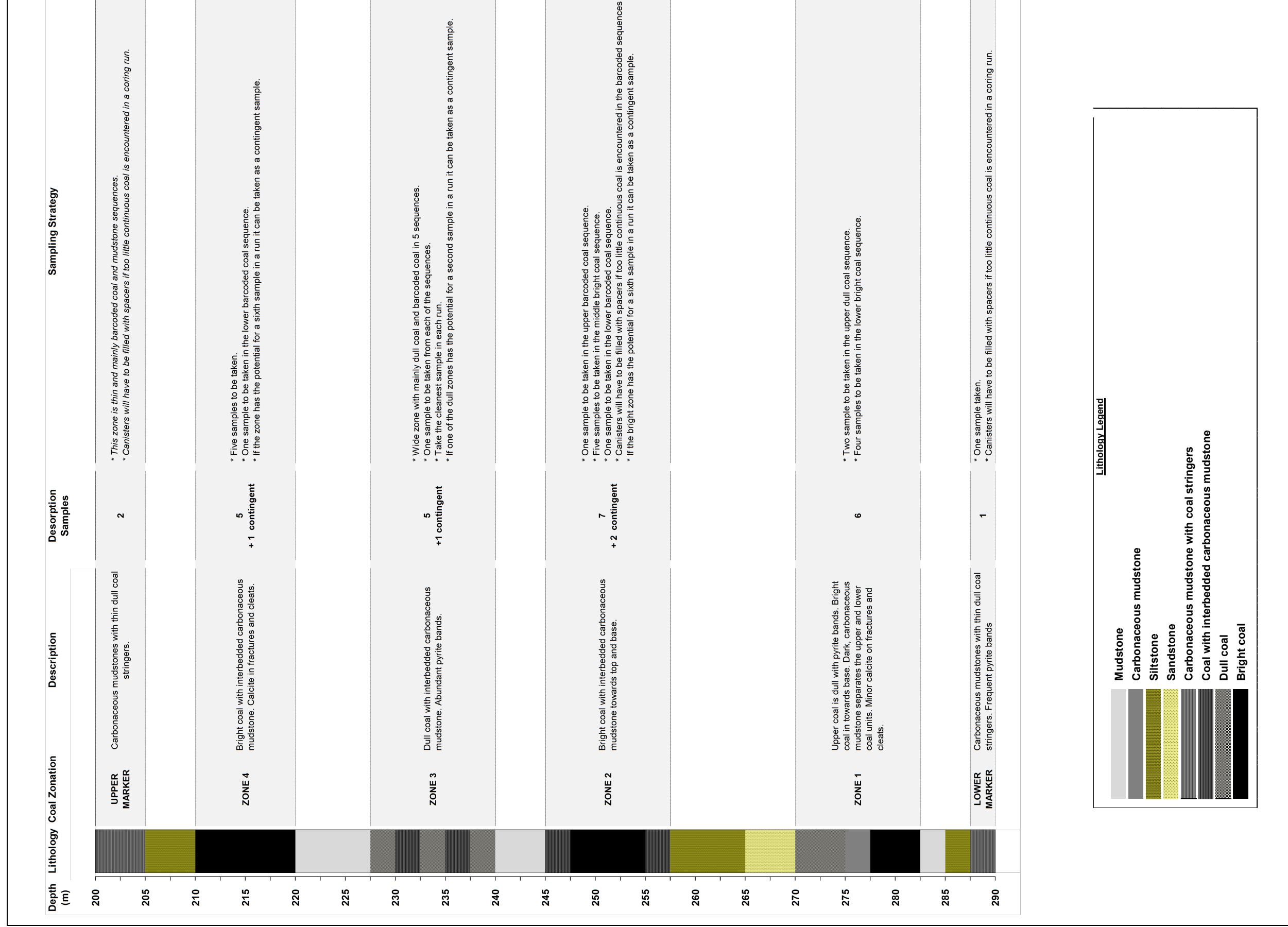


Figure 74 Desorption sample collection strategy.

Table 32 Sampling sequence of events.

SEQUENCE	ACTION	TIME MEASUREMENT	DESCRIPTION
1	<i>Start of coring run</i>		This is taken as the point when the coring bit starts cutting the core.
2	<i>Coring mid-point</i>	<u>Start recording time</u>	In Southern Africa 3m core barrels are used most often. In this case the mid-point will be at 1.5m. This is the point at which time recording must start, referred to as time zero ( $T_0$ ) (Standards Australia, 1999).
3	<i>End of coring run</i>		This is taken as the point when the core assembly has penetrated the full barrel length (3m).
4	<i>Core separation</i>		This process is where the base of the cut core is broken off the underlying formation by the drill rig
5	<i>Core barrel collection</i>		The wireline overshot is deployed to collect the core barrel (Figure 75).
6	<i>Core extraction</i>		The core barrel is brought to surface using the wireline winch mounted on the drill rig.
7	<i>Core removal from the inner barrel</i>		Once on surface the core inner barrel and catcher are unscrewed and the inner tube system is removed. The inner tube is pumped out of the inner barrel using a water plug and hydraulic pressure this minimises the amount of damage to the core. By using the triple tube system the inner tube is a split system than can be open with minimal effort further reducing time delays and damage to the core.
8	<i>Lithological description of the core</i>		The core has to be inspected for standard core recovery measurements and a brief lithological description taken. During this description potential samples need to be identified and marked out. It is advised to have desorption canisters on hand ready to be filled during the description process (Figure 76). Always ensure that the canister seal properly to prevent leakages prior to this phase.
9	<i>Sample Collection</i>		The samples identified during the lithological description phase need to be verified with the sampling strategy to prevent over or under sampling. The samples need to be cut from the core using either a hand held sampling saw or bolster and hammer. Bolsters work well in the Karoo cores. A useful tip with this phase is to have some halved PVC tubing, called a slip, on hand to place the samples in. The weight of the PVC tube needs to be written on in indelible ink as the sample has to be weighed prior to placing it in the desorption canister (Figure 77). The weight of the sample is important as gas content is expressed as volume per weight. If a significant amount of the sample is crushed the readings may be affected and in such cases it is best to not take the sample (Standards Australia, 1999).
10	<i>Transfer to desorption canister</i>		The selected sample on the slip can now be transferred to the desorption canisters. Ensure that all the material on the slip gets transferred to the canister. If a spacer was required the required length of spacer needs to be placed into the canister below the sample. Once the sample is in the canister the canister can be sealed.
11	<i>Prepare canister for the water bath or hotbox</i>		Once sealed the canisters can be moved to the hot box or water bath. Jin, et al. (2010) showed that oxygen in the canister can affect the gas composition measurements and as a result of this it is required to add a head space filler to the canister. The ASTM and AS standards provide for the addition of head space purging substances. The ASTM standards favours the use on an inert gas such as helium for this, however it is acceptable if distilled or formation water is used (ASTM International, 2010). If a gas is used the cap of the canister need to be prepared with a purge valve (Figure 78). In cases where the canisters do not allow for gas purging and formation water from nearby boreholes is not available distilled water must be used.
12	<i>Place canister in hotbox or water bath</i>	<u>Stop recording time</u>	The desorption canister is transferred to the hot box or water bath that has been pre-heated to the required reservoir temperature. This temperature can be obtained from the wireline logging. If no logging has taken place the temperature can be estimated based on the average surface temperature and geothermal gradient of the exploration area.

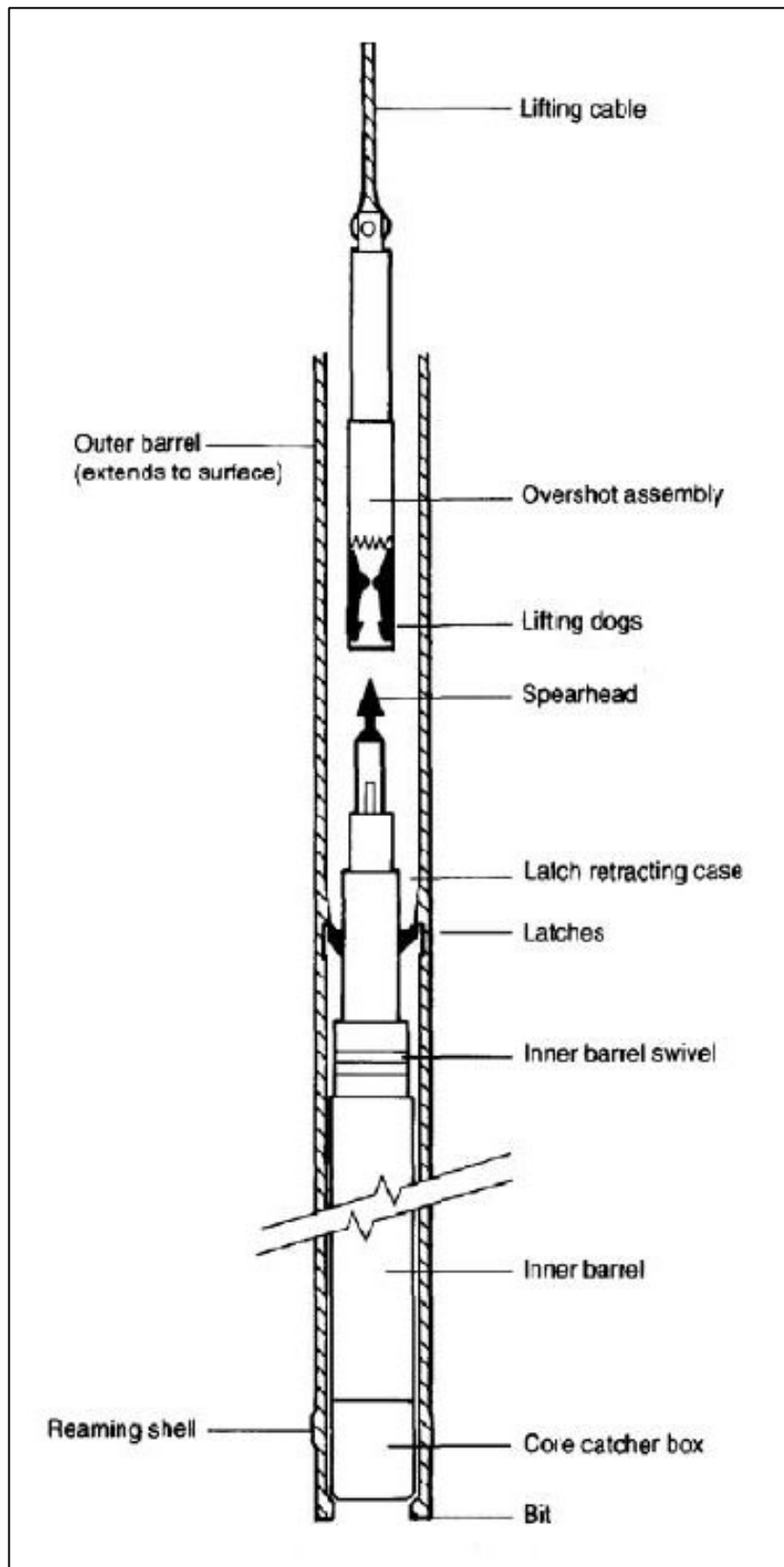


Figure 75 The wireline coring system collection mechanism (Massenga Drilling Rigs, n.d.)



Figure 76 Sample identification and collection (CBM Asia Development Corporation, 2012)



Figure 77 Coal sample selected for desorption on digital scale (Potgieter, 2015)

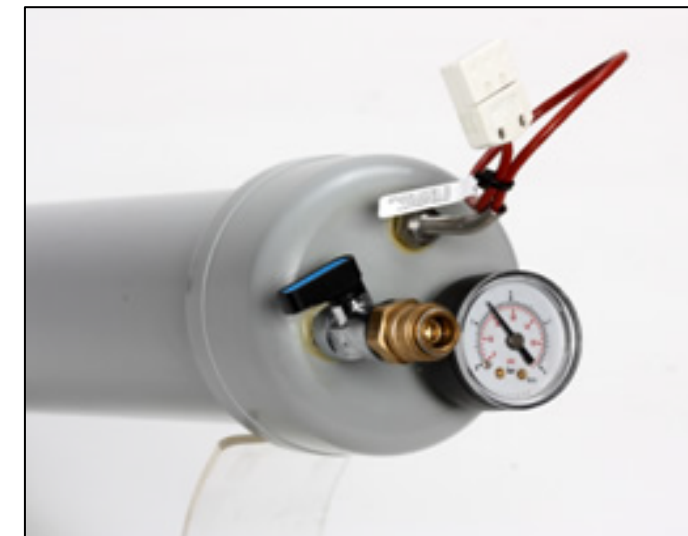


Figure 78 Desorption canister with purge and thermocouple valve (GEO Data, n.d.)

### 6.2.3. Gas Content Measurements

Gas content determination of the coal is comprised of three components 1) measureable gas, 2) lost gas and 3) residual gas. Each component is determined by different techniques as outlined in this section. The cumulative amount of gas that is desorbed from the coal is compared to the weight of the sample to express the gas content as a factor of volume to weight.

#### 6.2.3.1. Measureable Gas

The measurable gas (Q2) refers the physical amount of gas that is desorbed from the coal. These measurements are taken from the desorption canisters by opening the valve on the canister and having the gas displace water in a measuring cylinder. To facilitate easier reading of the measurements food colouring can be added to the water. The Australian Standard allows for the measurements to be taken either based on time or volume of gas. For field measurements it is advised to take all measurements based on time.

When taking the measurements there are two possible configurations. The first is a single canister measuring system where the canister either has to be removed from the water bath (Figure 79) or the measuring cylinder tube is connected to each canister individually. This is cumbersome on understaffed projects and by removing the canisters from the water bath the sample temperature is disturbed.

The second and preferred method is to have multiple measuring cylinders each connected to a specific desorption canister (Figure 80). With this configuration the geologist or assistant reads the desorbed volumes from the cylinders at specific time intervals without disturbing the samples. An added advantage of this configuration is that the cumulative volumes can be read directly rather than calculated based on point values reducing the chance for errors.



**Figure 79** Single sample desorbed gas content measuring apparatus (Weatherford Laboratories, n.d.).



**Figure 80** Continuous multiple sample desorbed gas content measuring apparatus (CSG Exploration & Production Services, n.d.).

Coal samples do not desorb at a fixed rate and as a result the measurements early on during the desorption process has to be more frequent than towards the end (Figure 81).

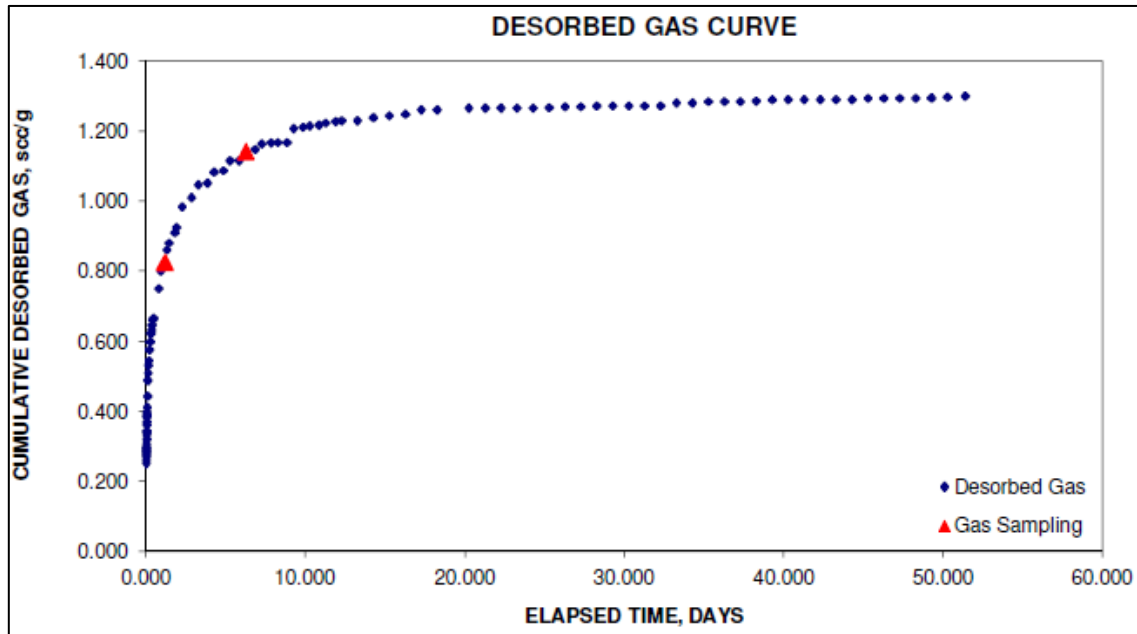


Figure 81 Cumulative measureable desorbed gas curve (Faiz, et al., 2013).

In Southern Africa the first 14 days of desorption is the key period when measurements have to be taken both often and at uniform intervals on all samples (Potgieter, 2015). With previous projects this sampling period was sub-divided into a number of time sections. Each timing section had different measurement intervals as outlined in Table 33. The end of desorption is regarded as the point where the sample equilibrates and the curve flat lines. A practical view of this point is when no additional gas is desorbed from the sample for a period of 5 days. As the project progresses it may be possible to determine the general number of days required for equilibrium e.g. 28 days. Once this timeframe is known a fixed time desorption programme can be developed.

**Table 33 Suggested desorption measurement intervals (Potgieter, 2015).**

Time Section (after T <sub>1</sub> )		Measurement Interval	Samples to be Taken	
			Gas Composition	Isotope
1.	0 – 10 minutes	1 minute		
2.	10 minutes – 1 hours	5 minutes		
3.	1 – 2 hours	15 minutes		
4.	2 – 6 hours	30 minutes		
5.	6 – 12 hours	1 hours		
6.	12 hours to 1 day	2 hours		
7.	1 – 2 days	4 hours	Sample	Sample
8.	2 – 5 days	8 hours		
9.	5 – 14 days	12 hours		
10.	14 days onwards	1 day		

Gas composition is an important aspect as CBM is not pure methane but a mixture of gasses, mainly methane, carbon dioxide and nitrogen. Resource estimations are based on total CBM, however sales gas will only be methane. When collecting the sample it is important to ensure the pure desorbed gas is sampled. To prevent any possible contamination the best point to take the gas sample is after about 2 days (Table 33). Gas composition samples need to be taken on each canister.

To fingerprint the origin of the gas (biogenic vs. thermogenic) isotope samples need to be collected. Isotope samples are collected in metal vessels known as IsoTubes (Figure 82 IsoTube gas sampling receptacle ) or gas tight packets. Due to logistics and

costs it is not always practical to sample every desorption canister for isotope analysis, however, it is important to generate a profile for the borehole and at least one isotope sample per zone is recommended. The samples should be taken shortly after the gas composition sampling (Table 33).



Figure 82 IsoTube gas sampling receptacle (Fieldwork Group, n.d.).

#### 6.2.3.2. Lost Gas

Lost gas (Q1) volumes are determined by extrapolating the first few hours of reading back to  $T_0$  (Waechter, et al., 2004). Waechter, et al. (2004) found that the accuracy of this extrapolation is higher where the sample collection time is faster and the initial desorption measurements were taken at a higher frequency as well as based on extended desorption measurements (Figure 83). A best fit polynomial method over extended time has shown to provide a superior fit (Figure 84) and more accurate Q1 determination (Waechter, et al., 2004).

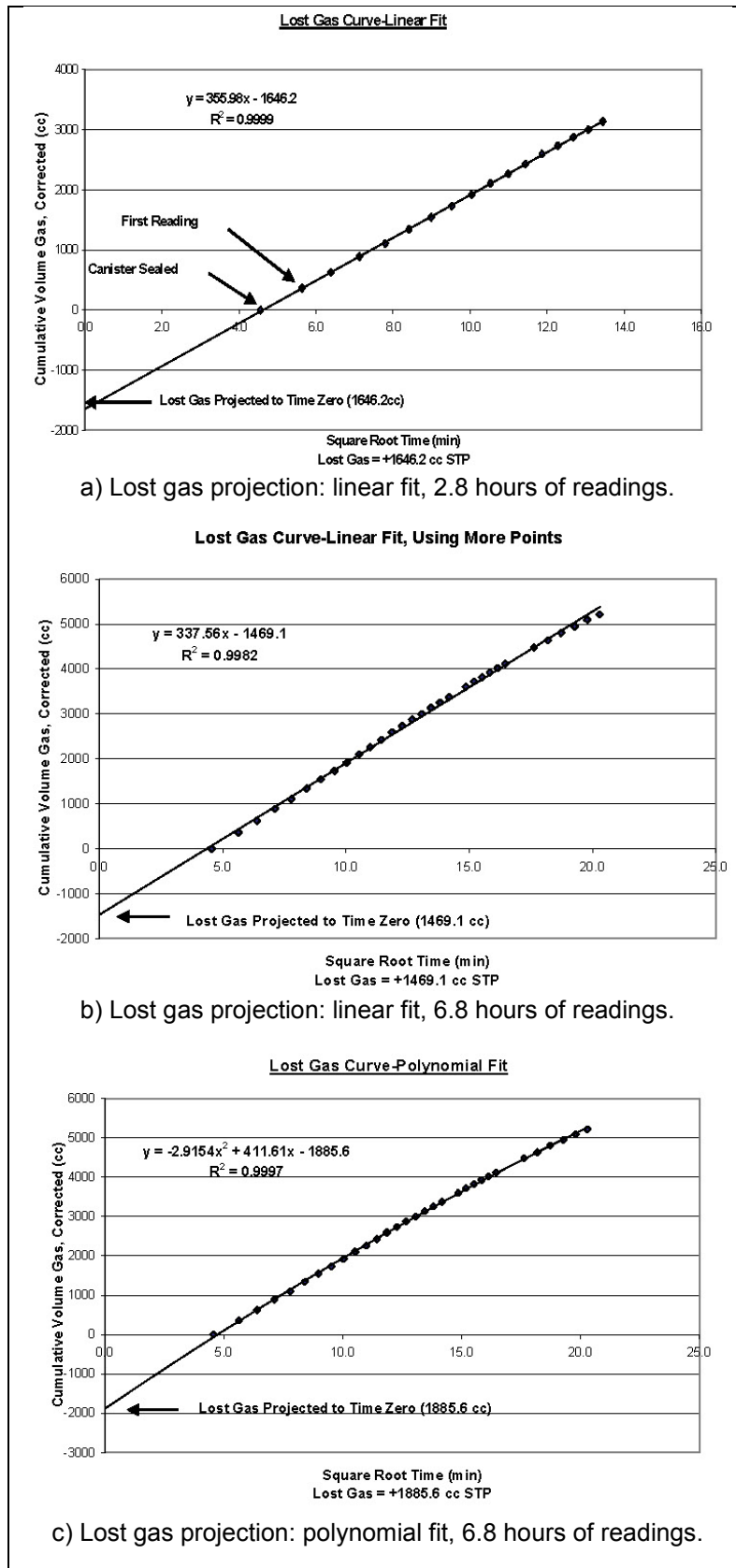
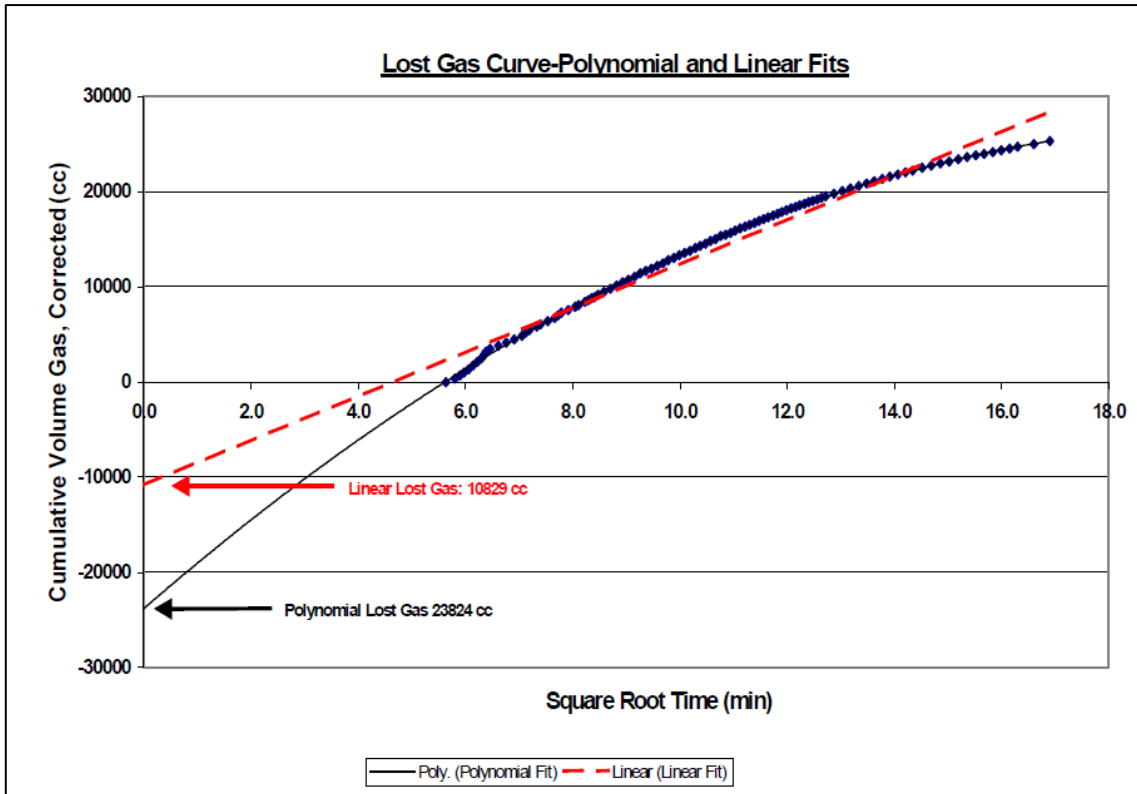


Figure 83

Curve fit lost gas estimations (Waechter, et al., 2004).



**Figure 84** Comparison of linear and polynomial fits in a coal with high gas content and high diffusion rate over a 4.4 hour period (Waechter, et al., 2004).

### 6.2.3.3. Residual Gas

Once the core desorption has been completed it is necessary to determine the residual gas content (Q3). The residual gas content is the amount of gas that is not extracted from the coal sample during the desorption analysis. To measure the residual gas content the core has to be removed from the desorption canister. Once the core is removed it must be cut in half using a slabbing saw (Figure 85). Half of the core will be kept for further coal analysis and half will be used to determine the Q3 content. In some cases only a quarter of the core is used for Q3 measurements, this requires a second slab on one of the core halves. The Q3 subsample has to be weighed again and placed in a gas tight Mill Pot and placed in a shaker (Figure 86 and Figure 87). The sample must be crushed to the point where 95% of the material will pass through a 212 $\mu$ m mesh (Standards Australia, 1999). The amount of gas liberated during the crushing is measured and reported as the residual gas content. Standards Australia (1999) requires to samples to be measured and compared. Equipment availability does not always allow for this.



Figure 85 Core slabbing equipment (GeoGas Pty Ltd, 2016).



**Figure 86** Residual gas content measurement milling canister (Weatherford Laboratories, n.d.).



**Figure 87** Residual gas mill pot in a shaker (GeoGas Pty Ltd, 2016).

#### 6.2.3.4. Total Gas Content

The total gas content of a sample is defined as the sum of the measurable gas, lost gas and residual gas. When the final data is reported the individual components and total gas content is provided. If the proximate analysis has been completed by the same contractor as the desorption evaluation the dry, ash-free gas content is often reported as part of the desorption summary sheet (Figure 88).

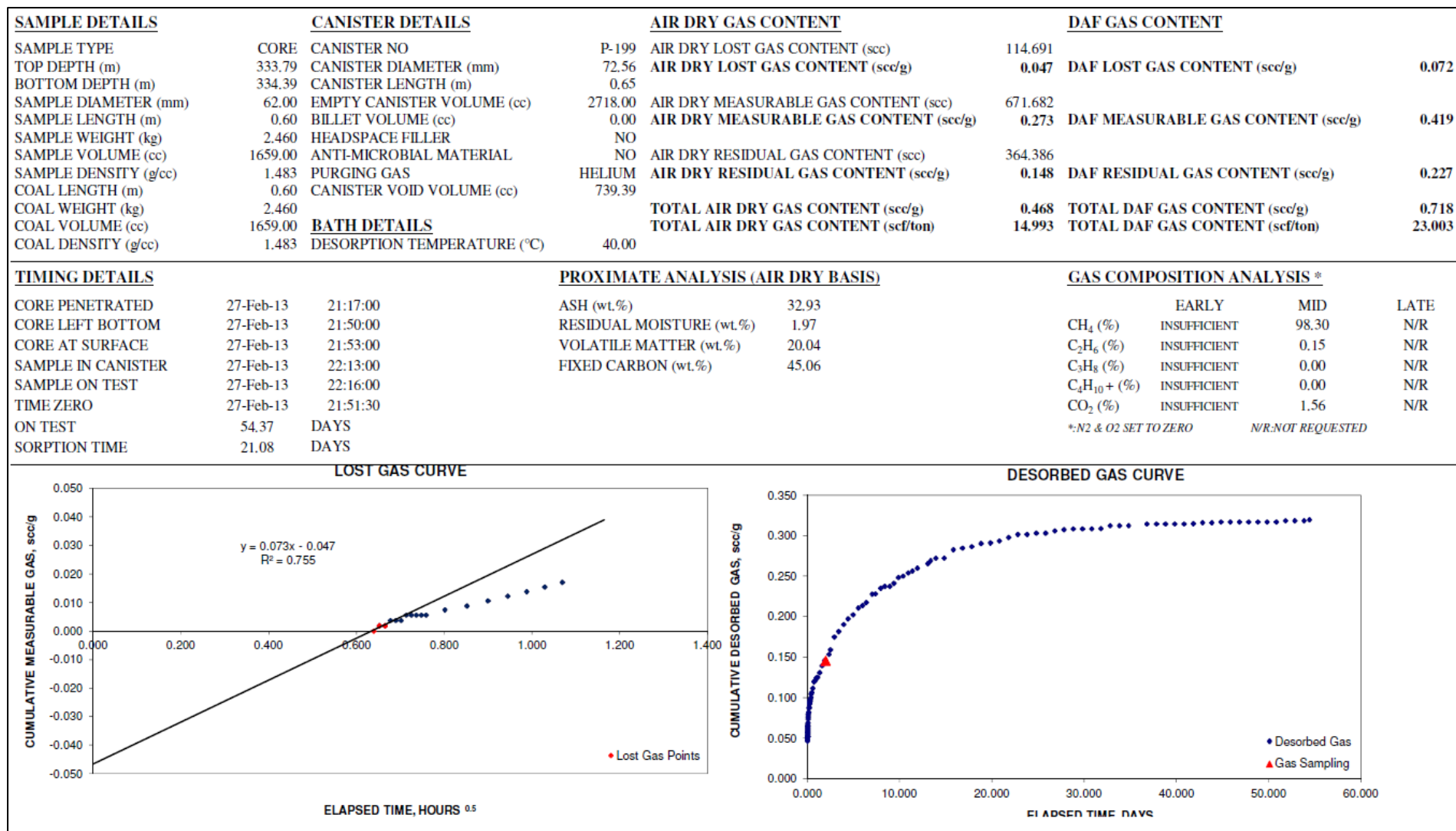


Figure 88 Desorption summary sheet (Kubu Energy, 2014).

#### 6.2.4. *Wireline Logging*

Wireline compensated density logs should be used as the primary coal identification tool. Along with the dual density tool a natural gamma, used for stratigraphic delineation, downhole temperature and, a multi-arm calliper, used to determine the borehole geometry, must be run as the minimum logging suite.

When running the density tool it is important to log at rates slower than 4m/min and maintain a constant logging speed. Although the density tool provides a calliper log along with the density log the multi-arm calliper is a good independent gauge for the accuracy of the density compensation. The temperature log is used to 1) determine the formation temperature and 2) indicate any possible water inflows. A number of the multi-arm calliper tools has a temperature sonde included, however if this is not the case a separate temperature sonde needs to be added to the logging suite.

Additional tools such as the sonic, resistivity, neutron, spontaneous potential, full waveform sonic and televiewer may be run depending on the requirement for additional petrophysical evaluations and budget constraints. Table 34 is summary of a number of tools showing tool descriptions and nominal logging speeds for a comprehensive logging suite as provided by Farr (2012).

It is very important to select a logging unit capable of reaching the operations. For a basic logging suite a 4x4 vehicle, like a Landcruiser, will suffice, however for more comprehensive logging suites in large diameter, deep boreholes, larger, purpose built trucks may be required (Figure 89).

Table 34

Wireline logging tool specifications and logging speeds (Farr, 2012).

<b>Basic Tool Suite Information and Descriptions</b>		
<b>Tool Name</b>	<b>Tool Description</b>	<b>Logging Speed</b>
Dummy	Weighted pipe to check if borehole has collapsed.	15m/min
Three-Arm Calliper	This is a three-arm calliper configuration used to measure the diameter of the borehole. It can be used in both open and cased holes.	10m/min
Compensated Density	The Compensated Density Logging Tool uses the two focused density detectors to compute borehole compensated density real time while logging. No post processing is required to produce compensated bulk density. Additionally, the tool also records natural gamma, calliper and focused guard resistivity.	3m/min
Acoustic Televiwer	The Acoustic Televiwer takes an oriented "picture" of the borehole using high-resolution sound waves. This acoustic picture is displayed in both amplitude and travel time. This information is used to detect bedding planes, fractures, and other hole anomalies without the need to have clear fluid fill in the boreholes. The televiwer digitizes 256 measurements around the borehole at each high-resolution sample interval (.005 meters/.02 feet). This data is oriented to North and displayed real-time while logging using the Visual Compu-Log software. Analysis includes colour adjustment, fracture dip and strike determination, and classification of anomaly. It allows information to be displayed on the graphical screen, plot, and in report format. Optionally, the tool can be equipped with a natural gamma sensor.	1m/m
Full Wave Sonic	The Full Wave Sonic Tool contains a single transmitter and dual receiver to record formation travel times. The full wave form data is also recorded simultaneously, along with near and far travel times, borehole compensated delta time, calculated sonic porosity, receiver gains, near/far amplitudes and natural gamma. The sonic or acoustic log uses the basic principle of sound waves traveling through media. The Century sonic system uses a single transmitter and dual receiver system for recording the travel times of the formation. The receivers are spaced (2 and 3 ft.) from the transmitter. Therefore, a 0.3 m (1ft.) calculation can be made to measure this interval transit time.	2m/min
Spontaneous Potential Resistivity	The Spontaneous Potential Resistivity Tool is a multi-parameter resistivity tool primarily used for water well logging and monitoring boreholes. The tool records nine different parameters simultaneously in one pass of the borehole. The nine parameters are the following: natural gamma, spontaneous potential, single point resistance, 16" normal resistivity, 64" normal resistivity, 48" lateral resistivity, fluid resistivity, temperature, and differential temperature.	5m/min
Multi-Parameter E-Log, Neutron	The Multi-Parameter E-Log, Neutron Logging Tool was developed to replace the E-Log Tool (9055) which was historically Century's most popular tool. The tool duplicates all parameters on the 9055 while adding the 16' normal, 64" normal, and lateral resistivities. The natural gamma circuit features a low dead time and the ability to measure very high count rates making it a favourite for uranium logging. The tool records ten different parameters simultaneously in one pass of the borehole. The ten parameters are the following: natural gamma, spontaneous potential, single point resistance, 16" normal resistivity, 64" normal resistivity, 48" lateral resistivity, neutron-neutron, temperature, delta temperature, slant angle (tilt) and azimuth (bearing). Slant angle, azimuth, and natural gamma are optional.	



a) Light weight wireline logging unit (Weatherford, 2016)



b) Weatherford's small-footprint slimline logging platform mounted on a 1.5-ton truck (Weatherford, 2007)



c) Light weight wireline logging unit in Mozambique (Weatherford, 2007)



d) Heavy duty logging unit (Farr, 2012)



e) Medium duty logging unit (Farr, 2012)

Figure 89 Examples of wireline logging units.

### 6.2.5. *Post-Desorption Sample Analyses*

The post-desorption sample analyses are subdivided into two categories, 1) basic analyses to be conducted on all desorption samples and 2) specialised analyses to be conducted on selected samples only.

#### 6.2.5.1. Basic Analyses

All desorption samples must have proximate analyses conducted on them, as this is the key to the DAF gas content determinations and coal quality determination. Grain density measurements have to be completed on each sample.

#### 6.2.5.2. Specialised Analyses

The specialised analyses referred to in this section are isotherm and petrography analyses.

When selecting samples for isotherm analysis it is important to have a representative distribution of the possible saturation values. Due to cost constraints it is rarely possible to conduct specialised analyses on all desorption samples. For representative sampling, the approach should be to have at least one sample over each zone and two contingent samples to test the heterogeneity in the most prospective zones (Figure 91). It is required to quarter the core samples for this method. The quarter to be retained for possible isotherm analysis must be stored in a manner to prevent any core degradation. Storage requirements will be provided by the laboratory responsible for the isotherm analyses.

The measured gas content values can be used to determine which samples to select, where the high gas content samples are compared to low gas content samples. This method has the potential to bias the readings toward a specific saturation state of the coal.

Comparatively lower gas content values are often excluded from the isotherm sampling programme. However, lower gas contents at higher saturation states could

be more productive across the field as shown in Figure 90. In the figure, both samples are under-saturated, however, the level of under-saturation in a lower quality coal is of such a nature that it may be able to produce gas quicker than a higher quality coal.

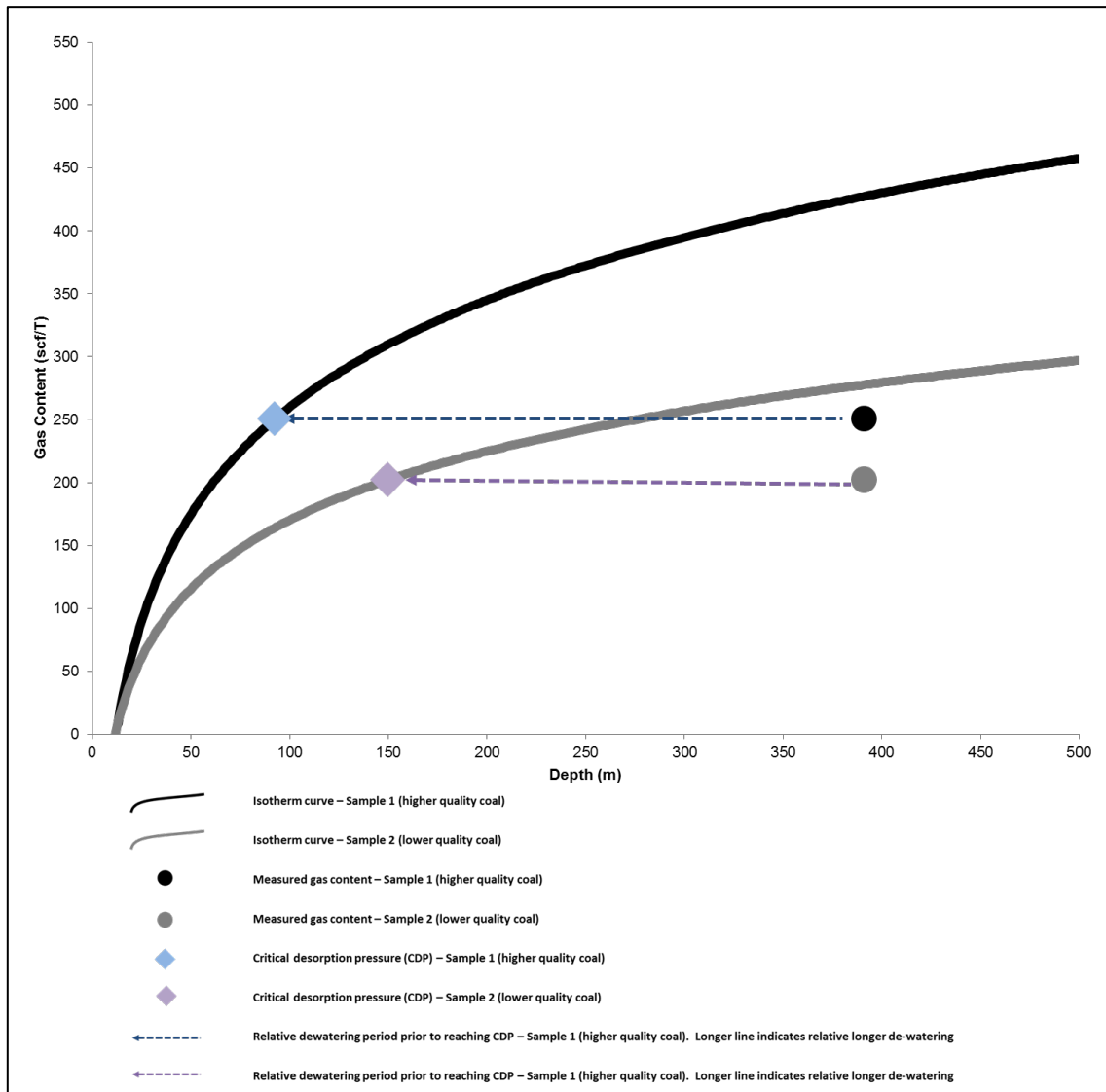


**Figure 90 Hypothetical production dynamics of 2 coal types and similar depths.**

It is advised to review the DAF gas content values of all samples in a zone and select the samples with values as close to the mode value as possible. This method works well in zones with a fairly uniform coal type and data distribution. In cases where a zone shows a great deal of heterogeneity with regards to the coal qualities and gas content values the data has to be evaluated further to determine the best

representation for the zone. Such a zone would typically require more than one sample analysed.

For the selection of the samples a ratio of DAF gas content to DAF fixed carbon can be used (Figure 92). This ratio provides a qualitative comparison of the sorptive capacity of every percent of fixed carbon of the coal. This ratio can be assumed as a proxy for the relative saturation states, but does not replace the isotherm analyses in any way. Due to different pressures encountered within different zones this ratio is not applicable for the comparison across zones.

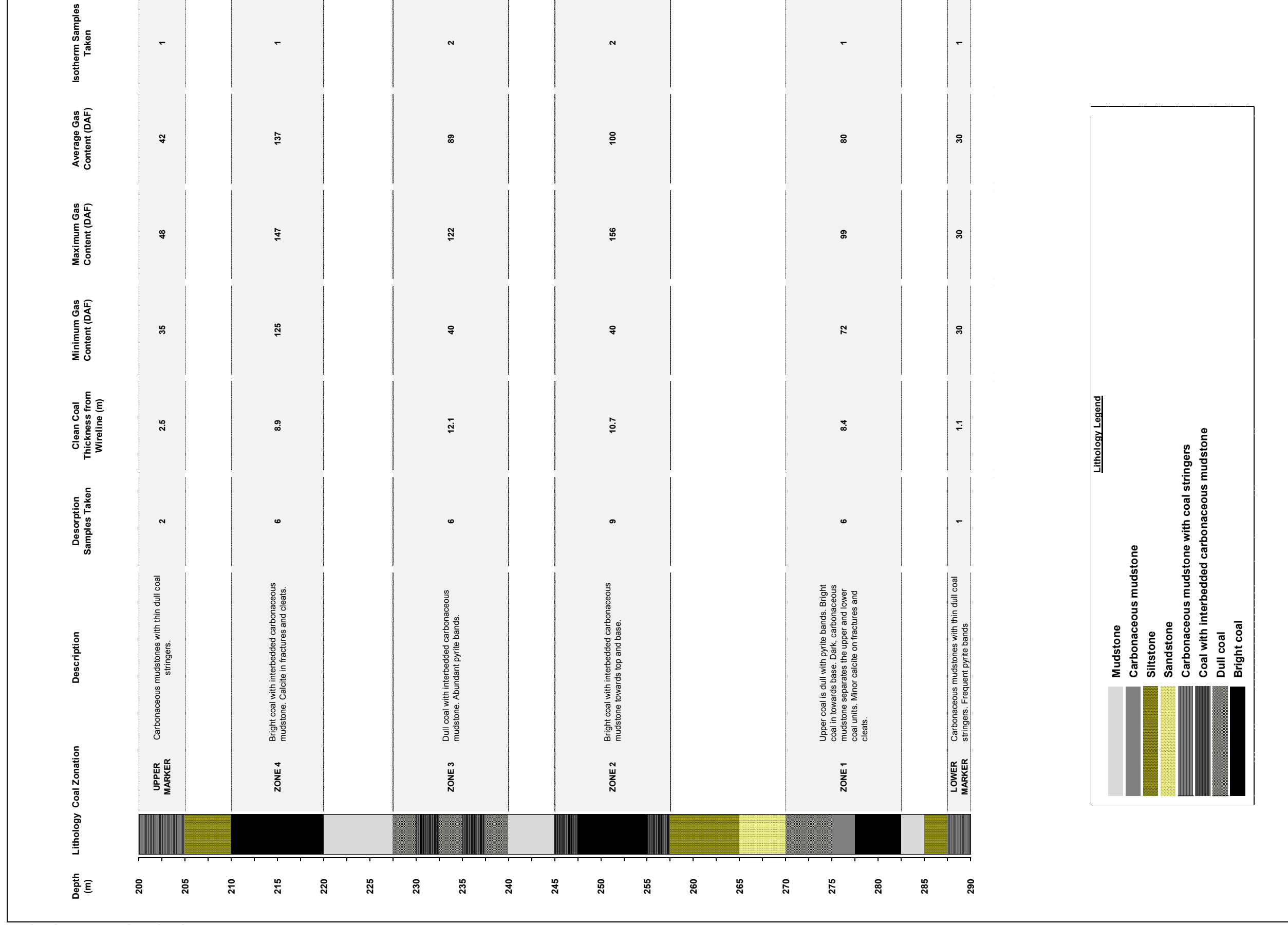
Higher ratios indicate coals where the fixed carbon desorbs greater volumes of gas per unit of carbon and the opposite is true for lower ratios. By comparing these base indices it is possible to eliminate bias in selecting subsamples related to the measured gas contents. An evaluation of this method (Figure 92) was completed based on 2 distinct coal types and compared to a sample from the Kubu exploration programme. A range of gas content values were used for each coal type to demonstrate how the ratio will change at different saturation states.

The premise is that higher gas content values for a specific coal type at similar depths will indicate higher saturation states. As the Kubu sample had isotherm data available, the gas content at 100% saturation was used to compare with the measured gas content (Figure 92). In cases where the relative saturations throughout the zone remain fairly constant the decision can be made to submit only one sample for isotherm analysis.

All samples selected for isotherm testing need to have a full petrography analysis with maceral typing and vitrinite reflectance measurements. Additional petrography samples may be taken for maturity profiling.

Figure 91

Isotherm sample selection.



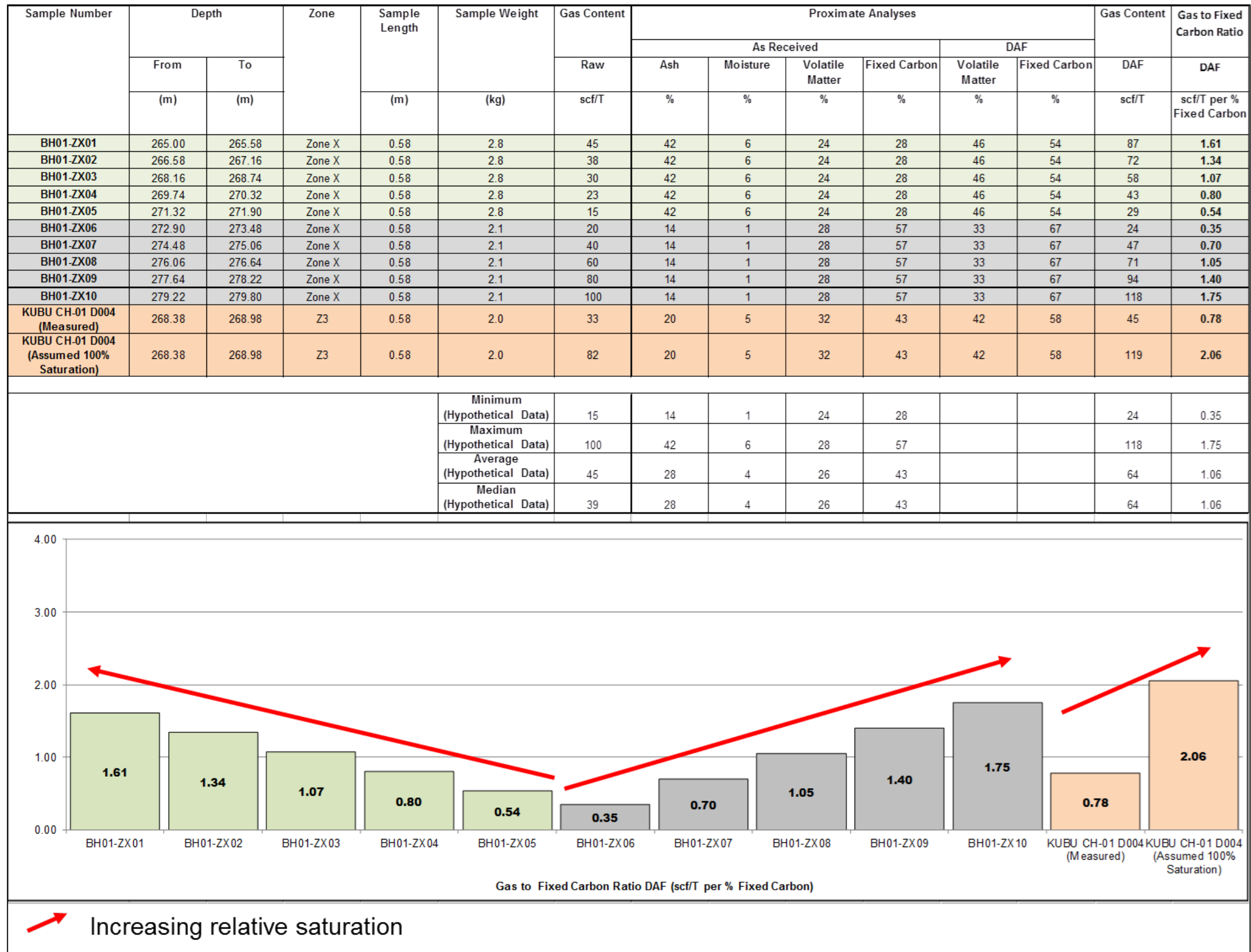


Figure 92 Example of desorption and coal data over a heterogeneous sampling zone.

### 6.2.6. *Data Reporting*

When reporting the sampling data in spread sheets it is imperative to quality check all information when adding the information. Adding incorrect data to the master sheet will affect all calculations and models.

The best approach is to have a master sheet, to which all data pertaining to a borehole can be added, that can be used for evaluation and modelling. When preparing the master sheet limitations and idiosyncrasies of the preferred modelling package needs to be taken into account as the input methods in various packages may differ vastly.

Always be mindful that a number of modelling packages have character limitations. A useful character limit to use in master sheets is twelve (12) characters and to achieve this, a coding system as shown in Table 35 can be used. This coding system allows for the creation of single row spread sheets that can be read by all modelling packages and database managers. The codes can be programmed into the package to recognise the analysis and units for quick reference decreasing the model processing time.

Although it may take some time to get fully accustomed with a coding system as proposed, the advantages relating to compatibility across modelling and evaluation platforms will increase processing efficiency.

Table 35 Proposed coding library for CBM exploration borehole, sampling and analysis information.

CODING LIBRARY FOR CBM EXPLORATION BOREHOLE, SAMPLING AND ANALYSIS INFORMATION									
DATA CATEGORY		SUB-CATEGORY				MEASUREMENT UNIT		EXAMPLE	
NAME	CODE	NAME	CODE	NAME	CODE	UNIT	CODE	VERBOSE	CODED
Borehole Number	BHID								
Sample Number	SPID								
Zone	ZON								
Marker Horizon	MH								
Depth	DT	From	FR	Metres	m	Top depth expressed in metres	DTFRm		
		To	TO	Feet	ft				
		Centre	CN						
Sample Weight	SW			kilograms	kg	Sample weight expressed in kilograms	SWkg		
				pounds	lb				
Sample Length	SL			centimetres	cm	Sample weight expressed in inches	SLin		
				Metres	m				
				inches	in				
				feet	ft				
Desorption Testing Gas Content	GC	Gas Content Lost Gas	Q1	Raw	RAW	Standard cubic feet per ton	scft	Dry, ash-free measureable gas content expressed in cubic meter per ton	GCQ2DAFcmT
		Gas Content Measureable Gas	Q2	As Received	AR	Standard cubic feet per tonne	scfT		
		Gas Content Residual Gas	Q3	Air Dried	AD	Cubic centimetre per gram	ccg		
		Gas Content Total Gas	Q4	Dry, Ash Free	DAF	Cubic meter per tonne	cmT		
Grain Density	GRD			Grams per cubic centimetre	gcc	Grain density in grams per cubic centimetre	GRDgcc		
				Pounds per cubic foot	pcf				
Gas Composition	GCO	Methane	CH4	Percent	pc	Measured methane content in percent	GCOCH4pc		
		Nitrogen	N2						
		Carbon Dioxide	CO2						
Proximate Analysis	PXM	Ash Content	A	Raw	RAW	As received fixed carbon measured during proximate analysis	PXMFCARpc		
		Moisture Content	M	As Received	AR				
		Volatile Matter	VM	Air Dried	AD				
		Fixed Carbon	FC	Dry, Ash Free	DAF				
				Ash Free	AF				
Isotherm Methane	IC4	Langmuir Pressure	PL	Pounds per square inch	psi	Dry, ash-free methane Langmuir volume expressed in standard cubic feet per tonne	IC4VLDAFscfT		
Isotherm Nitrogen	IN2			Kilopascal	kPa				
Isotherm Carbon Dioxide	ICO2			Mega Pascal	Mpa				
		Langmuir Volume	VL	Raw	RAW				
				Dry, Ash Free	DAF			Standard cubic feet per ton	scft
								Standard cubic feet per tonne	scfT
						Cubic centimetre per gram	ccg		
Formation Pressure Gradient	FPG			Cubic meter per tonne	cmT				
				Cubic meter per ton	cmf				
Formation Pressure	FP			Pounds per square inch per foot	psif	Formation pressure gradient expressed in pounds per square inch per foot	FPGpsif		
				Kilopascal per meter	kPam				
				Pounds per square inch	psi			Formation pressure expressed in pounds per square inch	FPpsi
				Kilopascal	kPa				
Saturation	SAT	Methane	C4	Raw	RAW	Raw methane saturation	SATC4RAWpc		
		Nitrogen	N2	Dry, Ash Free	DAF				
		Carbon Dioxide	CO2						
Petrography	PGH	Reflectance of Vitrinite	VR	Average	AVE	Average vitrinite reflectance	PGHVRAVEpc		
				Maximum	MAX				
				Minimum	MIN				
Gas to Fixed Carbon Ratio	CFR			Raw	RAW	Dry, ash free gas to fixed carbon ratio expressed in cubic centimetres per gram of gas per percent of fixed carbon	CFRDAFccgpc		
				Dry, Ash Free	DAF				
								Standard cubic feet per ton of gas per percent of fixed carbon	sctpc
								Standard cubic feet per tonne of gas per percent of fixed carbon	scTpc
						Cubic centimetres per gram of gas per percent of fixed carbon	ccgpc		
						Cubic meters per ton of gas per percent of fixed carbon	cmTpc		
						Cubic meters per tonne of gas per percent of fixed carbon	cmTpc		

## 7. SUMMARY

The growing energy demand coupled with a finite coal supply has resulted in industry leaders identifying and investigating new energy sources for future use. Natural gas is a transitional fuel during the period where low-carbon alternatives to coal and nuclear are investigated. In North America natural gas is being used extensively as the preferred energy source for domestic use and is one of the cleanest fossil fuels used for electricity generation. Currently two primary types of gas resources, conventional from high permeability reservoirs and unconventional from low permeability reservoirs, are being exploited. The most well-known of the unconventional gasses is Shale Gas that gained notoriety as a result of the completion method known as fracking. Another unconventional resource, currently being exploited in North America and Australia, is coal bed methane (CBM) where deep coal seams are exploited and gas produced. CBM was the focus of this evaluation. In the United States CBM has been produced commercially since the mid 1970's when operators started to modify existing petroleum industry technology.

CBM is the term used for the natural gas that is sourced by thermogenic alterations of coal or by biogenic action of indigenous microbes on the coal. During the coalification process the decomposition of the organic material produces methane gas which along with other gases, including nitrogen and carbon dioxide, is adsorbed onto the coal. The generation capability of biogenic methane is very difficult to measure or predict, however, biogenic gas generation has been investigated as a reservoir enrichment technique. The saturation state of a coal seam is determined by comparing the measured gas content to the maximum sorptive capacity of the coal. A saturated coal seam will produce gas nearly simultaneous to the initiation of the water pumping, whereas there is a long period of water abstraction required prior to any gas production in under-saturated seams. This reduces the overall production capability of a seam.

Southern Africa has very few producing conventional gas fields, mostly off-shore South Africa and Namibia. The vast marine shales of the Main Karoo Basin, in South Africa, and coal fields in Southern Africa have been the focus of these exploration efforts. The most notable programmes are the Waterberg CBM near

Lephalale, operated by Anglo Coal and planned Karoo shale gas project, operated by Shell in South Africa.

The CBM resources in Botswana and Zimbabwe have for the past two decades been seen as a potentially exploitable gas deposit and potential supplement and in time a substitute for coal as the primary energy source in the region. To date, there has been a great deal of speculation on the size of the potential resource with a wide range of values reported. The values are often based on either proprietary data or single point datasets that have been extrapolated to fit a regional study area. One of the major limitations noted with previous CBM resource evaluations was the lack of compensation for lower saturations. In a number of the previous evaluations reviewed full saturation was presumed as opposed to lower saturation values noted in a number of assessments. Currently there are no commercially producing CBM fields in Southern Africa, however, a number of companies, particularly Tlou in central Botswana and Anglo Coal in the Lephalale region in South Africa, have had some exploration success.

The Karoo Supergroup is the primary target for CBM exploration but is poorly exposed in Botswana and only a few outcrop descriptions could be made previously. The stratigraphic descriptions were mainly obtained from limited deep boreholes drilled in the 1970's aided by a deep resistivity survey. In Zimbabwe there has been a long history of coal mining and the stratigraphic nomenclature was developed from outcrops, drill logs and underground maps. The coal is found in the Permian Ecca Group and can occur as discrete seams in Zimbabwe or thin stringers in Botswana. The coal measures are found throughout the study area but, in north-eastern Botswana only four of the Anglo Coal Botswana boreholes intersected the coal indicating a pinch out of the lower Karoo strata.

Coal is ranked based on the constituents, physical properties and thermal maturity as the raw peat is transformed to anthracite. In the Mid-Zambezi Basin an apparent decrease in the coal rank over relatively short distance north-eastwards from Wankie to Sengwa and between Lusulu and Sengwa has been noted. In Botswana, evaluations of the Dukwi coalfield indicated that the coal is of low rank. It was possible to rank the coals within the study area using reported proximate analysis.

For the evaluation the ASTM standard of coal rank classification was used as it is relatable to gas holding capacities. In turn, these gas holding capacities were used to evaluate the CBM resource potential of the study area.

The calculated coal rank in the area ranged from subbituminous to medium volatile bituminous. Once an evaluation on the production capacity is attempted it is of utmost importance to isolate the primary producing zones and establish the regional continuity and possible compartmentalisation of these. With the sparse data this was not possible nor was it required at the regional scale of the assessment. The nett coal thickness, collected from published literature, was used for the resource assessment.

The evaluation of the Shangani Energy and Anglo Coal Botswana data indicate that there is a wide range of saturation levels present. Under-saturated coals have a long period of production where only water will be produced that lengthens the time from production start to delivery of the first commercial gas.

This under-saturation combined with lower permeabilities can lead to a very tight well spacing being required and raising the overall capital investment required for full field development. A further influence of under-saturation of the coal is that the estimated gas contents from laboratory testing are skewed and ultimately higher values are assumed. For this evaluation a range of saturation states, based on analogue data, were used to produce more accurate gas content distributions.

As a result of sparse field data the datasets required for the resources evaluation were separated into two categories, 1) Measured, datasets which had been obtained from published logs, papers and maps and subsequently modelled to show the regional distribution of the measurements, and 2) Inferred and Calculated datasets not explicitly or widely reported and subsequently interpreted and calculated from available data using previously reported techniques and analogues.

Schlumberger GeoX software was used for a probabilistic resource calculation using Monte Carlo simulations with ten thousand iterations. For the evaluation statistically calculated data distribution parameters were used as inputs. Recoverable resource

estimations were not conducted as this is highly dependent on data that is not available in the public domain. Statistical distributions of the area, coal thickness, coal density and gas content data were used to determine the input values to the GeoX volumetric calculation.

The resource estimation results showed a wide distribution of probable values. This is indicative of a poorly understood region with a great deal of assumption as opposed to good exploration data. The P50 resource value was 22 Tcf. This resource value was compared to major basins in Canada and the United States and found that the resource density ( $\text{g}/\text{cm}^3$ ) in the study area was significantly lower than the other basins.

The major basins in Canada and the US have a significantly higher resource density ( $\text{g}/\text{cm}^3$ ) than that of the study area indicating a lower prospectivity for CBM. Once more reliable regional data becomes available it will be possible to update this evaluation, however, from previous investigations within the region the general exploration and development potential is low and to date not a single project comparable to the North American basins have been found.

The primary challenge during the assessment of the study area was the availability of reliable geological and gas content data. If regional data collection and reporting was standardised it would be possible to assess the area with a greater amount of certainty. Practical guidelines, applicable on future CBM exploration programmes, were developed. These guidelines aim to ensure a uniform quality of data that can be used for regional assessments.

## **8. CONCLUSIONS**

Even with a resource value of 22Tcf, the major basins in Canada and the US have significantly higher resource densities than that of the Study Area indicating a lower prospectivity for CBM.

If saturation and permeability measurements become available for the study area it will be possible to evaluate the production potential and subsequent economic viability. Until such time the study area can be viewed as a stranded resource with no measureable economic value.

The CBM exploration industry in Southern Africa is still in its infancy. To date, because of the lack of Southern African standards, companies have placed greater emphasis on budget rather than data quality.

The culture of poor data collection and lack of publically available reports increases the difficulty of any evaluation such as this one. Using actual field data rather than the inferred gas contents will have an effect on a resource evaluation.

The guidelines developed during this study aim to improve the quality of data collected whilst being appreciative of cost.

## 9. RECOMMENDATIONS

Similar future regional evaluations need to be based on reliable, publically available data. This data reliability must be based on acceptable, standardised data collection methods. The Kubu Energy Relinquishment Report for the 2013 Botswana campaign should be seen as the best example for data reporting as the report included all field, laboratory and interpreted datasets in the publically available pack.

As a minimum the following data must be collected during a CBM exploration project:

- Coal thickness estimated from wireline logs;
- Stratigraphic depths measured during the drilling and refined using the wireline logs;
- Formation temperature from wireline logs;
- Proximate analysis and coal quality data;
- Gas content measured from core desorption;
- Gas saturations calculated from the comparison of the measured gas content analyses with the maximum gas holding capacity derived from adsorption isotherm measurements and
- Gas composition measured using gas chromatography.

The gas to fixed carbon ratio can be investigated further as a quantitative saturation state indicator, however this will require a great number of isotherm and pressure datasets that currently are not available in the public domain. A further limitation to this investigation is the lack of laboratories capable of conducting isotherm analyses in Southern Africa.

## 10. REFERENCES

- Adelmann, D. & Fiedler, K., 1998. Origin and characteristics of Late Permian submarine fan and deltaic sediments of the Laingsburg subbasin (SW Karoo Basin, Cape Province/South Africa). *Zeitschrift der deutschen Geologischen Gesellschaft*, Issue 149, pp. 27-38.
- Advanced Resources International, Inc., 2003. *Results of the Central Kalahari Karoo Basin Coalbed Methane Feasibility Study*, Arlington: Department of Geological Survey.
- Alberta Energy, 2008. *Natural Gas*, s.l.: Alberta Energy.
- Alberta Energy, 2012. *About Coalbed Methane*. [Online]  
Available at: <http://www.energy.alberta.ca/naturalgas/754.asp>  
[Accessed 22 April 2015].
- Al-Jubori, A. et al., 2009. Coalbed Methane: Clean Energy for the World. *Oilfield Review*, 21(2), pp. 4-13.
- Aminian, K., 2005. *Evaluation of Coalbed Methane Reservoirs*, s.l.: Petroleum & Natural Gas Engineering Department, West Virginia University.
- Anglo Coal Botswana, 2010. *Early Relinquishment Report: PL053/2009 - 058/2009 and 025/2009 - 039/2009*. Gaborone: Anglo Coal Botswana.
- Anon., 2004. The Karoo triple junction questioned: evidence from Jurassic and Proterozoic  $^{40}\text{Ar}/^{39}\text{Ar}$  ages and geochemistry of the giant Okavango dyke swarm (Botswana). *Earth and Planetary Science Letters*, Issue 222, p. 989– 1006.
- APF Energy, 2004. *Coalbed Methane Development in the Western Canadian Sedimentary Basin: A Significant Emerging Resource for North America*. s.l., s.n.
- Armaretti, T., 2014. *Unconventional Resources and the Petrobras Challenges in Argentina*. Bogota, s.n.
- ASTM International, 2010. *D7569 – 10: Standard Practice for Determination of Gas Content of Coal—Direct Desorption Method*. 1 ed. West Conshohocken: ASTM International.
- Australia Pacific LNG, 2011. *How CSG is produced*. [Online]  
Available at: <http://www.aplng.com.au/about-project/how-csg-produced>  
[Accessed 29 March 2015].

- Barker, O., 2006. *CBM Gas in Botswana*. Gaborone, Nyati Resources.
- Barker, O., 2006. *CBM Gas in Botswana*. Gaborone, Nyati Resources.
- Barker, O., 2012. *CBM in the Springbok Flats coalfield: A major untapped source of energy*. s.l., Fossil Fuel Foundation - Limpopo Conference.
- Bordy, E., 2009. *Sedimentological investigation of the coal-bearing Karoo succession in the Nata and Rainbow Gas Coal Project Areas of Botswana*, Grahamstown: Unpublished.
- Bordy, E., Knoll, F. & Bumby, A., 2010. New data on the palaeontology and sedimentology of the Lower Jurassic Lisbon Formation (Karoo Supergroup), Ellisras Basin, South Africa. *N. Jb. Geol. Paläont. Abh.*, Volume DOI: 10.1127/0077-7749/2010/0091.
- Bordy, E., Segwabe, T. & Makuke, B., 2010. Sedimentology of the Upper Triassic–Lower Jurassic (?) Mosolotsane Formation (Karoo Supergroup), Kalahari Karoo Basin, Botswana. *Journal of African Earth Sciences*, Issue 58, p. 127–140.
- Boyer, C. et al., 2011. Catuneanu, et al. (2005). *Catuneanu, et al. (2005)*, 23(3).
- Boyer, C., Frantz, J. & Jenkins, C., 2007. Hydrocarbons from non-conventional and alternative sources. In: *Encyclopaedia of hydrocarbons*. Rome: Istituto della enciclopedia Italiana, pp. 57-83.
- Cairncross, B., 2001. An overview of the Permian (Karoo) coal deposits of southern Africa. *African Earth Sciences*, Volume 33, p. 529–562.
- Cardott, B., 2012. *Introduction to Vitrinite Reflectance as a Thermal Maturity Indicator*. Tulsa, Oklahoma Geological Survey.
- Carney, J., Aldiss, D. & Lock, N., 1994. *The geology of Botswana*, s.l.: Geological Survey Department.
- Catuneanu, O. et al., 2005. The Karoo basins of south-central Africa. *Journal of African Earth Sciences*, Issue 43, p. 211–253.
- CBM Asia Development Corporation, 2012. *What is CBM*. [Online] Available at: <http://www.cbmasia.ca/What-Is-CBM> [Accessed 10 January 2016].
- Chilume, C., 2002. *Shared knowledge, a key to equitable utilisation of transboundary aquifers*. Tripoli, Internationally Shared Aquifer Resources Management.
- Computer Support Group, 2011. *Specific Gravity Of General Materials Table*. [Online]

- Available at: <http://www.csgnetwork.com/specificgravmattable.html>  
[Accessed 2015].
- Corrado, S., Zattin, M. & Aldega, L., 2010. Sedimentary vs. tectonic burial and exhumation along the Apennines (Italy). *Journal of the Virtual Explorer*, 36(The Geology of Italy: tectonics and life along plate margins).
- Crain, E., 2015. *Crain's Petrophysical Handbook - Density Log Basics*. [Online]  
Available at: <https://www.spec2000.net/07-densitylog.htm>  
[Accessed 2015].
- Crain, E., 2015. *Crain's Petrophysical Handbook. Special Cases - Coalbed Methane*. [Online]  
Available at: <https://www.spec2000.net/17-spec2000.htm>  
[Accessed 30 March 2015].
- CSG Exploration & Production Services, n.d. *Laboratory Images*. [Online]  
Available at: <http://www.csg-eps.com/LAB%20IMAGES.html>  
[Accessed 19 January 2016].
- Dowling, G., 2006. *Overview of the Anglo Coal Waterberg CBM Project*. Johannesburg, Fossil Fuel Foundation.
- Duguid, K., 1986. Wankie district coal measures. In: C. Anhaeusser & S. Maske, eds. *Mineral Deposits of Southern Africa*. s.l.:s.n., p. 2099–2104.
- Eddy, G., Rightmire, C. & Byren, C., 1982. *Relationship of Methane Content of Coal Rank and Depth: Theoretical vs. Observed*. Pittsburgh, Society of Petroleum Engineers.
- Faiz, M., Crozier, E. & Lee-King, A., 2013. *Influence of Coal Type, Rank and Thermal History on Gas Contents in the Kubu PLs, Botswana*, Brisbane: Kubu Energy.
- Faiz, M., Murphy, A., Hendry, P. & Midgley, D., 2012. *Geochemical and Microbiological Review of Coal Seam Gas – New Facts and Old Controversies*. Brisbane, Eastern Australian Basin Symposium.
- Faiz, M., Potgieter, J., Lee-King, A. & Crozier, E., 2014. *New insight into Permian coals of eastern Botswana and its impact on coal seam gas properties*. Sydney, The Society of Organic Petrology.
- Fallgren, P. et al., 2013. Comparison of coal rank for enhanced biogenic natural gas production. *International Journal of Coal Geology*, Issue 115, pp. 92-96.
- Farr, D., 2012. *Exploration Geophysics Logging Equipment* [Interview] 2012.

- Fieldwork Group, n.d. *IsoTubes*. [Online]  
Available at: <http://www.fieldworksupplies.co.nz/product/143-IsoTubes-1666>  
[Accessed 10 January 2016].
- Flores, R., 2002. Coalbed Methane in the Powder River Basin, Wyoming and Montana: An Assessment of the Tertiary-Upper Cretaceous Coalbed Methane Total Petroleum System. In: *Total Petroleum System and Assessment of Coalbed Gas in the Powder River Basin Province, Wyoming and Montana*. 1 ed. Denver(Colorado): United States Geological Survey.
- GEO Data, n.d. *Desorption*. [Online]  
Available at: <http://www.geo-data.de/index.php/en/petroleum-engineering/unconventional-services/desorption>  
[Accessed 19 January 2016].
- GeoGas Pty Ltd, 2016. *Sample Treatment*. [Online]  
Available at: <http://www.geogas.com.au/laboratory/sample-treatment>  
[Accessed 19 January 2016].
- Geological Survey Department, 1984. *The Petroleum Prospects of Botswana, Lobatse*: Geological Survey Department.
- Green, D., 1966. *The Karoo System in Bechuanaland*, Lobatse: Geological Survey Department.
- Gurba, L. & Weber, C., 2001. Effects of igneous intrusions on coalbed methane potential, Gunnedah Basin, Australia. *International Journal of Coal Geology*, Issue 46, pp. 113-131.
- Haddon, I. & McCarthy, T., 2005. The Mesozoic–Cenozoic interior sag basins of Central Africa: The Late-Cretaceous–Cenozoic Kalahari and Okavango basins. *Journal of African Earth Sciences*, Issue 43, pp. 316-333.
- Halliburton, 2008. *Halliburton*. 1 ed. s.l.:Halliburton.
- Hiller, K. & Shoko, O., 1996. Hydrocarbon source rock potential of the Karoo in Zimbabwe. *Journal of African Earth Sciences*, 23(1), pp. 31-43.
- Himmelsbach, T., Meier, J. & Böttcher, J., 2008. *Palaeo-Hydrogeology of the Okavango Basin and Makgadikgadi Pan (Botswana) in the Light of Climate Change and Regional Tectonics*. Kampala, s.n.

- Hogan, C., 2011. *Limnology: Makgadikgadi Pan*. [Online]  
Available at: <http://www.eoearth.org/view/article/170364/>  
[Accessed 15 December 2014].
- Hollub, V. & Schafer, P., 1992. *A Guide to Coalbed Methane Operations*, s.l.: Gas Research Institute.
- IHS Inc., 2014. *Langmuir Isotherm*. [Online]  
Available at:  
[http://www.fekete.com/SAN/WebHelp/FeketeHarmony/Harmony\\_WebHelp/Content/HTML\\_Files/Reference\\_Material/General\\_Concepts/Langmuir\\_Isotherm.htm](http://www.fekete.com/SAN/WebHelp/FeketeHarmony/Harmony_WebHelp/Content/HTML_Files/Reference_Material/General_Concepts/Langmuir_Isotherm.htm)  
[Accessed 05 12 2015].
- Iskhakov, R., 2013. *Coal-Bed Methane*. [Online]  
Available at: <http://large.stanford.edu/courses/2013/ph240/iskhakov1/>  
[Accessed 25 Jul 2015].
- Jansson, E., 2010. *What lies under the Kalahari sand?: U/Pb dating of Dwyka tillites, South Africa*, Göteborg: Göteborg University.
- Jenkins, C., 2008. *Practices and Pitfalls in Estimating Coalbed Methane Resources and Reserves*. San Antonio, American Association of Petroleum Geologists.
- Jin, H. et al., 2010. Coalbed gas desorption in canisters: Consumption of trapped atmospheric oxygen and implications for measured gas quality. *International Journal of Coal Geology*, Issue 81, pp. 64-72.
- Johnson, M. et al., 1996. Stratigraphy of the Karoo Supergroup in southern Africa: an overview. *Journal of African Earth Sciences*, 23(1), pp. 3-15.
- Jones, D. et al., 2001. Age of the Batoka basalts, northern Zimbabwe, and the duration of Karoo Large Igneous Province magmatism. *G-Cubed: Geochemistry, Geophysics, Geosystems*.
- Jourdan, F. et al., 2004. The Karoo triple junction questioned: evidence from Jurassic and Proterozoic  $^{40}\text{Ar}/^{39}\text{Ar}$  ages and geochemistry of the giant Okavango dyke swarm (Botswana). *Earth and Planetary Science Letters*, Issue 222, p. 989– 1006.
- Jourdan, F. et al., 2005. Karoo large igneous province: Brevity, origin, and relation to mass extinction questioned by new  $^{40}\text{Ar}/^{39}\text{Ar}$  age data. *Geology*, September, 33(9), pp. 745-748.

- Jourdan, F. et al., 2006. Basement control on dyke distribution in Large Igneous Provinces: Case study of the Karoo triple junction. *Earth and Planetary Science Letters*, Volume 241, p. 307– 322.
- Kentucky Geological Survey, 2011. *Classification and Rank of Coal*. [Online] Available at: <http://www.uky.edu/KGS/coal/coalkinds.htm> [Accessed 10 February 2015].
- Kinabo, B. et al., 2007. Early structural development of the Okavango rift zone, NW Botswana. *Journal of African Geosciences*, Issue 48, pp. 125-136.
- Krishan, M., 1940. *Classification of coal*. s.l., Geological Survey of India.
- Kubu Energy, 2014. *Application for Relinquishment of PL134/2010, 135/2010 and 136/2010*, Gaborone: Kubu Energy.
- Laubach, S., Marrett, R., Olson, J. & Scott, A., 1998. Characteristics and origins of coal cleat: A review. *International Journal of Coal Geology*, Issue 35, p. 175–207.
- Le Gall, B. et al., 2002. <sup>40</sup>Ar/<sup>39</sup>Ar geochronology and structural data from the giant Okavango and related mafic dyke swarms, Karoo igneous province, northern Botswana. *Earth and Planetary Science Letters* , Issue 202, pp. 595-606.
- Litynski, J., Vikara, D., Tennyson, M. & Webster, M., 2014. Using CO<sub>2</sub> for enhanced coalbed methane recovery and storage. *CBM Review*, June.
- Mapani, B., Finkelman, R. & Ravengai, S., 2013. Trace and heavy element distribution of the Hwange Coals in Zimbabwe: indicators of source rock chemistry, Coals in Zimbabwe: indicators of source rock chemistry, their formation in Southern Africa. *International Science and Technology Journal of Namibia*, 1(1), pp. 89-105.
- Maponga, O., 2014. *Zimbabwe's coal-bed methane potential*. Johannesburg, Fossil Fuel Foundation.
- Massenga Drilling Rigs, n.d. *Wireline Coring*. [Online] Available at: <http://www.massenzarigs.it/uk/contenuti/145/wireline-coring.html> [Accessed 10 January 2016].
- McCarthy, K. et al., 2011. Basic petroleum geochemistry for source rock evaluation. *Oilfield Review*, 23(2), pp. 32-23.

- McCarthy, T. & Rubidge, B., 2005. *Earth & Life: A southern african perspective on a 4.6-billion-year journey*. 1st ed. Cape Town: Struik.
- Middelkoop, W., 2009. [Online]  
Available at:  
[http://www.resourcestockdigest.com/precious\\_metals/index.php?&content\\_id=335](http://www.resourcestockdigest.com/precious_metals/index.php?&content_id=335)  
[Accessed 12 December 2014].
- Modie, B., 2007. *The palaeozoic palynostratigraphy of the Karoo Supergroup and palynofacies insight into palaeoenvironmental interpretations, Kalahari Karoo basin, Botswana*. Brest: Devant L'Universite de Bretagne Occidentale.
- Montana Bureau of Mines and Geology, n.d. *Energy: Coalbed Methane Research*. [Online]  
Available at: [http://www.mbmq.mtech.edu/energy/energy\\_cbm.asp](http://www.mbmq.mtech.edu/energy/energy_cbm.asp)  
[Accessed 28 March 2015].
- Moore, A. & Larkin, P., 2000. Drainage evolution in south-central Africa since the breakup of Gondwana. *South African Journal of Geology*, Volume 104, pp. 47-68.
- Mothibi, D., 1999. *National Geological Map of the Republic of Botswana*, Lobatse: Department of Geological Survey.
- Moyo, F., 2012. *The Hwange Coal Deposit. Presentation at the FFF & IEA Coal Indaba*. Johannesburg, Fossil Fuel Foundation.
- Mthandazo, N., 2015. Govt completes exploration of gas reserves. *News Day*, 1 December.
- Mukwakwami, N., 2013. *Coal Bed Methane: A clean energy elixir for Zimbabwe*. [Online]  
Available at: <https://projekt263.wordpress.com/2013/01/04/coal-bed-methane-a-clean-energy-elixir-for-zimbabwe/>  
[Accessed 03 04 2015].
- National Aeronautics and Space Administration, 2006. *NASA Jet Propulsion Laboratory California Institute of Technology*. [Online]  
Available at: <http://www2.jpl.nasa.gov/srtm/>  
[Accessed 28 May 2013].

- Nuccio, V., 2000. *Coal-Bed Methane: Potential and Concerns*, Denver: U.S. Geological Survey.
- Oesterlen, P. & Lepper, J., 2005. The Lower Karoo coal (k2–3) of the Mid-Zambezi basin, Zimbabwe: depositional analysis, coal genesis and palaeogeographic implications. *International Journal of Coal Geology*, Issue 61, p. 97–118.
- Origin Energy, 2015. *Natural Gas*. [Online]  
Available at: <https://www.originenergy.com.au/blog/about-energy/natural-gas.html>  
[Accessed 15 December 2015].
- Padcoal (Pvt) Ltd, 2011. *Gokwe Coal Field - A Rich Resource; Coal Special Grant SG152/10 - Nyagare Hills*, s.l.: Padcoal (Pvt) Ltd.
- Palloks, H. H., 1984. *An assessment of some of the coal deposits in North-West Zimbabwe*. Harare: Zimbabwe Geological Survey.
- Partridge, T. & Maud, R., 2000. *The Cenozoic of Southern Africa*. New York: Oxford.
- Persits, F. et al., 2011. *MAP SHOWING GEOLOGY, OIL AND GAS FIELDS, AND GEOLOGIC PROVINCES OF AFRICA*, s.l.: USGS.
- Petroleum Agency of South Africa, 2015. *Petroleum Exploration and Production Activities in South Africa*, Cape Town: Petroleum Agency of South Africa.
- Petters, S., 1991. Chapter 8: Paleozoic Sedimentary Basins in Africa. *Lecture Notes in Earth Sciences*, Volume 40, pp. 439-531.
- Pitfield, P., 1996. *Tectonic Map of Zimbabwe*, Harare: Government of Zimbabwe.
- Potgieter, J., 2015. *Personal Account*. s.l.:s.n.
- Potgieter, J., 2015. *Personal Account*. s.l.:s.n.
- Potgieter, J. & Andersen, N., 2012. *An evaluation of the coalbed methane potential of the central Kalahari area of Botswana from a geological perspective*, Centurion: GeoScientific & Exploration Services.
- Pridiyachi, V., n.d. *Coalbed Methane*, s.l.: s.n.
- Raath, M., Oesterlen, P. & Kitching, J., 1992. FIRST RECORD OF TRIASSIC RHYNCHOSAURIA (REPTILIA: DIAPSIDA) FROM THE LOWER ZAMBEZI VALLEY, ZIMBABWE. *Palaeontologica Africana*, Issue 29, pp. 1-10.

- Rainbow Gas and Coal Exploration (Pty) Ltd, 2011. *Early Final Relinquishment Report for Prospecting Licenses 36- 47/2007 and 90/2007*, Gaborone: Anglo Coal Botswana.
- Rice, D., 1993. Composition and Origins of Coalbed Gas. In: *Hydrocarbons from Coal*. s.l.:AAPG, pp. 159-184.
- Rycroft, M., 2014. *Gas to electric power generation potential*. [Online]  
Available at: <http://www.ee.co.za/article/gas-electric-power-generation-potential.html>  
[Accessed 14 December 2015].
- Sable Mining Africa Ltd, 2011. *Report and Accounts 2010 - 2011*, s.l.: Sable Mining.
- Sandvik Mining and Construction, 2015. *Core drilling tools. Diamond products*. s.l.:Sandvik Mining and Construction.
- SA-Venues, n.d. *Map - Botswana Attractions*. [Online]  
Available at: [http://www.sa-venues.com/maps/botswana\\_attractions.htm](http://www.sa-venues.com/maps/botswana_attractions.htm)  
[Accessed 15 12 2014].
- Schlumberger, n.d. *coal-bed methane*. [Online]  
Available at: [http://www.glossary.oilfield.slb.com/en/Terms/c/coal-bed\\_methane.aspx](http://www.glossary.oilfield.slb.com/en/Terms/c/coal-bed_methane.aspx)  
[Accessed 5 October 2015].
- Segwabe, T., 2008. *The Geological Framework and Depositional Environments of the Coal-Bearing Karoo Strata in the Central Kalahari Karoo Basin, Botswana*. M.Sc Thesis ed. Grahamstown: Rhodes University.
- Shell, 2012. *The Karoo*. [Online]  
Available at: <http://southafrica.shell.com/aboutshell/shell-businesses/e-and-p/karoo.html>  
[Accessed 16 January 2016].
- Sibanda, G., 2015. *Zim to set up own gas mines*, Harare: The Herald.
- Simpson, D., 2008. Coal Bed Methane. In: *Gas Well Deliquification*. 2nd ed. s.l.:Gulf, pp. 405-422.
- Smith, G., Cameron, A. & Bustin, R., 1994. Coal Resources of the Western Canada Sedimentary Basin. In: G. Mossop & I. Shetsen, eds. *Geological Atlas of the Western Canada Sedimentary Basin*. Edmonton: Alberta Geological Survey, p. Chapter 33.

- Smith, R., 1984. *The lithostratigraphy of the Karoo Supergroup in Botswana*, Lobatse: Geological Survey Department.
- Snyman, C., 1998. Coal. In: W. Wilson & C. Anhaeusser, eds. *The mineral resources of South Africa*. Pretoria: Council for Geosciences, pp. 136-205.
- Sparrow, J., 2012. *The Soutpansberg Coalfield: "The Forgotten Basin"*. s.l., Fossil Fuel Foundation - Limpopo Conference.
- SPE UGM SC, 2014. *Society of Petroleum Engineers*. [Online]  
Available at: <http://spe-sc.ft.ugm.ac.id/w/coal-as-oil-prone-source-rock/>  
[Accessed 1 February 2015].
- Spears, R., Alles, S. & Makhonin, A., 2014. Desorbed Canister Gas Sampling and Gas Isotopic Analysis Procedures and Practices: A Case Study of Two Coalbed Methane Wells from the Lower Saxony Basin, Germany. *Petrophysics*, 55(1).
- Standards Australia, 1999. *AS 3980—1999: Guide to the determination of gas content of coal—Direct desorption method*. 1 ed. Homebush: Standards Australia.
- Stansfield, B., 1973. *The geology of the area around Dukwe and Tlalamabele, Central District, Botswana*, Lobatse: Geological Survey of Botswana.
- Stoeckinger, W., 1991. Methods to measure directly the gas content of coals. In: *Open-file Report 91-52*. s.l.:Kansas Geological Survey, pp. 109-122.
- Swindell, G., 2007. *Powder River Basin Coalbed Methane Wells – Reserves and Rates*. Denver, Society of Petroleum Engineers.
- Thompson, A., 1981. *The Geology of the Lubimbi, Dhalia and Hankano Coalfields, Wankie and Lupane Districts*. Salisbury: Zimbabwe Geological Survey.
- Titley, M., 2013. *Mineral Resource Estimates for the Mutanga Uranium Project*, Ontario: CSA Global (UK) Ltd.
- Tlou Energy, 2014. *Lesedi CBM Project*. [Online]  
Available at: <http://tlouenergy.com/lesedi-cbm-project>  
[Accessed 28 September 2015].
- U.S. Energy Information Administration, 2011. *Annual Energy Outlook 2011*, s.l.: U.S. Energy Information Administration.
- UNESCO, 2004. *Managing Shared Aquifer Resources in Africa*, Saint-Denis: United Nations Educational,.

- Waechter, N., Hampton III, G. & Shipps, J., 2004. *Overview of Coal and Shale Gas Measurement: Field and Laboratory Procedures*. Tuscaloosa, Alabama, s.n.
- Walker, J., Geissman, J., Bowring, S. & Babcock, L., 2012. *Geologic Time Scale v.4.0*, Boulder: Geological Society of America.
- Weatherford Laboratories, n.d. *Wellsite Canister Desorption*. [Online]  
Available at: <https://labs.weatherford.com/services/field-services/wellsite-canister-gas-desorption>  
[Accessed 18 January 2016].
- Weatherford, 2007. *Advanced Slimline Logging for Minerals*, s.l.: Weatherford.
- Weatherford, 2016. *Slimline Logging Services*. [Online]  
Available at: <http://www.weatherford.com/products-services/drilling-formation-evaluation/wireline-services/slimline-logging-services>  
[Accessed 19 January 2016].
- World Coal Association, 2010. *World Coal Association*. [Online]  
Available at: <http://www.worldcoal.org/coal/uses-of-coal/coal-electricity/>  
[Accessed 10 March 2013].
- World Coal Institute, 2005. *The Coal Resource*, s.l.: World Coal Institute.
- Worldwide Geochemistry, n.d. *Maturation Parameters and Correlations*. [Online]  
Available at:  
<file:///C:/Users/Junior/Downloads/WorldwideThermal%20Maturity%20Parameters%20and%20Correlationsr%2024%20x%2032.pdf>  
[Accessed 1 February 2015].
- Zheng, A. et al., 2011. The Effect of Coal Seam Gas saturation on CBM Well Productivity-A Case Study of Central Region of Hedong Area. *Procedia Engineering*, Volume 26, pp. 1205-1213.

## 11. APPENDICES

Appendix A	Schedule of borehole data, indicating coal depth and thickness used in this study.	172
Appendix B	Schedule of borehole data, indicating coal quality and coal rank estimated from the ash-free fixed carbon, volatile matter and moisture values used in this evaluation.	180
Appendix C	Schedule of borehole data showing the Gas Content Calculated from the Eddy, et al. (1982) trend line Equations used in this evaluation.	196
Appendix D	List of isotherm samples collected and analysed by Kubu Energy (after Faiz, et al., 2013).	205
Appendix E	Gas content values from the Shangani Energy exploration data digitised from the Barker (2006) graph.	207

**Appendix A Schedule of borehole data, indicating coal depth and thickness used in this study.**

Sequence	Country	Area	Borehole ID / Field Name	Borehole Total Depth	Coal Interval		Sample Mid-Point	Composite Coal Thickness (m)	Data Source
					From (m)	To (m)	(m)		
1	Zimbabwe	Western Areas	M 53	292.12	284.19	291.57	287.88	7.38	Palloks (1984)
2	Zimbabwe	Western Areas	M 55	296.31	288.81	294.50	291.66	5.69	Palloks (1984)
3	Zimbabwe	Western Areas	M 56	257.03	249.09	254.76	251.93	5.67	Palloks (1984)
4	Zimbabwe	Western Areas	M 57	288.60	281.96	287.22	284.59	5.26	Palloks (1984)
5	Zimbabwe	Western Areas	M 58	253.24	243.00	252.28	247.64	9.28	Palloks (1984)
6	Zimbabwe	Western Areas	M 59	296.14	287.10	294.98	291.04	7.88	Palloks (1984)
7	Zimbabwe	Western Areas	M 60	289.11	279.04	287.36	283.20	8.32	Palloks (1984)
8	Zimbabwe	Western Areas	M 62	267.16	259.91	266.36	263.14	6.45	Palloks (1984)
9	Zimbabwe	Western Areas	M 63	260.35	252.67	258.78	255.73	6.11	Palloks (1984)
10	Zimbabwe	Western Areas	M 64	259.60	251.54	253.60	252.57	2.06	Palloks (1984)
11	Zimbabwe	Western Areas	M 65	105.14	88.63	103.81	96.22	9.46	Palloks (1984)
12	Zimbabwe	Western Areas	M 66	49.84	35.19	48.38	41.79	7.39	Palloks (1984)
13	Zimbabwe	Western Areas	M 67	42.27	24.70	34.33	29.52	3.90	Palloks (1984)
14	Zimbabwe	Western Areas	M 68	26.08	15.31	24.03	19.67	6.27	Palloks (1984)
15	Zimbabwe	Western Areas	M 69	112.09	100.61	109.31	104.96	5.72	Palloks (1984)
16	Zimbabwe	Western Areas	M 70	72.58	55.51	71.32	63.42	8.20	Palloks (1984)
17	Zimbabwe	Western Areas	M 71	32.79	15.75	31.62	23.69	9.20	Palloks (1984)
18	Zimbabwe	Western Areas	M 72	132.30	110.65	123.89	117.27	9.65	Palloks (1984)
19	Zimbabwe	Western Areas	M 73	117.47	99.06	116.83	107.95	8.70	Palloks (1984)
20	Zimbabwe	Western Areas	M 74	87.28	69.18	85.98	77.58	10.11	Palloks (1984)
21	Zimbabwe	Western Areas	M 75	53.74	33.00	51.43	42.22	13.91	Palloks (1984)
22	Zimbabwe	Western Areas	M 76	21.85	14.02	19.75	16.89	5.73	Palloks (1984)
23	Zimbabwe	Western Areas	M 77	115.68	87.78	113.39	100.59	7.76	Palloks (1984)
24	Zimbabwe	Western Areas	M 78	87.96	75.73	85.96	80.85	7.53	Palloks (1984)
25	Zimbabwe	Western Areas	M 79	51.58	36.51	51.28	43.90	8.86	Palloks (1984)
26	Zimbabwe	Western Areas	M 80	24.30	9.08	22.29	15.69	6.68	Palloks (1984)
27	Zimbabwe	Western Areas	M 81	108.01	90.86	106.31	98.59	8.27	Palloks (1984)
28	Zimbabwe	Western Areas	M 82	75.00	62.87	72.99	67.93	5.18	Palloks (1984)
29	Zimbabwe	Western Areas	M 83	36.13	25.38	34.13	29.76	5.82	Palloks (1984)
30	Zimbabwe	Western Areas	M 85	100.42	82.58	93.29	87.94	5.13	Palloks (1984)
31	Zimbabwe	Western Areas	M 86	67.60	56.68	65.15	60.92	3.66	Palloks (1984)
32	Zimbabwe	Western Areas	M 87	37.07	22.00	35.81	28.91	8.03	Palloks (1984)
33	Zimbabwe	Western Areas	M 88	9.36	4.20	8.90	6.55	4.70	Palloks (1984)
34	Zimbabwe	Western Areas	M 89	113.44	94.76	107.99	101.38	4.00	Palloks (1984)
35	Zimbabwe	Western Areas	M 90	92.90	75.70	86.42	81.06	4.40	Palloks (1984)
36	Zimbabwe	Western Areas	M 91	65.51	56.00	65.09	60.55	3.02	Palloks (1984)
37	Zimbabwe	Western Areas	M 92	38.70	20.31	37.26	28.79	9.12	Palloks (1984)
38	Zimbabwe	Western Areas	M 94	93.70	74.04	83.46	78.75	4.70	Palloks (1984)
39	Zimbabwe	Western Areas	M 95	58.48	43.11	57.73	50.42	8.74	Palloks (1984)
40	Zimbabwe	Western Areas	1740	169.90	156.38	168.90	162.64	12.52	Palloks (1984)

Sequence	Country	Area	Borehole ID / Field Name	Borehole Total Depth	Coal Interval		Sample Mid-Point	Composite Coal Thickness (m)	Data Source
					From (m)	To (m)	(m)		
41	Zimbabwe	Western Areas	1741	188.00	179.20	187.30	183.25	8.10	Palloks (1984)
42	Zimbabwe	Western Areas	1742	173.30	164.26	171.90	168.08	7.64	Palloks (1984)
43	Zimbabwe	Western Areas	1743	257.50	249.92	256.60	253.26	6.68	Palloks (1984)
44	Zimbabwe	Western Areas	1744	265.10	255.48	262.80	259.14	7.32	Palloks (1984)
45	Zimbabwe	Western Areas	1745	258.10	251.76	257.70	254.73	5.94	Palloks (1984)
46	Zimbabwe	Western Areas	1746	214.00	206.97	213.50	210.24	6.53	Palloks (1984)
47	Zimbabwe	Western Areas	1747	302.40	292.29	301.20	296.75	8.91	Palloks (1984)
48	Zimbabwe	Western Areas	1748	280.40	271.14	278.20	274.67	7.06	Palloks (1984)
49	Zimbabwe	Western Areas	1749	241.30	229.92	239.60	234.76	9.68	Palloks (1984)
50	Zimbabwe	Western Areas	1750	289.90	282.29	287.70	285.00	5.41	Palloks (1984)
51	Zimbabwe	Western Areas	1751	297.50	285.21	295.80	290.51	10.59	Palloks (1984)
52	Zimbabwe	Western Areas	1752	320.60	306.92	318.20	312.56	11.28	Palloks (1984)
53	Zimbabwe	Western Areas	1753				0.00		Palloks (1984)
54	Zimbabwe	Western Areas	1754	196.20	187.34	196.00	191.67	8.66	Palloks (1984)
55	Zimbabwe	Western Areas	1755	281.00	173.98	180.10	177.04	6.12	Palloks (1984)
56	Zimbabwe	Western Areas	1756	284.80	274.18	283.30	278.74	9.12	Palloks (1984)
57	Zimbabwe	Western Areas	1757	299.40	290.10	296.90	293.50	6.80	Palloks (1984)
58	Zimbabwe	Western Areas	1758	336.90	326.76	335.60	331.18	8.84	Palloks (1984)
59	Zimbabwe	Western Areas	1759	312.30	302.67	311.30	306.99	8.63	Palloks (1984)
60	Zimbabwe	Western Areas	1760	332.60	321.99	332.20	327.10	10.21	Palloks (1984)
61	Zimbabwe	Western Areas	1761	308.50	297.95	306.20	302.08	8.25	Palloks (1984)
62	Zimbabwe	Western Areas	1763	295.70			0.00		Palloks (1984)
63	Zimbabwe	Western Areas	1764A	326.40	313.47	325.47	319.47	11.73	Palloks (1984)
64	Zimbabwe	Entuba	E 1	280.72			0.00		Palloks (1984)
65	Zimbabwe	Entuba	E 2	56.46	34.89	47.39	41.14	12.50	Palloks (1984)
66	Zimbabwe	Entuba	E 3	46.63	33.00	43.38	38.19	10.38	Palloks (1984)
67	Zimbabwe	Entuba	E 3A	46.33	33.70	44.53	39.12	10.83	Palloks (1984)
68	Zimbabwe	Entuba	E 4	51.51	35.25	46.18	40.72	10.93	Palloks (1984)
69	Zimbabwe	Entuba	E 5	63.40	49.68	61.77	55.73	12.09	Palloks (1984)
70	Zimbabwe	Entuba	E 6	500.50	486.16	497.13	491.65	10.97	Palloks (1984)
71	Zimbabwe	Entuba	E 6	500.50	486.16	497.13	491.65	10.97	Palloks (1984)
72	Zimbabwe	Entuba	E 7	570.10	547.62	559.60	553.61	11.98	Palloks (1984)
73	Zimbabwe	Entuba	E 8	82.90	69.11	80.77	74.94	11.66	Palloks (1984)
74	Zimbabwe	Entuba	E 8	82.90	69.11	80.77	74.94	11.66	Palloks (1984)
75	Zimbabwe	Entuba	E 8	82.90	69.11	80.77	74.94	11.66	Palloks (1984)
76	Zimbabwe	Entuba	E 9	117.50	103.33	115.52	109.43	12.19	Palloks (1984)
77	Zimbabwe	Entuba	E 9A	62.92	54.86	64.26	59.56	9.40	Palloks (1984)
78	Zimbabwe	Entuba	E 9A	62.92	54.86	64.26	59.56	9.40	Palloks (1984)
79	Zimbabwe	Entuba	E 9A	62.92	54.86	64.26	59.56	9.40	Palloks (1984)
80	Zimbabwe	Entuba	E 10	48.02	34.16	46.33	40.25	12.17	Palloks (1984)
81	Zimbabwe	Entuba	E 12	61.57	47.72	57.06	52.39	9.34	Palloks (1984)

Sequence	Country	Area	Borehole ID / Field Name	Borehole Total Depth	Coal Interval		Sample Mid-Point	Composite Coal Thickness (m)	Data Source
					From (m)	To (m)	(m)		
82	Zimbabwe	Entuba	E 12	61.57	47.72	57.06	52.39	9.34	Palloks (1984)
83	Zimbabwe	Entuba	E 13	44.50	32.31	40.81	36.56	8.50	Palloks (1984)
84	Zimbabwe	Entuba	E 15	396.22	346.40	359.66	353.03	13.26	Palloks (1984)
85	Zimbabwe	Entuba	E 15	396.22	346.40	359.66	353.03	13.26	Palloks (1984)
86	Zimbabwe	Entuba	E 16A	63.40	49.07	62.00	55.54	12.93	Palloks (1984)
87	Zimbabwe	Entuba	E 16A	63.40	49.07	62.00	55.54	12.93	Palloks (1984)
88	Zimbabwe	Entuba	E 16A	63.40	49.07	62.00	55.54	12.93	Palloks (1984)
89	Zimbabwe	Entuba	E 17	46.63			0.00		Palloks (1984)
90	Zimbabwe	Entuba	E 17A	60.05	49.53	59.61	54.57	10.08	Palloks (1984)
91	Zimbabwe	Entuba	E 18	71.02	57.61	70.02	63.82	12.41	Palloks (1984)
92	Zimbabwe	Entuba	E 18	71.02	57.61	70.02	63.82	12.41	Palloks (1984)
93	Zimbabwe	Entuba	E 18	71.02	57.61	70.02	63.82	12.41	Palloks (1984)
94	Zimbabwe	Entuba	E 19	39.77			0.00		Palloks (1984)
95	Zimbabwe	Entuba	E 19A	45.87	39.01	43.84	41.43	4.83	Palloks (1984)
96	Zimbabwe	Entuba	E 19B	52.42	39.01	48.87	43.94	9.86	Palloks (1984)
97	Zimbabwe	Entuba	E 19C	54.56	41.15	53.04	47.10	11.89	Palloks (1984)
98	Zimbabwe	Entuba	E 19C	54.56	41.15	53.04	47.10	11.89	Palloks (1984)
99	Zimbabwe	Entuba	E 19C	54.56	41.15	53.04	47.10	11.89	Palloks (1984)
100	Zimbabwe	Entuba	E 20	55.83			0.00		Palloks (1984)
101	Zimbabwe	Entuba	E 21	183.49	171.00	181.98	176.49	10.98	Palloks (1984)
102	Zimbabwe	Entuba	E 22	45.24			0.00		Palloks (1984)
103	Zimbabwe	Entuba	E 24	68.05	55.44	65.84	60.64	10.40	Palloks (1984)
104	Zimbabwe	Entuba	E 24	68.05	55.44	65.84	60.64	10.40	Palloks (1984)
105	Zimbabwe	Entuba	E 25	87.13	55.91	67.57	61.74	11.66	Palloks (1984)
106	Zimbabwe	Entuba	E 26	109.28	94.14	104.10	99.12	9.87	Palloks (1984)
107	Zimbabwe	Entuba	E 27	281.64	270.05	281.18	275.62	11.13	Palloks (1984)
108	Zimbabwe	Entuba	E 28	29.56			0.00		Palloks (1984)
109	Zimbabwe	Entuba	E 29	116.13	100.58	114.66	107.62	14.08	Palloks (1984)
110	Zimbabwe	Entuba	E 29	116.13	100.58	114.66	107.62	14.08	Palloks (1984)
111	Zimbabwe	Entuba	E 30	63.40	53.34	61.57	57.46	8.23	Palloks (1984)
112	Zimbabwe	Entuba	E 30	63.40	53.34	61.57	57.46	8.23	Palloks (1984)
113	Zimbabwe	Entuba	E 31	170.99	161.39	170.38	165.89	8.99	Palloks (1984)
114	Zimbabwe	Entuba	E 32	115.21	105.77	114.60	110.19	8.83	Palloks (1984)
115	Zimbabwe	Entuba	E 32	115.21	105.77	114.60	110.19	8.83	Palloks (1984)
116	Zimbabwe	Entuba	E 33	101.19	89.97	100.35	95.16	10.38	Palloks (1984)
117	Zimbabwe	Entuba	E 33	101.19	89.97	100.35	95.16	10.38	Palloks (1984)
118	Zimbabwe	Entuba	E 34	174.04	161.08	173.35	167.22	12.27	Palloks (1984)
119	Zimbabwe	Entuba	E 34	174.04	161.08	173.35	167.22	12.27	Palloks (1984)
120	Zimbabwe	Entuba	E 34	174.04	161.08	173.35	167.22	12.27	Palloks (1984)
121	Zimbabwe	Entuba	E 35	181.05	170.69	180.74	175.72	10.05	Palloks (1984)
122	Zimbabwe	Entuba	E 36	215.18	204.08	212.58	208.33	8.50	Palloks (1984)

Sequence	Country	Area	Borehole ID / Field Name	Borehole Total Depth	Coal Interval		Sample Mid-Point	Composite Coal Thickness (m)	Data Source
					From (m)	To (m)	(m)		
123	Zimbabwe	Entuba	E 37	266.69	256.64	265.18	260.91	8.54	Palloks (1984)
124	Zimbabwe	Entuba	E 38	336.76	329.79	332.38	331.09	2.59	Palloks (1984)
125	Zimbabwe	Entuba	E 39	67.06	53.04	66.55	59.80	13.51	Palloks (1984)
126	Zimbabwe	Entuba	E 40	51.26	37.80	50.90	44.35	13.10	Palloks (1984)
127	Zimbabwe	Entuba	E 41	56.43	43.93	55.93	49.93	12.00	Palloks (1984)
128	Zimbabwe	Entuba	E 42	64.92	52.58	64.58	58.58	12.00	Palloks (1984)
129	Zimbabwe	Entuba	E 43	67.56	55.56	67.56	61.56	12.00	Palloks (1984)
130	Zimbabwe	Entuba	E 44	54.86	49.99	53.77	51.88	3.78	Palloks (1984)
131	Zimbabwe	Entuba	E 45	21.34	8.53	20.37	14.45	11.84	Palloks (1984)
132	Zimbabwe	Entuba	E 46	48.92	31.23	41.80	36.52	10.57	Palloks (1984)
133	Zimbabwe	Entuba	E 47	48.92	37.19	48.52	42.86	11.33	Palloks (1984)
134	Zimbabwe	Entuba	E 48	57.00	42.98	56.69	49.84	13.71	Palloks (1984)
135	Zimbabwe	Entuba	E 49	61.57	50.90	60.86	55.88	9.96	Palloks (1984)
136	Zimbabwe	Entuba	E 50	63.40	49.02	61.23	55.13	12.21	Palloks (1984)
137	Zimbabwe	Entuba	E 51	48.16	33.51	46.80	40.16	13.29	Palloks (1984)
138	Zimbabwe	Entuba	E 52	60.00	45.09	59.21	52.15	14.12	Palloks (1984)
139	Zimbabwe	Entuba	E 53	55.00	42.67	52.88	47.78	10.21	Palloks (1984)
140	Zimbabwe	Entuba	E 54	94.79	81.08	92.81	86.95	11.73	Palloks (1984)
141	Zimbabwe	Entuba	E 55	116.13	102.11	115.66	108.89	13.55	Palloks (1984)
142	Zimbabwe	Entuba	E 56	53.03	39.93	51.77	45.85	11.84	Palloks (1984)
143	Zimbabwe	Entuba	E 57	150.00	137.33	147.68	142.51	10.35	Palloks (1984)
144	Zimbabwe	Entuba	E 58	173.02	160.43	172.73	166.58	12.30	Palloks (1984)
145	Zimbabwe	Entuba	E 59	52.73	35.29	51.06	43.18	15.77	Palloks (1984)
146	Zimbabwe	Entuba	E 60	201.00	188.06	199.17	193.62	11.11	Palloks (1984)
147	Zimbabwe	Entuba	E 61	201.83	185.17	200.67	192.92	15.50	Palloks (1984)
148	Zimbabwe	Entuba	E 62	62.79	46.35	61.73	54.04	15.38	Palloks (1984)
149	Zimbabwe	Entuba	E 63	224.33	210.64	222.73	216.69	12.09	Palloks (1984)
150	Zimbabwe	Entuba	E 64	230.42	210.08	230.42	220.25	20.34	Palloks (1984)
151	Zimbabwe	Entuba	E 65	100.00	89.81	99.16	94.49	9.98	Palloks (1984)
152	Zimbabwe	Entuba	E 66	108.20	94.67	106.96	100.82	12.29	Palloks (1984)
153	Zimbabwe	Entuba	E 66A	106.71	94.59	105.73	100.16	11.14	Palloks (1984)
154	Zimbabwe	Entuba	E 67	90.83	76.88	89.99	83.44	13.11	Palloks (1984)
155	Zimbabwe	Entuba	E 68	91.44	74.19	87.99	81.09	13.80	Palloks (1984)
156	Zimbabwe	Entuba	E 69	153.64	140.85	153.54	147.20	12.69	Palloks (1984)
157	Zimbabwe	Entuba	E 70	161.00	150.27	160.67	155.47	10.40	Palloks (1984)
158	Zimbabwe	Entuba	E 71	162.00	151.91	161.46	156.69	9.55	Palloks (1984)
159	Zimbabwe	Entuba	E 72	154.00	144.13	152.90	148.52	8.77	Palloks (1984)
160	Zimbabwe	Entuba	E 73	215.63	203.05	214.63	208.84	11.58	Palloks (1984)
161	Zimbabwe	Entuba	E 74	195.73	183.99	194.54	189.27	10.55	Palloks (1984)
162	Zimbabwe	Entuba	E 75	198.73	189.20	197.66	193.43	8.46	Palloks (1984)
163	Zimbabwe	Entuba	E 76	180.74	176.02	180.12	178.07	4.10	Palloks (1984)

Sequence	Country	Area	Borehole ID / Field Name	Borehole Total Depth	Coal Interval		Sample Mid-Point	Composite Coal Thickness (m)	Data Source
					From (m)	To (m)	(m)		
164	Zimbabwe	Entuba	E 77	256.00	243.75	254.66	249.21	10.91	Palloks (1984)
165	Zimbabwe	Entuba	E 78	238.00	226.49	237.38	231.94	10.89	Palloks (1984)
166	Zimbabwe	Entuba	E 79	236.28	226.10	235.93	231.02	9.83	Palloks (1984)
167	Zimbabwe	Entuba	E 80B	256.30	246.14	255.40	250.77	9.26	Palloks (1984)
168	Zimbabwe	Entuba	E 81	249.85	241.28	249.18	245.23	7.82	Palloks (1984)
169	Zimbabwe	Entuba	E 82	333.99	325.23	333.69	329.46	8.46	Palloks (1984)
170	Zimbabwe	Entuba	E 83	323.48	314.62	323.22	318.92	8.60	Palloks (1984)
171	Zimbabwe	Entuba	E 84	269.82	261.14	269.66	265.40	8.52	Palloks (1984)
172	Zimbabwe	Entuba	E 85	323.86	315.49	323.26	319.38	7.77	Palloks (1984)
173	Zimbabwe	Entuba	E 87	12.75	6.08	10.50	8.29	4.42	Palloks (1984)
174	Zimbabwe	Entuba	E 88	63.94	53.54	63.85	58.70	10.31	Palloks (1984)
175	Zimbabwe	Entuba	E 89	54.04	48.46	52.94	50.70	4.48	Palloks (1984)
176	Zimbabwe	Entuba	E 90	50.10	38.60	48.87	43.74	10.27	Palloks (1984)
177	Zimbabwe	Entuba	E 91	63.80	49.38	61.10	55.24	11.72	Palloks (1984)
178	Zimbabwe	Entuba	E 92	59.10	47.50	59.08	53.29	11.58	Palloks (1984)
179	Zimbabwe	Entuba	E 93	77.61	64.22		64.22		Palloks (1984)
180	Zimbabwe	Entuba	E 94	70.91	58.92	69.31	64.12	10.39	Palloks (1984)
181	Zimbabwe	Entuba	E 96	212.23			0.00		Palloks (1984)
182	Zimbabwe	Entuba	E 97	272.59			0.00		Palloks (1984)
183	Zimbabwe	Entuba	E 98	122.12	110.50	121.60	116.05	11.10	Palloks (1984)
184	Zimbabwe	Entuba	E 99	227.61	218.85	227.13	222.99	8.28	Palloks (1984)
185	Zimbabwe	Entuba	E 101	240.24	229.08	238.44	233.76	9.36	Palloks (1984)
186	Zimbabwe	Entuba	E 102	211.65	201.80	210.60	206.20	8.80	Palloks (1984)
187	Zimbabwe	Entuba	E 103	102.54	93.46	101.82	97.64	8.36	Palloks (1984)
188	Zimbabwe	Entuba	E 104	129.85	119.41	125.83	122.62	6.42	Palloks (1984)
189	Zimbabwe	Lubu	LBW 1	172.52	11.12	13.14	12.13	2.02	Palloks (1984)
190	Zimbabwe	Lubu	LBW 1	172.52	16.17	20.23	18.20	3.73	Palloks (1984)
191	Zimbabwe	Lubu	LBW 1	172.52	28.82	43.33	36.08		Palloks (1984)
192	Zimbabwe	Lubu	LBW 1	172.52			0.00	10.53	Palloks (1984)
193	Zimbabwe	Lubu	LBW 2	241.86	84.71	88.66	86.69	2.80	Palloks (1984)
194	Zimbabwe	Lubu	LBW 2	241.86	95.94	111.56	103.75		Palloks (1984)
195	Zimbabwe	Lubu	LBW 2	241.86			0.00	13.57	Palloks (1984)
196	Zimbabwe	Lubu	LBW 4	98.98	41.51	43.51	42.51	2.00	Palloks (1984)
197	Zimbabwe	Lubu	LBW 4	98.98	51.90	70.13	61.02	17.92	Palloks (1984)
198	Zimbabwe	Lubu	LBW 5	76.81	32.76	36.41	34.59	3.26	Palloks (1984)
199	Zimbabwe	Lubu	LBW 5	76.81	40.53	56.83	48.68	16.20	Palloks (1984)
200	Zimbabwe	Lubu	LBW 6	126.64	65.61	74.10	69.86	9.09	Palloks (1984)
201	Zimbabwe	Lubu	LBW 6	126.64	15.00	98.00	56.50	7.96	Palloks (1984)
202	Zimbabwe	Lubu	LBW 6	126.64	83.56	92.70	88.13	8.65	Palloks (1984)
203	Zimbabwe	Lubu	LBW 7	107.08	55.05	58.99	57.02	3.69	Palloks (1984)
204	Zimbabwe	Lubu	LBW 7	107.08	64.65	82.28	73.47	15.68	Palloks (1984)

Sequence	Country	Area	Borehole ID / Field Name	Borehole Total Depth	Coal Interval		Sample Mid-Point	Composite Coal Thickness (m)	Data Source
					From (m)	To (m)	(m)		
205	Zimbabwe	Lubu	LBW 8	78.94	25.64	29.43	27.54	3.43	Palloks (1984)
206	Zimbabwe	Lubu	LBW 8	78.94	34.90	46.35	40.63	9.31	Palloks (1984)
207	Zimbabwe	Lubu	LBW 9	73.93	14.81	16.81	15.81	1.91	Palloks (1984)
208	Zimbabwe	Lubu	LBW 9	73.93	26.60	34.58	30.59	7.98	Palloks (1984)
209	Zimbabwe	Lubu	LBW 10	99.54	63.13	67.19	65.16	3.74	Palloks (1984)
210	Zimbabwe	Lubu	LBW 10	99.54	73.22	84.30	78.76	10.98	Palloks (1984)
211	Zimbabwe	Lubu	LBW 11	64.10	32.11	36.16	34.14	1.70	Palloks (1984)
212	Zimbabwe	Lubu	LBW 11	64.10	44.04	57.16	50.60	13.12	Palloks (1984)
213	Zimbabwe	Lubu	LBW 11	64.10			0.00	12.30	Palloks (1984)
214	Zimbabwe	Lubu	LBW 12	93.49	39.86	50.87	45.37	6.13	Palloks (1984)
215	Zimbabwe	Lubu	LBW 12	93.49	66.30	79.84	73.07	12.57	Palloks (1984)
216	Zimbabwe	Lubu	LBW 13	151.05	97.77	102.00	99.89	4.04	Palloks (1984)
217	Zimbabwe	Sengwa South	S 1	115.83	96.01	113.08	104.55	17.07	Palloks (1984)
218	Zimbabwe	Sengwa South	S 2	80.47	63.93	77.62	70.78	13.69	Palloks (1984)
219	Zimbabwe	Sengwa South	S 3	18.59	6.10	15.24	10.67	9.14	Palloks (1984)
220	Zimbabwe	Sengwa South	S 5	110.03	90.22	107.29	98.76	17.07	Palloks (1984)
221	Zimbabwe	Sengwa South	S 18	166.12	151.79	160.55	156.17	8.76	Palloks (1984)
222	Zimbabwe	Sengwa South	S 25	165.19	147.51	159.40	153.46	11.89	Palloks (1984)
223	Zimbabwe	Sengwa South	S 26	25.60	11.27	21.96	16.62	10.69	Palloks (1984)
224	Zimbabwe	Sengwa South	S 27	100.28	85.80	97.92	91.86	12.12	Palloks (1984)
225	Zimbabwe	Sengwa South	S 29	85.04	70.71	80.95	75.83	10.24	Palloks (1984)
226	Zimbabwe	Sengwa South	S 30	53.95	40.46	49.48	44.97	9.02	Palloks (1984)
227	Zimbabwe	Sengwa North	M 1	94.49	78.59	90.53	84.56	11.94	Palloks (1984)
228	Zimbabwe	Sengwa North	M 2	128.82	96.32	111.51	103.92	15.19	Palloks (1984)
229	Zimbabwe	Sengwa North	M 3	97.83	78.93	93.26	86.10	14.33	Palloks (1984)
230	Zimbabwe	Sengwa North	M 4	152.69	135.62	145.00	140.31	9.38	Palloks (1984)
231	Zimbabwe	Sengwa North	M 5	82.90	69.18	78.84	74.01	9.66	Palloks (1984)
232	Zimbabwe	Sengwa North	M 6	82.90	71.11	78.93	75.02	7.82	Palloks (1984)
233	Zimbabwe	Sengwa North	M 7	123.13	108.35	118.56	113.46	10.21	Palloks (1984)
234	Zimbabwe	Sengwa North	M 8	86.86	71.85	83.28	77.57	11.43	Palloks (1984)
235	Zimbabwe	Sengwa North	M 9	76.19	21.18	34.51	27.85	13.33	Palloks (1984)
236	Zimbabwe	Sengwa North	M 10	14.62	0.10	11.07	5.59	11.07	Palloks (1984)
237	Zimbabwe	Sengwa North	M 11	42.66	25.75	38.63	32.19	12.88	Palloks (1984)
238	Zimbabwe	Lusulu	L 256 (Type Borehole - Main & A Seams)		15.00	190.00	102.50	9.17	Palloks (1984)
239	Zimbabwe	Lusulu	L 252 (Type Borehole - Main Seam)*		22.50	197.50	110.00	6.15	Palloks (1984)
240	Zimbabwe	Lusulu	L 198 (Type Borehole - Lower & Middle Seam)*		26.60	97.77	62.19	4.15	Palloks (1984)
241	Zimbabwe	Wankie	Shallow (Average)		60.00	100.00	80.00	9.00	Mapani et al. (2013); Palloks (1984); Cairncross (2001) and Moyo (2012)
242	Zimbabwe	Wankie	Deep(Average)		200.00	700.00	450.00	9.00	Bakker (2006)
243	Zimbabwe	Gokwe	Gokwe Average		200.00	300.00	250.00	9.00	Oesterlen & Lepper (2005) and Padcoal (Pvt) Ltd

Sequence	Country	Area	Borehole ID / Field Name	Borehole Total Depth	Coal Interval		Sample Mid-Point	Composite Coal Thickness (m)	Data Source
					From (m)	To (m)	(m)		
									(2011)
244	Botswana	Northeast Botswana	N1/1		45.10	46.70	45.90	1.00	Smith (1984)
245	Botswana	Northeast Botswana	N1/2		41.00	89.00	65.00	5.50	Smith (1984)
246	Botswana	Northeast Botswana	N1/3		24.00	91.00	57.50	7.73	Smith (1984)
247	Botswana	Northeast Botswana	N2/1		52.70	118.10	85.40	19.60	Smith (1984)
248	Botswana	Northeast Botswana	N3/1		38.30	119.00	78.65	23.65	Smith (1984)
249	Botswana	Northeast Botswana	N4/1		113.30	189.00	151.15	14.03	Smith (1984)
250	Botswana	Northeast Botswana	N5/2		5.00	41.70	23.35	6.80	Smith (1984)
251	Botswana	Northeast Botswana	N5/1		10.40	41.20	25.80	4.10	Smith (1984)
252	Botswana	Northeast Botswana	N6/1		14.70	70.50	42.60	2.50	Smith (1984)
253	Botswana	Northeast Botswana	N8/2		75.35	124.50	99.93	11.50	Smith (1984)
254	Botswana	Northeast Botswana	N12/1		79.90	150.85	115.38	12.50	Smith (1984)
255	Botswana	Northeast Botswana	N9/1		75.40	124.60	100.00	8.74	Smith (1984)
256	Botswana	Northeast Botswana	N10/1		89.40	177.30	133.35	21.76	Smith (1984)
257	Botswana	Northeast Botswana	N11/3		110.60	153.50	132.05	8.15	Smith (1984)
258	Botswana	Northeast Botswana	N7/1				0.00		Smith (1984)
259	Botswana	Northeast Botswana	N7/2				0.00		Smith (1984)
260	Botswana	Northeast Botswana	N7/3				0.00		Smith (1984)
261	Botswana	Northeast Botswana	N8/1				0.00		Smith (1984)
262	Botswana	Northeast Botswana	N8/2				0.00		Smith (1984)
263	Botswana	Northeast Botswana	N12/1				0.00		Smith (1984)
264	Botswana	Northeast Botswana	N9/1				0.00		Smith (1984)
265	Botswana	Northeast Botswana	N10/1				0.00		Smith (1984)
266	Botswana	Northeast Botswana	N11/3				0.00		Smith (1984)
267	Botswana	Northeast Botswana	N11/2				0.00		Smith (1984)
268	Botswana	Northeast Botswana	N11/1				0.00		Smith (1984)
269	Botswana	Northeast Botswana	N12/1				0.00		Smith (1984)
270	Botswana	Northeast Botswana	N12/2				0.00		Smith (1984)
271	Botswana	Northeast Botswana	N12/3				0.00		Smith (1984)
272	Botswana	Northeast Botswana	Y1-01	595.00	499.74	566.30	533.02	10.65	Anglo Coal Botswana (2010)
273	Botswana	Northeast Botswana	Y1-02	769.00	705.54	737.14	721.34	1.29	Anglo Coal Botswana (2010)
274	Botswana	Northeast Botswana	Y1-03	808.00	705.73	792.74	749.24	16.75	Anglo Coal Botswana (2010)
275	Botswana	Northeast Botswana	Y1-04	638.18	587.20	605.50	596.35	2.85	Anglo Coal Botswana (2010)
276	Botswana	Northeast Botswana	PDM006C	701.34			0.00		Anglo Coal Botswana (2010)
277	Botswana	Northeast Botswana	PDM007A	287.00			0.00		Anglo Coal Botswana (2010)
278	Botswana	Northeast Botswana	PDM008	663.00			0.00		Anglo Coal Botswana (2010)
279	Botswana	Northeast Botswana	PDM009	526.00			0.00		Anglo Coal Botswana (2010)
280	Botswana	Northeast Botswana	PDM011	633.39			0.00		Anglo Coal Botswana (2010)
281	Botswana	Northeast Botswana	PDM014A	434.00			0.00		Anglo Coal Botswana (2010)
282	Botswana	Northeast Botswana	PDM015	396.00			0.00		Anglo Coal Botswana (2010)
283	Zimbabwe	Lubimbi	Lubimbi		11.80	190.00	100.90		Thompson (1981) and Oesterlen & Lepper (2005)

Sequence	Country	Area	Borehole ID / Field Name	Borehole Total Depth	Coal Interval		Sample Mid-Point	Composite Coal Thickness (m)	Data Source
					From (m)	To (m)	(m)		
284	Zimbabwe	Busi	Busi		60.00	80.00	70.00	10.00	Oesterlen & Lepper (2005)
285	Zimbabwe	Tjolutjo, Sawmills, and Insuza	Tjolutjo, Sawmills, and Insuza		270.00	330.00	300.00	5.00	Oesterlen & Lepper (2005)

**Appendix B** Schedule of borehole data, indicating coal quality and coal rank estimated from the ash-free fixed carbon, volatile matter and moisture values used in this evaluation.

Sequence	Borehole ID / Field Name	Coal Interval		Sample Mid-Point	Composite Coal Thickness (m)	Coal Quality Information							Coal Rank based on Ash-Free Fixed Carbon, Volatile Matter and Moisture Values			Code
		From (m)	To (m)	(m)		Yield (%)	Moisture (%)	Ash (%)	Volatile Matter (%)	Fixed Carbon (%)	Analysis Comments	Ash-Free			Long Text	
												Moisture (%)	Volatile Matter (%)	Fixed Carbon (%)		
1	M 53	284.19	291.57	287.88	7.38	53.4	1.1	8.0	25.2	65.7	Samples Washed at 1.4 g/cm <sup>3</sup>	1.2	27.4	71.4	Medium Volatile Bituminous	MVB
2	M 55	288.81	294.5	291.655	5.69	53.2	1.1	8.1	24.0	66.8	Samples Washed at 1.4 g/cm <sup>3</sup>	1.2	26.1	72.7	Medium Volatile Bituminous	MVB
3	M 56	249.09	254.76	251.925	5.67	57.9	1.2	8.2	23.3	67.3	Samples Washed at 1.4 g/cm <sup>3</sup>	1.3	25.4	73.3	Medium Volatile Bituminous	MVB
4	M 57	281.96	287.22	284.59	5.26	45.2	1.0	9.0	26.4	63.6	Samples Washed at 1.4 g/cm <sup>3</sup>	1.1	29.0	69.9	Medium Volatile Bituminous	MVB
5	M 58	243	252.28	247.64	9.28	78.9	1.1	7.6	25.3	66.0	Samples Washed at 1.4 g/cm <sup>3</sup>	1.2	27.4	71.4	Medium Volatile Bituminous	MVB
6	M 59	287.1	294.98	291.04	7.88	84.5	1.0	6.6	26.3	66.1	Samples Washed at 1.4 g/cm <sup>3</sup>	1.1	28.2	70.8	Medium Volatile Bituminous	MVB
7	M 60	279.04	287.36	283.2	8.32	83.1	1.2	6.7	26.2	65.9	Samples Washed at 1.4 g/cm <sup>3</sup>	1.3	28.1	70.6	Medium Volatile Bituminous	MVB
8	M 62	259.91	266.36	263.135	6.45	65.3	1.2	9.1	27.1	62.6	Samples Washed at 1.4 g/cm <sup>3</sup>	1.3	29.8	68.9	High Volatile Bituminous - A	HVB-A
9	M 63	252.67	258.78	255.725	6.11	75.8	1.2	8.9	29.8	60.1	Samples Washed at 1.4 g/cm <sup>3</sup>	1.3	32.7	66.0	High Volatile Bituminous - A	HVB-A
10	M 64	251.54	253.6	252.57	2.06		1.0	15.3	21.5	62.2	Samples Washed at 1.4 g/cm <sup>3</sup>	1.2	25.4	73.4	Medium Volatile Bituminous	MVB
11	M 65	88.63	103.81	96.22	9.46	43.2	1.1	9.8	32.6	56.5	Samples Washed at 1.4 g/cm <sup>3</sup>	1.2	36.1	62.6	High Volatile Bituminous - A	HVB-A
12	M 66	35.19	48.38	41.785	7.39	35.0	1.2	9.2	33.4	56.2	Samples Washed at 1.4 g/cm <sup>3</sup>	1.3	36.8	61.9	High Volatile Bituminous - B	HVB-B
13	M 67	24.7	34.33	29.515	3.9	51.0	1.3	9.2	33.7	55.8	Samples Washed at 1.4 g/cm <sup>3</sup>	1.4	37.1	61.5	High Volatile Bituminous - B	HVB-B
14	M 68	15.31	24.03	19.67	6.27		1.6	22.7	17.9	57.8	Samples Washed at 1.4 g/cm <sup>3</sup>	2.1	23.2	74.8	Medium Volatile Bituminous	MVB
15	M 69	100.61	109.31	104.96	5.72	47.6	1.3	8.1	33.6	57.0	Samples Washed at 1.4 g/cm <sup>3</sup>	1.4	36.6	62.0	High Volatile Bituminous - A	HVB-A
16	M 70	55.51	71.32	63.415	8.2	30.7	1.2	10.0	32.4	56.4	Samples Washed at 1.4 g/cm <sup>3</sup>	1.3	36.0	62.7	High Volatile Bituminous - A	HVB-A
17	M 71	15.75	31.62	23.685	9.2	28.3	1.4	10.2	32.1	56.3	Samples Washed at 1.4 g/cm <sup>3</sup>	1.6	35.7	62.7	High Volatile Bituminous - A	HVB-A

Sequence	Borehole ID / Field Name	Coal Interval		Sample Mid-Point	Composite Coal Thickness (m)	Coal Quality Information								Coal Rank based on Ash-Free Fixed Carbon, Volatile Matter and Moisture Values	Code	
		From (m)	To (m)	(m)		Yield (%)	Moisture (%)	Ash (%)	Volatile Matter (%)	Fixed Carbon (%)	Analysis Comments	Ash-Free				Long Text
												Moisture (%)	Volatile Matter (%)	Fixed Carbon (%)		
											g/cm <sup>3</sup>					
18	M 72	110.65	123.89	117.27	9.65	37.3	1.1	9.9	31.9	57.1	Samples Washed at 1.4 g/cm <sup>3</sup>	1.2	35.4	63.4	High Volatile Bituminous - A	HVB-A
19	M 73	99.06	116.83	107.945	8.7	40.0	1.4	10.4	31.9	56.3	Samples Washed at 1.4 g/cm <sup>3</sup>	1.6	35.6	62.8	High Volatile Bituminous - A	HVB-A
20	M 74	69.18	85.98	77.58	10.11	38.3	1.5	10.3	31.2	57.0	Samples Washed at 1.4 g/cm <sup>3</sup>	1.7	34.8	63.5	High Volatile Bituminous - A	HVB-A
21	M 75	33	51.43	42.215	13.91	49.7	1.8	9.8	31.4	57.0	Samples Washed at 1.4 g/cm <sup>3</sup>	2.0	34.8	63.2	High Volatile Bituminous - A	HVB-A
22	M 76	14.02	19.75	16.885	5.73		1.6	22.7	17.9	57.8	Samples Washed at 1.4 g/cm <sup>3</sup>	2.1	23.2	74.8	Medium Volatile Bituminous	MVB
23	M 77	87.78	113.39	100.585	7.76	54.7	1.5	9.7	31.4	57.4	Samples Washed at 1.4 g/cm <sup>3</sup>	1.7	34.8	63.6	High Volatile Bituminous - A	HVB-A
24	M 78	75.73	85.96	80.845	7.53		1.6	22.7	17.9	57.8	Samples Washed at 1.4 g/cm <sup>3</sup>	2.1	23.2	74.8	Medium Volatile Bituminous	MVB
25	M 79	36.51	51.28	43.895	8.86	45.7	1.7	9.8	31.3	57.2	Samples Washed at 1.4 g/cm <sup>3</sup>	1.9	34.7	63.4	High Volatile Bituminous - A	HVB-A
26	M 80	9.08	22.29	15.685	6.68	72.1	2.3	8.4	31.0	58.3	Samples Washed at 1.4 g/cm <sup>3</sup>	2.5	33.8	63.6	High Volatile Bituminous - A	HVB-A
27	M 81	90.86	106.31	98.585	8.27	34.6	1.7	10.5	30.8	57.0	Samples Washed at 1.4 g/cm <sup>3</sup>	1.9	34.4	63.7	High Volatile Bituminous - A	HVB-A
28	M 82	62.87	72.99	67.93	5.18	39.2	1.5	9.5	30.6	58.4	Samples Washed at 1.4 g/cm <sup>3</sup>	1.7	33.8	64.5	High Volatile Bituminous - A	HVB-A
29	M 83	25.38	34.13	29.755	5.82	41.6	1.7	9.4	30.7	58.2	Samples Washed at 1.4 g/cm <sup>3</sup>	1.9	33.9	64.2	High Volatile Bituminous - A	HVB-A
30	M 85	82.58	93.29	87.935	5.13	39.7	1.8	11.3	30.9	56.0	Samples Washed at 1.4 g/cm <sup>3</sup>	2.0	34.8	63.1	High Volatile Bituminous - A	HVB-A
31	M 86	56.68	65.15	60.915	3.66	36.4	1.7	10.9	30.4	57.0	Samples Washed at 1.4 g/cm <sup>3</sup>	1.9	34.1	64.0	High Volatile Bituminous - A	HVB-A
32	M 87	22	35.81	28.905	8.03	66.6	2.0	8.8	31.1	58.1	Samples Washed at 1.4 g/cm <sup>3</sup>	2.2	34.1	63.7	High Volatile Bituminous - A	HVB-A
33	M 88	4.2	8.9	6.55	4.7		1.6	22.7	17.9	57.8	Samples Washed at 1.4 g/cm <sup>3</sup>	2.1	23.2	74.8	Medium Volatile Bituminous	MVB

Sequence	Borehole ID / Field Name	Coal Interval		Sample Mid-Point	Composite Coal Thickness (m)	Coal Quality Information							Coal Rank based on Ash-Free Fixed Carbon, Volatile Matter and Moisture Values	Code		
		From (m)	To (m)	(m)		Yield (%)	Moisture (%)	Ash (%)	Volatile Matter (%)	Fixed Carbon (%)	Analysis Comments	Ash-Free			Long Text	
												Moisture (%)	Volatile Matter (%)			Fixed Carbon (%)
34	M 89	94.76	107.99	101.375	4	47.6	2.3	8.9	30.7	58.1	Samples Washed at 1.4 g/cm <sup>3</sup>	2.5	33.7	63.8	High Volatile Bituminous - A	HVB-A
35	M 90	75.7	86.42	81.06	4.4	47.6	2.0	8.1	31.6	58.3	Samples Washed at 1.4 g/cm <sup>3</sup>	2.2	34.4	63.4	High Volatile Bituminous - A	HVB-A
36	M 91	56	65.09	60.545	3.02	68.2	1.8	10.5	30.8	56.9	Samples Washed at 1.4 g/cm <sup>3</sup>	2.0	34.4	63.6	High Volatile Bituminous - A	HVB-A
37	M 92	20.31	37.26	28.785	9.12	45.0	2.0	9.0	31.4	57.6	Samples Washed at 1.4 g/cm <sup>3</sup>	2.2	34.5	63.3	High Volatile Bituminous - A	HVB-A
38	M 94	74.04	83.46	78.75	4.7	42.3	1.8	10.2	31.0	57.0	Samples Washed at 1.4 g/cm <sup>3</sup>	2.0	34.5	63.5	High Volatile Bituminous - A	HVB-A
39	M 95	43.11	57.73	50.42	8.74	38.5	1.9	10.4	31.1	56.6	Samples Washed at 1.4 g/cm <sup>3</sup>	2.1	34.7	63.2	High Volatile Bituminous - A	HVB-A
40	1740	156.38	168.9	162.64	12.52		1.4	17.5	21.0	60.1	Samples Washed at 1.6 g/cm <sup>3</sup>	1.7	25.5	72.8	Medium Volatile Bituminous	MVB
41	1741	179.2	187.3	183.25	8.1		1.4	20.2	21.0	57.4	Samples Washed at 1.6 g/cm <sup>3</sup>	1.8	26.3	71.9	Medium Volatile Bituminous	MVB
42	1742	164.26	171.9	168.08	7.64		1.7	23.3	21.3	53.7	Samples Washed at 1.6 g/cm <sup>3</sup>	2.2	27.8	70.0	Medium Volatile Bituminous	MVB
43	1743	249.92	256.6	253.26	6.68		1.5	16.2	21.3	61.0	Samples Washed at 1.6 g/cm <sup>3</sup>	1.8	25.4	72.8	Medium Volatile Bituminous	MVB
44	1744	255.48	262.8	259.14	7.32		1.0	15.3	21.5	62.2	Samples Washed at 1.6 g/cm <sup>3</sup>	1.2	25.4	73.4	Medium Volatile Bituminous	MVB
45	1745	251.76	257.7	254.73	5.94		1.0	15.3	21.5	62.2	Samples Washed at 1.6 g/cm <sup>3</sup>	1.2	25.4	73.4	Medium Volatile Bituminous	MVB
46	1746	206.97	213.5	210.235	6.53		1.3	23.7	19.7	55.3	Samples Washed at 1.6 g/cm <sup>3</sup>	1.7	25.8	72.5	Medium Volatile Bituminous	MVB
47	1747	292.29	301.2	296.745	8.91		1.7	12.8	23.0	62.5	Samples Washed at 1.6 g/cm <sup>3</sup>	1.9	26.4	71.7	Medium Volatile Bituminous	MVB
48	1748	271.14	278.2	274.67	7.06		2.0	13.5	22.9	61.6	Samples Washed at 1.6 g/cm <sup>3</sup>	2.3	26.5	71.2	Medium Volatile Bituminous	MVB
49	1749	229.92	239.6	234.76	9.68		1.0	15.3	21.5	62.2	Samples Washed at 1.6 g/cm <sup>3</sup>	1.2	25.4	73.4	Medium Volatile Bituminous	MVB
50	1750	282.29	287.7	284.995	5.41		1.1	20.0	20.1	58.8	Samples Washed at 1.6 g/cm <sup>3</sup>	1.4	25.1	73.5	Medium Volatile Bituminous	MVB

Sequence	Borehole ID / Field Name	Coal Interval		Sample Mid-Point (m)	Composite Coal Thickness (m)	Coal Quality Information								Coal Rank based on Ash-Free Fixed Carbon, Volatile Matter and Moisture Values	Code	
		From (m)	To (m)			Yield (%)	Moisture (%)	Ash (%)	Volatile Matter (%)	Fixed Carbon (%)	Analysis Comments	Ash-Free				Long Text
				Moisture (%)								Volatile Matter (%)	Fixed Carbon (%)			
51	1751	285.21	295.8	290.505	10.59		1.8	13.7	23.6	60.9	Samples Washed at 1.6 g/cm <sup>3</sup>	2.1	27.3	70.6	Medium Volatile Bituminous	MVB
52	1752	306.92	318.2	312.56	11.28		1.0	15.3	21.5	62.2	Samples Washed at 1.6 g/cm <sup>3</sup>	1.2	25.4	73.4	Medium Volatile Bituminous	MVB
53	1753			0			1.6	22.7	17.9	57.8	Samples Washed at 1.6 g/cm <sup>3</sup>	2.1	23.2	74.8	Medium Volatile Bituminous	MVB
54	1754	187.34	196	191.67	8.66		1.0	15.3	21.5	62.2	Samples Washed at 1.6 g/cm <sup>3</sup>	1.2	25.4	73.4	Medium Volatile Bituminous	MVB
55	1755	173.98	180.1	177.04	6.12		1.3	19.6	20.5	58.6	Samples Washed at 1.6 g/cm <sup>3</sup>	1.6	25.5	72.9	Medium Volatile Bituminous	MVB
56	1756	274.18	283.3	278.74	9.12		1.0	15.3	21.5	62.2	Samples Washed at 1.6 g/cm <sup>3</sup>	1.2	25.4	73.4	Medium Volatile Bituminous	MVB
57	1757	290.1	296.9	293.5	6.8		1.8	19.6	21.1	57.5	Samples Washed at 1.6 g/cm <sup>3</sup>	2.2	26.2	71.5	Medium Volatile Bituminous	MVB
58	1758	326.76	335.6	331.18	8.84		1.3	12.2	23.6	62.9	Samples Washed at 1.6 g/cm <sup>3</sup>	1.5	26.9	71.6	Medium Volatile Bituminous	MVB
59	1759	302.67	311.3	306.985	8.63		1.3	12.8	24.0	61.9	Samples Washed at 1.6 g/cm <sup>3</sup>	1.5	27.5	71.0	Medium Volatile Bituminous	MVB
60	1760	321.99	332.2	327.095	10.21		1.2	14.1	21.9	62.8	Samples Washed at 1.6 g/cm <sup>3</sup>	1.4	25.5	73.1	Medium Volatile Bituminous	MVB
61	1761	297.95	306.2	302.075	8.25		1.2	15.1	21.4	62.3	Samples Washed at 1.6 g/cm <sup>3</sup>	1.4	25.2	73.4	Medium Volatile Bituminous	MVB
62	1763			0			1.6	22.7	17.9	57.8	Samples Washed at 1.6 g/cm <sup>3</sup>	2.1	23.2	74.8	Medium Volatile Bituminous	MVB
63	1764A	313.47	325.47	319.47	11.73		0.9	10.5	25.7	62.9	Samples Washed at 1.6 g/cm <sup>3</sup>	1.0	28.7	70.3	Medium Volatile Bituminous	MVB
64	E 1			0							Raw Coal (Air Dried)					
65	E 2	34.89	47.39	41.14	12.5		1.1	15.6	21.0	62.3	Raw Coal (Air Dried)	1.3	24.9	73.8	Medium Volatile Bituminous	MVB
66	E 3	33	43.38	38.19	10.38		1.0	13.4	17.4	68.2	Raw Coal (Air Dried)	1.2	20.1	78.8	Low Volatile Bituminous	LVB
67	E 3A	33.7	44.53	39.115	10.83		1.2	11.2	20.4	67.2	Raw Coal (Air Dried)	1.4	23.0	75.7	Medium Volatile Bituminous	MVB
68	E 4	35.25	46.18	40.715	10.93		0.8	8.9	21.8	68.5	Raw Coal (Air Dried)	0.9	23.9	75.2	Medium Volatile Bituminous	MVB
69	E 5	49.68	61.77	55.725	12.09		1.0	8.4	21.6	69.0	Raw Coal (Air Dried)	1.1	23.6	75.3	Medium Volatile Bituminous	MVB

Sequence	Borehole ID / Field Name	Coal Interval		Sample Mid-Point	Composite Coal Thickness (m)	Coal Quality Information							Coal Rank based on Ash-Free Fixed Carbon, Volatile Matter and Moisture Values	Code		
		From (m)	To (m)	(m)		Yield (%)	Moisture (%)	Ash (%)	Volatile Matter (%)	Fixed Carbon (%)	Analysis Comments	Ash-Free			Long Text	
												Moisture (%)	Volatile Matter (%)			Fixed Carbon (%)
70	E 6	486.16	497.13	491.645	10.97		1.2	12.3	17.1	69.4	Raw Coal (Air Dried)	1.4	19.5	79.1	Low Volatile Bituminous	LVB
71	E 6	486.16	497.13	491.645	10.97		1.2	19.3	16.8	62.7	Raw Coal (Air Dried)	1.5	20.8	77.7	Low Volatile Bituminous	LVB
72	E 7	547.62	559.6	553.61	11.98		1.2	11.9	19.3	67.6	Raw Coal (Air Dried)	1.4	21.9	76.7	Medium Volatile Bituminous	MVB
73	E 8	69.11	80.77	74.94	11.66		0.9	7.0	24.6	67.5	Raw Coal (Air Dried)	1.0	26.5	72.6	Medium Volatile Bituminous	MVB
74	E 8	69.11	80.77	74.94	11.66		1.4	13.4	20.3	64.9	Raw Coal (Air Dried), Second Sample	1.6	23.4	74.9	Medium Volatile Bituminous	MVB
75	E 8	69.11	80.77	74.94	11.66		1.0	22.4	20.5	56.1	Raw Coal (Air Dried), Third Sample	1.3	26.4	72.3	Medium Volatile Bituminous	MVB
76	E 9	103.33	115.52	109.425	12.19		1.0	27.6	18.3	53.1	Raw Coal (Air Dried)	1.4	25.3	73.3	Medium Volatile Bituminous	MVB
77	E 9A	54.86	64.26	59.56	9.4		0.3	10.5	25.1	64.1	Raw Coal (Air Dried)	0.3	28.0	71.6	Medium Volatile Bituminous	MVB
78	E 9A	54.86	64.26	59.56	9.4		1.1	18.9	19.6	60.4	Raw Coal (Air Dried)	1.4	24.2	74.5	Medium Volatile Bituminous	MVB
79	E 9A	54.86	64.26	59.56	9.4		1.2	15.9	18.3	64.6	Raw Coal (Air Dried)	1.4	21.8	76.8	Medium Volatile Bituminous	MVB
80	E 10	34.16	46.33	40.245	12.17		1.0	8.8	22.1	68.1	Raw Coal (Air Dried)	1.1	24.2	74.7	Medium Volatile Bituminous	MVB
81	E 12	47.72	57.06	52.39	9.34		1.0	25.1	20.0	53.9	Raw Coal (Air Dried)	1.3	26.7	72.0	Medium Volatile Bituminous	MVB
82	E 12	47.72	57.06	52.39	9.34		0.9	11.5	22.0	65.6	Raw Coal (Air Dried), Second Sample	1.0	24.9	74.1	Medium Volatile Bituminous	MVB
83	E 13	32.31	40.81	36.56	8.5		1.7	15.4	20.5	62.4	Raw Coal (Air Dried)	2.0	24.2	73.8	Medium Volatile Bituminous	MVB
84	E 15	346.4	359.66	353.03	13.26		1.6	10.9	16.7	70.8	Raw Coal (Air Dried)	1.8	18.7	79.5	Low Volatile Bituminous	LVB
85	E 15	346.4	359.66	353.03	13.26		1.6	20.5	17.8	60.1	Raw Coal (Air Dried), Second Sample	2.0	22.4	75.6	Medium Volatile Bituminous	MVB
86	E 16A	49.07	62	55.535	12.93		1.3	12.8	21.0	64.9	Raw Coal (Air Dried)	1.5	24.1	74.4	Medium Volatile Bituminous	MVB
87	E 16A	49.07	62	55.535	12.93		1.3	16.1	19.7	62.9	Raw Coal (Air Dried), Second Sample	1.5	23.5	75.0	Medium Volatile Bituminous	MVB
88	E 16A	49.07	62	55.535	12.93		1.0	7.3	24.6	67.1	Raw Coal (Air Dried), Third Sample	1.1	26.5	72.4	Medium Volatile Bituminous	MVB
89	E 17			0							Raw Coal (Air Dried)					
90	E 17A	49.53	59.61	54.57	10.08		1.1	11.0	21.3	66.6	Raw Coal (Air Dried)	1.2	23.9	74.8	Medium Volatile Bituminous	MVB
91	E 18	57.61	70.02	63.815	12.41		1.7	13.1	17.8	67.4	Raw Coal (Air Dried)	2.0	20.5	77.6	Low Volatile Bituminous	LVB

Sequence	Borehole ID / Field Name	Coal Interval		Sample Mid-Point	Composite Coal Thickness (m)	Coal Quality Information							Coal Rank based on Ash-Free Fixed Carbon, Volatile Matter and Moisture Values	Code		
		From (m)	To (m)	(m)		Yield (%)	Moisture (%)	Ash (%)	Volatile Matter (%)	Fixed Carbon (%)	Analysis Comments	Ash-Free			Long Text	
												Moisture (%)	Volatile Matter (%)			Fixed Carbon (%)
92	E 18	57.61	70.02	63.815	12.41		1.7	12.6	17.8	67.9	Raw Coal (Air Dried), Second Sample	1.9	20.4	77.7	Low Volatile Bituminous	LVB
93	E 18	57.61	70.02	63.815	12.41		1.7	10.3	19.6	68.4	Raw Coal (Air Dried), Third Sample	1.9	21.9	76.3	Medium Volatile Bituminous	MVB
94	E 19			0							Raw Coal (Air Dried)					
95	E 19A	39.01	43.84	41.425	4.83		7.0	10.2	15.2	67.6	Raw Coal (Air Dried)	7.8	16.9	75.3	Medium Volatile Bituminous	MVB
96	E 19B	39.01	48.87	43.94	9.86		0.9	12.9	22.0	64.2	Raw Coal (Air Dried)	1.0	25.3	73.7	Medium Volatile Bituminous	MVB
97	E 19C	41.15	53.04	47.095	11.89		1.6	14.8	19.6	64.0	Raw Coal (Air Dried)	1.9	23.0	75.1	Medium Volatile Bituminous	MVB
98	E 19C	41.15	53.04	47.095	11.89		1.4	12.2	21.0	65.4	Raw Coal (Air Dried), Second Sample	1.6	23.9	74.5	Medium Volatile Bituminous	MVB
99	E 19C	41.15	53.04	47.095	11.89		1.1	8.3	25.9	64.7	Raw Coal (Air Dried), Third Sample	1.2	28.2	70.6	Medium Volatile Bituminous	MVB
100	E 20			0							Raw Coal (Air Dried)					
101	E 21	171	181.98	176.49	10.98		0.5	13.5	19.2	66.8	Raw Coal (Air Dried)	0.6	22.2	77.2	Low Volatile Bituminous	LVB
102	E 22			0							Raw Coal (Air Dried)					
103	E 24	55.44	65.84	60.64	10.4		0.2	21.5	19.9	58.4	Raw Coal (Air Dried)	0.3	25.4	74.4	Medium Volatile Bituminous	MVB
104	E 24	55.44	65.84	60.64	10.4		1.5	11.7	20.1	66.7	Raw Coal (Air Dried), Second Sample	1.7	22.8	75.5	Medium Volatile Bituminous	MVB
105	E 25	55.91	67.57	61.74	11.66		1.2	11.2	18.3	69.3	Raw Coal (Air Dried)	1.4	20.6	78.0	Low Volatile Bituminous	LVB
106	E 26	94.14	104.1	99.12	9.87		1.5	12.7	18.6	67.2	Raw Coal (Air Dried)	1.7	21.3	77.0	Medium Volatile Bituminous	MVB
107	E 27	270.05	281.18	275.615	11.13		1.0	15.5	18.1	65.4	Raw Coal (Air Dried)	1.2	21.4	77.4	Low Volatile Bituminous	LVB
108	E 28			0							Raw Coal (Air Dried)					
109	E 29	100.58	114.66	107.62	14.08		0.9	12.5	18.2	68.4	Raw Coal (Air Dried)	1.0	20.8	78.2	Low Volatile Bituminous	LVB
110	E 29	100.58	114.66	107.62	14.08		0.6	8.1	21.7	69.6	Raw Coal (Air Dried), Second Sample	0.7	23.6	75.7	Medium Volatile Bituminous	MVB
111	E 30	53.34	61.57	57.455	8.23		0.7	24.4	18.4	56.5	Raw Coal (Air Dried)	0.9	24.3	74.7	Medium Volatile Bituminous	MVB
112	E 30	53.34	61.57	57.455	8.23		0.7	14.8	19.2	65.3	Raw Coal (Air Dried), Second Sample	0.8	22.5	76.6	Medium Volatile Bituminous	MVB
113	E 31	161.39	170.38	165.885	8.99		0.7	27.0	19.4	52.9	Raw Coal (Air Dried)	1.0	26.6	72.5	Medium Volatile Bituminous	MVB

Sequence	Borehole ID / Field Name	Coal Interval		Sample Mid-Point (m)	Composite Coal Thickness (m)	Coal Quality Information							Coal Rank based on Ash-Free Fixed Carbon, Volatile Matter and Moisture Values		Code	
		From (m)	To (m)			Yield (%)	Moisture (%)	Ash (%)	Volatile Matter (%)	Fixed Carbon (%)	Analysis Comments	Ash-Free				Long Text
				Moisture (%)								Volatile Matter (%)	Fixed Carbon (%)			
114	E 32	105.77	114.6	110.185	8.83		0.7	11.5	17.3	70.5	Raw Coal (Air Dried)	0.8	19.5	79.7	Low Volatile Bituminous	LVB
115	E 32	105.77	114.6	110.185	8.83		0.8	8.3	21.2	69.7	Raw Coal (Air Dried), Second Sample	0.9	23.1	76.0	Medium Volatile Bituminous	MVB
116	E 33	89.97	100.35	95.16	10.38		1.2	22.2	18.4	58.2	Raw Coal (Air Dried)	1.5	23.7	74.8	Medium Volatile Bituminous	MVB
117	E 33	89.97	100.35	95.16	10.38		1.2	9.2	20.6	69.0	Raw Coal (Air Dried), Second Sample	1.3	22.7	76.0	Medium Volatile Bituminous	MVB
118	E 34	161.08	173.35	167.215	12.27		0.3	11.5	18.9	69.3	Raw Coal (Air Dried)	0.3	21.4	78.3	Low Volatile Bituminous	LVB
119	E 34	161.08	173.35	167.215	12.27		1.0	10.2	18.8	70.0	Raw Coal (Air Dried), Second Sample	1.1	20.9	78.0	Low Volatile Bituminous	LVB
120	E 34	161.08	173.35	167.215	12.27		0.6	12.1	23.8	63.6	Raw Coal (Air Dried), Third Sample	0.7	27.1	72.4	Medium Volatile Bituminous	MVB
121	E 35	170.69	180.74	175.715	10.05		0.9	10.1	20.7	68.3	Raw Coal (Air Dried)	1.0	23.0	76.0	Medium Volatile Bituminous	MVB
122	E 36	204.08	212.58	208.33	8.5		1.4	22.9	18.2	57.5	Raw Coal (Air Dried)	1.8	23.6	74.6	Medium Volatile Bituminous	MVB
123	E 37	256.64	265.18	260.91	8.54		0.9	19.9	17.9	61.3	Raw Coal (Air Dried), General quality for deep area used	1.1	22.3	76.5	Medium Volatile Bituminous	MVB
124	E 38	329.79	332.38	331.085	2.59		0.9	19.9	17.9	61.3	Raw Coal (Air Dried), General quality for deep area used	1.1	22.3	76.5	Medium Volatile Bituminous	MVB
125	E 39	53.04	66.55	59.795	13.51		1.3	19.3	18.1	61.3	Raw Coal (Air Dried)	1.6	22.4	76.0	Medium Volatile Bituminous	MVB
126	E 40	37.8	50.9	44.35	13.1		1.0	20.7	18.9	59.4	Raw Coal (Air Dried)	1.3	23.8	74.9	Medium Volatile Bituminous	MVB
127	E 41	43.93	55.93	49.93	12		1.2	19.9	18.2	60.7	Raw Coal (Air Dried)	1.5	22.7	75.8	Medium Volatile Bituminous	MVB
128	E 42	52.58	64.58	58.58	12		1.2	18.4	18.5	61.9	Raw Coal (Air Dried)	1.5	22.7	75.9	Medium Volatile Bituminous	MVB
129	E 43	55.56	67.56	61.56	12		1.2	19.3	18.6	60.9	Raw Coal (Air Dried)	1.5	23.0	75.5	Medium Volatile Bituminous	MVB
130	E 44	49.99	53.77	51.88	3.78		1.5	11.4	13.0	74.1	Raw Coal (Air Dried)	1.7	14.7	83.6	Low Volatile Bituminous	LVB
131	E 45	8.53	20.37	14.45	11.84		1.3	15.5	21.3	61.9	Raw Coal (Total Seam)	1.5	25.2	73.3	Medium Volatile Bituminous	MVB
132	E 46	31.23	41.8	36.515	10.57		0.6	15.5	21.5	62.4	Raw Coal (Total Seam)	0.7	25.4	73.8	Medium Volatile Bituminous	MVB
133	E 47	37.19	48.52	42.855	11.33		1.4	22.1	19.3	57.2	Raw Coal (Total Seam)	1.8	24.8	73.4	Medium Volatile Bituminous	MVB
134	E 48	42.98	56.69	49.835	13.71		1.2	24.4	18.1	56.3	Raw Coal (Total Seam)	1.6	23.9	74.5	Medium Volatile Bituminous	MVB

Sequence	Borehole ID / Field Name	Coal Interval		Sample Mid-Point (m)	Composite Coal Thickness (m)	Coal Quality Information							Coal Rank based on Ash-Free Fixed Carbon, Volatile Matter and Moisture Values		Code	
		From (m)	To (m)			Yield (%)	Moisture (%)	Ash (%)	Volatile Matter (%)	Fixed Carbon (%)	Analysis Comments	Ash-Free				Long Text
				Moisture (%)								Volatile Matter (%)	Fixed Carbon (%)			
135	E 49	50.9	60.86	55.88	9.96		1.2	18.0	21.4	59.4	Raw Coal (Total Seam)	1.5	26.1	72.4	Medium Volatile Bituminous	MVB
136	E 50	49.02	61.23	55.125	12.21		1.3	19.9	20.2	58.6	Raw Coal (Total Seam)	1.6	25.2	73.2	Medium Volatile Bituminous	MVB
137	E 51	33.51	46.8	40.155	13.29		1.2	23.0	19.0	56.8	Raw Coal (Total Seam)	1.6	24.7	73.8	Medium Volatile Bituminous	MVB
138	E 52	45.09	59.21	52.15	14.12		0.9	22.0	19.8	57.3	Raw Coal (Total Seam)	1.2	25.4	73.5	Medium Volatile Bituminous	MVB
139	E 53	42.67	52.88	47.775	10.21		1.3	15.0	19.9	63.8	Raw Coal (Total Seam)	1.5	23.4	75.1	Medium Volatile Bituminous	MVB
140	E 54	81.08	92.81	86.945	11.73		0.4	18.3	20.7	60.6	Raw Coal (Total Seam)	0.5	25.3	74.2	Medium Volatile Bituminous	MVB
141	E 55	102.11	115.66	108.885	13.55		1.1	20.6	18.9	59.4	Raw Coal (Total Seam)	1.4	23.8	74.8	Medium Volatile Bituminous	MVB
142	E 56	39.93	51.77	45.85	11.84		1.2	15.0	20.2	63.6	Raw Coal (Total Seam)	1.4	23.8	74.8	Medium Volatile Bituminous	MVB
143	E 57	137.33	147.68	142.505	10.35		1.0	15.1	19.7	64.2	Raw Coal (Total Seam)	1.2	23.2	75.6	Medium Volatile Bituminous	MVB
144	E 58	160.43	172.73	166.58	12.3		0.9	19.5	18.7	60.9	Raw Coal (Total Seam)	1.1	23.2	75.7	Medium Volatile Bituminous	MVB
145	E 59	35.29	51.06	43.175	15.77		1.5	17.2	20.2	61.1	Raw Coal (Total Seam)	1.8	24.4	73.8	Medium Volatile Bituminous	MVB
146	E 60	188.06	199.17	193.615	11.11		0.7	19.3	20.7	59.3	Raw Coal (Total Seam)	0.9	25.7	73.5	Medium Volatile Bituminous	MVB
147	E 61	185.17	200.67	192.92	15.5		1.0	26.0	18.1	54.9	Raw Coal (Total Seam)	1.4	24.5	74.2	Medium Volatile Bituminous	MVB
148	E 62	46.35	61.73	54.04	15.38		1.6	17.7	19.8	60.9	Raw Coal (Total Seam)	1.9	24.1	74.0	Medium Volatile Bituminous	MVB
149	E 63	210.64	222.73	216.685	12.09		1.1	24.5	18.2	56.2	Raw Coal (Total Seam)	1.5	24.1	74.4	Medium Volatile Bituminous	MVB
150	E 64	210.08	230.42	220.25	20.34		0.9	19.9	17.9	61.3	Raw Coal (Air Dried), General quality for deep area used	1.1	22.3	76.5	Medium Volatile Bituminous	MVB
151	E 65	89.81	99.16	94.485	9.98		1.2	20.4	18.0	60.4	Raw Coal (Total Seam)	1.5	22.6	75.9	Medium Volatile Bituminous	MVB
152	E 66	94.67	106.96	100.815	12.29		0.6	21.0	19.2	59.4	Raw Coal (Total Seam)	0.8	24.3	75.2	Medium Volatile Bituminous	MVB
153	E 66A	94.59	105.73	100.16	11.14		1.1	19.8	18.5	60.6	Raw Coal (Total Seam)	1.4	23.1	75.6	Medium Volatile Bituminous	MVB
154	E 67	76.88	89.99	83.435	13.11		1.4	22.9	17.5	58.2	Raw Coal (Total Seam)	1.8	22.7	75.5	Medium Volatile Bituminous	MVB
155	E 68	74.19	87.99	81.09	13.8		1.2	21.9	18.4	58.5	Raw Coal (Total Seam)	1.5	23.6	74.9	Medium Volatile Bituminous	MVB
156	E 69	140.85	153.54	147.195	12.69		1.0	15.9	17.9	65.2	Raw Coal (Total Seam)	1.2	21.3	77.5	Low Volatile Bituminous	LVB

Sequence	Borehole ID / Field Name	Coal Interval		Sample Mid-Point (m)	Composite Coal Thickness (m)	Coal Quality Information							Coal Rank based on Ash-Free Fixed Carbon, Volatile Matter and Moisture Values		Code	
		From (m)	To (m)			Yield (%)	Moisture (%)	Ash (%)	Volatile Matter (%)	Fixed Carbon (%)	Analysis Comments	Ash-Free				Long Text
				Moisture (%)								Volatile Matter (%)	Fixed Carbon (%)			
157	E 70	150.27	160.67	155.47	10.4		0.8	18.1	19.5	61.6	Raw Coal (Total Seam)	1.0	23.8	75.2	Medium Volatile Bituminous	MVB
158	E 71	151.91	161.46	156.685	9.55		0.9	22.8	18.5	57.8	Raw Coal (Total Seam)	1.2	24.0	74.9	Medium Volatile Bituminous	MVB
159	E 72	144.13	152.9	148.515	8.77		0.8	19.6	18.5	61.1	Raw Coal (Total Seam)	1.0	23.0	76.0	Medium Volatile Bituminous	MVB
160	E 73	203.05	214.63	208.84	11.58		1.0	20.7	17.3	61.0	Raw Coal (Total Seam)	1.3	21.8	76.9	Medium Volatile Bituminous	MVB
161	E 74	183.99	194.54	189.265	10.55		0.9	19.0	18.3	61.8	Raw Coal (Total Seam)	1.1	22.6	76.3	Medium Volatile Bituminous	MVB
162	E 75	189.2	197.66	193.43	8.46		0.9	31.8	16.9	50.4	Raw Coal (Total Seam)	1.3	24.8	73.9	Medium Volatile Bituminous	MVB
163	E 76	176.02	180.12	178.07	4.1		0.6	15.8	18.8	64.8	Raw Coal (Total Seam)	0.7	22.3	77.0	Medium Volatile Bituminous	MVB
164	E 77	243.75	254.66	249.205	10.91		1.0	19.4	16.8	62.8	Raw Coal (Total Seam)	1.2	20.8	77.9	Low Volatile Bituminous	LVB
165	E 78	226.49	237.38	231.935	10.89		1.0	18.6	17.5	62.9	Raw Coal (Total Seam)	1.2	21.5	77.3	Low Volatile Bituminous	LVB
166	E 79	226.1	235.93	231.015	9.83		0.8	22.9	17.1	59.2	Raw Coal (Total Seam)	1.0	22.2	76.8	Medium Volatile Bituminous	MVB
167	E 80B	246.14	255.4	250.77	9.26		1.0	18.4	18.4	62.2	Raw Coal (Total Seam)	1.2	22.5	76.2	Medium Volatile Bituminous	MVB
168	E 81	241.28	249.18	245.23	7.82		0.8	19.4	17.0	62.8	Raw Coal (Total Seam)	1.0	21.1	77.9	Low Volatile Bituminous	LVB
169	E 82	325.23	333.69	329.46	8.46		0.9	22.1	17.7	59.3	Raw Coal (Total Seam)	1.2	22.7	76.1	Medium Volatile Bituminous	MVB
170	E 83	314.62	323.22	318.92	8.6		0.9	19.5	17.9	61.7	Raw Coal (Total Seam)	1.1	22.2	76.6	Medium Volatile Bituminous	MVB
171	E 84	261.14	269.66	265.4	8.52		1.0	20.2	17.5	61.3	Raw Coal (Total Seam)	1.3	21.9	76.8	Medium Volatile Bituminous	MVB
172	E 85	315.49	323.26	319.375	7.77		0.8	25.4	16.5	57.3	Raw Coal (Total Seam)	1.1	22.1	76.8	Medium Volatile Bituminous	MVB
173	E 87	6.08	10.5	8.29	4.42		1.1	18.9	19.6	60.4	Raw Coal (Air Dried), General quality for open cast area used	1.4	24.2	74.5	Medium Volatile Bituminous	MVB
174	E 88	53.54	63.85	58.695	10.31		1.1	18.9	19.6	60.4	Raw Coal (Total Seam)	1.4	24.2	74.5	Medium Volatile Bituminous	MVB
175	E 89	48.46	52.94	50.7	4.48		1.1	18.9	19.6	60.4	Raw Coal (Total Seam)	1.4	24.2	74.5	Medium Volatile Bituminous	MVB
176	E 90	38.6	48.87	43.735	10.27		1.1	9.8	20.9	68.2	Raw Coal (Total Seam)	1.2	23.2	75.6	Medium Volatile Bituminous	MVB
177	E 91	49.38	61.1	55.24	11.72		0.9	11.4	21.5	66.2	Raw Coal (Total Seam)	1.0	24.3	74.7	Medium Volatile Bituminous	MVB
178	E 92	47.5	59.08	53.29	11.58		1.1	18.9	19.6	60.4	Raw Coal (Total Seam)	1.4	24.2	74.5	Medium Volatile Bituminous	MVB

Sequence	Borehole ID / Field Name	Coal Interval		Sample Mid-Point	Composite Coal Thickness (m)	Coal Quality Information							Coal Rank based on Ash-Free Fixed Carbon, Volatile Matter and Moisture Values	Code		
		From (m)	To (m)	(m)		Yield (%)	Moisture (%)	Ash (%)	Volatile Matter (%)	Fixed Carbon (%)	Analysis Comments	Ash-Free			Long Text	
												Moisture (%)	Volatile Matter (%)			Fixed Carbon (%)
179	E 93	64.22		64.22			1.1	18.9	19.6	60.4	Raw Coal (Air Dried), General quality for open cast area used	1.4	24.2	74.5	Medium Volatile Bituminous	MVB
180	E 94	58.92	69.31	64.115	10.39		1.1	18.9	19.6	60.4	Raw Coal (Total Seam)	1.4	24.2	74.5	Medium Volatile Bituminous	MVB
181	E 96			0							Raw Coal (Total Seam)					
182	E 97			0							Raw Coal (Total Seam)					
183	E 98	110.5	121.6	116.05	11.1		0.9	19.9	17.9	61.3	Raw Coal (Air Dried), General quality for deep area used	1.1	22.3	76.5	Medium Volatile Bituminous	MVB
184	E 99	218.85	227.13	222.99	8.28		0.9	19.9	17.9	61.3	Raw Coal (Air Dried), General quality for deep area used	1.1	22.3	76.5	Medium Volatile Bituminous	MVB
185	E 101	229.08	238.44	233.76	9.36		0.9	19.9	17.9	61.3	Raw Coal (Air Dried), General quality for deep area used	1.1	22.3	76.5	Medium Volatile Bituminous	MVB
186	E 102	201.8	210.6	206.2	8.8		0.9	19.9	17.9	61.3	Raw Coal (Air Dried), General quality for deep area used	1.1	22.3	76.5	Medium Volatile Bituminous	MVB
187	E 103	93.46	101.82	97.64	8.36		1.1	18.9	19.6	60.4	Raw Coal (Total Seam)	1.4	24.2	74.5	Medium Volatile Bituminous	MVB
188	E 104	119.41	125.83	122.62	6.42		0.9	19.9	17.9	61.3	Raw Coal (Air Dried), General quality for deep area used	1.1	22.3	76.5	Medium Volatile Bituminous	MVB
189	LBW 1	11.12	13.14	12.13	2.02		1.1	37.6	25.9	35.4	Raw Coal (Air Dried)	1.8	41.5	56.7	High Volatile Bituminous - B	HVB-B
190	LBW 1	16.17	20.23	18.2	3.73		1.0	41.7	22.2	35.1	Raw Coal (Air Dried)	1.7	38.1	60.2	High Volatile Bituminous - B	HVB-B
191	LBW 1	28.82	43.33	36.075			1.1	27.3	23.4	48.2	Raw Coal (Air Dried), General quality information used	1.5	32.2	66.3		
192	LBW 1			0	10.53		1.0	29.9	23.4	45.7	Raw Coal (Air Dried)	1.4	33.4	65.2	High Volatile Bituminous - A	HVB-A
193	LBW 2	84.71	88.66	86.685	2.8		1.1	39.0	24.2	35.5	Raw Coal (Air Dried)	1.8	39.7	58.2	High Volatile Bituminous - B	HVB-B
194	LBW 2	95.94	111.56	103.75			1.1	27.3	23.4	48.2	Raw Coal (Air Dried), General quality information used	1.5	32.2	66.3		
195	LBW 2			0	13.57		1.1	23.7	22.0	53.2	Raw Coal (Air Dried)	1.4	28.8	69.7	Medium Volatile Bituminous	MVB

Sequence	Borehole ID / Field Name	Coal Interval		Sample Mid-Point (m)	Composite Coal Thickness (m)	Coal Quality Information							Coal Rank based on Ash-Free Fixed Carbon, Volatile Matter and Moisture Values		Code	
		From (m)	To (m)			Yield (%)	Moisture (%)	Ash (%)	Volatile Matter (%)	Fixed Carbon (%)	Analysis Comments	Ash-Free				Long Text
				Moisture (%)								Volatile Matter (%)	Fixed Carbon (%)			
196	LBW 4	41.51	43.51	42.51	2		1.0	34.6	25.0	39.4	Raw Coal (Air Dried)	1.5	38.2	60.2	High Volatile Bituminous - B	HVB-B
197	LBW 4	51.9	70.13	61.015	17.92		1.0	24.7	23.0	51.3	Raw Coal (Air Dried)	1.3	30.5	68.1	High Volatile Bituminous - A	HVB-A
198	LBW 5	32.76	36.41	34.585	3.26		0.9	46.6	21.1	31.5	Raw Coal (Air Dried)	1.7	39.5	59.0	High Volatile Bituminous - B	HVB-B
199	LBW 5	40.53	56.83	48.68	16.2		0.9	27.6	23.9	47.6	Raw Coal (Air Dried)	1.2	33.0	65.7	High Volatile Bituminous - A	HVB-A
200	LBW 6	65.61	74.1	69.855	9.09		1.1	27.3	23.4	48.2	Raw Coal (Air Dried), General quality information used	1.5	32.2	66.3		
201	LBW 6	15	98	56.5	7.96		0.9	44.1	18.4	30.8	Raw Coal (Air Dried)	1.6	32.9	55.1	High Volatile Bituminous - B	HVB-B
202	LBW 6	83.56	92.7	88.13	8.65		1.0	23.9	25.6	49.5	Raw Coal (Air Dried)	1.3	33.6	65.0	High Volatile Bituminous - A	HVB-A
203	LBW 7	55.05	58.99	57.02	3.69		1.0	43.5	22.2	33.4	Raw Coal (Air Dried)	1.8	39.3	59.1	High Volatile Bituminous - B	HVB-B
204	LBW 7	64.65	82.28	73.465	15.68		1.0	32.4	23.1	43.5	Raw Coal (Air Dried)	1.5	34.2	64.3	High Volatile Bituminous - A	HVB-A
205	LBW 8	25.64	29.43	27.535	3.43		0.8	42.5	20.9	35.8	Raw Coal (Air Dried)	1.4	36.3	62.3	High Volatile Bituminous - A	HVB-A
206	LBW 8	34.9	46.35	40.625	9.31		0.9	25.8	24.2	49.1	Raw Coal (Air Dried)	1.2	32.6	66.2	High Volatile Bituminous - A	HVB-A
207	LBW 9	14.81	16.81	15.81	1.91		1.1	35.3	25.1	38.5	Raw Coal (Air Dried)	1.7	38.8	59.5	High Volatile Bituminous - B	HVB-B
208	LBW 9	26.6	34.58	30.59	7.98		0.9	32.3	22.3	44.5	Raw Coal (Air Dried)	1.3	32.9	65.7	High Volatile Bituminous - A	HVB-A
209	LBW 10	63.13	67.19	65.16	3.74		1.1	38.5	20.8	34.9	Raw Coal (Air Dried)	1.8	33.8	56.7	High Volatile Bituminous - B	HVB-B
210	LBW 10	73.22	84.3	78.76	10.98		0.9	29.2	21.9	48.0	Raw Coal (Air Dried)	1.3	30.9	67.8	High Volatile Bituminous - A	HVB-A
211	LBW 11	32.11	36.16	34.135	1.7		1.6	37.9	24.3	37.8	Raw Coal (Air Dried)	2.6	39.1	60.9	High Volatile Bituminous - B	HVB-B
212	LBW 11	44.04	57.16	50.6	13.12		1.1	27.3	23.4	48.2	Raw Coal (Air Dried), General quality information used	1.5	32.2	66.3		
213	LBW 11			0	12.3		2.7	24.6	25.3	47.4	Raw Coal (Air Dried)	3.6	33.6	62.9	High Volatile Bituminous - A	HVB-A
214	LBW 12	39.86	50.87	45.365	6.13		2.2	40.3	23.7	33.8	Raw Coal (Air Dried)	3.7	39.7	56.6	High Volatile Bituminous - B	HVB-B
215	LBW 12	66.3	79.84	73.07	12.57		2.1	20.4	21.3	56.2	Raw Coal (Air Dried)	2.6	26.8	70.6	Medium Volatile Bituminous	MVB
216	LBW 13	97.77	102	99.885	4.04		0.8	39.3	18.7	41.2	Raw Coal (Air Dried)	1.3	30.8	67.9	High Volatile Bituminous - A	HVB-A
217	S 1	96.01	113.08	104.545	17.07		3.8	26.2	24.4	45.6	Raw Coal	5.1	33.1	61.8	High Volatile Bituminous - B	HVB-B
218	S 2	63.93	77.62	70.775	13.69		4.4	22.9	21.6	51.1	Raw Coal	5.7	28.0	66.3	High Volatile Bituminous - A	HVB-A
219	S 3	6.1	15.24	10.67	9.14		4.4	27.3	20.6	47.7	Raw Coal	6.1	28.3	65.6	High Volatile Bituminous - A	HVB-A
220	S 5	90.22	107.29	98.755	17.07		5.2	17.7	20.9	56.2	Raw Coal	6.3	25.4	68.3	High Volatile Bituminous - A	HVB-A

Sequence	Borehole ID / Field Name	Coal Interval		Sample Mid-Point	Composite Coal Thickness (m)	Coal Quality Information							Coal Rank based on Ash-Free Fixed Carbon, Volatile Matter and Moisture Values			Code
		From (m)	To (m)	(m)		Yield (%)	Moisture (%)	Ash (%)	Volatile Matter (%)	Fixed Carbon (%)	Analysis Comments	Ash-Free			Long Text	
												Moisture (%)	Volatile Matter (%)	Fixed Carbon (%)		
221	S 18	151.79	160.55	156.17	8.76		2.8	19.4	26.6	51.2	Raw Coal	3.5	33.0	63.5	High Volatile Bituminous - A	HVB-A
222	S 25	147.51	159.4	153.455	11.89		3.2	25.8	21.3	49.7	Raw Coal	4.3	28.7	67.0	High Volatile Bituminous - A	HVB-A
223	S 26	11.27	21.96	16.615	10.69		3.6	26.5	18.6	51.3	Raw Coal	4.9	25.3	69.8	Medium Volatile Bituminous	MVB
224	S 27	85.8	97.92	91.86	12.12		3.4	22.9	21.0	52.7	Raw Coal	4.4	27.2	68.4	High Volatile Bituminous - A	HVB-A
225	S 29	70.71	80.95	75.83	10.24		3.6	22.8	21.4	52.2	Raw Coal	4.7	27.7	67.6	High Volatile Bituminous - A	HVB-A
226	S 30	40.46	49.48	44.97	9.02		5.1	11.5	22.0	61.4	Raw Coal	5.8	24.9	69.4	Medium Volatile Bituminous	MVB
227	M 1	78.59	90.53	84.56	11.94		3.0	27.2	22.3	47.5	Raw Coal	4.1	30.6	65.2	High Volatile Bituminous - A	HVB-A
228	M 2	96.32	111.51	103.915	15.19		3.0	27.7	21.8	47.5	Raw Coal	4.1	30.2	65.7	High Volatile Bituminous - A	HVB-A
229	M 3	78.93	93.26	86.095	14.33		3.6	17.5	23.5	55.4	Raw Coal	4.4	28.5	67.2	High Volatile Bituminous - A	HVB-A
230	M 4	135.62	145	140.31	9.38		3.3	24.2	23.0	49.5	Raw Coal	4.4	30.3	65.3	High Volatile Bituminous - A	HVB-A
231	M 5	69.18	78.84	74.01	9.66		2.2	26.9	23.1	47.8	Raw Coal	3.0	31.6	65.4	High Volatile Bituminous - A	HVB-A
232	M 6	71.11	78.93	75.02	7.82		2.0	37.6	20.7	39.7	Raw Coal	3.2	33.2	63.6	High Volatile Bituminous - A	HVB-A
233	M 7	108.35	118.56	113.455	10.21		3.6	18.3	23.0	55.1	Raw Coal	4.4	28.2	67.4	High Volatile Bituminous - A	HVB-A
234	M 8	71.85	83.28	77.565	11.43		4.0	21.9	22.0	52.1	Raw Coal	5.1	28.2	66.7	High Volatile Bituminous - A	HVB-A
235	M 9	21.18	34.51	27.845	13.33		5.0	18.7	21.5	54.8	Raw Coal	6.2	26.4	67.4	High Volatile Bituminous - A	HVB-A
236	M 10	0.1	11.07	5.585	11.07		5.3	18.2	21.5	55.0	Raw Coal	6.5	26.3	67.2	High Volatile Bituminous - A	HVB-A
237	M 11	25.75	38.63	32.19	12.88		4.5	20.6	20.4	54.5	Raw Coal	5.7	25.7	68.6	High Volatile Bituminous - A	HVB-A
238	L 256 (Type Borehole - Main & A Seams)*	15	190	102.5	9.17		12.0	18.8	24.1	45.1	Raw Coal - Fixed Carbon Calculated	14.8	29.7	55.5	High Volatile Bituminous - B	HVB-B
239	L 252 (Type Borehole - Main Seam)*	22.49766 667	197.4976 667	109.9976 667	6.15		13.5	16.0	27.4	43.1	Raw Coal - Fixed Carbon Calculated	16.1	32.6	51.3	High Volatile Bituminous - C	HVB-C
240	L 198 (Type Borehole - Lower & Middle Seam)*	26.6	97.77	62.185	4.15		11.9	13.0	29.3	45.8	Raw Coal - Fixed Carbon Calculated	13.7	33.7	52.6	High Volatile Bituminous - C	HVB-C
241	Shallow (Average)*	60	100	80	9		0.8	9.8	23.8	65.8	High ash bright thin bands with interbedded mudstone reported, some Fischer oil noted	0.8	26.3	72.9	Medium Volatile Bituminous	MVB
242	Deep(Average)*	200	700	450	9		0.8	9.8	23.8	65.8	High ash bright thin bands with interbedded mudstone reported	0.8	26.3	72.9	Medium Volatile Bituminous	MVB

Sequence	Borehole ID / Field Name	Coal Interval		Sample Mid-Point (m)	Composite Coal Thickness (m)	Coal Quality Information							Coal Rank based on Ash-Free Fixed Carbon, Volatile Matter and Moisture Values		Code	
		From (m)	To (m)			Yield (%)	Moisture (%)	Ash (%)	Volatile Matter (%)	Fixed Carbon (%)	Analysis Comments	Ash-Free				Long Text
				Moisture (%)								Volatile Matter (%)	Fixed Carbon (%)			
243	Gokwe Average	200	300	250	9		4.0	25.0	22.0	49.0	Reported by Padcoal (Pvt) Ltd (2011) as part of an investment brochure. Ash values reported as between 20 & 30 % by Oesterlen & Lepper (2005)	5.3	29.3	65.3	High Volatile Bituminous - A	HVB-A
244	N1/1	45.1	46.7	45.9	1						No Analysis Data Provided. High ash lower quality coal. Report				Subbituminous	SBIT
245	N1/2	41	89	65	5.5						No Analysis Data Provided. High ash lower quality coal. Report				Subbituminous	SBIT
246	N1/3	24	91	57.5	7.73						No Analysis Data Provided. High ash lower quality coal. Report				Subbituminous	SBIT
247	N2/1	52.7	118.1	85.4	19.6						No Analysis Data Provided. High ash lower quality coal. Report				Subbituminous	SBIT
248	N3/1	38.3	119	78.65	23.65						No Analysis Data Provided. High ash lower quality coal. Report				Subbituminous	SBIT
249	N4/1	113.3	189	151.15	14.03						No Analysis Data Provided. High ash lower quality coal. Report				Subbituminous	SBIT
250	N5/2	5	41.7	23.35	6.8						No Analysis Data Provided. High ash lower quality coal. Report				Subbituminous	SBIT
251	N5/1	10.4	41.2	25.8	4.1						No Analysis Data Provided. High ash lower quality coal. Report				Subbituminous	SBIT

Sequence	Borehole ID / Field Name	Coal Interval		Sample Mid-Point	Composite Coal Thickness (m)	Coal Quality Information							Coal Rank based on Ash-Free Fixed Carbon, Volatile Matter and Moisture Values	Code		
		From (m)	To (m)	(m)		Yield (%)	Moisture (%)	Ash (%)	Volatile Matter (%)	Fixed Carbon (%)	Analysis Comments	Ash-Free			Long Text	
												Moisture (%)	Volatile Matter (%)			Fixed Carbon (%)
252	N6/1	14.7	70.5	42.6	2.5						No Analysis Data Provided. High ash lower quality coal. Report				Subbituminous	SBIT
253	N8/2	75.35	124.5	99.925	11.5						No Analysis Data Provided. High ash lower quality coal. Report				Subbituminous	SBIT
254	N12/1	79.9	150.85	115.375	12.5						No Analysis Data Provided. High ash lower quality coal. Report				Subbituminous	SBIT
255	N9/1	75.4	124.6	100	8.74						No Analysis Data Provided. High ash lower quality coal. Report				Subbituminous	SBIT
256	N10/1	89.4	177.3	133.35	21.76						No Analysis Data Provided. High ash lower quality coal. Report				Subbituminous	SBIT
257	N11/3	110.6	153.5	132.05	8.15						No Analysis Data Provided. High ash lower quality coal. Report				Subbituminous	SBIT
258	N7/1			0							No Coal Intersected					
259	N7/2			0							No Coal Intersected					
260	N7/3			0							No Coal Intersected					
261	N8/1			0							No Coal Intersected					
262	N8/2			0							No Coal Intersected					
263	N12/1			0							No Coal Intersected					
264	N9/1			0							No Coal Intersected					
265	N10/1			0							No Coal Intersected					
266	N11/3			0							No Coal Intersected					
267	N11/2			0							No Coal Intersected					
268	N11/1			0							No Coal					

Sequence	Borehole ID / Field Name	Coal Interval		Sample Mid-Point (m)	Composite Coal Thickness (m)	Coal Quality Information							Coal Rank based on Ash-Free Fixed Carbon, Volatile Matter and Moisture Values	Code			
		From (m)	To (m)			Yield (%)	Moisture (%)	Ash (%)	Volatile Matter (%)	Fixed Carbon (%)	Analysis Comments	Ash-Free					
				Moisture (%)								Volatile Matter (%)	Fixed Carbon (%)		Long Text		
269	N12/1			0							Intersected						
270	N12/2			0							No Coal Intersected						
271	N12/3			0							No Coal Intersected						
272	Y1-01	499.74	566.3	533.02	10.652						No Analysis Data Provided. High ash lower quality coal. Only developed in the Nata Area				Subbituminous	SBIT	
273	Y1-02	705.536	737.136	721.336	1.29						No Analysis Data Provided. High ash lower quality coal. Only developed in the Nata Area				Subbituminous	SBIT	
274	Y1-03	705.73	792.74	749.235	16.75						No Analysis Data Provided. High ash lower quality coal. Only developed in the Nata Area				Subbituminous	SBIT	
275	Y1-04	587.2	605.5	596.35	2.85						No Analysis Data Provided. High ash lower quality coal. Only developed in the Nata Area				Subbituminous	SBIT	
276	PDM006C			0							No Coal Intersected						
277	PDM007A			0							No Coal Intersected						
278	PDM008			0							No Coal Intersected						
279	PDM009			0							No Coal Intersected						
280	PDM011			0							No Coal Intersected						
281	PDM014A			0							No Coal Intersected						
282	PDM015			0							No Coal Intersected						

Sequence	Borehole ID / Field Name	Coal Interval		Sample Mid-Point	Composite Coal Thickness (m)	Coal Quality Information							Coal Rank based on Ash-Free Fixed Carbon, Volatile Matter and Moisture Values	Code		
		From (m)	To (m)	(m)		Yield (%)	Moisture (%)	Ash (%)	Volatile Matter (%)	Fixed Carbon (%)	Analysis Comments	Ash-Free			Long Text	
												Moisture (%)	Volatile Matter (%)			Fixed Carbon (%)
283	Lubimbi	11.8	190	100.9						High ash bright thin bands with interbedded mudstone reported, some Fischer oil noted. High Volatile Bituminous B Assumed				High Volatile Bituminous C	HVB-C	
284	Busi	60	80	70	10					High ash lower quality coal reported				Subbituminous	SBIT	
285	Tjolutjo, Sawmills, and Insuza	270	330	300	5					High ash lower quality coal reported (bituminous)				Subbituminous	SBIT	

Appendix C Schedule of borehole data showing the Gas Content Calculated from the Eddy, et al. (1982) trend line Equations used in this evaluation.

Sequence	Borehole ID / Field Name	Coal Interval			Nett Coal Thickness (m)	Coal Quality				Eddy, et al. (1982) Trend Line Equation	Gas Content Calculated from Eddy, et al. (1982) Trend Line Equations (scf/T)											
		From (m)	To (m)	Sample Mid-Point (m)		Ash-Free			Coal Rank Code		Full Saturation (100%)			75% Saturation			50% Saturation			25% Saturation		
						Moisture (%)	Volatile Matter (%)	Fixed Carbon (%)			Minimum	Maximum	Average	Minimum	Maximum	Average	Minimum	Maximum	Average	Minimum	Maximum	Average
1	M 53	284.19	291.57	287.88	7.38	1.2	27.4	71.4	MVB	$y = 122.88\ln(x) - 305.91$	388	391	390	291	294	292	194	196	195	97	98	97
2	M 55	288.81	294.5	291.655	5.69	1.2	26.1	72.7	MVB	$y = 122.88\ln(x) - 305.91$	390	393	392	293	295	294	195	196	196	98	98	98
3	M 56	249.09	254.76	251.925	5.67	1.3	25.4	73.3	MVB	$y = 122.88\ln(x) - 305.91$	372	375	374	279	281	280	186	187	187	93	94	93
4	M 57	281.96	287.22	284.59	5.26	1.1	29.0	69.9	MVB	$y = 122.88\ln(x) - 305.91$	387	390	388	291	292	291	194	195	194	97	97	97
5	M 58	243	252.28	247.64	9.28	1.2	27.4	71.4	MVB	$y = 122.88\ln(x) - 305.91$	369	374	371	277	280	279	185	187	186	92	93	93
6	M 59	287.1	294.98	291.04	7.88	1.1	28.2	70.8	MVB	$y = 122.88\ln(x) - 305.91$	390	393	391	292	295	293	195	196	196	97	98	98
7	M 60	279.04	287.36	283.2	8.32	1.3	28.1	70.6	MVB	$y = 122.88\ln(x) - 305.91$	386	390	388	290	292	291	193	195	194	97	97	97
8	M 62	259.91	266.36	263.135	6.45	1.3	29.8	68.9	HVB-A	$y = 78.864\ln(x) - 193.00$	246	247	246	184	186	185	123	124	123	61	62	62
9	M 63	252.67	258.78	255.725	6.11	1.3	32.7	66.0	HVB-A	$y = 78.864\ln(x) - 193.00$	243	245	244	182	184	183	122	123	122	61	61	61
10	M 64	251.54	253.6	252.57	2.06	1.2	25.4	73.4	MVB	$y = 122.88\ln(x) - 305.91$	373	374	374	280	281	280	187	187	187	93	94	93
11	M 65	88.63	103.81	96.22	9.46	1.2	36.1	62.6	HVB-A	$y = 78.864\ln(x) - 193.00$	161	173	167	120	130	125	80	87	84	40	43	42
12	M 66	35.19	48.38	41.785	7.39	1.3	36.8	61.9	HVB-B	$y = 52.803\ln(x) - 141.04$	47	64	56	35	48	42	23	32	28	12	16	14
13	M 67	24.7	34.33	29.515	3.9	1.4	37.1	61.5	HVB-B	$y = 52.803\ln(x) - 141.04$	(1)	46	(1)	(1)	34	(1)	(1)	23	(1)	(1)	11	(1)
14	M 68	15.31	24.03	19.67	6.27	2.1	23.2	74.8	MVB	$y = 122.88\ln(x) - 305.91$	(1)	(1)	(1)	(1)	(1)	(1)	(1)	(1)	(1)	(1)	(1)	(1)
15	M 69	100.61	109.31	104.96	5.72	1.4	36.6	62.0	HVB-A	$y = 78.864\ln(x) - 193.00$	171	177	174	128	133	130	85	89	87	43	44	43
16	M 70	55.51	71.32	63.415	8.2	1.3	36.0	62.7	HVB-A	$y = 78.864\ln(x) - 193.00$	124	144	134	93	108	101	62	72	67	31	36	34
17	M 71	15.75	31.62	23.685	9.2	1.6	35.7	62.7	HVB-A	$y = 78.864\ln(x) - 193.00$	(1)	79	(1)	(1)	60	(1)	(1)	40	(1)	(1)	20	(1)
18	M 72	110.65	123.89	117.27	9.65	1.2	35.4	63.4	HVB-A	$y = 78.864\ln(x) - 193.00$	178	187	183	134	140	137	89	94	91	45	47	46
19	M 73	99.06	116.83	107.945	8.7	1.6	35.6	62.8	HVB-A	$y = 78.864\ln(x) - 193.00$	169	182	176	127	137	132	85	91	88	42	46	44
20	M 74	69.18	85.98	77.58	10.11	1.7	34.8	63.5	HVB-A	$y = 78.864\ln(x) - 193.00$	141	158	150	106	119	113	71	79	75	35	40	38
21	M 75	33	51.43	42.215	13.91	2.0	34.8	63.2	HVB-A	$y = 78.864\ln(x) - 193.00$	83	118	102	62	88	77	41	59	51	21	29	26
22	M 76	14.02	19.75	16.885	5.73	2.1	23.2	74.8	MVB	$y = 122.88\ln(x) - 305.91$	(1)	(1)	(1)	(1)	(1)	(1)	(1)	(1)	(1)	(1)	(1)	(1)
23	M 77	87.78	113.39	100.585	7.76	1.7	34.8	63.6	HVB-A	$y = 78.864\ln(x) - 193.00$	160	180	171	120	135	128	80	90	85	40	45	43
24	M 78	75.73	85.96	80.845	7.53	2.1	23.2	74.8	MVB	$y = 122.88\ln(x) - 305.91$	226	241	234	169	181	175	113	121	117	56	60	58
25	M 79	36.51	51.28	43.895	8.86	1.9	34.7	63.4	HVB-A	$y = 78.864\ln(x) - 193.00$	91	118	105	68	88	79	45	59	53	23	29	26
26	M 80	9.08	22.29	15.685	6.68	2.5	33.8	63.6	HVB-A	$y = 78.864\ln(x) - 193.00$	(1)	(1)	(1)	(1)	(1)	(1)	(1)	(1)	(1)	(1)	(1)	(1)
27	M 81	90.86	106.31	98.585	8.27	1.9	34.4	63.7	HVB-A	$y = 78.864\ln(x) - 193.00$	163	175	169	122	131	127	81	88	85	41	44	42
28	M 82	62.87	72.99	67.93	5.18	1.7	33.8	64.5	HVB-A	$y = 78.864\ln(x) - 193.00$	134	145	140	100	109	105	67	73	70	33	36	35
29	M 83	25.38	34.13	29.755	5.82	1.9	33.9	64.2	HVB-A	$y = 78.864\ln(x) - 193.00$	(1)	85	(1)	(1)	64	(1)	(1)	43	(1)	(1)	21	(1)
30	M 85	82.58	93.29	87.935	5.13	2.0	34.8	63.1	HVB-A	$y = 78.864\ln(x) - 193.00$	155	165	160	116	124	120	78	82	80	39	41	40
31	M 86	56.68	65.15	60.915	3.66	1.9	34.1	64.0	HVB-A	$y = 78.864\ln(x) - 193.00$	125	136	131	94	102	98	63	68	66	31	34	33
32	M 87	22	35.81	28.905	8.03	2.2	34.1	63.7	HVB-A	$y = 78.864\ln(x) - 193.00$	(1)	89	(1)	(1)	67	(1)	(1)	45	(1)	(1)	22	(1)
33	M 88	4.2	8.9	6.55	4.7	2.1	23.2	74.8	MVB	$y = 122.88\ln(x) - 305.91$	(1)	(1)	(1)	(1)	(1)	(1)	(1)	(1)	(1)	(1)	(1)	(1)

Sequence	Borehole ID / Field Name	Coal Interval			Nett Coal Thickness (m)	Coal Quality				Eddy, et al. (1982) Trend Line Equation	Gas Content Calculated from Eddy, et al. (1982) Trend Line Equations (scf/T)											
		From (m)	To (m)	Sample Mid-Point (m)		Ash-Free			Coal Rank Code		Full Saturation (100%)			75% Saturation			50% Saturation			25% Saturation		
						Moisture (%)	Volatile Matter (%)	Fixed Carbon (%)			Minimum	Maximum	Average	Minimum	Maximum	Average	Minimum	Maximum	Average	Minimum	Maximum	Average
34	M 89	94.76	107.99	101.375	4	2.5	33.7	63.8	HVB-A	$y = 78.864\ln(x) - 193.00$	166	176	171	124	132	128	83	88	86	41	44	43
35	M 90	75.7	86.42	81.06	4.4	2.2	34.4	63.4	HVB-A	$y = 78.864\ln(x) - 193.00$	148	159	154	111	119	115	74	79	77	37	40	38
36	M 91	56	65.09	60.545	3.02	2.0	34.4	63.6	HVB-A	$y = 78.864\ln(x) - 193.00$	124	136	131	93	102	98	62	68	65	31	34	33
37	M 92	20.31	37.26	28.785	9.12	2.2	34.5	63.3	HVB-A	$y = 78.864\ln(x) - 193.00$	(1)	92	(1)	(1)	69	(1)	(1)	46	(1)	(1)	23	(1)
38	M 94	74.04	83.46	78.75	4.7	2.0	34.5	63.5	HVB-A	$y = 78.864\ln(x) - 193.00$	146	156	151	110	117	114	73	78	76	37	39	38
39	M 95	43.11	57.73	50.42	8.74	2.1	34.7	63.2	HVB-A	$y = 78.864\ln(x) - 193.00$	104	127	116	78	95	87	52	63	58	26	32	29
40	1740	156.38	168.9	162.64	12.52	1.7	25.5	72.8	MVB	$y = 122.88\ln(x) - 305.91$	315	324	320	236	243	240	157	162	160	79	81	80
41	1741	179.2	187.3	183.25	8.1	1.8	26.3	71.9	MVB	$y = 122.88\ln(x) - 305.91$	332	337	334	249	253	251	166	169	167	83	84	84
42	1742	164.26	171.9	168.08	7.64	2.2	27.8	70.0	MVB	$y = 122.88\ln(x) - 305.91$	321	327	324	241	245	243	160	163	162	80	82	81
43	1743	249.92	256.6	253.26	6.68	1.8	25.4	72.8	MVB	$y = 122.88\ln(x) - 305.91$	373	376	374	279	282	281	186	188	187	93	94	94
44	1744	255.48	262.8	259.14	7.32	1.2	25.4	73.4	MVB	$y = 122.88\ln(x) - 305.91$	375	379	377	281	284	283	188	189	188	94	95	94
45	1745	251.76	257.7	254.73	5.94	1.2	25.4	73.4	MVB	$y = 122.88\ln(x) - 305.91$	373	376	375	280	282	281	187	188	187	93	94	94
46	1746	206.97	213.5	210.235	6.53	1.7	25.8	72.5	MVB	$y = 122.88\ln(x) - 305.91$	349	353	351	262	265	263	175	177	176	87	88	88
47	1747	292.29	301.2	296.745	8.91	1.9	26.4	71.7	MVB	$y = 122.88\ln(x) - 305.91$	392	395	394	294	297	295	196	198	197	98	99	98
48	1748	271.14	278.2	274.67	7.06	2.3	26.5	71.2	MVB	$y = 122.88\ln(x) - 305.91$	383	386	384	287	289	288	191	193	192	96	96	96
49	1749	229.92	239.6	234.76	9.68	1.2	25.4	73.4	MVB	$y = 122.88\ln(x) - 305.91$	362	367	365	272	276	274	181	184	182	91	92	91
50	1750	282.29	287.7	284.995	5.41	1.4	25.1	73.5	MVB	$y = 122.88\ln(x) - 305.91$	387	390	389	291	292	291	194	195	194	97	97	97
51	1751	285.21	295.8	290.505	10.59	2.1	27.3	70.6	MVB	$y = 122.88\ln(x) - 305.91$	389	393	391	292	295	293	194	197	196	97	98	98
52	1752	306.92	318.2	312.56	11.28	1.2	25.4	73.4	MVB	$y = 122.88\ln(x) - 305.91$	398	402	400	298	302	300	199	201	200	99	101	100
53	1753					2.1	23.2	74.8	MVB	$y = 122.88\ln(x) - 305.91$	(1)	(1)	(1)	(1)	(1)	(1)	(1)	(1)	(1)	(1)	(1)	(1)
54	1754	187.34	196	191.67	8.66	1.2	25.4	73.4	MVB	$y = 122.88\ln(x) - 305.91$	337	343	340	253	257	255	169	171	170	84	86	85
55	1755	173.98	180.1	177.04	6.12	1.6	25.5	72.9	MVB	$y = 122.88\ln(x) - 305.91$	328	332	330	246	249	248	164	166	165	82	83	83
56	1756	274.18	283.3	278.74	9.12	1.2	25.4	73.4	MVB	$y = 122.88\ln(x) - 305.91$	384	388	386	288	291	289	192	194	193	96	97	96
57	1757	290.1	296.9	293.5	6.8	2.2	26.2	71.5	MVB	$y = 122.88\ln(x) - 305.91$	391	394	392	293	295	294	195	197	196	98	98	98
58	1758	326.76	335.6	331.18	8.84	1.5	26.9	71.6	MVB	$y = 122.88\ln(x) - 305.91$	405	409	407	304	307	305	203	204	204	101	102	102
59	1759	302.67	311.3	306.985	8.63	1.5	27.5	71.0	MVB	$y = 122.88\ln(x) - 305.91$	396	400	398	297	300	298	198	200	199	99	100	99
60	1760	321.99	332.2	327.095	10.21	1.4	25.5	73.1	MVB	$y = 122.88\ln(x) - 305.91$	404	407	406	303	306	304	202	204	203	101	102	101
61	1761	297.95	306.2	302.075	8.25	1.4	25.2	73.4	MVB	$y = 122.88\ln(x) - 305.91$	394	397	396	296	298	297	197	199	198	99	99	99
62	1763					2.1	23.2	74.8	MVB	$y = 122.88\ln(x) - 305.91$	(1)	(1)	(1)	(1)	(1)	(1)	(1)	(1)	(1)	(1)	(1)	(1)
63	1764A	313.47	325.47	319.47	11.73	1.0	28.7	70.3	MVB	$y = 122.88\ln(x) - 305.91$	400	405	403	300	304	302	200	202	201	100	101	101
64	E 1																					
65	E 2	34.89	47.39	41.14	12.5	1.3	24.9	73.8	MVB	$y = 122.88\ln(x) - 305.91$	131	168	151	98	126	113	65	84	75	33	42	38
66	E 3	33	43.38	38.19	10.38	1.2	20.1	78.8	LVB	$y = 141.59\ln(x) - 316.94$	178	217	199	134	163	149	89	108	99	45	54	50
67	E 3A	33.7	44.53	39.115	10.83	1.4	23.0	75.7	MVB	$y = 122.88\ln(x) - 305.91$	126	161	145	95	120	108	63	80	72	32	40	36

Sequence	Borehole ID / Field Name\	Coal Interval			Nett Coal Thickness (m)	Coal Quality				Eddy, et al. (1982) Trend Line Equation	Gas Content Calculated from Eddy, et al. (1982) Trend Line Equations (scf/T)											
		From (m)	To (m)	Sample Mid-Point (m)		Ash-Free			Coal Rank Code		Full Saturation (100%)			75% Saturation			50% Saturation			25% Saturation		
						Moisture (%)	Volatile Matter (%)	Fixed Carbon (%)			Minimum	Maximum	Average	Minimum	Maximum	Average	Minimum	Maximum	Average	Minimum	Maximum	Average
68	E 4	35.25	46.18	40.715	10.93	0.9	23.9	75.2	MVB	$y = 122.88\ln(x) - 305.91$	132	165	150	99	124	112	66	83	75	33	41	37
69	E 5	49.68	61.77	55.725	12.09	1.1	23.6	75.3	MVB	$y = 122.88\ln(x) - 305.91$	174	201	188	131	151	141	87	100	94	44	50	47
70	E 6	486.16	497.13	491.645	10.97	1.4	19.5	79.1	LVB	$y = 141.59\ln(x) - 316.94$	559	562	561	419	422	420	280	281	280	140	141	140
71	E 6	486.16	497.13	491.645	10.97	1.5	20.8	77.7	LVB	$y = 141.59\ln(x) - 316.94$	559	562	561	419	422	420	280	281	280	140	141	140
72	E 7	547.62	559.6	553.61	11.98	1.4	21.9	76.7	MVB	$y = 122.88\ln(x) - 305.91$	469	472	470	352	354	353	234	236	235	117	118	118
73	E 8	69.11	80.77	74.94	11.66	1.0	26.5	72.6	MVB	$y = 122.88\ln(x) - 305.91$	215	234	225	161	175	168	107	117	112	54	58	56
74	E 8	69.11	80.77	74.94	11.66	1.6	23.4	74.9	MVB	$y = 122.88\ln(x) - 305.91$	215	234	225	161	175	168	107	117	112	54	58	56
75	E 8	69.11	80.77	74.94	11.66	1.3	26.4	72.3	MVB	$y = 122.88\ln(x) - 305.91$	215	234	225	161	175	168	107	117	112	54	58	56
76	E 9	103.33	115.52	109.425	12.19	1.4	25.3	73.3	MVB	$y = 122.88\ln(x) - 305.91$	264	278	271	198	208	203	132	139	136	66	69	68
77	E 9A	54.86	64.26	59.56	9.4	0.3	28.0	71.6	MVB	$y = 122.88\ln(x) - 305.91$	186	206	196	140	154	147	93	103	98	47	51	49
78	E 9A	54.86	64.26	59.56	9.4	1.4	24.2	74.5	MVB	$y = 122.88\ln(x) - 305.91$	186	206	196	140	154	147	93	103	98	47	51	49
79	E 9A	54.86	64.26	59.56	9.4	1.4	21.8	76.8	MVB	$y = 122.88\ln(x) - 305.91$	186	206	196	140	154	147	93	103	98	47	51	49
80	E 10	34.16	46.33	40.245	12.17	1.1	24.2	74.7	MVB	$y = 122.88\ln(x) - 305.91$	128	165	148	96	124	111	64	83	74	32	41	37
81	E 12	47.72	57.06	52.39	9.34	1.3	26.7	72.0	MVB	$y = 122.88\ln(x) - 305.91$	169	191	181	127	143	135	85	96	90	42	48	45
82	E 12	47.72	57.06	52.39	9.34	1.0	24.9	74.1	MVB	$y = 122.88\ln(x) - 305.91$	169	191	181	127	143	135	85	96	90	42	48	45
83	E 13	32.31	40.81	36.56	8.5	2.0	24.2	73.8	MVB	$y = 122.88\ln(x) - 305.91$	121	150	136	91	112	102	61	75	68	30	37	34
84	E 15	346.4	359.66	353.03	13.26	1.8	18.7	79.5	LVB	$y = 141.59\ln(x) - 316.94$	511	516	514	383	387	385	256	258	257	128	129	128
85	E 15	346.4	359.66	353.03	13.26	2.0	22.4	75.6	MVB	$y = 122.88\ln(x) - 305.91$	413	417	415	309	313	311	206	209	207	103	104	104
86	E 16A	49.07	62	55.535	12.93	1.5	24.1	74.4	MVB	$y = 122.88\ln(x) - 305.91$	172	201	188	129	151	141	86	101	94	43	50	47
87	E 16A	49.07	62	55.535	12.93	1.5	23.5	75.0	MVB	$y = 122.88\ln(x) - 305.91$	172	201	188	129	151	141	86	101	94	43	50	47
88	E 16A	49.07	62	55.535	12.93	1.1	26.5	72.4	MVB	$y = 122.88\ln(x) - 305.91$	172	201	188	129	151	141	86	101	94	43	50	47
89	E 17																					
90	E 17A	49.53	59.61	54.57	10.08	1.2	23.9	74.8	MVB	$y = 122.88\ln(x) - 305.91$	174	196	186	130	147	139	87	98	93	43	49	46
91	E 18	57.61	70.02	63.815	12.41	2.0	20.5	77.6	LVB	$y = 141.59\ln(x) - 316.94$	257	285	272	193	213	204	129	142	136	64	71	68
92	E 18	57.61	70.02	63.815	12.41	1.9	20.4	77.7	LVB	$y = 141.59\ln(x) - 316.94$	257	285	272	193	213	204	129	142	136	64	71	68
93	E 18	57.61	70.02	63.815	12.41	1.9	21.9	76.3	MVB	$y = 122.88\ln(x) - 305.91$	192	216	205	144	162	154	96	108	102	48	54	51
94	E 19																					
95	E 19A	39.01	43.84	41.425	4.83	7.8	16.9	75.3	MVB	$y = 122.88\ln(x) - 305.91$	144	159	152	108	119	114	72	79	76	36	40	38
96	E 19B	39.01	48.87	43.94	9.86	1.0	25.3	73.7	MVB	$y = 122.88\ln(x) - 305.91$	144	172	159	108	129	119	72	86	79	36	43	40
97	E 19C	41.15	53.04	47.095	11.89	1.9	23.0	75.1	MVB	$y = 122.88\ln(x) - 305.91$	151	182	167	113	137	126	75	91	84	38	46	42
98	E 19C	41.15	53.04	47.095	11.89	1.6	23.9	74.5	MVB	$y = 122.88\ln(x) - 305.91$	151	182	167	113	137	126	75	91	84	38	46	42
99	E 19C	41.15	53.04	47.095	11.89	1.2	28.2	70.6	MVB	$y = 122.88\ln(x) - 305.91$	151	182	167	113	137	126	75	91	84	38	46	42
100	E 20																					
101	E 21	171	181.98	176.49	10.98	0.6	22.2	77.2	LVB	$y = 141.59\ln(x) - 316.94$	411	420	416	308	315	312	206	210	208	103	105	104

Sequence	Borehole ID / Field Name	Coal Interval			Nett Coal Thickness (m)	Coal Quality				Eddy, et al. (1982) Trend Line Equation	Gas Content Calculated from Eddy, et al. (1982) Trend Line Equations (scf/T)												
		From (m)	To (m)	Sample Mid-Point (m)		Ash-Free			Coal Rank Code		Full Saturation (100%)			75% Saturation			50% Saturation			25% Saturation			
						Moisture (%)	Volatile Matter (%)	Fixed Carbon (%)			Minimum	Maximum	Average	Minimum	Maximum	Average	Minimum	Maximum	Average	Minimum	Maximum	Average	
102	E 22																						
103	E 24	55.44	65.84	60.64	10.4	0.3	25.4	74.4	MVB	$y = 122.88\ln(x) - 305.91$	187	209	199	141	156	149	94	104	99	47	52	50	
104	E 24	55.44	65.84	60.64	10.4	1.7	22.8	75.5	MVB	$y = 122.88\ln(x) - 305.91$	187	209	199	141	156	149	94	104	99	47	52	50	
105	E 25	55.91	67.57	61.74	11.66	1.4	20.6	78.0	LVB	$y = 141.59\ln(x) - 316.94$	253	280	267	190	210	200	126	140	133	63	70	67	
106	E 26	94.14	104.1	99.12	9.87	1.7	21.3	77.0	MVB	$y = 122.88\ln(x) - 305.91$	253	265	259	189	199	194	126	132	129	63	66	65	
107	E 27	270.05	281.18	275.615	11.13	1.2	21.4	77.4	LVB	$y = 141.59\ln(x) - 316.94$	476	481	479	357	361	359	238	241	239	119	120	120	
108	E 28																						
109	E 29	100.58	114.66	107.62	14.08	1.0	20.8	78.2	LVB	$y = 141.59\ln(x) - 316.94$	336	354	346	252	266	259	168	177	173	84	89	86	
110	E 29	100.58	114.66	107.62	14.08	0.7	23.6	75.7	MVB	$y = 122.88\ln(x) - 305.91$	261	277	269	196	208	202	130	138	134	65	69	67	
111	E 30	53.34	61.57	57.455	8.23	0.9	24.3	74.7	MVB	$y = 122.88\ln(x) - 305.91$	183	200	192	137	150	144	91	100	96	46	50	48	
112	E 30	53.34	61.57	57.455	8.23	0.8	22.5	76.6	MVB	$y = 122.88\ln(x) - 305.91$	183	200	192	137	150	144	91	100	96	46	50	48	
113	E 31	161.39	170.38	165.885	8.99	1.0	26.6	72.5	MVB	$y = 122.88\ln(x) - 305.91$	319	325	322	239	244	242	159	163	161	80	81	81	
114	E 32	105.77	114.6	110.185	8.83	0.8	19.5	79.7	LVB	$y = 141.59\ln(x) - 316.94$	343	354	349	257	266	262	172	177	174	86	89	87	
115	E 32	105.77	114.6	110.185	8.83	0.9	23.1	76.0	MVB	$y = 122.88\ln(x) - 305.91$	267	277	272	200	208	204	133	138	136	67	69	68	
116	E 33	89.97	100.35	95.16	10.38	1.5	23.7	74.8	MVB	$y = 122.88\ln(x) - 305.91$	247	260	254	185	195	190	123	130	127	62	65	63	
117	E 33	89.97	100.35	95.16	10.38	1.3	22.7	76.0	MVB	$y = 122.88\ln(x) - 305.91$	247	260	254	185	195	190	123	130	127	62	65	63	
118	E 34	161.08	173.35	167.215	12.27	0.3	21.4	78.3	LVB	$y = 141.59\ln(x) - 316.94$	403	413	408	302	310	306	201	207	204	101	103	102	
119	E 34	161.08	173.35	167.215	12.27	1.1	20.9	78.0	LVB	$y = 141.59\ln(x) - 316.94$	403	413	408	302	310	306	201	207	204	101	103	102	
120	E 34	161.08	173.35	167.215	12.27	0.7	27.1	72.4	MVB	$y = 122.88\ln(x) - 305.91$	319	328	323	239	246	242	159	164	162	80	82	81	
121	E 35	170.69	180.74	175.715	10.05	1.0	23.0	76.0	MVB	$y = 122.88\ln(x) - 305.91$	326	333	329	244	250	247	163	166	165	81	83	82	
122	E 36	204.08	212.58	208.33	8.5	1.8	23.6	74.6	MVB	$y = 122.88\ln(x) - 305.91$	348	353	350	261	264	263	174	176	175	87	88	88	
123	E 37	256.64	265.18	260.91	8.54	1.1	22.3	76.5	MVB	$y = 122.88\ln(x) - 305.91$	376	380	378	282	285	283	188	190	189	94	95	94	
124	E 38	329.79	332.38	331.085	2.59	1.1	22.3	76.5	MVB	$y = 122.88\ln(x) - 305.91$	407	408	407	305	306	305	203	204	204	102	102	102	
125	E 39	53.04	66.55	59.795	13.51	1.6	22.4	76.0	MVB	$y = 122.88\ln(x) - 305.91$	182	210	197	137	157	148	91	105	98	46	52	49	
126	E 40	37.8	50.9	44.35	13.1	1.3	23.8	74.9	MVB	$y = 122.88\ln(x) - 305.91$	140	177	160	105	133	120	70	88	80	35	44	40	
127	E 41	43.93	55.93	49.93	12	1.5	22.7	75.8	MVB	$y = 122.88\ln(x) - 305.91$	159	189	175	119	141	131	79	94	87	40	47	44	
128	E 42	52.58	64.58	58.58	12	1.5	22.7	75.9	MVB	$y = 122.88\ln(x) - 305.91$	181	206	194	136	155	146	90	103	97	45	52	49	
129	E 43	55.56	67.56	61.56	12	1.5	23.0	75.5	MVB	$y = 122.88\ln(x) - 305.91$	188	212	200	141	159	150	94	106	100	47	53	50	
130	E 44	49.99	53.77	51.88	3.78	1.7	14.7	83.6	LVB	$y = 141.59\ln(x) - 316.94$	237	247	242	178	185	182	118	124	121	59	62	61	
131	E 45	8.53	20.37	14.45	11.84	1.5	25.2	73.3	MVB	$y = 122.88\ln(x) - 305.91$	(1)	(1)	(1)	(1)	(1)	(1)	(1)	(1)	(1)	(1)	(1)	(1)	
132	E 46	31.23	41.8	36.515	10.57	0.7	25.4	73.8	MVB	$y = 122.88\ln(x) - 305.91$	117	153	136	88	115	102	58	76	68	29	38	34	
133	E 47	37.19	48.52	42.855	11.33	1.8	24.8	73.4	MVB	$y = 122.88\ln(x) - 305.91$	138	171	156	104	128	117	69	86	78	35	43	39	
134	E 48	42.98	56.69	49.835	13.71	1.6	23.9	74.5	MVB	$y = 122.88\ln(x) - 305.91$	156	190	174	117	143	131	78	95	87	39	48	44	
135	E 49	50.9	60.86	55.88	9.96	1.5	26.1	72.4	MVB	$y = 122.88\ln(x) - 305.91$	177	199	188	133	149	141	88	99	94	44	50	47	

Sequence	Borehole ID / Field Name	Coal Interval			Nett Coal Thickness (m)	Coal Quality				Eddy, et al. (1982) Trend Line Equation	Gas Content Calculated from Eddy, et al. (1982) Trend Line Equations (scf/T)											
		From (m)	To (m)	Sample Mid-Point (m)		Ash-Free			Coal Rank Code		Full Saturation (100%)			75% Saturation			50% Saturation			25% Saturation		
						Moisture (%)	Volatile Matter (%)	Fixed Carbon (%)			Minimum	Maximum	Average	Minimum	Maximum	Average	Minimum	Maximum	Average	Minimum	Maximum	Average
136	E 50	49.02	61.23	55.125	12.21	1.6	25.2	73.2	MVB	$y = 122.88\ln(x) - 305.91$	172	200	187	129	150	140	86	100	93	43	50	47
137	E 51	33.51	46.8	40.155	13.29	1.6	24.7	73.8	MVB	$y = 122.88\ln(x) - 305.91$	126	167	148	94	125	111	63	83	74	31	42	37
138	E 52	45.09	59.21	52.15	14.12	1.2	25.4	73.5	MVB	$y = 122.88\ln(x) - 305.91$	162	196	180	122	147	135	81	98	90	41	49	45
139	E 53	42.67	52.88	47.775	10.21	1.5	23.4	75.1	MVB	$y = 122.88\ln(x) - 305.91$	155	182	169	116	136	127	78	91	85	39	45	42
140	E 54	81.08	92.81	86.945	11.73	0.5	25.3	74.2	MVB	$y = 122.88\ln(x) - 305.91$	234	251	243	176	188	182	117	125	121	59	63	61
141	E 55	102.11	115.66	108.885	13.55	1.4	23.8	74.8	MVB	$y = 122.88\ln(x) - 305.91$	263	278	270	197	208	203	131	139	135	66	69	68
142	E 56	39.93	51.77	45.85	11.84	1.4	23.8	74.8	MVB	$y = 122.88\ln(x) - 305.91$	147	179	164	110	134	123	74	90	82	37	45	41
143	E 57	137.33	147.68	142.505	10.35	1.2	23.2	75.6	MVB	$y = 122.88\ln(x) - 305.91$	299	308	303	224	231	228	149	154	152	75	77	76
144	E 58	160.43	172.73	166.58	12.3	1.1	23.2	75.7	MVB	$y = 122.88\ln(x) - 305.91$	318	327	323	239	245	242	159	164	161	80	82	81
145	E 59	35.29	51.06	43.175	15.77	1.8	24.4	73.8	MVB	$y = 122.88\ln(x) - 305.91$	132	177	157	99	133	118	66	89	78	33	44	39
146	E 60	188.06	199.17	193.615	11.11	0.9	25.7	73.5	MVB	$y = 122.88\ln(x) - 305.91$	338	345	341	253	258	256	169	172	171	84	86	85
147	E 61	185.17	200.67	192.92	15.5	1.4	24.5	74.2	MVB	$y = 122.88\ln(x) - 305.91$	336	346	341	252	259	256	168	173	170	84	86	85
148	E 62	46.35	61.73	54.04	15.38	1.9	24.1	74.0	MVB	$y = 122.88\ln(x) - 305.91$	165	201	184	124	151	138	83	100	92	41	50	46
149	E 63	210.64	222.73	216.685	12.09	1.5	24.1	74.4	MVB	$y = 122.88\ln(x) - 305.91$	352	358	355	264	269	266	176	179	177	88	90	89
150	E 64	210.08	230.42	220.25	20.34	1.1	22.3	76.5	MVB	$y = 122.88\ln(x) - 305.91$	351	363	357	263	272	268	176	181	178	88	91	89
151	E 65	89.81	99.16	94.485	9.98	1.5	22.6	75.9	MVB	$y = 122.88\ln(x) - 305.91$	247	259	253	185	194	190	123	129	127	62	65	63
152	E 66	94.67	106.96	100.815	12.29	0.8	24.3	75.2	MVB	$y = 122.88\ln(x) - 305.91$	253	268	261	190	201	196	127	134	130	63	67	65
153	E 66A	94.59	105.73	100.16	11.14	1.4	23.1	75.6	MVB	$y = 122.88\ln(x) - 305.91$	253	267	260	190	200	195	127	133	130	63	67	65
154	E 67	76.88	89.99	83.435	13.11	1.8	22.7	75.5	MVB	$y = 122.88\ln(x) - 305.91$	228	247	238	171	185	178	114	124	119	57	62	59
155	E 68	74.19	87.99	81.09	13.8	1.5	23.6	74.9	MVB	$y = 122.88\ln(x) - 305.91$	223	244	234	167	183	176	112	122	117	56	61	59
156	E 69	140.85	153.54	147.195	12.69	1.2	21.3	77.5	LVB	$y = 141.59\ln(x) - 316.94$	384	396	390	288	297	292	192	198	195	96	99	97
157	E 70	150.27	160.67	155.47	10.4	1.0	23.8	75.2	MVB	$y = 122.88\ln(x) - 305.91$	310	318	314	233	239	236	155	159	157	78	80	79
158	E 71	151.91	161.46	156.685	9.55	1.2	24.0	74.9	MVB	$y = 122.88\ln(x) - 305.91$	311	319	315	234	239	236	156	159	158	78	80	79
159	E 72	144.13	152.9	148.515	8.77	1.0	23.0	76.0	MVB	$y = 122.88\ln(x) - 305.91$	305	312	309	229	234	231	152	156	154	76	78	77
160	E 73	203.05	214.63	208.84	11.58	1.3	21.8	76.9	MVB	$y = 122.88\ln(x) - 305.91$	347	354	350	260	265	263	174	177	175	87	88	88
161	E 74	183.99	194.54	189.265	10.55	1.1	22.6	76.3	MVB	$y = 122.88\ln(x) - 305.91$	335	342	338	251	256	254	167	171	169	84	85	85
162	E 75	189.2	197.66	193.43	8.46	1.3	24.8	73.9	MVB	$y = 122.88\ln(x) - 305.91$	338	344	341	254	258	256	169	172	171	85	86	85
163	E 76	176.02	180.12	178.07	4.1	0.7	22.3	77.0	MVB	$y = 122.88\ln(x) - 305.91$	329	332	331	247	249	248	165	166	165	82	83	83
164	E 77	243.75	254.66	249.205	10.91	1.2	20.8	77.9	LVB	$y = 141.59\ln(x) - 316.94$	461	467	464	346	351	348	231	234	232	115	117	116
165	E 78	226.49	237.38	231.935	10.89	1.2	21.5	77.3	LVB	$y = 141.59\ln(x) - 316.94$	451	458	454	338	343	341	225	229	227	113	114	114
166	E 79	226.1	235.93	231.015	9.83	1.0	22.2	76.8	MVB	$y = 122.88\ln(x) - 305.91$	360	365	363	270	274	272	180	183	181	90	91	91
167	E 80B	246.14	255.4	250.77	9.26	1.2	22.5	76.2	MVB	$y = 122.88\ln(x) - 305.91$	371	375	373	278	281	280	185	188	186	93	94	93
168	E 81	241.28	249.18	245.23	7.82	1.0	21.1	77.9	LVB	$y = 141.59\ln(x) - 316.94$	460	464	462	345	348	347	230	232	231	115	116	116
169	E 82	325.23	333.69	329.46	8.46	1.2	22.7	76.1	MVB	$y = 122.88\ln(x) - 305.91$	405	408	406	304	306	305	202	204	203	101	102	102

Sequence	Borehole ID / Field Name	Coal Interval			Nett Coal Thickness (m)	Coal Quality				Eddy, et al. (1982) Trend Line Equation	Gas Content Calculated from Eddy, et al. (1982) Trend Line Equations (scf/T)											
		From (m)	To (m)	Sample Mid-Point (m)		Ash-Free			Coal Rank Code		Full Saturation (100%)			75% Saturation			50% Saturation			25% Saturation		
						Moisture (%)	Volatile Matter (%)	Fixed Carbon (%)			Minimum	Maximum	Average	Minimum	Maximum	Average	Minimum	Maximum	Average	Minimum	Maximum	Average
170	E 83	314.62	323.22	318.92	8.6	1.1	22.2	76.6	MVB	$y = 122.88\ln(x) - 305.91$	401	404	402	301	303	302	200	202	201	100	101	101
171	E 84	261.14	269.66	265.4	8.52	1.3	21.9	76.8	MVB	$y = 122.88\ln(x) - 305.91$	378	382	380	283	286	285	189	191	190	94	95	95
172	E 85	315.49	323.26	319.375	7.77	1.1	22.1	76.8	MVB	$y = 122.88\ln(x) - 305.91$	401	404	403	301	303	302	201	202	201	100	101	101
173	E 87	6.08	10.5	8.29	4.42	1.4	24.2	74.5	MVB	$y = 122.88\ln(x) - 305.91$	(1)	(1)	(1)	(1)	(1)	(1)	(1)	(1)	(1)	(1)	(1)	(1)
174	E 88	53.54	63.85	58.695	10.31	1.4	24.2	74.5	MVB	$y = 122.88\ln(x) - 305.91$	183	205	195	137	154	146	92	102	97	46	51	49
175	E 89	48.46	52.94	50.7	4.48	1.4	24.2	74.5	MVB	$y = 122.88\ln(x) - 305.91$	171	182	177	128	136	132	85	91	88	43	45	44
176	E 90	38.6	48.87	43.735	10.27	1.2	23.2	75.6	MVB	$y = 122.88\ln(x) - 305.91$	143	172	158	107	129	119	72	86	79	36	43	40
177	E 91	49.38	61.1	55.24	11.72	1.0	24.3	74.7	MVB	$y = 122.88\ln(x) - 305.91$	173	199	187	130	150	140	87	100	94	43	50	47
178	E 92	47.5	59.08	53.29	11.58	1.4	24.2	74.5	MVB	$y = 122.88\ln(x) - 305.91$	168	195	183	126	146	137	84	98	91	42	49	46
179	E 93	64.22		64.22		1.4	24.2	74.5	MVB	$y = 122.88\ln(x) - 305.91$	206	(1)	206	154	(1)	154	103	(1)	103	51	(1)	51
180	E 94	58.92	69.31	64.115	10.39	1.4	24.2	74.5	MVB	$y = 122.88\ln(x) - 305.91$	195	215	205	146	161	154	97	107	103	49	54	51
181	E 96																					
182	E 97																					
183	E 98	110.5	121.6	116.05	11.1	1.1	22.3	76.5	MVB	$y = 122.88\ln(x) - 305.91$	272	284	278	204	213	209	136	142	139	68	71	70
184	E 99	218.85	227.13	222.99	8.28	1.1	22.3	76.5	MVB	$y = 122.88\ln(x) - 305.91$	356	361	359	267	271	269	178	180	179	89	90	90
185	E 101	229.08	238.44	233.76	9.36	1.1	22.3	76.5	MVB	$y = 122.88\ln(x) - 305.91$	362	367	364	271	275	273	181	183	182	90	92	91
186	E 102	201.8	210.6	206.2	8.8	1.1	22.3	76.5	MVB	$y = 122.88\ln(x) - 305.91$	346	351	349	260	264	262	173	176	174	87	88	87
187	E 103	93.46	101.82	97.64	8.36	1.4	24.2	74.5	MVB	$y = 122.88\ln(x) - 305.91$	252	262	257	189	197	193	126	131	129	63	66	64
188	E 104	119.41	125.83	122.62	6.42	1.1	22.3	76.5	MVB	$y = 122.88\ln(x) - 305.91$	282	288	285	211	216	214	141	144	143	70	72	71
189	LBW 1	11.12	13.14	12.13	2.02	1.8	41.5	56.7	HVB-B	$y = 52.803\ln(x) - 141.04$	(1)	(1)	(1)	(1)	(1)	(1)	(1)	(1)	(1)	(1)	(1)	(1)
190	LBW 1	16.17	20.23	18.2	3.73	1.7	38.1	60.2	HVB-B	$y = 52.803\ln(x) - 141.04$	(1)	(1)	(1)	(1)	(1)	(1)	(1)	(1)	(1)	(1)	(1)	(1)
191	LBW 1	28.82	43.33	36.075		1.5	32.2	66.3														
192	LBW 1				10.53	1.4	33.4	65.2	HVB-A	$y = 78.864\ln(x) - 193.00$	(1)	(1)	(1)	(1)	(1)	(1)	(1)	(1)	(1)	(1)	(1)	(1)
193	LBW 2	84.71	88.66	86.685	2.8	1.8	39.7	58.2	HVB-B	$y = 52.803\ln(x) - 141.04$	93	96	95	70	72	71	47	48	47	23	24	24
194	LBW 2	95.94	111.56	103.75		1.5	32.2	66.3														
195	LBW 2				13.57	1.4	28.8	69.7	MVB	$y = 122.88\ln(x) - 305.91$	(1)	(1)	(1)	(1)	(1)	(1)	(1)	(1)	(1)	(1)	(1)	(1)
196	LBW 4	41.51	43.51	42.51	2	1.5	38.2	60.2	HVB-B	$y = 52.803\ln(x) - 141.04$	56	58	57	42	44	43	28	29	28	14	15	14
197	LBW 4	51.9	70.13	61.015	17.92	1.3	30.5	68.1	HVB-A	$y = 78.864\ln(x) - 193.00$	118	142	131	89	107	98	59	71	66	30	36	33
198	LBW 5	32.76	36.41	34.585	3.26	1.7	39.5	59.0	HVB-B	$y = 52.803\ln(x) - 141.04$	43	49	46	32	37	35	22	24	23	11	12	12
199	LBW 5	40.53	56.83	48.68	16.2	1.2	33.0	65.7	HVB-A	$y = 78.864\ln(x) - 193.00$	99	126	113	74	94	85	49	63	57	25	31	28
200	LBW 6	65.61	74.1	69.855	9.09	1.5	32.2	66.3														
201	LBW 6	15	98	56.5	7.96	1.6	32.9	55.1	HVB-B	$y = 52.803\ln(x) - 141.04$	(1)	101	72	(1)	76	54	(1)	51	36	(1)	25	18
202	LBW 6	83.56	92.7	88.13	8.65	1.3	33.6	65.0	HVB-A	$y = 78.864\ln(x) - 193.00$	156	164	160	117	123	120	78	82	80	39	41	40
203	LBW 7	55.05	58.99	57.02	3.69	1.8	39.3	59.1	HVB-B	$y = 52.803\ln(x) - 141.04$	71	74	72	53	56	54	35	37	36	18	19	18

Sequence	Borehole ID / Field Name	Coal Interval			Nett Coal Thickness (m)	Coal Quality				Eddy, et al. (1982) Trend Line Equation	Gas Content Calculated from Eddy, et al. (1982) Trend Line Equations (scf/T)											
		From (m)	To (m)	Sample Mid-Point (m)		Ash-Free			Coal Rank Code		Full Saturation (100%)			75% Saturation			50% Saturation			25% Saturation		
						Moisture (%)	Volatile Matter (%)	Fixed Carbon (%)			Minimum	Maximum	Average	Minimum	Maximum	Average	Minimum	Maximum	Average	Minimum	Maximum	Average
204	LBW 7	64.65	82.28	73.465	15.68	1.5	34.2	64.3	HVB-A	$y = 78.864\ln(x) - 193.00$	136	155	146	102	116	109	68	77	73	34	39	36
205	LBW 8	25.64	29.43	27.535	3.43	1.4	36.3	62.3	HVB-A	$y = 78.864\ln(x) - 193.00$	(1)	(1)	(1)	(1)	(1)	(1)	(1)	(1)	(1)	(1)	(1)	(1)
206	LBW 8	34.9	46.35	40.625	9.31	1.2	32.6	66.2	HVB-A	$y = 78.864\ln(x) - 193.00$	87	110	99	65	82	74	44	55	50	22	27	25
207	LBW 9	14.81	16.81	15.81	1.91	1.7	38.8	59.5	HVB-B	$y = 52.803\ln(x) - 141.04$	(1)	(1)	(1)	(1)	(1)	(1)	(1)	(1)	(1)	(1)	(1)	(1)
208	LBW 9	26.6	34.58	30.59	7.98	1.3	32.9	65.7	HVB-A	$y = 78.864\ln(x) - 193.00$	(1)	86	77	(1)	65	58	(1)	43	38	(1)	22	19
209	LBW 10	63.13	67.19	65.16	3.74	1.8	33.8	56.7	HVB-B	$y = 52.803\ln(x) - 141.04$	78	81	80	58	61	60	39	41	40	19	20	20
210	LBW 10	73.22	84.3	78.76	10.98	1.3	30.9	67.8	HVB-A	$y = 78.864\ln(x) - 193.00$	146	157	151	109	118	114	73	78	76	36	39	38
211	LBW 11	32.11	36.16	34.135	1.7	2.6	39.1	60.9	HVB-B	$y = 52.803\ln(x) - 141.04$	42	48	45	32	36	34	21	24	23	11	12	11
212	LBW 11	44.04	57.16	50.6	13.12	1.5	32.2	66.3														
213	LBW 11				12.3	3.6	33.6	62.9	HVB-A	$y = 78.864\ln(x) - 193.00$	(1)	(1)	(1)	(1)	(1)	(1)	(1)	(1)	(1)	(1)	(1)	(1)
214	LBW 12	39.86	50.87	45.365	6.13	3.7	39.7	56.6	HVB-B	$y = 52.803\ln(x) - 141.04$	54	66	60	40	50	45	27	33	30	13	17	15
215	LBW 12	66.3	79.84	73.07	12.57	2.6	26.8	70.6	MVB	$y = 122.88\ln(x) - 305.91$	209	232	221	157	174	166	105	116	111	52	58	55
216	LBW 13	97.77	102	99.885	4.04	1.3	30.8	67.9	HVB-A	$y = 78.864\ln(x) - 193.00$	168	172	170	126	129	128	84	86	85	42	43	43
217	S 1	96.01	113.08	104.545	17.07	5.1	33.1	61.8	HVB-B	$y = 52.803\ln(x) - 141.04$	100	109	104	75	81	78	50	54	52	25	27	26
218	S 2	63.93	77.62	70.775	13.69	5.7	28.0	66.3	HVB-A	$y = 78.864\ln(x) - 193.00$	135	150	143	101	113	107	67	75	71	34	38	36
219	S 3	6.1	15.24	10.67	9.14	6.1	28.3	65.6	HVB-A	$y = 78.864\ln(x) - 193.00$	(1)	(1)	(1)	(1)	(1)	(1)	(1)	(1)	(1)	(1)	(1)	(1)
220	S 5	90.22	107.29	98.755	17.07	6.3	25.4	68.3	HVB-A	$y = 78.864\ln(x) - 193.00$	162	176	169	122	132	127	81	88	85	41	44	42
221	S 18	151.79	160.55	156.17	8.76	3.5	33.0	63.5	HVB-A	$y = 78.864\ln(x) - 193.00$	203	208	205	152	156	154	102	104	103	51	52	51
222	S 25	147.51	159.4	153.455	11.89	4.3	28.7	67.0	HVB-A	$y = 78.864\ln(x) - 193.00$	201	207	204	151	155	153	100	103	102	50	52	51
223	S 26	11.27	21.96	16.615	10.69	4.9	25.3	69.8	MVB	$y = 122.88\ln(x) - 305.91$	(1)	(1)	(1)	(1)	(1)	(1)	(1)	(1)	(1)	(1)	(1)	(1)
224	S 27	85.8	97.92	91.86	12.12	4.4	27.2	68.4	HVB-A	$y = 78.864\ln(x) - 193.00$	158	169	163	119	126	123	79	84	82	40	42	41
225	S 29	70.71	80.95	75.83	10.24	4.7	27.7	67.6	HVB-A	$y = 78.864\ln(x) - 193.00$	143	154	148	107	115	111	71	77	74	36	38	37
226	S 30	40.46	49.48	44.97	9.02	5.8	24.9	69.4	MVB	$y = 122.88\ln(x) - 305.91$	149	174	162	112	130	121	74	87	81	37	43	40
227	M 1	78.59	90.53	84.56	11.94	4.1	30.6	65.2	HVB-A	$y = 78.864\ln(x) - 193.00$	151	162	157	113	122	118	76	81	78	38	41	39
228	M 2	96.32	111.51	103.915	15.19	4.1	30.2	65.7	HVB-A	$y = 78.864\ln(x) - 193.00$	167	179	173	125	134	130	84	89	87	42	45	43
229	M 3	78.93	93.26	86.095	14.33	4.4	28.5	67.2	HVB-A	$y = 78.864\ln(x) - 193.00$	152	165	158	114	124	119	76	82	79	38	41	40
230	M 4	135.62	145	140.31	9.38	4.4	30.3	65.3	HVB-A	$y = 78.864\ln(x) - 193.00$	194	199	197	146	150	148	97	100	98	49	50	49
231	M 5	69.18	78.84	74.01	9.66	3.0	31.6	65.4	HVB-A	$y = 78.864\ln(x) - 193.00$	141	151	146	106	114	110	71	76	73	35	38	37
232	M 6	71.11	78.93	75.02	7.82	3.2	33.2	63.6	HVB-A	$y = 78.864\ln(x) - 193.00$	143	152	148	107	114	111	72	76	74	36	38	37
233	M 7	108.35	118.56	113.455	10.21	4.4	28.2	67.4	HVB-A	$y = 78.864\ln(x) - 193.00$	177	184	180	132	138	135	88	92	90	44	46	45
234	M 8	71.85	83.28	77.565	11.43	5.1	28.2	66.7	HVB-A	$y = 78.864\ln(x) - 193.00$	144	156	150	108	117	113	72	78	75	36	39	38
235	M 9	21.18	34.51	27.845	13.33	6.2	26.4	67.4	HVB-A	$y = 78.864\ln(x) - 193.00$	(1)	86	(1)	(1)	65	(1)	(1)	43	(1)	(1)	22	(1)
236	M 10	0.1	11.07	5.585	11.07	6.5	26.3	67.2	HVB-A	$y = 78.864\ln(x) - 193.00$	(1)	(1)	(1)	(1)	(1)	(1)	(1)	(1)	(1)	(1)	(1)	(1)
237	M 11	25.75	38.63	32.19	12.88	5.7	25.7	68.6	HVB-A	$y = 78.864\ln(x) - 193.00$	(1)	95	81	(1)	71	61	(1)	48	40	(1)	24	20

Sequence	Borehole ID / Field Name	Coal Interval			Nett Coal Thickness (m)	Coal Quality				Eddy, et al. (1982) Trend Line Equation	Gas Content Calculated from Eddy, et al. (1982) Trend Line Equations (scf/T)											
		From (m)	To (m)	Sample Mid-Point (m)		Ash-Free			Coal Rank Code		Full Saturation (100%)			75% Saturation			50% Saturation			25% Saturation		
						Moisture (%)	Volatile Matter (%)	Fixed Carbon (%)			Minimum	Maximum	Average	Minimum	Maximum	Average	Minimum	Maximum	Average	Minimum	Maximum	Average
238	L 256 (Type Borehole - Main & A Seams)*	15	190	102.5	9.17	14.8	29.7	55.5	HVB-B	$y = 52.803\ln(x) - 141.04$	(1)	136	103	(1)	102	78	(1)	68	52	(1)	34	26
239	L 252 (Type Borehole - Main Seam)*	22.49766667	197.4976667	109.9976667	6.15	16.1	32.6	51.3	HVB-C	$y = 30.948\ln(x) - 69.666$	(1)	94	76	(1)	70	57	(1)	47	38	(1)	23	19
240	L 198 (Type Borehole - Lower & Middle Seam)*	26.6	97.77	62.185	4.15	13.7	33.7	52.6	HVB-C	$y = 30.948\ln(x) - 69.666$	(1)	72	58	(1)	54	44	(1)	36	29	(1)	18	15
241	Shallow (Average)*	60	100	80	9	0.8	26.3	72.9	MVB	$y = 122.88\ln(x) - 305.91$	197	260	233	148	195	174	99	130	116	49	65	58
242	Deep(Average)*	200	700	450	9	0.8	26.3	72.9	MVB	$y = 122.88\ln(x) - 305.91$	345	499	445	259	374	334	173	250	222	86	125	111
243	Gokwe Average	200	300		9	5.3	29.3	65.3	HVB-A	$y = 78.864\ln(x) - 193.00$	225	257	242	169	193	182	112	128	121	56	64	61
244	N1/1	45.1	46.7	45.9	1				SBIT	$y = 6.2975\ln(x) - 7.8369$	16	16	16	12	12	12	8	8	8	4	4	4
245	N1/2	41	89	65	5.5				SBIT	$y = 6.2975\ln(x) - 7.8369$	16	20	18	12	15	14	8	10	9	4	5	5
246	N1/3	24	91	57.5	7.73				SBIT	$y = 6.2975\ln(x) - 7.8369$	(1)	21	18	(1)	15	13	(1)	10	9	(1)	5	4
247	N2/1	52.7	118.1	85.4	19.6				SBIT	$y = 6.2975\ln(x) - 7.8369$	17	22	20	13	17	15	9	11	10	4	6	5
248	N3/1	38.3	119	78.65	23.65				SBIT	$y = 6.2975\ln(x) - 7.8369$	15	22	20	11	17	15	8	11	10	4	6	5
249	N4/1	113.3	189	151.15	14.03				SBIT	$y = 6.2975\ln(x) - 7.8369$	22	25	24	16	19	18	11	13	12	5	6	6
250	N5/2	5	41.7	23.35	6.8				SBIT	$y = 6.2975\ln(x) - 7.8369$	(1)	16	(1)	(1)	12	(1)	(1)	8	(1)	(1)	4	(1)
251	N5/1	10.4	41.2	25.8	4.1				SBIT	$y = 6.2975\ln(x) - 7.8369$	(1)	16	(1)	(1)	12	(1)	(1)	8	(1)	(1)	4	(1)
252	N6/1	14.7	70.5	42.6	2.5				SBIT	$y = 6.2975\ln(x) - 7.8369$	(1)	19	16	(1)	14	12	(1)	9	8	(1)	5	4
253	N8/2	75.35	124.5	99.925	11.5				SBIT	$y = 6.2975\ln(x) - 7.8369$	19	23	21	15	17	16	10	11	11	5	6	5
254	N12/1	79.9	150.85	115.375	12.5				SBIT	$y = 6.2975\ln(x) - 7.8369$	20	24	22	15	18	17	10	12	11	5	6	6
255	N9/1	75.4	124.6	100	8.74				SBIT	$y = 6.2975\ln(x) - 7.8369$	19	23	21	15	17	16	10	11	11	5	6	5
256	N10/1	89.4	177.3	133.35	21.76				SBIT	$y = 6.2975\ln(x) - 7.8369$	20	25	23	15	19	17	10	12	11	5	6	6
257	N11/3	110.6	153.5	132.05	8.15				SBIT	$y = 6.2975\ln(x) - 7.8369$	22	24	23	16	18	17	11	12	11	5	6	6
258	N7/1																					
259	N7/2																					
260	N7/3																					
261	N8/1																					
262	N8/2																					
263	N12/1																					
264	N9/1																					
265	N10/1																					
266	N11/3																					

Sequence	Borehole ID / Field Name\	Coal Interval			Nett Coal Thickness (m)	Coal Quality			Eddy, et al. (1982) Trend Line Equation	Gas Content Calculated from Eddy, et al. (1982) Trend Line Equations (scf/T)												
		From (m)	To (m)	Sample Mid-Point (m)		Ash-Free				Coal Rank Code	Full Saturation (100%)			75% Saturation			50% Saturation			25% Saturation		
						Moisture (%)	Volatile Matter (%)	Fixed Carbon (%)			Minimum	Maximum	Average	Minimum	Maximum	Average	Minimum	Maximum	Average	Minimum	Maximum	Average
267	N11/2																					
268	N11/1																					
269	N12/1																					
270	N12/2																					
271	N12/3																					
272	Y1-01	499.74	566.3	533.02	10.652			SBIT	$y = 6.2975\ln(x) - 7.8369$	31	32	32	23	24	24	16	16	16	8	8	8	
273	Y1-02	705.536	737.136	721.336	1.29			SBIT	$y = 6.2975\ln(x) - 7.8369$	33	34	34	25	25	25	17	17	17	8	8	8	
274	Y1-03	705.73	792.74	749.235	16.75			SBIT	$y = 6.2975\ln(x) - 7.8369$	33	34	34	25	26	25	17	17	17	8	9	8	
275	Y1-04	587.2	605.5	596.35	2.85			SBIT	$y = 6.2975\ln(x) - 7.8369$	32	33	32	24	24	24	16	16	16	8	8	8	
276	PDM006C																					
277	PDM007A																					
278	PDM008																					
279	PDM009																					
280	PDM011																					
281	PDM014A																					
282	PDM015																					
283	Lubimbi	11.8	190	100.9				HVB-C	$y = 30.948\ln(x) - 69.666$	(1)	93	73	(1)	70	55	(1)	46	37	(1)	23	18	
284	Busi	60	80	70	10			SBIT	$y = 6.2975\ln(x) - 7.8369$	18	20	19	13	15	14	9	10	9	4	5	5	
285	Tjolotjo, Sawmills, and Insuza	270	330	300	5			SBIT	$y = 6.2975\ln(x) - 7.8369$	27	29	28	21	22	21	14	14	14	7	7	7	

Appendix D List of isotherm samples collected and analysed by Kubu Energy (after Faiz, et al., 2013).

Sample Sequence	Borehole	Depth From	Depth To	Sample Mid-Point Depth	Sample Number	Zone	Sampling					Intrusives	Sample Analyses										Vitrinite Reflectance	Selected for Comparison to Eddy et al. (1982) Measured Data	
							Gas Description			Proximate Analysis	Vitrinite Reflectance		Proximity to Intrusive <30m Vertical	Thickest Intrusive Thickness (m)	Measured Gas Content		Proximate Analysis								
							Methane	Nitrogen	Carbon Dioxide						Raw	Dry, Ash-Free	Air Dried				Ash-Free				
																	Moisture	Ash	Volatiles Matter	Fixed Carbon	Moisture	Volatiles Matter			Fixed Carbon
(m)	(m)	(m)	scf/T	scf/T	%	%	%	%	%	%	%	%	%	%	%	%									
1	135C9	405.7	406.3	406	CH-9-002	UMH	✓	✓		✓	✓	✓	1.61	11.33	20.14	3.81	39.94	22.04	34.21	6.34	36.70	56.96	0.51		
2	135C9	420.8	421.4	421.1	CH-9-008	Z3	✓	✓		✓	✓	✓	1.61	74.60	184.70	1.52	58.09	6.03	34.37	3.63	14.38	81.99	3.67		
3	135C9	444.21	444.81	444.51	CH-9-018	Z3	✓	✓		✓	✓	✓	43.46	20.61	35.86	1.91	40.61	15.51	41.97	3.22	26.12	70.67	1.30		
4	135C9	504.6	505.2	504.9	CH-9-028	Z2	✓	✓		✓	✓	✓	43.46	26.86	120.29	3.40	74.27	5.95	16.38	13.22	23.11	63.66	4.71		
5	135C9	520.86	521.46	521.16	CH-9-031	Z1	✓	✓		✓	✓	✓	43.46	37.31	52.34	2.07	26.64	17.82	53.46	2.82	24.29	72.88	1.88		
6	134C8	370.48	370.86	370.67	CH-8-002	UMH	✓	✓		✓	✓	✓		13.09	19.37	3.36	29.07	33.58	33.99	4.74	47.34	47.92	0.40		
7	134C8	385.62	386.22	385.92	CH-8-005	Z3	✓	✓		✓	✓	✓	73.43	9.03	12.19	3.15	22.79	27.91	46.15	4.08	36.15	59.77	0.62		
8	134C8	387.88	388.48	388.18	CH-8-012	Z3	✓	✓	✓	✓	✓	✓	73.43	40.07	79.16	2.66	46.71	16.99	33.64	5.00	31.88	63.12	0.90		
9	134C7	403.83	404.43	404.13	CH-7-002	UMH	✓	✓		✓	✓	✓		11.30	17.69	6.36	29.78	32.85	31.01	9.06	46.78	44.16	0.50		
10	134C7	432.36	432.96	432.66	CH-7-011	Z3	✓	✓		✓	✓	✓		17.77	21.85	4.78	13.91	33.51	47.81	5.55	38.92	55.53	0.54		
11	134C7	439.95	440.55	440.25	CH-7-016	Z3	✓	✓	✓	✓	✓	✓		17.12	23.18	3.52	22.65	28.88	44.95	4.55	37.34	58.11	0.54		
12	134C7	462.86	463.14	463	CH-7-021	Z2	✓	✓		✓	✓	✓		26.78	32.12	3.72	12.91	32.05	51.33	4.27	36.80	58.94	0.55	✓	
13	134C7	485.62	486.22	485.92	CH-7-025	Z1	✓	✓		✓	✓	✓	21.25	100.26	130.89	1.30	22.10	9.42	67.18	1.67	12.09	86.24	3.88		
14	134C6	319.59	320.19	319.89	CH-6-002	Z3	✓	✓		✓	✓	✓		21.78	42.05	5.99	42.21	23.38	28.41	10.37	40.46	49.17	0.47	✓	
15	134C6	328.84	329.4	329.12	CH-6-008	Z3	✓	✓		✓	✓	✓		37.11	47.18	5.27	16.07	34.62	44.04	6.28	41.25	52.47	0.51	✓	
16	134C6	340.05	340.64	340.345	CH-6-013	Z2	✓	✓		✓	✓	✓		39.94	49.05	4.98	13.60	32.00	49.41	5.77	37.04	57.19	0.60	✓	
17	134C6	355.5	355.99	355.745	CH-6-016	Z1	✓	✓	✓	✓	✓	✓		12.43	36.05	2.42	63.10	13.18	21.30	6.57	35.72	57.71	0.65		
18	135C5	247.77	248.5	248.135	CH-05-D1	UMH	✓	✓		✓	✓	✓	13.83	26.84	36.47	1.85	24.56	22.65	50.94	2.45	30.03	67.52	1.00		
19	135C5	283	283.25	283.125	CH-05-D2	Z3	✓	✓		✓	✓	✓	1.21	22.39	45.63	2.43	48.50	6.57	42.50	4.71	12.75	82.54	5.33		
20	135C5	325.77	328.46	327.115	CH-05-D5	Z3	✓	✓		✓	✓	✓	2.91	13.11	19.74	2.21	31.35	23.61	42.83	3.22	34.39	62.39	1.40		
21	135C5	335.26	336.29	335.775	CH-05-D9	Z2	✓	✓		✓	✓	✓	29.47	23.98	29.47	1.37	17.26	22.11	59.25	1.66	26.73	71.61	1.22		
22	135C5	344.1	345.23	344.665	CH-05-D11	Z1	✓	✓		✓	✓	✓	29.47	42.64	104.80	2.27	57.05	8.38	32.30	5.28	19.52	75.20	5.44		
23	135C4	380.82	381.53	381.175	CH-04-D1	UMH	✓	✓		✓	✓	✓		15.06	26.60	1.13	42.25	14.25	42.37	1.95	24.68	73.37	1.91		
24	135C4	437.06	437.41	437.235	CH-04-D3	Z3	✓	✓		✓	✓	✓		22.37	141.78	2.27	81.96	4.21	11.57	12.56	23.31	64.12	5.53		
25	135C4	459.9	460.02	459.96	CH-04-D10	Z2	✓	✓	✓	✓	✓	✓		56.73	67.23	2.31	13.30	28.53	55.86	2.66	32.91	64.43	0.84	✓	
26	135C4	478.79	479.34	479.065	CH-04-D15	Z1	✓	✓		✓	✓	✓	5.14	23.42	29.15	2.50	17.16	27.13	53.20	3.02	32.76	64.23	0.87		
27	135C4	490.4	490.64	490.52	CH-04-D19	Z1	✓	✓	✓	✓	✓	✓	5.14	82.23	96.53	1.06	13.75	11.27	73.92	1.23	13.07	85.70	1.59		
28	136C3	364.7	365	364.85	CH-03-005	Z3	✓	✓		✓	✓	✓		37.55	50.12	2.10	22.98	29.07	45.84	2.73	37.75	59.52	0.83	✓	
29	136C3	374.94	375.54	375.24	CH-03-012	Z3	✓	✓		✓	✓	✓		13.04	25.51	3.51	45.38	21.51	29.60	6.43	39.38	54.19	0.52		

Sample Sequence	Borehole	Depth From	Depth To	Sample Mid-Point Depth	Sample Number	Zone	Sampling					Intrusives		Sample Analyses										
							Gas Description	Isotherm Analyses			Proximate Analysis	Vitrinite Reflectance	Proximity to Intrusive <30m Vertical	Thickest Intrusive Thickness (m)	Measured Gas Content		Proximate Analysis							Vitrinite Reflectance
								Methane	Nitrogen	Carbon Dioxide					Raw	Dry, Ash-Free	Air Dried				Ash-Free			
																	Moisture	Ash	Volatiles Matter	Fixed Carbon	Moisture	Volatiles Matter	Fixed Carbon	
																	scf/T	scf/T	%	%	%	%	%	
30	136C3	410.45	410.68	410.565	CH-03-013	Z2	✓	✓		✓	✓	29.84	28.06	33.45	4.32	11.79	31.45	52.44	4.89	35.65	59.45	0.64		
31	136C3	417.95	418.55	418.25	CH-03-016	Z2	✓	✓	✓	✓	✓	29.84	35.31	46.93	3.14	21.62	21.12	54.12	4.00	26.95	69.05	0.92		
32	136C3	420.95	421.55	421.25	CH-03-018	Z1	✓	✓		✓	✓	29.84	38.70	54.22	2.05	26.58	17.49	53.88	2.79	23.83	73.39	1.39		
33	136C2	257.64	258.25	257.945	CH-02-003	Z3	✓	✓		✓	✓		5.80	8.49	4.88	26.79	33.52	34.82	6.66	45.78	47.56	0.46		
34	136C2	272.49	273.09	272.79	CH-02-007	Z3	✓	✓		✓	✓	50.12	22.97	32.60	2.69	26.84	27.69	42.78	3.67	37.85	58.48	0.77		
35	136C2	276.51	276.74	276.625	CH-02-009	Z3	✓	✓		✓	✓	50.12	52.83	68.52	1.45	21.45	16.30	60.81	1.85	20.75	77.41	1.52		
36	136C2	357.97	358.27	358.12	CH-02-011	Z2	✓	✓		✓	✓	50.12	31.01	47.87	0.76	34.45	18.77	46.02	1.16	28.63	70.20	1.57		
37	136C1	245.82	246.29	246.055	CH-01 D002	UMH	✓	✓		✓	✓		18.45	25.55	5.65	22.11	28.74	43.49	7.25	36.90	55.84	0.44		
38	136C1	268.38	268.98	268.68	CH-01 D004	Z3	✓	✓		✓	✓		33.23	44.71	5.45	20.23	31.50	42.82	6.84	39.49	53.68	0.47	✓	
39	136C1	275.24	275.44	275.34	CH-01 D005	Z3	✓	✓		✓	✓		33.13	45.05	5.43	21.04	30.70	42.84	6.87	38.87	54.25	0.49	✓	
40	136C1	277.3	277.9	277.6	CH-01 D006	Z3	✓	✓	✓	✓	✓		33.32	51.03	4.71	29.99	25.84	39.46	6.73	36.91	56.36	0.47	✓	
41	136C1	279.96	280.17	280.065	CH-01 D008	Z3	✓	✓	✓	✓	✓		32.33	39.16	5.08	12.37	32.94	49.62	5.79	37.59	56.62	0.50	✓	

Selected for Comparison to Eddy et al. (1982)  
Measured Data

**Appendix E Gas content values from the Shangani Energy exploration data digitised from the Barker (2006) graph.**

Sequence	Area	Borehole Name	Depth Digitised from Baker (2006) Graph	Gas Content Digitised from Baker (2006) Graph
			(m)	(scf/T)
1	Hwange	C6-Hwange	682	328
2	Hwange	C6-Hwange	700	337
3	Hwange	C6-Hwange	732	409
4	Hwange	C6-Hwange	738	280
5	Hwange	C6-Hwange	775	284
6	Hwange	C6-Hwange	738	261
7	Hwange	C6-Hwange	699	250
8	Hwange	C6-Hwange	698	243
9	Hwange	C6-Hwange	679	244
10	Hwange	C6-Hwange	688	252
11	Hwange	C6-Hwange	734	246
12	Hwange	C6-Hwange	753	243
13	Hwange	C6-Hwange	753	227
14	Hwange	C6-Hwange	769	235
15	Hwange	C6-Hwange	740	221
16	Hwange	C6-Hwange	694	211
17	Hwange	C6-Hwange	676	195
18	Hwange	C6-Hwange	671	188
19	Hwange	C6-Hwange	683	182
20	Hwange	C6-Hwange	676	167
21	Hwange	C6-Hwange	687	141
22	Hwange	C6-Hwange	674	106
23	Hwange	C6-Hwange	739	113
24	Hwange	C6-Hwange	756	112
25	Hwange	C6-Hwange	762	101
26	Hwange	C6-Hwange	771	59
27	Hwange	C6-Hwange	760	56
28	Hwange	C6-Hwange	765	51
29	Hwange	C6-Hwange	745	44
30	Hwange	C6-Hwange	741	31
31	Hwange	C6-Hwange	766	30
32	Hwange	C6-Hwange	677	56
33	Sengwa	RTZ-Sengwa	261	9
34	Sengwa	RTZ-Sengwa	270	15
35	Sengwa	RTZ-Sengwa	270	15
36	Sengwa	RTZ-Sengwa	268	24
37	Sengwa	RTZ-Sengwa	268	24
38	Sengwa	RTZ-Sengwa	278	31

Sequence	Area	Borehole Name	Depth Digitised from Baker (2006) Graph	Gas Content Digitised from Baker (2006) Graph
			(m)	(scf/T)
39	Sengwa	RTZ-Sengwa	284	30
40	Sengwa	RTZ-Sengwa	284	30
41	Sengwa	RTZ-Sengwa	281	21
42	Sengwa	RTZ-Sengwa	288	19
43	Sengwa	RTZ-Sengwa	293	33
44	Sengwa	RTZ-Sengwa	303	32
45	Sengwa	RTZ-Sengwa	310	29
46	Sengwa	RTZ-Sengwa	310	29
47	Sengwa	RTZ-Sengwa	311	20
48	Sengwa	RTZ-Sengwa	316	28
49	Sengwa	RTZ-Sengwa	326	27
50	Sengwa	RTZ-Sengwa	326	27
51	Sengwa	RTZ-Sengwa	336	29
52	Sengwa	RTZ-Sengwa	336	29
53	Sengwa	RTZ-Sengwa	336	29
54	Sengwa	RTZ-Sengwa	338	39
55	Sengwa	RTZ-Sengwa	332	42
56	Sengwa	RTZ-Sengwa	332	42
57	Sengwa	RTZ-Sengwa	332	42
58	Sengwa	RTZ-Sengwa	332	42
59	Sengwa	RTZ-Sengwa	338	39
60	Sengwa	RTZ-Sengwa	342	32
61	Sengwa	RTZ-Sengwa	336	29
62	Sengwa	RTZ-Sengwa	332	20
63	Sengwa	RTZ-Sengwa	332	20
64	Gwaai	C2-Gwaai	327	4
65	Gwaai	C2-Gwaai	284	3
66	Gwaai	C2-Gwaai	306	3
67	Gwaai	C2-Gwaai	303	12
68	Gwaai	C2-Gwaai	295	26
69	Gwaai	C2-Gwaai	304	37
70	Gwaai	C2-Gwaai	290	37
71	Gwaai	C2-Gwaai	294	53
72	Gwaai	C2-Gwaai	294	53
73	Gwaai	C2-Gwaai	302	77
74	Gwaai	C2-Gwaai	309	79
75	Gwaai	C2-Gwaai	309	87
76	Gwaai	C2-Gwaai	309	100
77	Gwaai	C2-Gwaai	298	116
78	Gwaai	C2-Gwaai	219	46

Sequence	Area	Borehole Name	Depth Digitised from Baker (2006) Graph	Gas Content Digitised from Baker (2006) Graph
			(m)	(scf/T)
79	Gwaai	C2-Gwaai	242	53
80	Gwaai	C2-Gwaai	264	54
81	Gwaai	C2-Gwaai	249	39
82	Gwaai	C2-Gwaai	222	26
83	Gwaai	C2-Gwaai	208	21
84	Gwaai	C2-Gwaai	201	19
85	Gwaai	C2-Gwaai	220	14
86	Gwaai	C2-Gwaai	209	7
87	Gwaai	C2-Gwaai	219	5
88	Gwaai	C2-Gwaai	172	6
89	Gwaai	C2-Gwaai	248	1
90	Gwaai	C2-Gwaai	275	5
91	Gwaai	C3-Gwaai	348	169
92	Gwaai	C3-Gwaai	358	216
93	Gwaai	C3-Gwaai	402	199
94	Gwaai	C3-Gwaai	411	188
95	Gwaai	C3-Gwaai	414	177
96	Gwaai	C3-Gwaai	414	168
97	Gwaai	C3-Gwaai	414	168
98	Gwaai	C3-Gwaai	441	166
99	Gwaai	C3-Gwaai	420	151
100	Gwaai	C3-Gwaai	438	151
101	Gwaai	C3-Gwaai	438	151
102	Gwaai	C3-Gwaai	442	209
103	Gwaai	C3-Gwaai	443	221
104	Gwaai	C3-Gwaai	410	109
105	Gwaai	C3-Gwaai	407	122
106	Gwaai	C3-Gwaai	425	132
107	Gwaai	C3-Gwaai	418	131
108	Gwaai	C3-Gwaai	442	145
109	Gwaai	C3-Gwaai	399	143
110	Gwaai	C3-Gwaai	409	152
111	Gwaai	C3-Gwaai	427	110
112	Gwaai	C3-Gwaai	424	101
113	Gwaai	C3-Gwaai	424	101
114	Gwaai	C3-Gwaai	436	97
115	Gwaai	C3-Gwaai	448	107
116	Gwaai	C3-Gwaai	448	91
117	Gwaai	C3-Gwaai	421	90
118	Gwaai	C3-Gwaai	437	72

Sequence	Area	Borehole Name	Depth Digitised from Baker (2006) Graph	Gas Content Digitised from Baker (2006) Graph
			(m)	(scf/T)
119	Gwaai	C3-Gwaai	434	59
120	Gwaai	C3-Gwaai	446	50
121	Gwaai	C3-Gwaai	449	58
122	Gwaai	C3-Gwaai	437	49
123	Gwaai	C3-Gwaai	353	47
124	Gwaai	C3-Gwaai	352	40
125	Gwaai	C3-Gwaai	374	51
126	Gwaai	C3-Gwaai	379	70
127	Gwaai	C3-Gwaai	361	65
128	Gwaai	C3-Gwaai	351	67
129	Gwaai	C3-Gwaai	352	77
130	Gwaai	C3-Gwaai	345	76
131	Gwaai	C3-Gwaai	339	71
132	Gwaai	C3-Gwaai	347	98
133	Gwaai	C3-Gwaai	335	108
134	Gwaai	C3-Gwaai	365	119
135	Gwaai	C3-Gwaai	359	153
136	Gwaai	C3-Gwaai	342	157
137	Gwaai	C3-Gwaai	413	24
138	Gwaai	C3-Gwaai	413	16
139	Gwaai	C3-Gwaai	418	12
140	Gwaai	C3-Gwaai	429	4
141	Gwaai	C3-Gwaai	414	2
142	Gwaai	C3-Gwaai	443	18
143	Gwaai	C3-Gwaai	414	2
144	Gwaai	C3-Gwaai	405	13
145	Gwaai	C3-Gwaai	360	9
146	Gwaai	C3-Gwaai	350	6
147	Gwaai	C3-Gwaai	243	29
148	Gwaai	C3-Gwaai	251	20
149	Gwaai	C3-Gwaai	255	62
150	Gwaai	C3-Gwaai	255	62
151	Gwaai	C3-Gwaai	230	2
152	Gwaai	C4-Gwaai	424	277
153	Gwaai	C4-Gwaai	422	262
154	Gwaai	C4-Gwaai	410	262
155	Gwaai	C4-Gwaai	398	262
156	Gwaai	C4-Gwaai	392	255
157	Gwaai	C4-Gwaai	408	235
158	Gwaai	C4-Gwaai	407	228

Sequence	Area	Borehole Name	Depth Digitised from Baker (2006) Graph	Gas Content Digitised from Baker (2006) Graph
			(m)	(scf/T)
159	Gwaai	C4-Gwaai	424	247
160	Gwaai	C4-Gwaai	431	210
161	Gwaai	C4-Gwaai	422	214
162	Gwaai	C4-Gwaai	428	195
163	Gwaai	C4-Gwaai	428	179
164	Gwaai	C4-Gwaai	427	167
165	Gwaai	C4-Gwaai	431	154
166	Gwaai	C4-Gwaai	431	154
167	Gwaai	C4-Gwaai	382	160
168	Gwaai	C4-Gwaai	393	159
169	Gwaai	C4-Gwaai	395	169
170	Gwaai	C4-Gwaai	395	179
171	Gwaai	C4-Gwaai	395	179
172	Gwaai	C4-Gwaai	396	188
173	Gwaai	C4-Gwaai	386	198
174	Gwaai	C4-Gwaai	408	146
175	Gwaai	C4-Gwaai	410	140
176	Gwaai	C4-Gwaai	418	131
177	Gwaai	C4-Gwaai	418	131
178	Gwaai	C4-Gwaai	417	121
179	Gwaai	C4-Gwaai	417	113
180	Gwaai	C4-Gwaai	437	106
181	Gwaai	C4-Gwaai	434	96
182	Gwaai	C4-Gwaai	432	44
183	Gwaai	C4-Gwaai	432	37
184	Gwaai	C4-Gwaai	384	4
185	Gwaai	C4-Gwaai	374	9
186	Gwaai	C4-Gwaai	380	25
187	Gwaai	C4-Gwaai	392	28
188	Gwaai	C4-Gwaai	384	36
189	Gwaai	C4-Gwaai	383	43
190	Gwaai	C4-Gwaai	341	62
191	Gwaai	C4-Gwaai	334	53
192	Gwaai	C4-Gwaai	209	67
193	Gwaai	C4-Gwaai	218	66
194	Gwaai	C4-Gwaai	236	63
195	Gwaai	C4-Gwaai	236	63
196	Gwaai	C4-Gwaai	246	69
197	Gwaai	C4-Gwaai	258	74
198	Gwaai	C4-Gwaai	258	74

Sequence	Area	Borehole Name	Depth Digitised from Baker (2006) Graph	Gas Content Digitised from Baker (2006) Graph
			(m)	(scf/T)
199	Gwaai	C4-Gwaai	263	61
200	Gwaai	C4-Gwaai	254	49
201	Gwaai	C4-Gwaai	254	40
202	Gwaai	C4-Gwaai	254	31
203	Gwaai	C4-Gwaai	258	24
204	Gwaai	C4-Gwaai	266	27
205	Gwaai	C4-Gwaai	287	14
206	Gwaai	C4-Gwaai	197	7
207	Gwaai	C4-Gwaai	266	93
208	Gwaai	C4-Gwaai	286	105
209	Gwaai	C4-Gwaai	246	104
210	Gwaai	C4-Gwaai	255	106
211	Gwaai	C4-Gwaai	256	120
212	Gwaai	C4-Gwaai	256	129
213	Gwaai	C4-Gwaai	221	130
214	Gwaai	C4-Gwaai	245	159
215	Gwaai	C4-Gwaai	256	224
216	Gwaai	C4-Gwaai	334	85
217	Gwaai	C4-Gwaai	333	99
218	Gwaai	C4-Gwaai	346	136
219	Gwaai	C4-Gwaai	348	122
220	Gwaai	C4-Gwaai	361	131
221	Gwaai	C4-Gwaai	352	113
222	Gwaai	C4-Gwaai	362	106
223	Gwaai	C4-Gwaai	362	97
224	Gwaai	C4-Gwaai	373	105
225	Gwaai	C4-Gwaai	379	112
226	Gwaai	C4-Gwaai	390	108
227	Gwaai	C4-Gwaai	404	97
228	Gwaai	C4-Gwaai	399	105
229	Gwaai	C4-Gwaai	348	23
230	Gwaai	C4-Gwaai	345	16
231	Gwaai	C4-Gwaai	345	16
232	Gwaai	C4-Gwaai	340	9
233	Lupane	C5-Lupane	505	175
234	Lupane	C5-Lupane	525	159
235	Lupane	C5-Lupane	519	155
236	Lupane	C5-Lupane	558	141
237	Lupane	C5-Lupane	545	129
238	Lupane	C5-Lupane	553	127

Sequence	Area	Borehole Name	Depth Digitised from Baker (2006) Graph	Gas Content Digitised from Baker (2006) Graph
			(m)	(scf/T)
239	Lupane	C5-Lupane	563	110
240	Lupane	C5-Lupane	563	110
241	Lupane	C5-Lupane	555	98
242	Lupane	C5-Lupane	567	91
243	Lupane	C5-Lupane	579	66
244	Lupane	C5-Lupane	558	55
245	Lupane	C5-Lupane	558	47
246	Lupane	C5-Lupane	544	37
247	Lupane	C5-Lupane	508	26
248	Lupane	C5-Lupane	514	47
249	Lupane	C5-Lupane	535	50
250	Lupane	C5-Lupane	514	69
251	Lupane	C5-Lupane	502	60
252	Lupane	C5-Lupane	492	55
253	Lupane	C5-Lupane	485	71
254	Lupane	C5-Lupane	499	73
255	Lupane	C5-Lupane	506	82
256	Lupane	C5-Lupane	496	94
257	Lupane	C5-Lupane	479	91
258	Lupane	C5-Lupane	460	84
259	Lupane	C5-Lupane	485	71
260	Lupane	C5-Lupane	494	79
261	Lupane	C5-Lupane	543	97
262	Lupane	C5-Lupane	528	94
263	Lupane	C5-Lupane	529	107
264	Lupane	C5-Lupane	524	112
265	Lupane	C5-Lupane	518	124
266	Lupane	C5-Lupane	510	118
267	Lupane	C5-Lupane	469	125
268	Lupane	C5-Lupane	453	124
269	Lupane	C5-Lupane	469	125
270	Lupane	C5-Lupane	559	87
271	Lupane	C5-Lupane	552	77
272	Lupane	C5-Lupane	552	69
273	Lupane	C5-Lupane	525	69
274	Lupane	C5-Lupane	420	51
275	Lupane	C5-Lupane	408	82
276	Lupane	C5-Lupane	445	69
277	Lupane	C5-Lupane	439	78
278	Lupane	C5-Lupane	401	41

Sequence	Area	Borehole Name	Depth Digitised from Baker (2006) Graph	Gas Content Digitised from Baker (2006) Graph
			(m)	(scf/T)
279	Lupane	C5-Lupane	413	50
280	Entuba	ZG-Entuba	363	3
281	Entuba	ZG-Entuba	363	3
282	Entuba	ZG-Entuba	373	3
283	Entuba	ZG-Entuba	496	5
284	Entuba	ZG-Entuba	501	10
285	Entuba	ZG-Entuba	485	6
286	Entuba	ZG-Entuba	496	5
287	Entuba	ZG-Entuba	467	10
288	Entuba	ZG-Entuba	467	21
289	Entuba	ZG-Entuba	483	20
290	Entuba	ZG-Entuba	478	31
291	Entuba	ZG-Entuba	474	42
292	Entuba	ZG-Entuba	473	36
293	Entuba	ZG-Entuba	401	21
294	Entuba	ZG-Entuba	401	21
295	Entuba	ZG-Entuba	392	88
296	Entuba	ZG-Entuba	388	104
297	Entuba	ZG-Entuba	392	88
298	Entuba	ZG-Entuba	388	79
299	Entuba	ZG-Entuba	388	79
300	Entuba	ZG-Entuba	388	79
301	Entuba	ZG-Entuba	390	66
302	Entuba	ZG-Entuba	397	67
303	Entuba	ZG-Entuba	396	60
304	Entuba	ZG-Entuba	390	58
305	Entuba	ZG-Entuba	381	61
306	Entuba	ZG-Entuba	392	42
307	Entuba	ZG-Entuba	378	29
308	Entuba	ZG-Entuba	368	27
309	Entuba	ZG-Entuba	360	26
310	Entuba	ZG-Entuba	365	37
311	Entuba	ZG-Entuba	365	54
312	Entuba	ZG-Entuba	393	17
313	Entuba	ZG-Entuba	394	25